Modeling of spatially distributed nitrate transport to investigate the effects of drought and river restoration in the Bode catchment, Central Germany

---

Kumulative Dissertation

zur Erlangung des akademischen Grades

"doctor rerum naturalium"

(Dr. rer. nat.)

in der Wissenschaftsdisziplin "Geoökologie"

eingereicht an der

Mathematisch-Naturwissenschaftlichen Fakultät

der Universität Potsdam

von

Xiangqian Zhou

Hauptbetreuer: Prof. Dr. Michael Rode, Universität Potsdam/Helmholtz-Zentrum für Umweltforschung – UFZ, Deutschland

Betreuer: Prof. Dr. Ralf Merz, Martin-Luther Universität Halle-Wittenberg/ Helmholtz-Zentrum für Umweltforschung – UFZ, Deutschland

Published online on the
Publication Server of the University of Potsdam:
https://doi.org/10.25932/publishup-62105
https://nbn-resolving.org/urn:nbn:de:kobv:517-opus4-621059

Preface

This dissertation is prepared and submitted in accordance with the guidelines for the degree of Doctor of Philosophy in Faculty of Science (Discipline Geoecology) at the University of Potsdam, Germany. The Ph.D. study was under the supervision of Prof. Dr. Michael Rode (Helmholtz Centre for Environmental Research – UFZ) and Prof. Dr. Ralf Merz (Helmholtz Centre for Environmental Research – UFZ). The study was carried out at UFZ.

The study was mainly funded by the Chinese Scholarship Council (CSC) for a period of four years (No. 201706710031) and partially supported by the Department of Aquatic Ecosystem Analysis and Management (ASAM), UFZ.

Hydromorphological alteration and diffuse pollution are the main drivers of European water bodies fail to achieve the 'good ecology status' according to the European Environment Agency report (EEA, 2018). In addition, the increase occurrences of extreme weather events such as droughts and heat waves has worsened the situation, which are projected to become more frequent and severe in the future. This results in a complex situation, perturbing remarkably the hydrological cycle and its associated processes including the runoff partitioning and nutrient transport to river network. Thus, sustainable management of catchments requires scientific understanding of the impacts of drought on nitrate dynamics and the stream restoration on nitrate retention at river network scale. A scientifically-based and integrated hydrological and water quality decision making tool capable to guide sustainable water management considering the increasing extreme climate conditions are needed. To this end, a process-based and distributed hydrological water quality model is required to provide scientific evidence of the hydrological and water quality processes under changing climate conditions. This model can be used for investigating mitigation measurements (such as spatially-targeted mitigation measures) to improve water quality.

The newly developed grid-based hydrological water quality model (mHM-Nitrate) balancing between processes complexity and an accurate representation of catchment heterogeneity, was implemented in the well-monitored Bode catchment, in central Germany with heterogeneous climate and catchment characteristics. First, we investigate the impact of calibration schemes on the spatiotemporal transferability of mHM-Nitrate model parameters by evaluating the spatiotemporal performance of nitrate concentration at non-calibrated water quality sampling locations. The Bode catchment experienced sequential drought from 2015-2018 and nitrate concentrations showed varying trends at different gauging stations. This allows us to evaluate the mHM-Nitrate model's ability to simulate discharge and nitrate dynamics in extreme weather events, as well as to investigate the mechanism of the impacts of drought on stream nitrate dynamics. Finally, we investigate the impact of stream restoration through re-meandering on nitrate concentration at river network scale based on the well-calibrated mHM-Nitrate model.

The dissertation is presented as an accumulation of three peer-reviewed publications, including a general Introduction and a general Discussion as Chapter 1 and Chapter 5, respectively. Chapters 2 – 4 present the three peer-reviewed manuscripts as detailed below:

Chapter 2: Ghaffar S., Zhou, X., Jomaa, S., Yang, X. and Rode, M. 2022. Improving the calibration of a fully distributed hydrological water quality model. Submitted.

Chapter 3: Zhou, X., Jomaa, S., Yang, X., Merz, R., Wang, Y. and Rode, M. 2022. Exploring the relations between sequential droughts and stream nitrogen dynamics in central Germany through catchment-scale mechanistic modelling. Journal of Hydrology 614, 128615. https://doi.org/10.1016/j.jhydrol.2022.128615

Chapter 4: Zhou, X., Jomaa, S., Yang, X., Merz, R., Wang, Y. and Rode, M. 2022. Stream restoration can reduce nitrate levels in agricultural landscapes. Accepted.

Acknowledgement

It is not an easy task to pursue a PhD and it is even harder without the support of my supervisor and colleagues. I am deeply grateful to them and cannot express my gratitude in words.

First and foremost, it is my great pleasure to thank my supervisor, Prof. Michael Rode, for accepting me to do my PhD in his team. I still remember how excited I was when he told me I could join him after interview online. In the beginning of my PhD, I was not completely clear about my topic. It is always a pleasure talking to him, and every time we talk he provides me with a lot of ideas and asks me some questions that are difficult to answer but which help me think deeply. He is not only helpful at work, he is also been inviting us to have a beer discussion and boat ride on the Elbe River. I really appreciate his kindness and the warm atmosphere he creates in our office.

I would like to thank Prof. Ralf Merz for his co-supervision of my PhD, he always has constructive ideas and good suggestions during our discussion.

I would also like to express my thanks to all my colleagues in our team and UFZ. Thanks to my friend Dr Seifeddine Jomaa, who taught me how to analyze data and write a scientific paper and encouraged me pursuing my passion for science. I am very grateful for you inviting me over to your place after work to have dinner with your family. I enjoyed being with you all.

I am also very thankful to Xiaoqiang Yang, thank you for hosting me when I came to Germany. Whenever I have a modeling problem you always have a solution. It is difficult to debug the model without your help. I also want to thank my friends: Salman Ghaffar, Ghulam Abbas, it is nice to work together in the same office and play football together on weekends.

Last but not least, I would also thank Sanyuan Jiang, Jingshui Huang, Xiaolin Zhang, YaoLi, Mufeng Chen, Dr Christiane Katterfeld and Martina Klapputh. Particularly, my greatest appreciation goes to my HIGRAD teachers who taught me how to program.

Finally, I would express my deep gratitude to my parents and sister for their emotional support and forever love. Even though my parents didn't have a high degree, they always encouraged me to study hard and didn't make me worry. Especially, I would express my grateful thanks to my wife, Yanping Wang, for her understanding, encouragement and moral support.

Contents

Abstract

The European Water Framework Directive (WFD) has identified river morphological alteration and diffuse pollution as the two main pressures affecting water bodies in Europe at the catchment scale. Consequently, river restoration has become a priority to achieve the WFD's objective of good ecological status. However, little is known about the effects of stream morphological changes, such as re-meandering, on in-stream nitrate retention at the river network scale. Therefore, catchment nitrate modeling is necessary to provide guidance for the implementation of spatially targeted and cost-effective mitigation measures. Meanwhile, Germany, like many other regions in central Europe, has experienced consecutive summer droughts from 2015-2018, resulting in significant changes in river nitrate concentrations in various catchments. However, the mechanistic exploration of catchment nitrate responses to changing weather conditions is still lacking.

Firstly, a fully distributed, process-based catchment Nitrate model (mHM-Nitrate) was used, which was properly calibrated and comprehensively evaluated at numerous spatially distributed nitrate sampling locations. Three calibration schemes were designed, taking into account land use, stream order, and mean NO_3^- concentrations, and they varied in spatial coverage but used data from the same time period (2011–2019). The model performance for discharge was similar among the three schemes, with Nash-Sutcliffe Efficiency (NSE) scores ranging from 0.88 to 0.92. However, for nitrate concentrations, scheme 2 outperformed schemes 1 and 3 when compared to observed data from eight gauging stations. This was likely because scheme 2 incorporated a diverse range of data, including low discharge values and nitrate concentrations, and thus provided a better representation of within-catchment heterogenous. Therefore, the study suggests that strategically selecting gauging stations that reflect the full range of within-catchment heterogeneity is more important for calibration than simply increasing the number of stations.

Secondly, the mHM-Nitrate model was used to reveal the causal relations between sequential droughts and nitrate concentration in the Bode catchment (3200 km^2) in central Germany, where stream nitrate concentrations exhibited contrasting trends from upstream to downstream reaches. The model was evaluated using data from six gauging stations, reflecting different levels of runoff components and their associated nitrate-mixing from upstream to downstream. Results indicated that the mHM-Nitrate model reproduced dynamics of daily discharge and nitrate concentration well, with Nash-Sutcliffe Efficiency ≥ 0.73 for discharge and Kling-Gupta Efficiency ≥ 0.50 for nitrate concentration at most stations. Particularly, the spatially contrasting trends of nitrate concentration were successfully captured by the model. The decrease of nitrate concentration in the lowland area in drought years (2015-2018) was presumably due to (1) limited terrestrial export loading (ca. 40% lower than that of normal years 2004-2014), and (2) increased in-stream retention efficiency (20% higher in summer within the whole river network). From a mechanistic modelling perspective, this study provided insights into spatially heterogeneous flow and nitrate dynamics and effects of sequential droughts, which shed light on water-quality responses to future climate change, as droughts are projected to be more frequent.

Thirdly, this study investigated the effects of stream restoration via re-meandering on in-stream nitrate retention at network-scale in the well-monitored Bode catchment. The mHM-Nitrate model showed good performance in reproducing daily discharge and nitrate concentrations, with median Kling-Gupta values of 0.78 and 0.74, respectively. The mean and standard deviation of gross nitrate retention efficiency, which accounted for both denitrification and assimilatory uptake, were 5.1±0.61% and 74.7±23.2% in winter and summer, respectively, within the stream network. The study found that in the summer, denitrification rates were about two times higher in lowland sub-catchments dominated by agricultural lands than in mountainous sub-catchments dominated by forested areas, with median ± SD of 204±22.6 and 102±22.1 mg N m^{-2} d^{-1}, respectively. Similarly, assimilatory uptake rates were approximately five times higher in streams surrounded by lowland agricultural areas than in those in higher-elevation, forested areas, with median ± SD of 200±27.1 and 39.1±8.7 mg N m^{-2} d^{-1}, respectively. Therefore, restoration strategies targeting lowland agricultural areas may have greater potential for increasing nitrate retention. The study also found that restoring stream sinuosity could increase net nitrate retention efficiency by up to 25.4±5.3%, with greater effects seen in small streams. These results suggest that restoration efforts should consider augmenting stream sinuosity to increase nitrate retention and decrease nitrate concentrations at the catchment scale.

Chapter 1: Introduction

1.1. Problem statement

In recent decades, eutrophication has become a worldwide aquatic environmental problem due to excess nutrients from intensive human activities. Over the 20th century, the global nutrient input to surface waters increased from 34 to 64 Tg N y^{-1}, and agriculture was the dominant contribution to the nutrient source (19% - 51% of total input) on the global scale (Beusen et al., 2016). Streams and rivers are essential parts of surface water ecosystems, they serve as water supply, irrigation, transportation and recreation and have great social, economic and ecosystem significance to humans. However, many streams and rivers have been polluted by excess nitrogen input from agriculture, urban wastewater and other sources. For example, around 60% of European surface water bodies failed to achieve good ecological status according to the European Environment Agency report (EEA, 2018). Good ecological status is introduced by the European Water Framework Directive (WFD), defined as a slight variation from undisturbed conditions in terms of the quality of the biological elements, the hydromorphological and chemical elements (EU, 2000). Hydromorphological alteration and diffuse source pollution are two dominant pressures on Europe's surface water bodies, which affect 40% and 38% of surface water bodies (mainly rivers), respectively (EEA, 2018). In addition, 13% of European water bodies have been heavily modified (e.g., straightening and channelization, dams and weirs) to facilitate agricultural land use and flood protection (EEA, 2018). In Germany, more than 37% of rivers are heavily modified by channelization and/or straightening (Pander et al., 2017).

Hydrological water quality models of catchments are required for quantifying nutrient transport and transformation and investigating river restoration's effect on nitrate retention in river networks. Many parameters are included in the model that cannot be directly measured in the field in order to model spatial variability in hydrological and biogeochemical processes at the catchment scale (Li, Weller and Jordan, 2010). Model calibration is a prerequisite to apply the catchment model by optimizing the model parameters to match the model simulations with observations (Engel et al., 2007; Moriasi et al., 2012; Saraswat et al., 2015). This increases the reliability of the model to accurately represent the spatiotemporal variability of hydrological and biogeochemical processes at the catchment scale (White and Chaubey, 2005). Conventionally, the hydrological water quality model was calibrated at a single site usually the catchment outlet, which may not give a satisfactory model performance at internal sub-catchments in spatially heterogeneous catchments because model parameters could not be well constrained only using the information at the catchment outlet (Cao et al., 2006; Refsgaard et al., 2016). Many studies found that hydrological water quality model calibration at multi-site outperforms over calibration only at the catchment outlet (e.g., Ghaffar et al., 2021; Her and Chaubey, 2015; Jiang et al., 2015; Zhang, Srinivasan and Van Liew, 2008). In contrast, several studies have reported that multi-site calibration did not improve or had almost the same model performance as single-site calibration (e.g., Franco, Oliveira and Bonumá, 2020; Lerat et al., 2012; Wang et al., 2012; Wu et al., 2022a). However, previous studies were mostly restricted to semi-distributed hydrological water quality models (e.g, SWAT(Arnold et al., 2012; Leta, Griensven and Bauwens, 2017; Zhang, Srinivasan and Van Liew, 2008), HYPE (Ghaffar et al.,

2021; Jiang et al., 2015; Lindström et al., 2010)), few studies investigated the effect of calibrating multi-sites compared to a single-site on the performance of a fully distributed hydrological water quality model.

At the catchment scale nitrate turnover processes are expected to change due to climate change (Hesse and Krysanova, 2016; Mosley, 2015; Whitehead et al., 2009), especially due to an increase in drought events (Ballard, Sinha and Michalak, 2019; Zwolsman and van Bokhoven, 2007). In Germany, mean annual temperature increased by 1.5°C from 1881-2018, with ca. 0.3°C of that increase occurring from 2014-2018 (UBA, 2019). Using an ensemble of climate-change scenarios, Huang, Krysanova and Hattermann (2015) reported that most rivers in Germany will experience more frequent droughts. The influence of drought on nitrate dynamics has received increasing attention in recent decades (e.g., Baldwin et al., 2005; Lutz et al., 2016; Mosley, 2015; van Vliet and Zwolsman, 2008; Whitehead et al., 2009; Yevenes, Figueroa and Parra, 2018; Zwolsman and van Bokhoven, 2007). Numerous studies have reported that droughts can have spatiotemporally varying impacts on nitrate transport and transformation processes due to the heterogeneous changes in hydrological processes within catchments (e.g., Leitner et al., 2020; Lintern et al., 2018b; Lutz et al., 2016). These studies are generally based on data-driven and statistical analyses, but conclusions drawn from them are site-specific and often do not provide a full understanding of the factors that influence the effects of drought on nitrate dynamics and their spatial heterogeneity. Thus, it is crucial to identify the mechanisms that underlie water-quality trends under drought conditions to ensure future water quality and develop effective management strategies. Furthermore, the scientific understanding gained from analyzing deterministic trends can help to predict future trends. However, how sequential droughts influence stream nitrate responses has not yet been mechanistically explored.

To achieve a good ecological status, river restoration has received increasing attention (Newcomer Johnson et al., 2016; Wohl et al., 2015). There have been variant measures, for example, re-connect streams with their floodplain in agricultural streams (Roley et al., 2012), re-meandering of straightened rivers (Lorenz et al., 2009; Pedersen et al., 2014), and connecting with ponds (Passy et al., 2012). Several studies have investigated the effects of river restoration on stream nitrate retention at reach scale (Bukaveckas, 2007; Craig et al., 2008; Kaushal et al., 2008; Klocker et al., 2009; Kunz et al., 2017c; Lin et al., 2021; Veraart et al., 2014; Wagenschein and Rode, 2008). However, systemic investigation of the effects of stream restoration (i.e., re-meandering) on stream nitrate retention at the river network scale is still missing. This can be explained by the following challenges of the (i) difficulty in disentangling the contribution of geomorphology among other controlling factors to the variability of nutrient retention (Lin et al., 2016), (ii) the lack of detailed historical information on river morphology (at the natural condition) for the whole river network, and (iii) the uncertainty of disentangling terrestrial and in-stream N processes.

1.2. Background and state-of-art

1.2.1. Nutrient transport, transformation and retention processes at catchment scale

The processes of nutrient transport, nutrient transformation, and nutrient retention in a watershed rely on complex interactions among hydrologic, biogeochemical, and

geomorphologic processes in both terrestrial landscapes and river networks (Grimm et al., 2003; Rode et al., 2010; Ye et al., 2012). The scheme of nutrient transport, transformation and retention within a catchment is shown in Figure 1.1. The interactions between these processes occur at a variety of temporal and spatial scales, and these processes are affected by climate and catchment characteristics (e.g., geology and soil property, land use and land cover, and topography) (Li et al., 2020; Lintern et al., 2018a; Lohse et al., 2009). Climate patterns affect nitrate transport and transformation in both terrestrial and in-stream ecosystems through changes in hydrological and biogeochemical processes (Baron et al., 2012; Suddick et al., 2012). For instance, more nutrient is transported to rivers in periods with high precipitation and high discharge than in drought periods (Howarth et al., 2012). While higher water temperature during drought could result in higher nitrate transformation rates (e.g., denitrification rate and assimilatory uptake rate by crop/plant) in soils and streams (Homyak et al., 2017; Mosley, 2015; Sprague, 2005; Whitehead et al., 2006). Soil properties are closely related to the parent geology, and soil properties affect dissolved nutrient transport through influence on the infiltration process. For example, Kyllmar et al. (2014) found that more nitrate is leached to streams from highly permeable soils (e.g., sandy loam soil) compared to less permeable soil (e.g., clay soil) due to higher hydrological conductivity. Land use and land cover not only influence nutrient transport but also the nutrient source. There was a positive relationship between stream nutrient concentration and the share of agriculture areas in the catchment (Djodjic, Bieroza and Bergstrom, 2021; Ladrera et al., 2019). However, some studies reported that there was no strong relationship between nitrate concentration in streams and the share of agriculture areas (Lintern et al., 2018b; Ruiz et al., 2002). The different findings could be explained by different agricultural practices (such as fertilities application). Catchment topographic properties (e.g., slope, curvature) can influence nutrient transport and transformation though affect the flow path and water residence time (Onderka et al., 2012; Wagener et al., 2007). Numerous studies have demonstrated a strong correlation between topographic properties and nitrogen flux export from catchments. Topography also affects the hydrologic flushing mechanism by affecting the delivery of flushable N (Creed and Beall, 2009; Lei, Wagner and Fohrer, 2021). For example, more N export can be seen in catchments with larger, hydrologically connected variable source areas.

The river network is an important site where nutrient transformation and retention occur (Alexander, Smith and Schwarz, 2000). In-stream retention plays an important role in retaining anthropogenic nitrogen and preventing it from reaching downstream waterbodies (Mulholland et al., 2008; Mulholland and Webster, 2010). Nutrient retention in the river network includes two processes: temporary storage of nutrients in biomass (i.e., assimilatory uptake) and permanent removal from the stream ecosystems (i.e., denitrification) (Ye et al., 2012). Assimilatory uptake slows downstream transport of dissolved inorganic nitrogen, which may be remineralized and removed via coupled nitrification and denitrification, or ultimately be exported from the reach in inorganic form (Arango et al., 2008). Denitrification permanently removes nitrogen in water by converting nitrate to gaseous N_2 as the final product, following the reaction sequence: $NO_3^- \rightarrow NO_2^- \rightarrow NO \rightarrow N_2O \rightarrow N_2$, which is performed by particular groups of heterotrophic bacteria (Groffman et al., 2006).

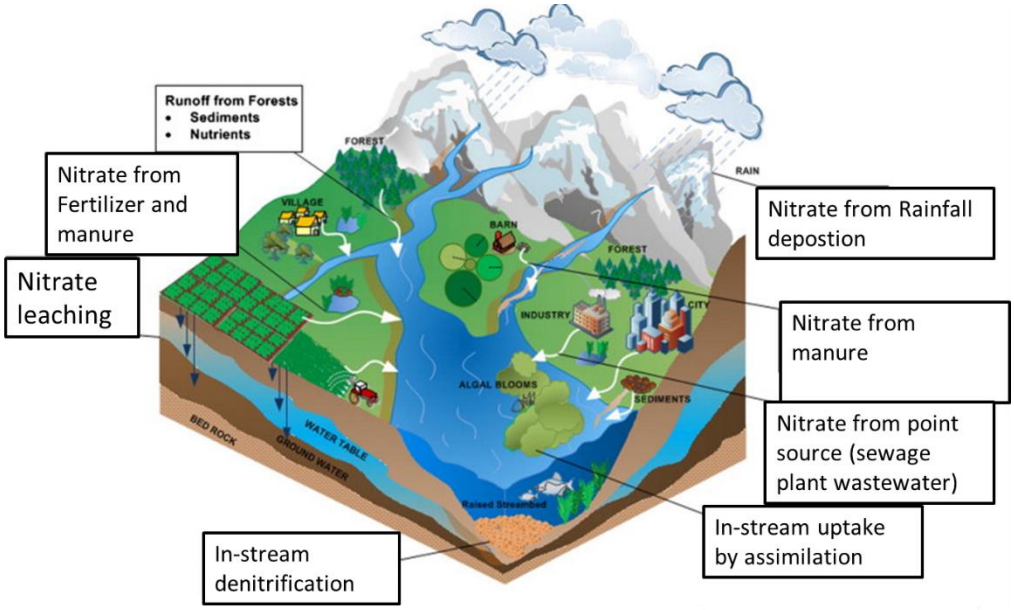

Figure 1.1 The scheme of nitrate transport, transformation and retention processes in a catchment.

Water quality models have been developed and widely used as scientific tools for quantifying the nutrient source, transport and transformation in river ecosystems, as well as examining different land management strategies and climate change scenarios across different environmental conditions (Arheimer et al., 2005; Engel et al., 2007; Fu et al., 2020; Fu et al., 2019; Rode et al., 2010). At the river network scale, several models have been developed to quantify nitrogen retention during transport in river networks, such as FrAMES (Wollheim et al., 2008a; Wollheim et al., 2008b), THREW (Tian et al., 2006; Ye et al., 2012) and NEXSS (Gomez-Velez and Harvey, 2014; Kiel and Bayani Cardenas, 2014). These models have typically parameterized nutrient transformation and retention processes based on local field measurements and extrapolate empirical equations to the whole river network (Ye et al., 2017). A common limitation of these river network models is that they assume the lateral water and nutrient inflows from land to the stream network are homogenous along the streams. They do not account for spatial and temporal distribution of nitrate loading which may contribute to large uncertainty to model simulation results (Helton, Hall and Bertuzzo, 2018; Wollheim et al., 2008a). Therefore, an integrated hydrological water quality model that consider nitrate transport, transformation and retention simultaneously at both terrestrial landscapes and river networks within a catchment is essential.

1.2.2. Hydrological water quality models

In hydrological science and environmental management research, hydrological water quality models have been widely used to quantify nonpoint source pollution inputs to receiving waterbodies and determine their source areas as well as to predict the impacts of climate change and land-use change on water quality (Wellen, Kamran-Disfani and Arhonditsis, 2015). Hydrological water quality models provide a framework for integrating the current understandings of the hydrological and biogeochemical processes and scaling them up to a wide range of spatial and temporal scales. Over the past decades, many hydrological water

quality models have been developed and applied in different environments all over the world (Moriasi et al., 2012). There are numerous papers about different aspects of catchment hydrological water quality models, such as model use model purpose, software availability and documentation, (Engel et al., 2007; Saraswat et al., 2015; Yuan, Sinshaw and Forshay, 2020)), model development (e.g., process representation, spatial heterogeneities and scales, (Baffaut et al., 2015; Breuer et al., 2008; Horn et al., 2004)) and model performance (e.g., calibration, validation and uncertainty analysis, (Daggupati et al., 2015; Efstratiadis and Koutsoyiannis, 2010; Moriasi et al., 2015; Moriasi et al., 2012)).

Wellen, Kamran-Disfani and Arhonditsis (2015) evaluated the current state of distributed catchment water quality models and summarized the five models mostly used worldwide. These are the Soil Water Assessment Tool (SWAT) (Arnold et al., 1998), the Integrated Catchment model (INCA) (Whitehead, Wilson and Butterfield, 1998), the Agricultural Nonpoint Source Pollution Model (AGNPS/AnnAGNPS) (Young, 1989), Hydrological Simulation Program Fortran (HSPF) (Bicknell, 1997), and HBV-NP (now revised as Hydrological Predictions for the Environment (HYPE) (Lindström et al., 2010). The summary of the main processes represented in these models was given in Table 1.1.

SWAT is a semi-distributed, process-based hydrological water quality model that operates on a continuous daily time step. It simulates the hydrological processes, nutrient loss and sediment yield (Arnold, 1998). In the SWAT model, a watershed is divided into small sub-watersheds which are further subdivided into hydrologic response units (HRUs) based on unique land use, soil and topographic characteristics. The HRUs represent percentages of the sub-watershed area and are not spatially identified within a SWAT simulation (Gassman et al., 2007). The hydrological processes are simulated for each HRU, including canopy interception of precipitation, snowmelt, tile drainage, surface runoff, infiltration, redistribution of water within the soil profile, evapotranspiration, lateral subsurface flow and return flow from shallow aquifers. Once the loadings of water, sediment and nutrients from the land phase to the main channel have been determined, the loadings are routed through the streams and reservoirs within the watershed (Arnold et al., 2012).

INCA is a semi-distributed, process-based model that simulates the nitrogen cycle in both the land phase and riverine phase (Whitehead, Wilson and Butterfield, 1998). The model simulates the nitrogen export from different land-use types within a river system, and the in-stream nitrate and ammonium concentrations at a daily time step. INCA represents a catchment as a series of sub-catchments consisting of regular grids (Wade et al., 2002). INCA depends on external inputs, such as hydrologically effective rainfall (HER; the fraction of precipitation which contributes to runoff) and soil moisture deficits (SMD; the difference between the current depth of water and the water holding capacity), there are conceptual problems when water storage representation differ between INCA and external rainfall-runoff models used to estimate HER and SMD (Futter et al., 2014).

AnnAGNPS is a distributed parameter, continuous simulation watershed model (Bingner, Theurer and Yuan, 2003), based originally on the single event model, Agricultural Non-Point Source (AGNPS) (Young, 1989). It was developed by the USDA Agriculture Research Service and the USDA Natural Resources Conservation Service to evaluate non-point source pollution

from watersheds. The AnnAGNPS can simulate surface runoff, sediment and nutrients loading on a daily time step. It discretizes a watershed into homogenous, unique land management and soil cells. The hydrological processes considered within AnnAGNPS are similar to SWAT except the groundwater flow, the nutrient processes consider plant uptake, fertilization, residue decomposition, mineralization and transport in the soil while neglecting the in-stream processes (Abdelwahab et al., 2016; Parajuli et al., 2009).

HSPF is a process-based, continuous simulation watershed model that was jointly developed by the US Environmental Protection Agency and the US Geological Survey (Bicknell, 1997). It can be used to simulate nonpoint source runoff and pollutant loadings from upland areas in a watershed and performs flow and water quality routing in streams and well-mixed lakes and impoundments (B. Duda et al., 2012; Bicknell, 1997). Within HSPF, the watershed is divided into pervious and impervious areas, which are further grouped by land use and subbasin. For the pervious land area, the PERLND module estimates the water budget, snow and ice, sediment, solute transport, nitrogen and phosphorus cycles. For the impervious land area, the IMPLND module estimates fewer processes, including snow and ice, water budget and sediment. In-stream processes (routing, transformation) are estimated in the RCHRES module.

HYPE is a process-based, semi-distributed hydrological water quality model, which was developed by the Swedish Meteorological and Hydrological Institute based on the hydrological model HBV (Bergström, 1976; Lindstrom et al., 1997) and the water quality model HBV-NP(Andersson et al., 2005; Arheimer et al., 2005; Lindström, Rosberg and Arheimer, 2005). Within HYPE, the watershed is divided into small sub-watersheds which are further subdivided into land classes.

These models usually disaggregate a catchment into sub-catchments based on surface topography and further into homogenous classes (e.g., HRUs in SWAT and Soil and Land-use Classes in HYPE) within each sub-catchment based on land-use, soil type and topographic characteristics combinations. The classes are not coupled to geographic locations but define as a fraction of a sub-catchment area (Lindström et al., 2010). Consequently, spatial information on class locations is missing. Furthermore, terrestrial processes simulated in a class are aggregated and directly routed to the sub-catchment outlet. Therefore, interactions between neighboring classes are lost (Gassman et al., 2007; Rathjens et al., 2015). In addition, the river length in the sub-catchment is estimated as the total length of each sub-catchment and could not reflect the river network structure within the sub-catchment. Detailed spatial information, such as nutrient status (e.g., soil moisture concentration) and dynamics (e.g., leaching and percolation) in specific locations are missing (Rathjens et al., 2015). Recently, a new hydrological grid-based nitrate model (mHM-Nitrate) was developed by Yang et al. (2018) based on the advanced implementations of the mesoscale Hydrological Model (mHM) (Samaniego, Kumar and Attinger, 2010) and the HYPE model (Lindström et al., 2010). It can provide detailed spatial information on nitrate concentrations and fluxes, which offers promising opportunities for further evaluation of nutrient transport and removal processes spatiotemporally.

Table 1.1. Comparison of hydrological and water quality processes and fluxes representation of five widely used catchment water quality model.

Processes	SWAT	INCA	AGNPS/AnnAGNPS	HSPF	HYPE
Hydrology	surface runoff, lateral flow (return flow), groundwater flow	surface runoff, lateral flow (return flow), groundwater flow	surface runoff, lateral flow (return flow), flow through till drainage	surface runoff, lateral flow (return flow), groundwater flow	surface runoff, lateral flow (return flow), groundwater flow, flow through till drainage
Soil nitrogen pools	NO_3, NH_4, active (stable) organic N, plant residue	NO_3, NH_4, groundwater NO_3 (NH_4), organic N	active (stable) inorganic N, stable organic N	NO_3, solution (adsorbed) NH_4, plant N above/below ground, litter N, particulate (solution) labile organic N, particulate (solution) refractory organic N	active (stable) organic N, dissolved inorganic N, dissolved organic N
Soil nitrogen fluxes	plant uptake, denitrification, volatilization, nitrification, decay, residue mineralization	plant uptake, denitrification, nitrification, ammonia mineralization (decay), ammonia immobilization	plant uptake, denitrification, volatilization, nitrification, decay, residue mineralization, immobilization, leaching	plant uptake, denitrification, mineralization, immobilization, litterfall, plant N return, sorption	plant uptake, denitrification, degradation, mineralization, dissolution
In-stream processes	transport capacity, deposition, impoundments	deposition, entrainment	-	deposition, scour, adsorption, advection, decay processes	assimilatory uptake, denitrification

1.2.3. Hydrological water quality model calibration and uncertainty

Model calibration is a prerequisite to apply the catchment hydrological water quality model and to increase the reliability of the model in accurately representing the spatiotemporal variability of hydrological and biogeochemical processes at the catchment scale (White and Chaubey, 2005). Model calibration is a process optimizing the model parameters to match the model simulations with observations (Daggupati et al., 2015; Saraswat et al., 2015). The schematic representation of calibration is shown in Figure 2. The most common methods for

estimating parameter values are manual trial and error and automatic calibration. During manual calibration, parameter values were adjusted one by one based on expert knowledge of hydrological and water quality processes, which are subjective and labor intensive (Vrugt et al., 2003). Automatic calibration has become popular as computing efficiency increases as well as the development of optimization algorithms (Efstratiadis and Koutsoyiannis, 2010). As Gupta, Sorooshian and Yapo (1998) noted that automatic calibration involves a number of important components: (1) selecting appropriate calibration data, (2) defining an objective function that measures the difference between model predictions and the calibration data, and (3) selecting an optimization algorithm for optimizing the selected objective function.

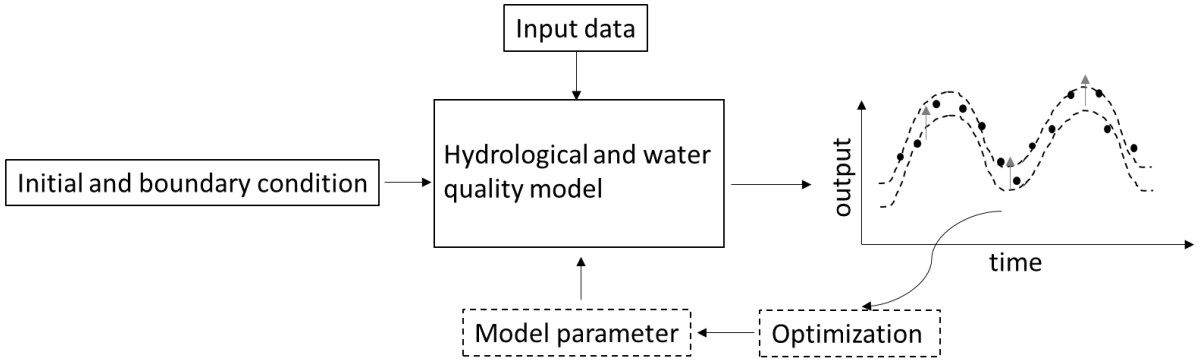

Figure 2. The schematic represent of model calibration (figure based on ideas from Vrugt et al. (2008)). Model parameters are adjusted to match the model simulation (represented by dashed lines) as close to observation (represented by dots) as possible.

Traditionally, only discharge observed at catchment outlet was used for calibration. However, the model simulated discharge integrated multiple processes of the catchment and the impacts of sub-catchment scale variability are averaged out. Therefore, model calibration becomes an ill-posed inverse or one-to-many mapping problem (Gupta, Sorooshian and Yapo, 1998; Jakeman and Hornberger, 1993). The ill-posed inverse problem may be resolved by (1) including additional observation data from internal stations (Her and Chaubey, 2015; Refsgaard, 1997; Wu et al., 2022a), (2) sensitivity analysis to select most sensitive parameters before calibration (Pianosi et al., 2016; Song et al., 2015; Yang, Jomaa and Rode, 2019), (3) relating model parameters to catchment characteristics to reduce the dimensionality of calibrated parameters by regionalization (Götzinger and Bárdossy, 2007; Pokhrel, Gupta and Wagener, 2008; Samaniego, Kumar and Attinger, 2010; Samaniego et al., 2017), (4) using multi-criteria and multi-objective stepwise or simultaneously calibration (Ahmadi et al., 2014; Arnold et al., 2012; Efstratiadis and Koutsoyiannis, 2010; Franco, Oliveira and Bonumá, 2020; Moriasi et al., 2012), (5) using multiple fluxes and states (e.g., soil moisture (Gavahi et al., 2020; Han, Merwade and Heathman, 2012; Rajib, Merwade and Yu, 2016), snow cover/depth (Duethmann et al., 2014; Finger et al., 2011; Parajka and Blöschl, 2008), groundwater level (Demirel et al., 2018; Refsgaard, 1997)) in addition to discharge to calibrate hydrological water quality models, (6) calibration against hydrologic signatures (Gupta, Wagener and Liu, 2008; McMillan, 2021).

Numerous studies reported that calibration of hydrological water quality models at multiple sites perform over single-site calibration (e.g., Ghaffar et al., 2021; Her and Chaubey, 2015; Jiang et al., 2015; Li, Weller and Jordan, 2010; Zhang, Srinivasan and Van Liew, 2008). For

example, Leta, van Griensven and Bauwens (2017) calibrated the SWAT model using single-site calibration at the catchment outlet, sequential calibration from upstream to downstream and simultaneous multi-site calibration. They found that the sequential calibration and the simultaneous multi-site calibration performed better than single-site calibration, and they recommend simultaneous multi-site calibration because several objective functions at multiple stations can be used simultaneously and calibration data information can be shared among stations simultaneously. Similarly, Ghaffar et al. (2021) compared single-site and multisite calibrate at the Selke catchment in central Germany based on the HYPE model. They found that multi-site calibration, as opposed to calibration solely at the catchment outlet, enhanced model performance of discharge, nitrate, and total phosphorus content at the calibration stations as well as at internal, non-calibrated stations. In contrast, several studies have reported that multi-site calibration did not improve or had almost the same model performance as single-site calibration (e.g., Franco, Oliveira and Bonumá, 2020; Lerat et al., 2012; Wang et al., 2012; Wu et al., 2022a). They explained the unimproved model performance with high degree of similarity between flow data used to evaluate the model performance (Lerat et al., 2012), errors on the boundary conditions and errors on the model representation of spatial varied hydro-geologic properties (Wang et al., 2012) and hydrologic processes (Wu et al., 2022a). Shrestha et al. (2016) found that the performance of the SWAT model for different variables differed between multi-site and single-site calibration. Model performance for discharge and total suspended sediment loadings did not improve with multi-site calibration compared to single-site calibration, while it improved for total nitrogen and total phosphorus loadings.

The selection of objective functions is crucial for automatic calibration (Muleta, 2012), because different objective functions highlight different aspects of the variable for calibration, such as the Nash Sutcliffe efficiency (NSE) which depends on the peaks (Krause, Boyle and Bäse, 2005), and percent bias (PBIAS) which depends on the relative deviation (Gupta, Sorooshian and Yapo, 1999; Moriasi et al., 2015). When using multiple variables (e.g., discharge and different nutrient fractions) and/or multi-site (Ahmadi et al., 2014; Zhang, Srinivasan and Van Liew, 2008), it becomes difficult to optimize the objective function. There are two main approaches of multi-objective optimization. First, the objective function can be aggregated to one objective function and then used to the single objective optimization algorithm (e.g., Shuffled Complex Evolution (SCE-UA) algorithm (Duan, Sorooshian and Gupta, 1992), Dynamically Dimensioned Search (DDS) (Tolson and Shoemaker, 2007)). This method has been criticized for using arbitrary weights (Efstratiadis and Koutsoyiannis, 2010). Nevertheless, the single-objective optimization method is easier to analyze statistically and computationally less intensive. A second method is to use multi-objective evolutionary algorithms to optimize the different objective functions at multiple sites simultaneously and find a set of multiple Pareto optimal solutions (Khu, Madsen and di Pierro, 2008; Zhang, Srinivasan and Van Liew, 2008).

Hydrological water quality models are mathematical representation of real systems. Generally, they are described based on incomplete scientific knowledge of the study catchment's hydrological and biogeochemical processes, thus they are inherent in simplifications and assumptions (Beven, 1993; Beven, 2007; Beven and Binley, 1992; Beven and Freer, 2001; Gupta, Beven and Wagener, 2005). Uncertainties in measurement of input data (e.g.,

precipitation and temperature) and output data (e.g., discharge and nitrate concentration data), model structure and parameters contribute to model simulation uncertainty (Vrugt et al., 2005; Wagener and Gupta, 2005), especially for spatially distributed hydrological water quality models which contain more parameters than lumped and semi-distributed hydrological water quality models. There also could be multiple parameters sets providing good model performance, resulted in equifinality of parameters (Beven, 1993; Beven, 2001; Beven and Freer, 2001). Several studies reported that hydrological water quality model calibration using multiple variables (such as nitrogen concentration, remotely satellite derived soil moisture, evapotranspiration, land surface temperature) in conjunction with discharge data could reduce model simulation uncertainty and increase reliability of model internal processes (Bergström, Lindström and Pettersson, 2002; Dembélé et al., 2020a; Dembélé et al., 2020b; Immerzeel and Droogers, 2008; Rajib et al., 2018; Stisen et al., 2018; Zhang et al., 2021).

Many uncertainty analysis frameworks have been introduced for hydrological models, such as the Generalized Likelihood Uncertainty Estimation (GLUE) methodology (Beven and Binley, 1992), Bayesian Recursive Estimation (BaRE) (Thiemann et al., 2001), the Shuffled Complex Evolution Metropolis algorithm (SCEM-UA) (Vrugt et al., 2003), the dynamic identifiability analysis framework (DYNIA) (Wagener et al., 2003), the Simultaneous Optimization and Data Assimilation (SODA) method (Vrugt et al., 2005), the Integrated Bayesian Uncertainty Estimator (IBUNE) (Ajami, Duan and Sorooshian, 2007), the DiffeRential Evolution Adaptive Metropolis algorithm (DREAM) (Vrugt et al., 2008), and the Integrated Parameter Estimation and Uncertainty Analysis Tool (IPEAT) (Yen et al., 2014). While considerable efforts have been made by the hydrological modelling community to develop uncertainty analysis techniques, they are rarely applied to distributed, process-based hydrological water quality models maybe due to the model's complexity (Wellen, Kamran-Disfani and Arhonditsis, 2015). Jiang et al. (2015) found that multi-site calibration can reduce model simulation uncertainty and improve model simulation on stream inorganic nitrogen concentration compared to single-site calibration only at catchment outlet based on the HYPE model combined with DREAM$_{(ZS)}$ in a nested catchment in Central Germany. In contrast, Her and Chaubey (2015) reported that calibration at three stations increased the uncertainty of SWAT model simulations on discharge substantially compared to single-site calibration only at the catchment outlet.

1.2.4. River restoration effects on stream nitrate retention

Over the past three decades, best agricultural and urban management practices have been implemented in the European Union to reduce nitrate loads to streams and rivers (European Commission, 1991a; European Commission, 1991b). In spite of this, around 60% of European surface water bodies do not meet good ecological standards, as reported by the European Environment Agency (2018). According to the European Water Framework Directive (WFD), river morphological alteration and diffuse pollution are the two dominant pressures on Europe's waters (Carvalho et al., 2019). To achieve a good ecological status targeted by the WFD, river restoration have been received increased attention in recent decades (Newcomer Johnson et al., 2016; Wohl, Lane and Wilcox, 2015).

The effects of stream restoration on nitrate retention have been studied through both empirical field-based measurements (Baker, Bledsoe and Price, 2012; Doyle, Stanley and Harbor, 2003;

Gucker and Boechat, 2004; Opdyke, David and Rhoads, 2006; Stanley and Doyle, 2002; Tatariw et al., 2013; Wollheim et al., 2001) and model simulations at reach scale (Alexander et al., 2009; Alexander, Smith and Schwarz, 2000; Wagenschein and Rode, 2008; Wollheim et al., 2006; Ye et al., 2012). The field-based measurements are mainly conducted using isotope tracer or nutrient addition experiments in separate stream reaches with distinct channel characteristics to calculate the nutrient spiraling metrics: uptake length (S_w), uptake rate coefficient (k), uptake velocity (V_f), uptake rate (U). Then these metrics are related to geomorphologic parameters to analyze the relationship between channel characteristics and nutrient retention (net uptake or denitrification). For instance, Doyle, Stanley and Harbor (2003) studied the relative influences of biochemical uptake processes and dynamic hydrology and geomorphology (hydrogeomorphology) on molybdate reactive phosphorus (MRP) retention within a stream. They surveyed channel cross sections before and following dam removal to quantify changing channel form and used paired upstream and downstream measurements of MRP concentration to compute three retention metrics: uptake rate, mass transfer coefficient and uptake length. They found that hydrogeomorphology can control nutrient retention on the reach scale only when hydrogeomorphic variation is greater than uptake rate variability. Gucker and Boechat (2004) evaluated ammonium retention in headwater streams by combining a one-dimensional transport model (OTIS) with the nutrient spiraling concept. They found that channel morphology determined stream transient storage zone sizes and residence times, which in turn, is a strong determinant of ammonium retention potential. Opdyke, David and Rhoads (2006) studied the influence of in-stream geomorphologic characteristics (riffle, point bar, cut-bank pool, run, or separation zone) variability on sediment denitrification in agricultural streams. Sediment denitrification was measured at two paired channelized and meandering stream reaches in the headwaters of the Embarras River basin in east-central Illinois, between June 2003 and February 2005 using the chloramphenicol-amended acetylene inhibition procedure. They found that differences in benthic organic matter and the percentage of fine-grained sediments in the streambeds controlled much of the spatial variations in sediment denitrification among the geomorphological features. Bukaveckas (2007) found that stream restoration through re-meandering and installing pool-riffle sequences in a channelized stream reduced downstream transport of nutrients (nitrate and phosphorus) due to decreased flow velocity in the restored channel than the channelized one. It was found that in-stream uptake rate coefficient (k) was 30-fold higher in the restored channel than in its pre-restoration channel, while change of uptake velocity (V_f) was relatively small (Bukaveckas, 2007).

However, there are few limitations of the field experiment studies: (1) differences between sites or reaches are unlikely to be limited to channel morphology alone (Doyle, Stanley and Harbor, 2003). For instance, other factors such as water temperature, ambient water chemistry and community composition varying from site to site, may cause significant among sites difference in nutrient dynamics independent of effects of channel morphology, (2) the spiraling metrics derived from nutrient addition experiments could not differentiate the nitrate retention processes (e.g., assimilatory uptake and denitrification), which need combined with other methods such as isotope tracer addition (Mulholland et al., 2009) and N2:Ar method (Groffman et al., 2006) (3) these experimental studies mainly are limited to small streams and in short

term period (low flow period). This leads to considerable uncertainties which are particularly related to estimates of reaction rates covering the total variability of flows and site characteristics. In particular, the lack of substantial continuous nitrogen removal data for larger rivers results in significant uncertainties in network-scale total nitrogen loss estimates (Tank et al., 2008; Wollheim et al., 2017; Ye et al., 2017).

Recently developed in situ high frequency, high-resolution nitrate sensors provide the opportunities to measure in-stream nitrate assimilatory uptake rate at high temporal frequencies (Hensley and Cohen, 2020; Hensley, Cohen and Korhnak, 2014; Kunz et al., 2017c; Rode et al., 2016b), which allow inferring uptake rates scale across river size. For example, Kunz et al. (2017c) combined two stations' high-frequency time series and longitudinal profiling of nitrate concentration to assess differences in nitrogen processing dynamics in a natural versus a channelized impounded reach in a fourth order river, Germany. They found that net mass removal rates of nitrate were markedly higher in the unmodified reach and seasonal variations in temperature and insolation affected the relative contribution of assimilatory versus dissimilatory uptake processes. Nitrate retention in river networks results from complex interactions of hydrological, geomorphological and biogeochemical processes (Ensign and Doyle, 2006; Ye et al., 2012). Hydrological processes influence nutrient retention by affecting the interaction between available nutrients and biogeochemical active sites (Hall, Bernhardt and Likens, 2002). On the other side, river morphology can directly affect nutrient retention through physical processes (e.g., water velocity, water residence time) in a river (Bukaveckas, 2007; Doyle, Stanley and Harbor, 2003), river morphology can also affect nutrient retention indirectly by creating spatiotemporal variability of aquatic communities (e.g., macrophytes and phytoplankton) and their associated biological processes (Lin et al., 2016). The fully distributed hydrological water quality model (mHM-Nitrate) provides the ability to scale up the in-stream nitrate retention rate from field measurements to river network scale and to distinguish the effects of stream restoration via stream morphological changes from hydrological processes on stream nitrate retention at river network scale.

1.3. Knowledge gaps

Distributed hydrological water quality models are needed for water quality management in order to provide detailed spatial information to identify key nonpoint source pollution source areas and implement agricultural mitigating measures at the field scale. Some grid-based water quality models have been developed, such as grid-based structure of AGNPS (Liu et al., 2008), grid version of SWAT model (Rathjens and Oppelt, 2012; Rathjens et al., 2015), integration of grid-based Water Flow and Balance Simulation Model (WaSiM-ETH) and AGNPS (Rode and Lindenschmidt, 2001). A common issue with these models is an imbalance between spatial representation and model complexity that leads to high computational demand. The recently developed fully distributed mHM-Nitrate model can balance the model complexity and representation of nitrate transport and in-stream retention processes (Yang et al., 2018). However, the mHM-Nitrate model has been not tested in large heterogenous mesoscale catchment.

According to literature review, the model performance was affected by using different calibration stations (single-site vs multi-site). However, previous studies based on semi-

distributed hydrological water quality models, the effects of calibration stations on the spatial and spatiotemporal transferability of distributed hydrological water quality parameters is unclear.

Droughts occurred more frequently in recent decades and are projected to be more serve in future, it is crucial to identify the mechanisms that underlie water-quality trends under drought conditions to ensure future water quality and develop effective management strategies. Although there were some studies found that droughts can have spatiotemporally varying impacts on nitrate transport and transformation processes, these studies are just based on data-driven and statistical analysis. No study has examined the mechanisms underlying how sequential drought affects the nitrate concentration.

As review in section 1.2.4, although numerous studies have investigated the impact of stream restoration on nitrate retention, these studies were only at reach scale. Systemic investigation of the effects of stream restoration (i.e., re-meandering) on stream nitrate retention at the river network scale is still missing.

1.4. Objectives

Based on the above mentioned problem statement and literature review, three objectives were defined to address the knowledge gap in understanding nitrate dynamics and the effects of drought and stream restoration on nitrate retention.

The first objective was to evaluate the effect of calibration schemes on the spatiotemporal performance of the mHM-Nitrate model using different calibration schemes and a large number of nitrate sampling locations (Chapter 2);

The second objective was to investigate the effect of sequential drought on stream nitrate dynamics in the Bode catchment using the mHM-Nitrate model (Chapter 3);

The third objective was to investigate the effect of stream restoration (i.e., re-meandering) on stream nitrate retention at the river network scale based on the well calibrated mHM-Nitrate model in the Bode catchment (Chapter 4).

Chapter 2: Improving the calibration of a fully distributed hydrological water quality model

Salman Ghaffar[a]*, Xiangqian Zhou[a]*, Seifeddine Jomaa[a], Xiaoqiang Yang[a,b], Michael Rode[a,c]

[a]Department of Aquatic Ecosystem Analysis and Management, Helmholtz Centre for Environmental Research – UFZ, Magdeburg, Germany

[b]Yangtze Institute for Conservation and Development, Hohai University, Nanjing 210098, China

[c]Institute of Environmental Science and Geography, University of Potsdam, Potsdam-Golm, Germany

*Corresponding authors: Salman Ghaffar (salman.ghaffar@ufz.de), Xiangqian Zhou (xiangqian.zhou@ufz.de)

2.1. Abstract

Distributed hydrological water quality models are increasingly being used to manage natural resources at the catchment scale. While the models must be properly calibrated to ensure spatial and temporal reliability, there are no guidelines for selecting the most useful gauging stations. We investigated the influence of calibration schemes on the spatiotemporal performance of a fully distributed process-based hydrological water quality model (mHM-Nitrate). More specifically, we examined how calibration schemes affected simulations of discharge (Q) and nitrate (NO_3^-) concentrations for the heterogeneous Bode catchment in central Germany. Accounting for land use, stream order, and mean NO_3^- concentrations, we designed three calibration schemes that varied in spatial coverage but that used data from the same time period (2011–2019): scheme 1 used data from the catchment outlet station; scheme 2 used data from the catchment outlet station and two upstream stations found in sub-catchments dominated by forests and farmland, respectively; and scheme 3 used data from the catchment outlet station and seven upstream stations varying in land use and size. Model performance was validated using Q and NO_3^- observations from the 8 gauging stations (2015–2019) and NO_3^- observations from 94 spatially distributed sampling locations (1994–2019).

For Q, model performance was similar among the three schemes (NSE—scheme 1: 0.92, scheme 2: 0.88, and scheme 3: 0.90). For NO_3^- concentrations, performance was better with scheme 2 than with schemes 1 and 3 when simulated values were compared to observed values from the eight gauging stations. Similarly, scheme 2 did better than scheme 1 at replicating NO_3^- concentrations at the spatially distributed sampling locations (PBIAS values < 15.0%: 34 vs. 9 locations, respectively), while schemes 2 and 3 yielded similar results. This finding may be attributable to the fact that scheme 2 incorporated a broader range of data, including low Q values and NO_3^- concentrations, and thus provided a better representation of within-catchment diversity. As a consequence, hydrological and water quality parameters were better constrained, which resulted in improved simulations at upstream stations in forested areas and at the spatially distributed sampling locations. Conversely, even though scheme 3 included data from five more gauging stations than did scheme 2, there were no further improvements in

catchment representation. Moreover, simulated NO_3^- concentrations were more accurate when the model used scheme 2 versus scheme 3, as seen in the narrower 95% uncertainty boundaries for scheme 2. Thus, adding observations that contained similar information on catchment characteristics did not seem to improve model performance; instead, it appeared to increase levels of uncertainty. Our results suggest that, to optimize parameter calibration, it is necessary to strategically select gauging stations that reflect the full range of within-catchment heterogeneity rather than simply seeking to maximize station number.

Keywords:

Multi-site calibration, Spatiotemporal validation, Hydrological water quality model, Uncertainty, Parameter transferability

Highlights:

- Single- and multi-site calibration approaches generally led to similar model performance for discharge (Q) at the catchment outlet.
- For accurate simulation of Q and nitrate throughout the watershed, single-site calibration only at the catchment outlet is not sufficient.
- The quality of the nitrate model simulation depends less on the number of calibration stations than on their representativeness of the catchment characteristics.

2.2. Introduction

Distributed hydrological water quality models provide crucial support for water management decisions. The models include many parameters that represent spatial variability in hydrological and biogeochemical processes at the catchment scale that cannot be measured directly in the field (Li, Weller and Jordan, 2010). Thus, parameters must be calibrated to optimize model performance (Engel et al., 2007; Moriasi et al., 2012; Saraswat et al., 2015).

Most commonly, hydrological water quality models are calibrated using measurements made at the catchment outlet and may thus poorly simulate dynamics at sites within catchments, given spatial variability in conditions (Cao et al., 2006; Refsgaard et al., 2016; Refsgaard, Stisen and Koch, 2022). As spatially structured discharge and water quality data become increasingly available, researchers are calling for multi-objective calibration strategies that allow for the inclusion of multiple sites, variables, and criteria (Daggupati et al., 2015; Efstratiadis and Koutsoyiannis, 2010; Khu, Madsen and di Pierro, 2008).

However, to date, findings are mixed regarding the performance of single- versus multi-site calibration techniques. Many studies have found that, for catchment outlets, multi-site calibration yields more accurate results than does single-site calibration (e.g., Ghaffar et al., 2021; Her and Chaubey, 2015; Jiang et al., 2015; Zhang, Srinivasan and Van Liew, 2008). For example, Shrestha et al. (2016) found such to be the case for a SWAT model (Arnold et al., 2012; Arnold et al., 1998) simulating total nitrogen (TN) and total phosphorus (TP) loads. Ghaffar et al. (2021) reported the same for a HYPE model (Lindström et al., 2010) seeking to replicate nitrate (NO_3^-) and TP concentrations across a suite of monitoring stations in central Germany's Selke catchment.

In contrast, several other studies have found that performance was largely equivalent for multi-site and single-site calibration techniques (e.g., Franco, Oliveira and Bonumá, 2020; Lerat et al., 2012; Wu et al., 2022a). They explained the unimproved model performance with high degree of similarity between flow data used to evaluate the model performance (Lerat et al., 2012), errors in boundary conditions as well as in representations of spatially structured hydrogeological properties (Wang et al., 2012) and hydrological processes (Wu et al., 2022a). However, it is important to note that previous studies have largely utilized semi-distributed hydrological and water quality models (e.g., SWAT: (Leta, Griensven and Bauwens, 2017; Zhang, Srinivasan and Van Liew, 2008) and HYPE: (Ghaffar et al., 2021; Jiang et al., 2015) and that station choice has frequently been driven by availability. Guidance is lacking when it comes to selecting the most useful gauging stations when calibrating fully distributed hydrological water quality models.

Compared to their lumped and semi-distributed counterparts, fully distributed hydrological water quality models incorporate detailed spatial information for sites within catchments while also including a broader range of parameters (Khu, Madsen and di Pierro, 2008; Refsgaard, 1997). The applicability of parameters across spatial and temporal scales (i.e., parameter transferability) presents a major challenge for the construction of distributed hydrological water quality models (Beven, 2001; Samaniego, Kumar and Attinger, 2010). Parameters defined using information from calibration locations can be applied to other locations using a process

called regionalization, as per Bloschl and Sivapalan (1995). Regionalization can be based on spatial proximity (Oudin et al., 2008a; Parajka, Merz and Bloschl, 2005), similarity in climatic and catchment characteristics (Beck et al., 2016; Merz and Blöschl, 2004; Oudin et al., 2008b; Parajka, Merz and Bloschl, 2005), and non-linear transfer functions that relate the parameters to catchment characteristics (e.g., land use, soil type, and geological type) (Hundecha and Bárdossy, 2004; Pokhrel, Gupta and Wagener, 2008; Wagener and Wheater, 2006). Samaniego, Kumar and Attinger (2010) specifically developed a multi-scale parameter regionalization (MPR) method, whose appeal stems from the fact that only the coefficients in the transfer functions (i.e., the global parameters) need calibration, and not the parameters for each grid, substantially reducing the dimensionality of the calibrated parameters (Parajka et al., 2013; Singh, Archfield and Wagener, 2014). When model parameters are tied to catchment characteristics, calibration data drawn from diverse gauging stations are assumed to better represent within-catchment heterogeneity and to enhance model performance at spatial scales. However, little is known about the impact of different calibration schemes on the spatial and temporal performance of fully distributed hydrological water quality models.

Hydrological water quality models are typically developed using current knowledge about the physical and chemical processes taking place in the focal catchment, an endeavor that inherently involves simplifications and assumptions (Beven, 2007; Gupta, Beven and Wagener, 2005). Uncertainty in model simulations is rooted in uncertainty from the measurement data, used as input and for calibration, as well as from model structure and parameterization (Vrugt et al., 2005; Wagener and Gupta, 2005). Such is especially true for spatially distributed hydrological water quality models, which contain more parameters than those of a lumped or semi-distributed model. While the hydrological modelling community has spent considerable time and effort designing uncertainty analysis techniques, the latter are rarely applied to distributed process-based hydrological water quality models, perhaps due to model complexity (Wellen, Kamran-Disfani and Arhonditsis, 2015). In addition, contrasting estimates of model simulation uncertainty have been obtained with single- versus multi-site calibration techniques. Jiang et al. (2015) found that, compared to single-site calibration, multi-site calibration reduced the uncertainty around estimates of Q and NO_3^- concentrations in the HYPE model. In contrast, Her and Chaubey (2015) found the opposite effect for Q estimates from a SWAT model: better performance was obtained using single-site than multi-site calibration. Finally, Shrestha et al. (2016) reported mixed results: for a SWAT model, single-site calibration resulted in less uncertainty for simulated Q values, while multi-site calibration accomplished the same for simulated TN and TP loading values. Thus, there is a pressing need to explore the impact of multi-calibration techniques on the uncertainty associated with fully distributed models.

Recently, Yang et al. (2018) developed a fully distributed hydrological water quality model (mHM-Nitrate) that is based on both the mesoscale hydrological model (mHM) (Samaniego, Kumar and Attinger, 2010) and the HYPE model (Lindström et al., 2010). The mHM-Nitrate model appears to successfully handle different catchment characteristics (Wu et al., 2022b; Yang et al., 2019), but it is unknown how well it deals with parameter transferability across space. Our study's overarching aim was to evaluate the effects of different calibration schemes on the spatiotemporal performance of the mHM-Nitrate model. The specific objectives were

as follows: (i) to evaluate and compare three calibration schemes that differed in gauging station number and representation of within-catchment diversity (e.g., land use and stream order); (ii) to assess parameter transferability across space under the three calibration schemes using NO_3^- data from a large number of sampling locations; and (iii) to examine the effects of the three calibration schemes on the degree of uncertainty associated with simulated NO_3^- concentrations. Ideally, the study's results should help guide the choice of effective calibration schemes, depending on the availability of Q and water quality data.

2.3. Study area and methods

2.3.1. Study area

The Bode catchment has a area of 3,200 km^2 and is located in central Germany (Figure 2.1). It is part of the Harz/Central German Lowland Observatory, within the broader TERENO Earth observation network focused on integrated, multi-scale monitoring and intensive research (Wollschläger et al., 2016). There is dramatic spatial heterogeneity across the catchment, which extends from the Harz Mountains in the southwest to the lowlands of central Germany in the northeast. There is also a marked elevational gradient, ranging from 1,142 m above sea level (a.s.l.) at Brocken, the highest peak in the Harz Mountains, to 70 m a.s.l. in the central lowlands. These extremes are reflected in dramatic differences in mean annual precipitation at these two locations, equal to 1,500 mm and 500 mm, respectively (climatic data: 1990–2019). In the mountains, mean monthly temperature ranges from -0.4℃ in January to 16.6℃; for the lowlands, these figures are 1.3℃ and 18.9℃, respectively. In the mountains, land surfaces are dominated by forests, with some pastures (10%), agricultural fields (8%), and urban areas and lakes (7%). In the lowlands, land surfaces are largely dedicated to cultivating crops (81%), primarily winter wheat, winter barley, rapeseed, and sugar beet. There is much less representation of other land use categories: forests (7%), pastures (3%), and urban areas and small lakes (9%) (Figure 1a). The predominant soil types in the mountains and lowlands are cambisols and chernozems, respectively.

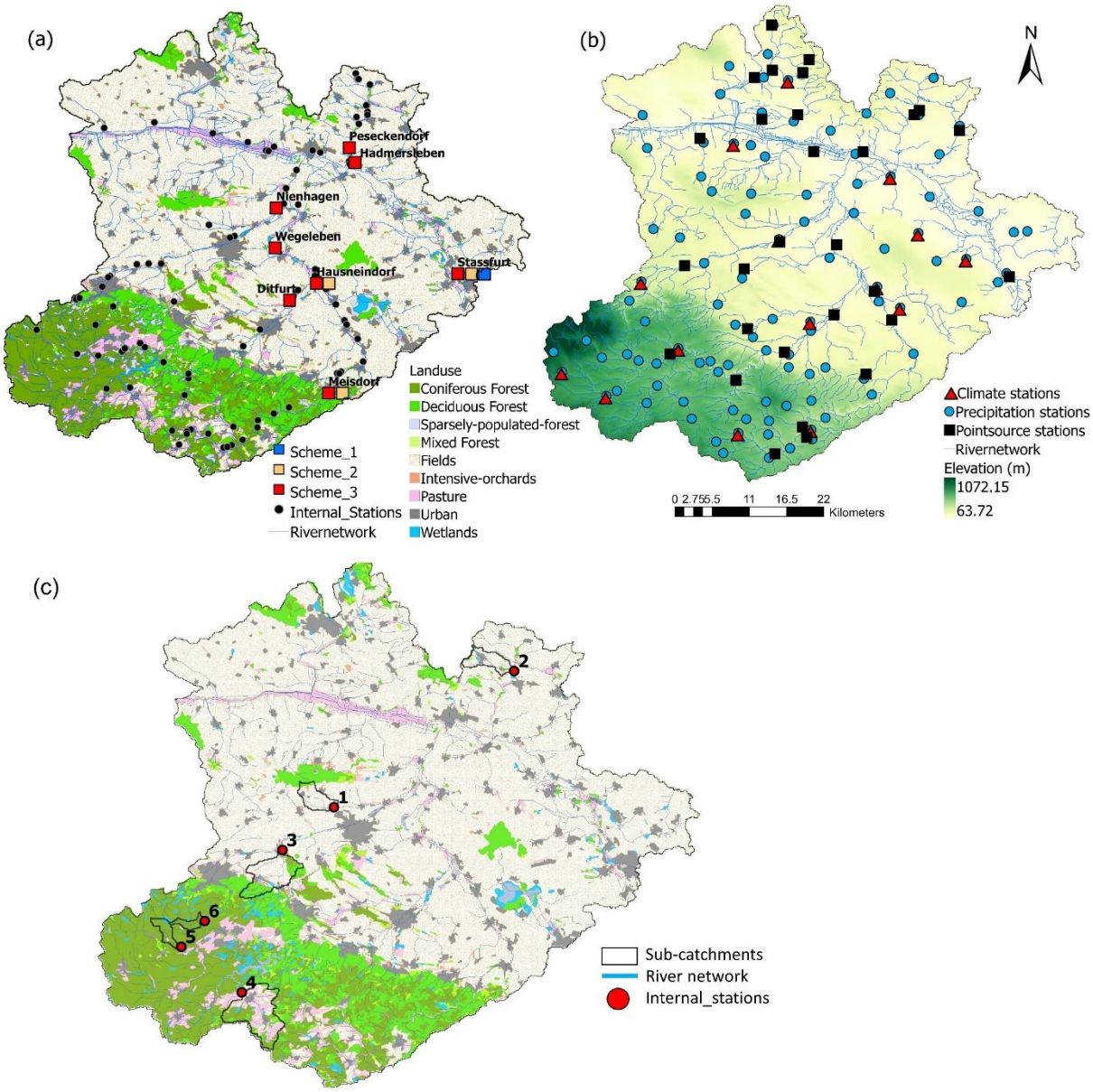

Figure 2.1. Maps of the Bode catchment showing (a) land use, the gauging stations, and the spatially distributed sampling locations as well as (b) elevation and the meteorological stations and (c) location of 6 internal stations presented in section 3.2.

We gathered observations of daily precipitation, daily temperature (maximum, mean, and minimum), and potential evapotranspiration to use as model input. These measurements spanned the period between 1993–2019 and were provided by the German Weather Service (DWD); they came from 78 rain gauges and 13 climate stations within the study area. To create the meteorological forcing dataset for the model, the daily precipitation and temperature data were spatially interpolated to 1 km × 1 km grid data using the External Drift Kriging method. This interpolation approach uses elevation, an external variable, to predict orographic effects on precipitation and temperature (Hundecha and Bárdossy, 2004). The daily potential evapotranspiration values were calculated using the Hargreaves and Samani (1985) method and interpolated at the same scale of spatial resolution.

To set up the mHM-Nitrate model, several sources of geographical data were used. Elevation measurements (spatial resolution: 90 m × 90 m) were obtained from the Shuttle Radar Topography Mission (SRTM) (Jarvis, 2008). The digitized geological map and the soil map (scale: 1:1,000,000) were provided by the German Federal Institute for Geosciences and Natural Resources (BGR) (https://produktcenter.bgr.de; last accessed 1 June 2020). The land cover data came from CORINE Land Cover 2012, which contains information on land cover/land use in the year 2012 (https://gdz.bkg.bund.de/index.php/default/open-data.html; last accessed 1 June 2020). These datasets were resampled to generate model input (spatial resolution: 100 m × 100 m).

For model calibration and validation, we used measurements of Q and NO_3^- concentrations from eight gauging stations. Daily measurements of Q at these stations were provided by the State Agency for Flood Protection and Water Management of Saxony-Anhalt (LHW) (http://gldweb.dhi-wasy.com/gld-portal/; last accessed 10 April 2020). High-frequency (15 minutes) NO_3^- concentrations for four stations (Meisdorf, Hausneindorf, Hadmersleben, and Stassfurt) between 2010 and 2019 were obtained from the Helmholtz Center for Environmental Research—UFZ; we aggregated these high-frequency measurements to daily values. For the other four stations (Ditfurt, Wegeleben, Nienhagen, and Peseckendorf), the NO_3^- data were low-frequency measurements collected every two weeks to every two months from 1994 to 2019 by LHW (http://gldweb.dhi-wasy.com/gld-portal/; last accessed 10 April 2020). Finally, we also gathered low-frequency NO_3^- measurements from 94 sampling locations to spatially validate the mHM-Nitrate model. The catchment characteristics at these sites are described in the Supplementary Materials (Table S2.1).

2.3.2. mHM-Nitrate model

The mHM-Nitrate model is a grid-based catchment nitrate model that balances process complexity and model representation (Yang et al., 2018). Hydrological processes in the model includes the following: canopy interception, snow accumulation and melt, evapotranspiration, infiltration, soil moisture dynamics, runoff generation, percolation and flood routing along the river network. Nitrate-process descriptions come mainly from the HYPE model (Lindström et al., 2010), with additional considerations of nitrate retention in deep groundwater, spatially distributed crop rotations and time-varying point-source inputs. Nitrate processes are fully integrated into the hydrological cycling. Major N inputs include wet atmospheric deposition via precipitation, fertiliser and manure application and plant/crop residues. In each soil layer, four N pools are defined (i.e., active solid organic N, inactive solid organic N, dissolved organic N and dissolved inorganic N), along with soil N processes of denitrification, plant/crop uptake and transformations among the four N pools. In-stream N transformations include denitrification, primary production and mineralization. More detailed descriptions of the mHM-Nitrate model can be found in Yang et al. (2018), and source code can be found in Yang and Rode (2020).

2.3.3. Model setup

The mHM-Nitrate model was setup at a daily time step from 1993-2019 based on the available hydrometeorological and geographical data (Table 2.1). The model was calibrated and

validated for the period of 2010-2014 and 2015-2019 respectively. Using 94 water quality sampling locations with low frequency data, an extensive spatial-temporal validation of the mHM-Nitrate model was performed under three different calibration schemes. The frequency of the water quality data for water quality sampling locations is given in Table S2.1 in Supplement material. To exclude the effect of reservoir on the discharge, the observed daily discharge and NO_3^- concentration at the gauging station (Thale) were used as input data.

Table 2.1. Description of spatio-temporal input data for the mHM-Nitrate model setup in the Bode catchment.

Data type	Data description/properties	Resolution	Source
Geographical data	Elevation	100 m	State Survey Office
	Stream network	-	State Survey Office
	Soil type	100 m	State Survey Office
	Land use	100 m	Corrine Land Cover 2012
Meteorological data	Daily precipitation and mean air temperature	1 km	German Weather Service-DWD
Agricultural practices	Manure and inorganic fertiliser application, timing and amount for fertilisation, sowing and harvesting	Land use dependent	Field survey and literature
Soil nitrogen content	Initial nitrogen storage		Literature review
Sewage treatment plants	N load	Daily time step	Operating reports of sewage treatment plants

2.3.4. Calibration schemes

The parameters of the mHM-nitrate model were related to catchment characteristics. Based on catchment characteristics, land use, mean NO_3^- concentration, and stream order, three calibration schemes were designed. In scheme. Scheme 1 used only data from the catchment outlet station (Stassfurt). Scheme 2 used data from Stassfurt and two gauging stations upstream (Meisdorf and Hausneindorf) (Table 2.1 and Figure 2.2). Scheme 3 used data from Stassfurt and seven gauging stations upstream (Figures 2.1a and 2.2).

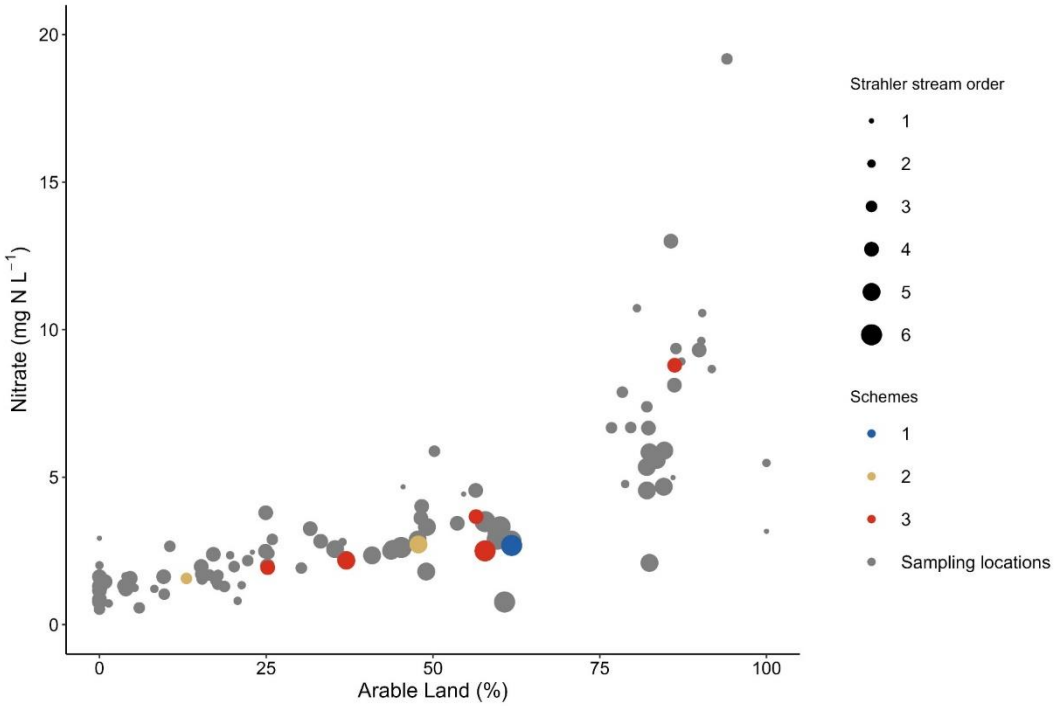

Figure 2.2. Relationship between nitrate concentration and share of arable land use with information on stream order of the sub-catchments represented by the eight gauging stations and the 94 spatially distributed sampling locations. Station inclusion within the calibration schemes is indicated (with higher-level schemes including the stations found in lower-level schemes).

The eight gauging stations used in scheme 3 reflect different combinations of land use and meteorological conditions found in the Bode catchment (Table 2). Compared to scheme 2, scheme 3 includes data from five additional gauging stations that are associated with larger streams (stream order: 4–6) (Krabbenhoft et al., 2022). There are four main gauging stations along the Bode River: Ditfurt (upstream), Wegeleben (intermediate stream), Hadmersleben (downstream), and Stassfurt (catchment outlet). Ditfurt and Wegeleben are in a forest-dominated subcatchment, while Hadmersleben and Stassfurt locate in an area dominated by farmlands. The headwaters of the Selke and Holtemme Rivers are located in the mountains, a region with extensive forests (71.9%) and low NO_3^- concentrations. In contrast, the lowlands are covered by agricultural fields, and NO_3^- concentrations are high. The Meisdorf station is located in the mountainous Upper Selke, while the Hausneindorf station is the Selke's outlet, an area with a mixture of forests and farms. The Nienhagen station is the Holtemme outlet, whose upstream and downstream areas are dominated by forest and agricultural surfaces (Ehrhardt et al., 2019), respectively. At Nienhagen, Q values are heavily affected by the presence of weirs (Kunz et al., 2017b). The Peseckendorf station is the outlet of the Geesgraben stream, which merges into the Bode after Hadmersleben; the surrounding area is predominantly covered by crops (88.8%).

Table 2. Subcatchment characteristics for the eight gauging stations. Abbreviations: Subcatch = subcatchment; Precip = precipitation; Q = discharge; and NO_3^- = nitrate concentration range (mean).

Station	Subcatch	Area (km^2)	Elevation (m)	Precip (mm y^{-1})	% Forest	% Farm land	Stream order	Q (mm y^{-1})	NO_3^- (mg N L^{-1})
Meisdorf	Selke	180	199–597	690	73.1	12.8	3	186	0.01–5.14 (1.57)

Hausneind.	Selke	458	106–597	590	37.8	48.5	5	99	0.44–8.55 (2.73)
Ditfurt	Bode	714	107–1072	783	56.4	25.3	4	211	1.30–2.90 (1.93)
Wegeleben	Bode	1230	94–1072	698	46.9	36.9	5	166	1.10–4.75 (2.24)
Nienhagen	Holtemme	260	94–931	678	31.6	54.2	4	162	1.22–10.4 (4.59)
Peseckend.	Geesgraben	137	76–200	546	3.0	88.8	4	58	0.77–17.0 (8.80)
Hadmersl.	Bode	2620	76–1072	639	29.2	56.6	6	132	0.47–11.0 (2.51)
Stassfurt	Bode	3179	66–1072	617	24.7	61.6	6	114	0.46–8.10 (2.68)

2.3.5. Model calibration and validation

Parameter sensitivity analysis was performed using the Morris method (Morris, 1991). We calculated the elementary effect (EE) of each parameter using the Sensitivity Analysis For Everybody toolbox (SAFE; Pianosi, Sarrazin and Wagener, 2015). We identified the eight most sensitive hydrological parameters and the six most sensitive water quality parameters (Table S2.2) based on the ranked values of the sensitivity indices (absolute mean and standard deviation of EE). This suite of parameters was then used in mHM-Nitrate model calibration. A more detailed description of the parameter sensitivity analysis is available in Zhou et al. (2022).

Instead of using an optimization algorithm, like a dynamically dimensioned search (DDS) (Tolson and Shoemaker, 2007), we opted for a sequential multi-criteria method (Wu et al., 2021) to filter out sets of behavioral parameters for each calibration scheme. This process involved two steps. During the first step, 300,000 parameter sets were created for the eight sensitive hydrological parameters. Next, the best 100 parameter sets were selected for each calibration scheme, a decision guided by the ranks of both the Nash-Sutcliffe coefficient (NSE) and percent bias (PBIAS) values for Q at the relevant gauging stations. During the second step, 300,000 parameter sets were generated for the six sensitive water quality parameters, which were combined with the 100 best Q parameter sets. For each calibration scheme, we selected the best 100 parameter sets from this second step based on the ranks of the NSE and PBIAS values for Q and NO_3^- concentrations for the relevant gauging stations. The preliminary calibration results revealed that 300,000 iterations allowed the objective function values to converge upon minimum values. This procedure made it possible to compare the three calibration schemes, as this allows each calibration scheme to achieve its own best performance from the same parameter space.

Following the split-sample test, this calibration procedure was applied to the mHM-Nitrate model incorporating Q and NO_3^- concentrations from 2011 to 2014. Each calibration scheme was validated (time period: 2015–2019) at all eight gauging stations for both Q and NO_3^- concentrations (Table 2.3). NSE and PBIAS were used as performance evaluation criteria. However, it is difficult to draw conclusions about the relative performance of calibration schemes when sample size is small. Therefore, we carried out spatiotemporal validation of the model using NO_3^- data from the 94 spatially distributed sampling locations (i.e., low-frequency

measurements for 1994–2019). In this case, only PBIAS was used to evaluate model performance, which is satisfactory when values are less than 35%, according to Moriasi et al. (2015).

2.3.6. The value of added calibration stations on parameter distributions and model performance

To assess the value of additional calibration stations on the identification of the model, the cumulative parameter distributions were computed for all calibration schemes utilizing the top 100 model runs from the second calibration phase of calibration schemes. To the extent that additional calibration stations change the cumulative distribution function of the individual model parameters due to model calibration, the cumulative distribution function of the realized performance measure of the 100 model runs of the different calibration schemes should also change (Nijzink et al., 2018). Significant differences in these cumulative distribution functions can be tested statistically and should allow an assessment of the added value of a modified data set introduced by additional calibration stations for model identification. In this study, we determined the statistical significance of the differences in these cumulative distribution functions between calibration schemes using the two-sample Kolmogorov-Smirnov (Conover, 1999) test (D):

$$D = max|F(\theta_i) - G(\theta_i)| \quad (1)$$

where $F(\theta_i)$ and $G(\theta_i)$ are the empirical cumulative distribution functions of the parameter θ_i for calibration scheme 1(2) and 2(3). The null hypothesis is that the two samples are from the same continuous distribution. If D is closer to zero, it indicates that the probability of the two samples being drawn from the same population is higher. Moreover, the two-sample Kolmogorov-Smirnov test generates a p-value that corresponds to the calculated D statistic. A higher p-value (> 0.05) provides stronger support for the null hypothesis. The relative occurrences of certain, significant, KS statistics can be inspected by means of cumulative frequency plots.

2.3.7. Uncertainty analysis

To compare model uncertainty among the three calibration schemes, 95% uncertainty boundaries were calculated based on the 2.5th and 97.5th percentiles of the cumulative distributions for the best 100 model runs from the second calibration step. The R-factor quantifies differences between observed and simulated data and is calculated by dividing the average distance between the upper and lower 95% uncertainty boundaries by the standard deviation of the observed data (Abbaspour et al., 2007). The R-factor expresses the width of the 95% uncertainty and a value less than 1 is being desirable. The uncertainty analysis was performed for both Q and NO_3^- concentrations at all the gauging stations included in schemes 2 and 3. We compared model uncertainty for schemes 2 and 3 by comparing results for the stations shared by the schemes (Stassfurt, Hausneindorf, and Meisdorf).

2.4. Results

The mHM-Nitrate model was calibrated under three calibration schemes for discharge and NO_3^- parameters. The calibrated parameters are presented in Table S2.1 (Supplementary material) with their description, physical meanings, initial and optimized values.

2.4.1. Model performance at gauging stations

The model performance of discharge (Q) for at the catchment outlet (Stassfurt station) was similar across the three calibration schemes (NSE—scheme 1: 0.82, scheme 2: 0.87, and scheme 3: 0.88; PBIAS—scheme 1: 0.30%, scheme 2: 0.0%, and scheme 3: -8.60%; Table 2.4). During the calibration period, at the Meisdorf and Hausneindorf stations, performance was lower for scheme 3 than for scheme 2 (NSE—scheme 2: 0.58 to 0.69 vs. scheme 3: 0.53 to 0.66; PBIAS—scheme 2: -7.80% to -23.5% vs. scheme 3: -20.2% to -32.0%). During the validation period, water balance was well captured across all the calibration schemes and gauging stations, with the exception of Nienhagen (PBIAS—scheme 1: -3.7% to 7.1%, scheme 2: -7.7% to 2.6%, and scheme 3: -12.7% to 1.4%). Performance was lowest at the Peseckendorf and Nienhagen stations across the three schemes, albeit lower for scheme 1 than for schemes 2 and 3 (NSE—scheme 1: -0.34 to 0.13 vs. scheme 2: 0.17 to 0.29 and scheme 3: 0.36 to 0.45; Table 2.4). It was also better at the Stassfurt, Meisdorf, and Hausneindorf stations during the validation period than during the calibration period across all calibration schemes (NSE—lower ranges: 0.53–0.88 and upper ranges: 0.71–0.92).

Model performance of NO_3^- concentration at the catchment outlet Stassfurt station decreased from Scheme 1 to 2 and 3 during the calibration period (NSE—scheme 1: 0.67, scheme 2: 0.64, and scheme 3: 0.62; PBIAS—scheme 1: 0.40%, scheme 2: -6.90%, and scheme 3: 7.10%). Also, during the calibration period, model performance at the Meisdorf station was better at scheme 2 (PBIAS: -2.60%) than scheme 3 (PBIAS: -23.2%). At Hausneindorf, scheme 3 yielded better performance than did scheme 2 (PBIAS: -7.90% vs. 1.20%, respectively). During the validation period, performance was better at scheme 2 than at scheme 1 for all the gauging stations except for Nienhagen station, with PBIAS values in ranges —scheme 2: 1.8–33.9% and scheme 1: -10.1–23.3%, respectively. While NO_3^- concentration model performance decreased from Scheme 2 to 3 at all gauging stations except Nienhagen station, with larger absolute PBAIS values in Scheme 3 than Scheme 2.

Table 2.4. Model performance of discharge and NO_3^- concentration at gauging stations under Scheme 1, Scheme 2 and Scheme 3.

Schemes	Stations	Discharge				NO_3^-			
		Calibration		Validation		Calibration		Validation	
		NSE	PBIAS (%)	NSE	PBIAS (%)	NSE	PBIAS (%)	NSE	PBIAS (%)
Scheme 1	Stassfurt	0.82	0.30	0.92	4.20	0.67	0.40	0.33	12.5
	Meisdorf	-	-	0.71	7.10	-	-	0.32	33.9
	Hausneindorf	-	-	0.77	0.70	-	-	-0.08	8.10

	Wegeleben	-	-	0.92	-3.70	-	-	-1.19	16.4
	Hadmersleben	-	-	0.93	2.90	-	-	0.01	20.9
	Peseckendorf	-	-	-0.34	-3.50	-	-	-3.84	23.0
	Ditfurt	-	-	0.97	-0.20	-	-	-4.36	8.80
	Nienhagen	-	-	0.13	44.7	-	-	-0.66	1.80
Scheme2	Stassfurt	0.87	0.00	0.88	0.60	0.64	-6.90	0.23	9.30
	Meisdorf	0.58	-23.5	0.72	-1.70	0.66	-2.60	0.67	-10.1
	Hausneindorf	0.69	-7.80	0.76	-3.00	0.27	-7.90	0.31	-4.00
	Wegeleben	-	-	0.92	-3.10	-	-	-0.14	4.00
	Hadmersleben	-	-	0.92	2.60	-	-	0.26	14.3
	Peseckendorf	-	-	0.17	-7.70	-	-	-2.72	23.3
	Ditfurt	-	-	0.96	2.20	-	-	-2.18	1.60
	Nienhagen	-	-	0.29	38.8	-	-	-0.17	-9.10
Scheme 3	Stassfurt	0.88	-8.60	0.90	1.40	0.62	7.10	-0.33	16.8
	Meisdorf	0.53	-32.0	0.71	-12.0	0.53	-23.2	0.71	-14.0
	Hausneindorf	0.66	-20.2	0.73	-12.7	0.31	1.20	0.20	-7.80
	Wegeleben	0.87	-12.6	0.92	-5.60	0.37	-9.50	-1.39	11.0
	Hadmersleben	0.87	-9.10	0.92	-0.90	0.21	14.0	-0.49	23.8
	Peseckendorf	0.56	-21.6	0.45	-9.80	-0.44	-15.6	-1.70	24.7
	Ditfurt	0.94	-3.40	0.96	1.00	0.35	-9.80	-3.56	9.20
	Nienhagen	0.68	6.00	0.36	29.9	0.59	-14.2	0.39	-3.20

The seasonal dynamics of Q were captured by scheme 2 at its three gauging stations during both the calibration and validation periods as well as during low- and high-flow conditions (Figures 2.3a, 2.3c, and 2.3e). The same was true for the seasonal dynamics of NO_3^- concentrations (i.e., high values during high-flow periods and low values during low-flow periods; Figures 2.3b, 2.3d, and 2.3f). In addition, over the period from 2011 to 2019, NO_3^- concentrations followed a constant seasonal pattern at the Meisdorf station (Figure 2.3b) but tended to decline at the Hausneindorf and Stassfurt stations (Figures 2.3d and 2.3f), which were well captured by the model. Model performance for NO_3^- concentrations was greatest at the Meisdorf station (NSE—calibration: 0.66 and validation: 0.67; Table 2.4). It was lowest at the Hausneindorf station (NSE—calibration: 0.27 and validation: 0.31; Table 2.4). At Stassfurt, Meisdorf, and Hausneindorf, model performance for NO_3^- concentrations were satisfactory (PBIAS ranged between -7.9% and 9.3% during calibration and validation).

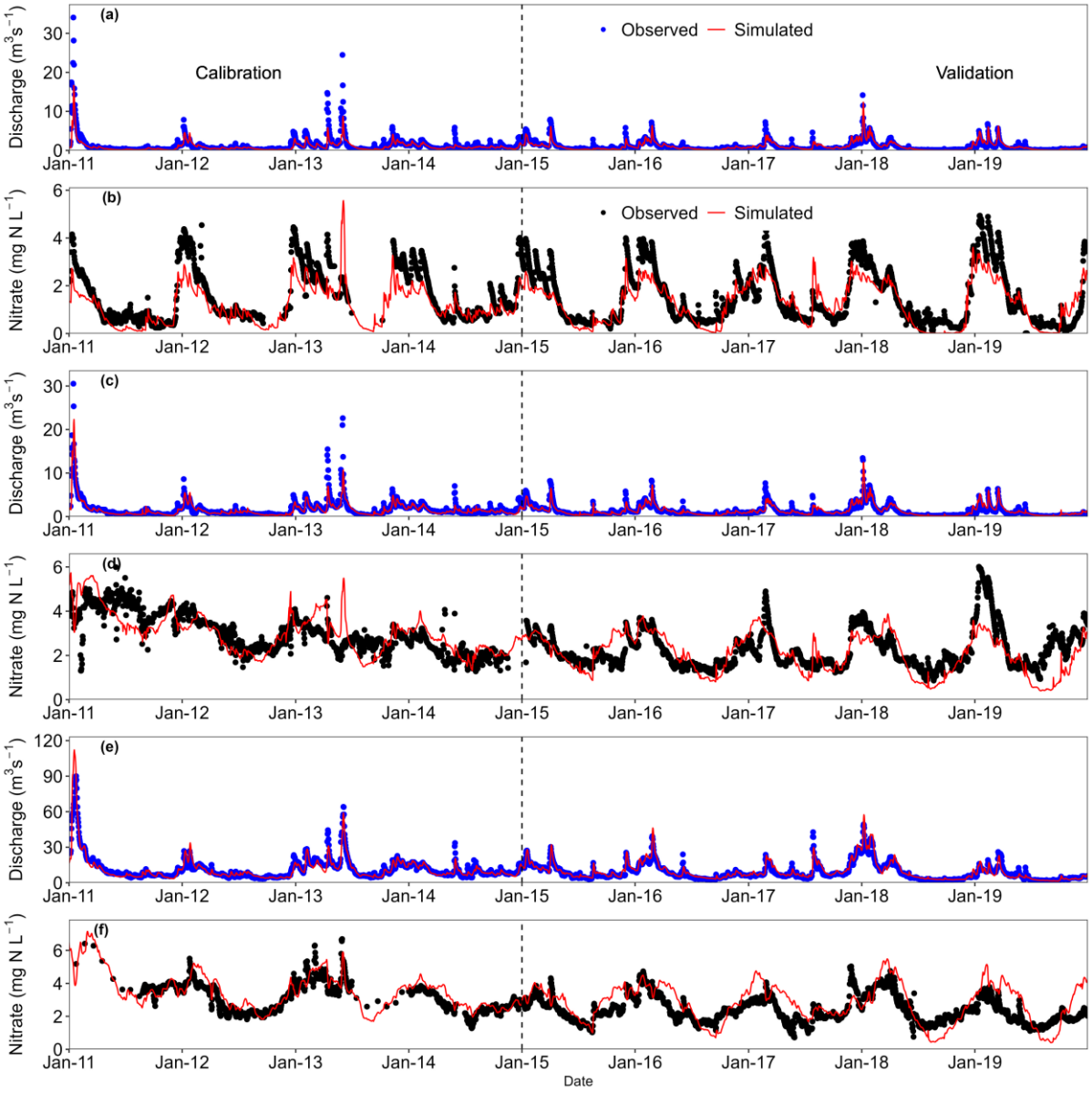

Figure 2.3. Model simulated and observed discharge and $\mathbf{NO_3^-}$ concentration at (a-b) Meisdorf, (c-d) Hausneindorf and (e-f) Stassfurt stations at Scheme 2.

2.4.2. Model performance at water quality sampling locations

We further tested how the calibration schemes affected model performance using NO_3^- data from the 94 spatially distributed sampling locations. Performance was generally better for scheme 2 than for scheme 1 (PBIAS $\leq$ 15.0%: 34 vs. 9 sampling stations, respectively, and PBIAS > 45%: 12 vs. 65 sampling stations, respectively) (Table 2.5). Performance was similar for schemes 2 and 3 (PBIAS $\leq$ 15.0%: 34 vs. 35 sampling locations, respectively).

Table 2.5. Number of water quality sampling locations under different PBIAS ranges for three calibration schemes.

PBIAS (%)	Scheme 1	Scheme 2	Scheme 3
0.00 – 15.0	9	34	35
15.1 – 25.0	9	19	16

25.1 – 35.0	8	17	20
35.1 – 45.0	3	12	10
> 45.1	65	12	13

We also examined how catchment characteristics might influence model performance by looking at the spatial distributions of the PBIAS values for all 94 sampling locations across the three calibration schemes (Figure 2.4). The model performance for NO_3^- concentration at each stream order and land use (farmland vs. forest) are shown in Figure S2.1. Overall, more locations showed a good level of performance (PBIAS $\leq$ 15.0%) at scheme 2 versus scheme 1; no such difference was seen between schemes 2 and 3. More specifically, performance was better at scheme 2 than scheme 1 in areas dominated by farmlands for all stream orders (Figure S2.1). Additionally, performance was better for scheme 3 than scheme 2 except in the case of stream orders 2 and 4 in agricultural areas and stream order 5 in forested areas (Figure S2.1). With schemes 2 and 3, a few stations had high PBIAS values (> 45.0%; 12 and 13 stations, respectively). For forested areas, scheme 2 led to much better performance than did scheme 1 but was not significantly better than scheme 3.

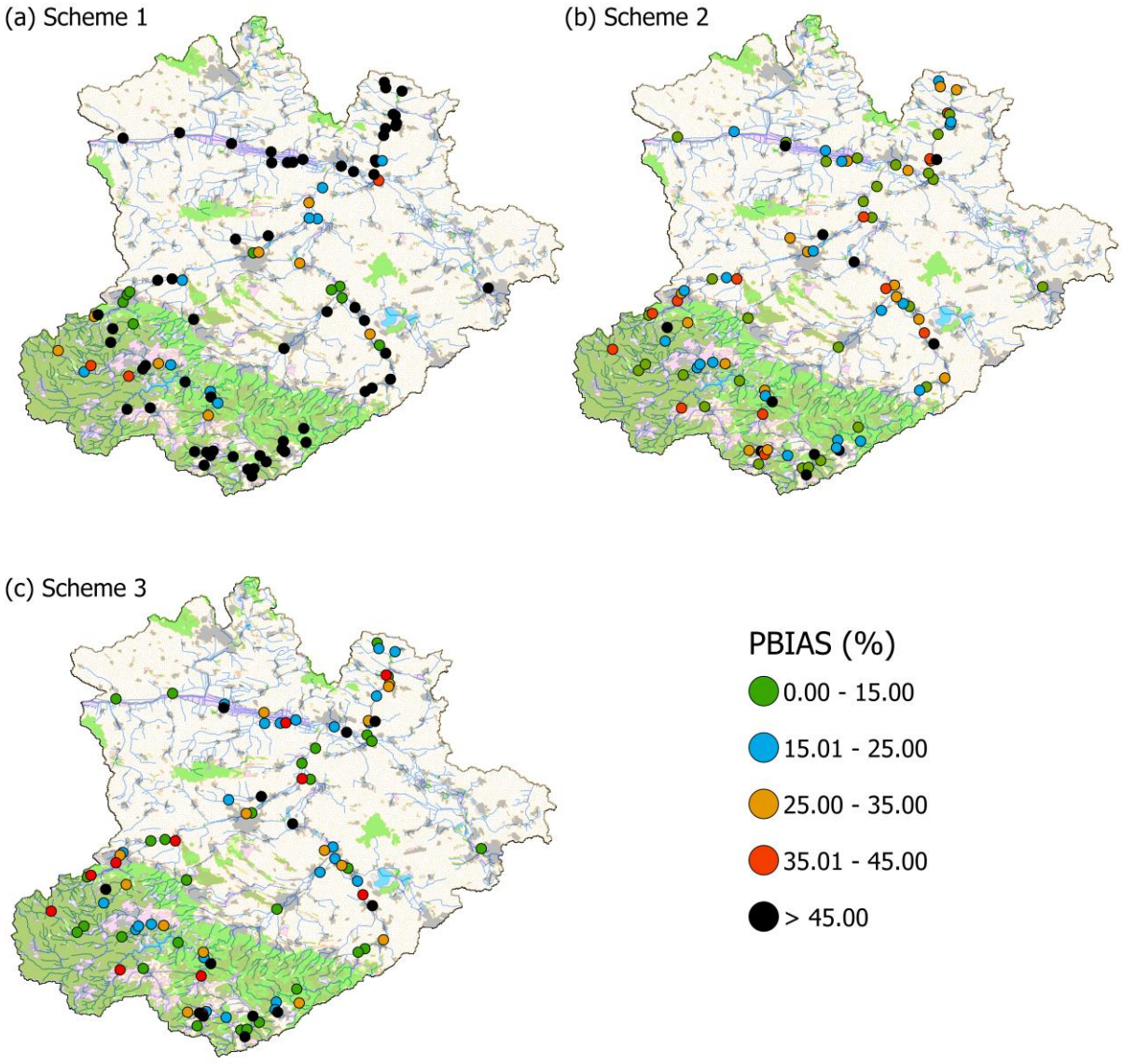

Figure 2.4. Spatial evaluation of mHM-Nitrate model performance on $\mathbf{NO_3^-}$ concentration for all water quality sampling locations under three calibration schemes.

We used the optimized parameter sets for scheme 2 to explore model performance in greater detail at six spatially distributed sampling locations that displayed distinct characteristics (map: Figure 2.1c; observed and simulated NO_3^- concentrations: Figure 2.6; PBIAS: Table 2.6). There was variation in the duration and frequency of the validation data for the six sampling locations. Seasonal patterns of NO_3^- concentrations were well captured by the model over different levels of NO_3^- (Figure 2.5), with PBIAS values ranging from -17.1% to 14.5% (Table 2.6). This result indicates that the mHM-Nitrate model was capable of representing NO_3^- dynamics within different subcatchments when scheme 2 was applied. The largest difference between mean observed and simulated NO_3^- concentrations occurred at NO_3^- sampling location 2 (Figure 2.5c) with PBIAS value of -17.1%, which represents an arable dominated sub-catchment. The best fit between mean observed and simulated NO_3^- concentration was found at NO_3^- sampling location 4 (Figure 2.5d; PBIAS = -9.3%), which is found in a mountainous sub-catchment that contains a mixture of farmland and pasture (Figure 2.1c).

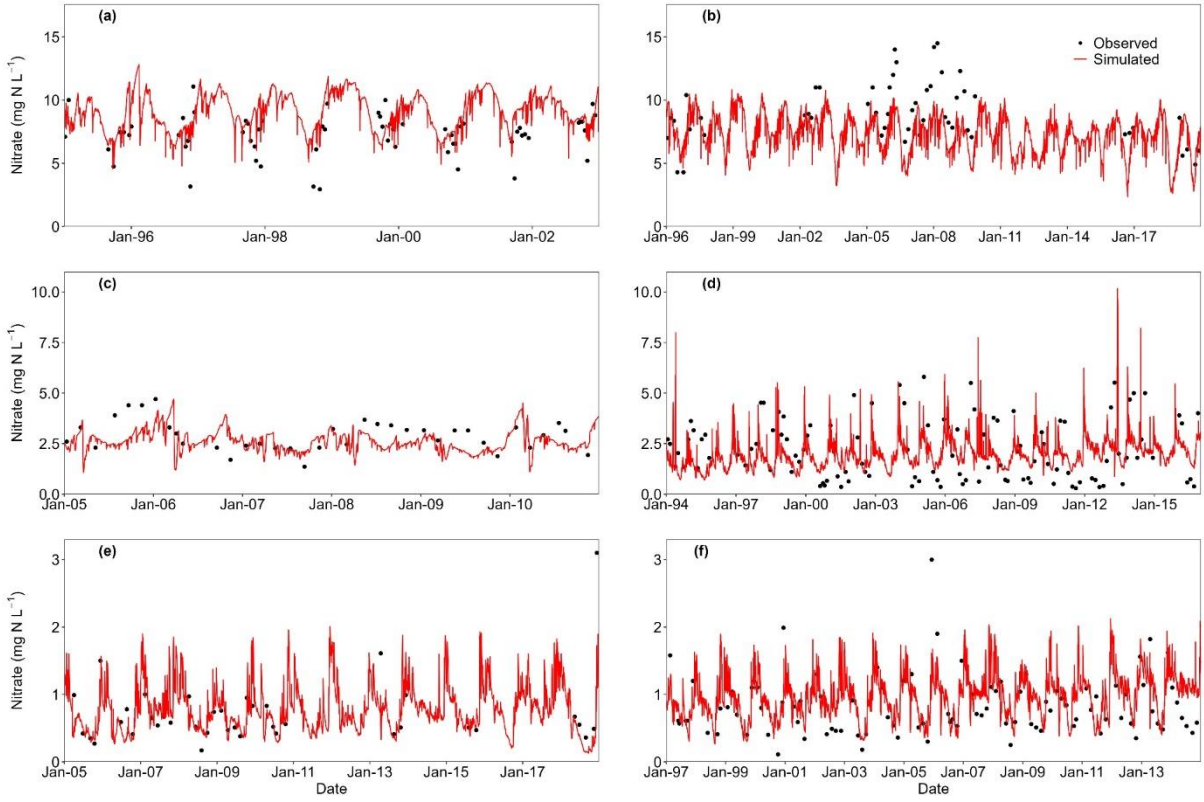

Figure 2.5. Observed and simulated nitrate (NO_3^-) concentrations (calibration scheme 2) for the six sampling locations displaying distinct characteristics.

Table 2.6. Summary of catchment characteristics represented by the six sampling locations, model performance for nitrate (NO_3^-) concentrations (PBIAS values), minimum and maximum values of simulated and observed NO_3^- concentrations at the sampling locations, and range (mean) of NO_3^- concentrations.

Sampling location	Sub-catchment area (km2)	Dominant land use	PBIAS (%)	Simulated NO_3^- concentration (mg N L^{-1})	Observed NO_3^- concentration (mg N L^{-1})
1	11.8	Arable (87.2%)	12.8	4.6-12.9 (9.1)	2.9-11.1 (7.4)
2	12.6	Arable (78.3%)	-17.1	2.4-10.8 (7.4)	4.3-14.5 (8.9)
3	26.4	Arable (53.6%) Forest (40.1%)	-12.6	1.1-4.7 (2.6)	1.4-4.7 (2.9)
4	37.1	Arable (22.2%) Pasture (29.0%)	-9.3	0.8-10.2 (2.0)	0.3-5.8 (2.2)
5	6.1	Forest (96.0%)	-11.7	0.1-2.0 (0.7)	0.2-3.1 (0.7)
6	3.9	Forest (100%)	14.5	0.3-2.1 (1.0)	0.1-3.0 (0.8)

2.4.3. Model parameter distributions

For the three calibration schemes, we constructed cumulative distribution functions for the most sensitive hydrological and water quality parameters using the best 100 model runs (Figure 2.6). From the results, it is clear that the hydrological parameters—infiltration shape factor (infil) and potential evapotranspiration (pet) differ significantly between schemes 1 and 2 as well as between schemes 2 and 3 ($p < 0.01$) (Figure 2.6 and Table 2.7). In the mHM-Nitrate

model, soil infiltration is parameterized using the power function of soil saturation, whose exponent is determined by the infiltration shape factor (infil). Cuntz et al. (2015) reported that, as a parameter, infil is highly related to soil saturation, where higher infiltration occurs in mountain soils than in lowland soils. Because the Meisdorf station was included in scheme 2, a greater range of soil types were represented, allowing infil to be better defined. In contrast, scheme 1 averaged all the soil types present in the catchment, as reflected by the narrower ranges of infil for scheme 2 versus 1 (Figure 2.6). The cumulative distributions of four water quality parameters, namely in-stream denitrification rate (denitri), primary production rate (pprt), primary production coefficient in non-agriculture stream (pprt_na), and primary production coefficient in agriculture stream (pprt_agri), showed dissimilarities between scheme 1 and schemes 2 and 3. However, there were no differences in the cumulative parameter distributions between scheme 2 and scheme 3 ($p > 0.05$) (Figure 2.6 and Table 2.7). The four water quality parameters were better constrained for scheme 2 than scheme 1, as reflected by their narrower ranges in the former versus the latter (Figure 2.6). Yang, Jomaa and Rode (2019) found the control factors for denitri and pprt varied between the Meisdorf and Hausneindorf stations. At Meisdorf, both parameters have a strong correlation with stream discharge and benthic area, while at Hausneindorf they are highly correlated with terrestrial flows and fluxes. In summary, parameter distributions were dramatically affected by the increase in station number between scheme 1 and scheme 2. In contrast, the additional stations added in scheme 3 had little to no effect.

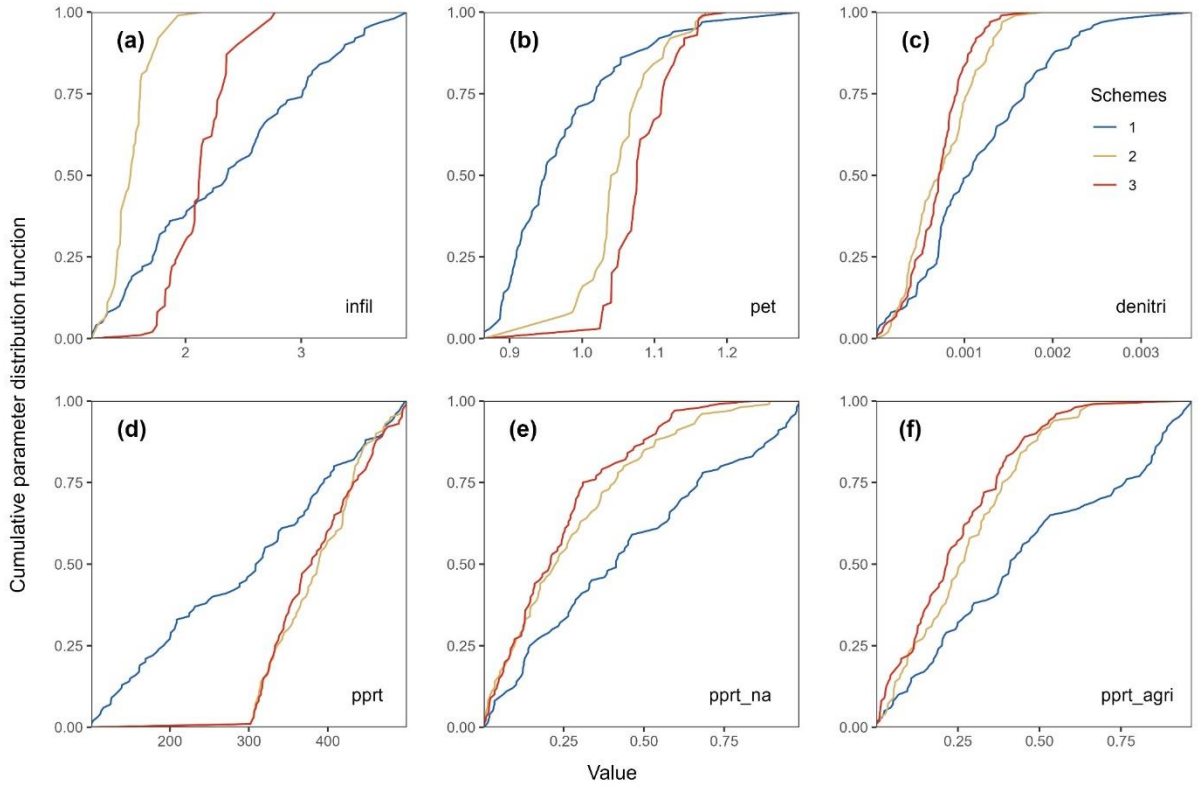

Figure 2.6. Cumulative distributions for the hydrological parameters infil (a) and pet (b) and four the water quality parameters, in-stream denitrification rate (denitri) (c), primary production rate (pprt) (d), primary production coefficient in non-agriculture stream (pprt_na) (e), and primary production coefficient in agriculture stream (pprt_agri) (f) across the three calibration schemes.

2.4.4. Uncertainty analysis of NO_3^- concentration

We calculated the 95% uncertainty boundaries for simulated daily NO_3^- concentrations at the Meisdorf, Hausneindorf, and Stassfurt stations for schemes 2 and 3 (Figure 2.7). The associated R-factors are given in Table 2.8. The 95% uncertainty boundaries for simulated daily Q associated with schemes 2 and 3 are available in the Supplementary Materials (Figure S2.3). Whether under low- or high-flow conditions, 95% uncertainty boundaries for daily NO_3^- concentrations were narrower for scheme 2 than for scheme 3 (Figure 2.7). For instance, they were nearly twice as wide for scheme 3 than scheme 2 at Hausneindorf (R-factor = 4.13 vs. 2.18, respectively) and Stassfurt (R-factor = 4.52 vs. 2.79, respectively) (Table 2.8). Furthermore, over 60% of the observed NO_3^- concentrations lay within the 95% uncertainty boundaries for scheme 2. When scheme 2 was used, the Meisdorf station, located in a forested subcatchment, displayed lower levels of uncertainty than did the Hausneindorf and Stassfurt stations, which are found in a subcatchment dominated by farmland. The same was also true for scheme 3. This finding was reflected in the narrower 95% uncertainty boundaries for Meisdorf versus Hausneindorf and Stassfurt (Figures 2.7a-b vs. 2.7c-f), as well as in the lower R-factor values for Meisdorf (scheme 2 = 0.92; scheme 3 = 1.08; Table 2.8).

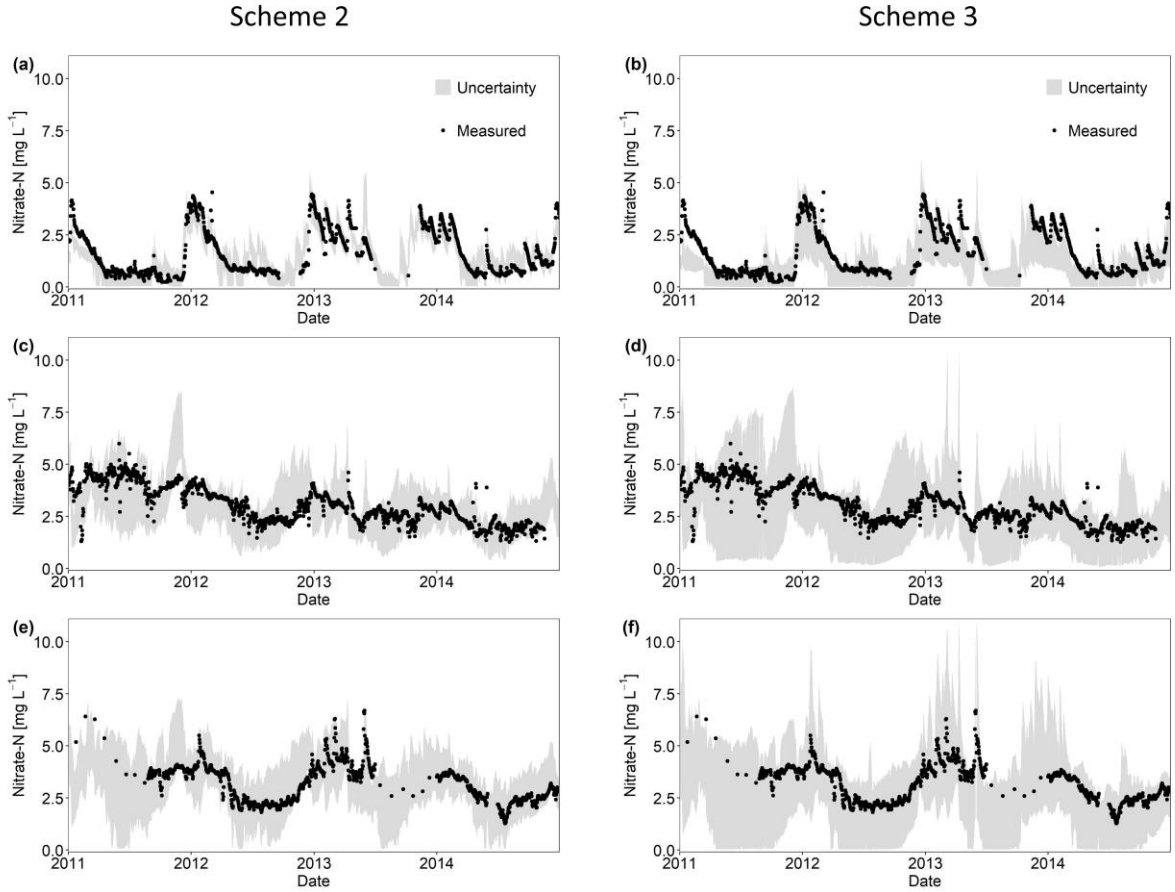

Figure 2.7. Comparison of 95% uncertainty boundaries for the simulated nitrate ($\mathbf{NO_3^-}$) concentrations obtained with schemes 2 and 3 for three gauging stations: Meisdorf (a-b), Hausneindorf (c-d), and Stassfurt (e-f).

Table 2.8. R-factor values for nitrate ($\mathbf{NO_3^-}$) concentrations at three gauging stations for schemes 2 and 3.

Stations	Criterion	Scheme 2	Scheme 3
Meisdorf	R-factor	0.92	1.08
Hausneindorf	R-factor	2.18	4.13

Stassfurt	R-factor	2.79	4.52

2.5. Discussion

2.5.1. Evaluation of model performance at calibration schemes

We evaluated the ability of the mHM-Nitrate model to simulate discharge and nitrate concentrations at eight gauging stations. We specifically examined the transferability of hydrological and water quality parameters at spatial scales.

2.5.1.1. Model performance for discharge under three calibration schemes

During model validation, simulated discharge at the catchment outlet was similar whether the calibration data came from a single site (scheme 1: catchment outlet station) or multiple sites (scheme 2: 3 stations and scheme 3: 8 stations) (Table 2.4). This result suggests that, for discharge, the number of stations used during calibration did not affect model performance at the catchment outlet. Our finding is consistent with those of Chiang et al. (2014); Wang et al. (2012); Wu et al. (2022a).

That said, performance was better with scheme 2 than scheme 1 when discharge was simulated for all eight gauging stations, except in the case of Hausneindorf (Table 2.4). This result could have arisen because multi-site calibration better constrains model parameters by including information on catchment characteristics (e.g., land use and soil types) at upstream stations (here, Meisdorf and Hausneindorf); these characteristics are frequently heterogeneous in space and shape hydrological parameters (e.g., infil and pet, Figures 2.6a and 2.6b). Jiang et al. (2015) reported that, compared to single-site calibration, multi-site calibration may better capture dynamics in large, diverse catchments because it accounts for the effects of different hydrological processes (e.g., slow groundwater dynamics and quick interflows). For example, in the Bode catchment, interflow is the primary form of runoff in mountainous areas (Jiang et al., 2014), while the share of groundwater increases from the mountains to the lowlands (Zhou et al., 2022).

In contrast, model performance was similar for schemes 2 and 3 (NSE values for the eight gauging stations; Table 2.4), which suggests that adding more sites does not always improve simulations for upstream stations. This finding is consistent with those of previous studies (Her and Chaubey (2015); Wang et al. (2012); Xie et al. (2021)) and could potentially be explained by station choice and the failure of scheme 3 to introduce any new catchment characteristics. As a result, schemes 2 and 3 displayed similar cumulative distributions for their hydrological parameters (Figures 2.6a-b). Therefore, during calibration, it may be challenging to optimize model parameters by relying on station number only.

2.5.1.2. Model performance for NO_3^- concentration under three calibration schemes

Simulated nitrate concentrations were significantly better for all gauging stations (with the exception of Nienhagen) when scheme 2 versus scheme 1 was used (Table 2.4). This improvement may be attributed to the inclusion of Meisdorf in scheme 2. The station is found in a forested subcatchment, which likely led to changes in the values of land-use-dependent parameters (e.g., pprt_na, pprt_agri; Figures 6e and 6f). These parameters were optimized in

scheme 2 and, additionally, improved model performance at non-calibrated stations, such as Wegeleben and Ditfurt. Both stations are located in subcatchments with intermediate levels of forest cover (> 30% and > 56.4%, respectively). Similarly, the inclusion of Hausneindorf in scheme 2 improved model performance at Hadmersleben, which had not been part of the calibration process, because the two stations occur in regions with similar levels of farmlands (Table 2.2). This finding indicates that utilizing multi-site calibration schemes that capture diverse catchment characteristics can improve simulated nitrate concentrations even at locations that were not included in the calibration process. This result concurs with those of previous studies (Chiang et al., 2014; Jiang et al., 2015; Shrestha et al., 2016), which found that such improvements result from the fact that multi-site calibration schemes can account for dramatic variability in observed nitrate concentrations and hydrological regimes across catchments. These schemes can thus better constrain parameters associated with nitrate transport and transformation.

In contrast, model performance was slightly lower at all stations (except Nienhagen) for scheme 3 than scheme 2 (PBIAS values; Table 2.4), which suggests that adding more gauging stations to the calibration process cannot, by itself, result in further improvements to simulations of nitrate concentrations. This finding may have two explanations. First, the five additional gauging stations (Wegeleben, Hadmersleben, Peseckendorf, Ditfurt, and Nienhagen) included in scheme 3 did not introduce additional diversity in catchment characteristics, which was the case when Meisdorf and Hausneindorf were included in scheme 2 (Figure 2.2). For instance, except for Peseckendorf, four of the five additional stations have farmland surface areas and mean nitrate concentrations that are similar to that of Hausneindorf, which led to similar model parameter distributions for schemes 2 and 3 (Figures 2.6c-f). Second, three of the five additional stations have low-frequency measurements of nitrate concentrations (i.e., once or twice per month). Jiang et al. (2019) found that, when the HYPE model was applied to the Selke catchment, performance was better when calibration used nitrate concentrations that were collected daily versus every two weeks. The slight decline in performance from scheme 2 to scheme 3 could be affected by the model's attempt to satisfyingly balance the large number of additional observations resulting from site addition (Jiang et al., 2015). In other words, multi-site calibration approaches try to identify the parameter set that represents the best compromise given the presence of multiple subcatchments, which is a more intensive task than simply focusing on a single catchment outlet.

2.5.1.3. Comparison of hydrological and water quality model performance

In brief, the model's accuracy for predicting both discharge and NO_3^- concentration improved when using Scheme 2 compared to Scheme 1. However, while the model's accuracy for discharge remained consistent between Scheme 2 and 3, its accuracy for nitrate decreased in Scheme 3. On one hand, hydrology is a physical process that is well understood and can be easily quantified through measurements and modeling. On the other hand, nitrate dynamics are much more complex and can be influenced by a variety of specific factors that are unique to a particular location, such as the amount of fertilizer applied and the level of moisture in the soil. Nitrogen fertilizer application rates are often uncertain and can vary depending on crop type and management practices. Nitrate uptake by plants is also difficult to predict, as it is influenced

by a range of factors such as soil moisture, temperature, and nutrient availability. Overall, nitrate simulations are likely to be more accurate in mountainous regions where quick flowing systems lead to less storage and transformation of nitrate (Table 2.4). In lowland agricultural systems, nitrate can persist in soils for several years and in groundwater for even longer time scales, leading to legacy effects that can complicate stream nitrate dynamics (Ehrhardt et al., 2019; Hrachowitz et al., 2015).

2.5.2. Simulating nitrate concentrations across space

Scheme 1, which solely utilized data from the catchment outlet, was unable to accurately simulate nitrate dynamics at upstream sites within the large, heterogeneous Bode catchment. Indeed, PBIAS values were high (> 45%) for many of the 94 spatially distributed sampling locations when scheme 1 was used (Figure 2.4a and Table 2.5). The model performed much better when scheme 2 was employed. Its addition of two gauging stations to the calibration process thus appeared to greatly influence model performance at the catchment scale.

However, little to no further improvement was seen with scheme 3 and its five additional gauging stations. This assertion has two sources of support: schemes 2 and 3 had similar numbers of sampling locations within the different PBIAS ranges (Table 2.5) and displayed similar cumulative distributions for their parameters (Figure 2.6). Comparing cumulative parameter distributions can help identify informative calibration stations.

Further results of the model performance of NO_3^- concentration at Scheme 2 shows varying performances among NO_3^- sampling locations that represent different catchment characteristics (e.g., precipitation, land use, and fertilizer inputs) (Figure 2.5). At sampling location 4, NO_3^- concentration was overestimated in summer, but the PBIAS value of the whole period was negative, it means that the model underestimated NO_3^- concentrations during other times of the year. This could be due to errors in the representation of hydrological processes, such as groundwater recharge, which can affect nitrate transport and concentration in the groundwater. This suggests that spatial representation of groundwater processes (such as groundwater NO_3^- concentration) are needed to be refined to obtain better model performance for small sub-catchments. Faramarzi et al. (2015) and Gao et al. (2016) concluded that the hydrological water quality models that only rely on calibration without refining internal process representation (e.g., groundwater NO_3^- concentration) will often not result in further improvement. Nevertheless, the above analysis indicates that Scheme 2 is sufficient to ensure the satisfactory model performance at NO_3^- sampling locations, since 75% of the NO_3^- sampling locations showed absolute PBIAS $\leq$35% (Figure 2.4b and Table 2.5) and the mHM-Nitrate model was capable to present different magnitudes of NO_3^- levels for different sub-catchments which differ in their catchment characteristics (Figure 2.5). These findings are in line with Ghaffar et al. (2021), where they found that considering archetypal gauging stations in the calibration process leads better spatial validation of the model at internal locations that were not originally considered in calibration. These stations represent the maximum catchment characteristics in heterogeneous catchments in terms of dominant land-use and meteorological features. This highlights the need for multiple internal stations/locations to validate the model's capacity to accurately capture the complexity of natural processes and identify which process needs to be improved (Beven, 2001; Daggupati et al., 2015).

2.5.3. Impact of calibration approaches on model uncertainty

For the three gauging stations, there was more uncertainty around simulated nitrate concentrations for scheme 3 than for scheme 2 (Figure 2.7), likely because scheme 3 included stations with low-frequency measurements. This result highlights the effect of measurement frequency on simulation uncertainty. Indeed, low-frequency measurements may not capture the full range of variability in nitrate dynamics. Furthermore, multi-site calibration approaches that rely on low-frequency data may give rise to spatial representation issues, given that water quality can vary widely across heterogenous catchments and be influenced by local factors, such as land use and soil type. This finding is in line with those of previous studies (Jiang et al., 2019; Khorashadi Zadeh et al., 2019; Ullrich and Volk, 2010). For example, Jiang et al. (2019) found that, for the HYPE model, uncertainty was reduced when the calibration process used nitrate concentrations that had been collected daily versus every two weeks. Our work also highlights the urgent need to establish suitable sampling procedures for gathering long-term, high-frequency water quality data to build reliable databases for model calibration and evaluation.

2.5.4. Implication of spatial evaluation of distributed hydrological water quality model

As hydrological water quality models become increasingly complex and monitoring data becomes more available, the question of how to improve their performance has become a crucial issue (Beven, 2001; Refsgaard et al., 2016; Refsgaard, Stisen and Koch, 2022). One crucial aspect is the increased attention on evaluating the spatial pattern performance of distributed process-based hydrological water quality models. Spatial evaluation of distributed hydrological water quality models allows us to better understand the spatial variability of hydrological and water processes and to gain insights into the underlying processes that govern the behavior of the system. This is important for identification of areas that require intervention to improve water quality.

It is possible to use remote sensing data such as soil moisture to evaluate spatial pattern performance of models for water quantity (Rajib, Merwade and Yu, 2016), but this approach cannot be applied to spatially evaluate models for nitrate and other chemicals. Water quality monitoring or sampling is always required for this purpose. However, spatially distributed models can greatly benefit from using long-term monitoring data that is available from authorities. This data is more densely available than discharge data and is readily accessible in many European communities and other regions. In our study, we demonstrated the usefulness of this type of data for evaluating the spatial performance of the distributed model, even when discharge measurements were not available.

2.6. Conclusion

Using three different approaches, we calibrated a fully distributed process-based mHM-Nitrate model that was then validated spatially and temporally at 8 gauging stations (discharge and nitrate concentrations) and 94 spatially distributed sampling locations (nitrate concentrations) within the heterogeneous Bode catchment in central Germany. Scheme 1 used only data from the catchment outlet; scheme 2 used data from the catchment outlet and two upstream stations;

and scheme 3 used data from the catchment outlet and seven additional upstream stations. Our study found that, for simulated discharge, model performance was similar at the catchment outlet for the three calibration schemes. Furthermore, model performance did not improve consistently across the upstream gauging stations.

In contrast, for nitrate concentrations, scheme 2 was better than scheme 1 when it came to simulating dynamics at sampling locations that had not been part of the calibration process. That said, model performance across the sampling locations was similar for schemes 2 and 3. Our results indicate that increasing the number of stations used in calibration does not necessarily improve simulations of nitrate concentrations. Additionally, we found that the use of low-frequency calibration data may increase the degree of model uncertainty.

In conclusion, this study offers valuable insights into the selection of gauging stations for model calibration. It suggests that differences in cumulative parameter distributions can serve as an indicator of which stations can provide useful additional representation. Furthermore, our work highlights that this selection process must account for diversity in catchment characteristics, such as land use, meteorological patterns, and elevation. In this way, the calibration data will better represent spatial patterns, and the model will yield more accurate predictions. Overall, this study provides valuable insights into calibration-related decision-making when carrying out fully distributed hydrological water quality models to simulate dynamics within spatially heterogeneous catchments.

2.7. References

Abbaspour, K.C. et al., 2007. Modelling hydrology and water quality in the pre-alpine/alpine Thur watershed using SWAT. Journal of Hydrology, 333(2-4): 413-430. DOI:10.1016/j.jhydrol.2006.09.014

Arnold, J.G. et al., 2012. Swat: Model Use, Calibration, and Validation. Transactions of the Asabe, 55(4): 1491-1508.

Arnold, J.G., Srinivasan, R., Muttiah, R.S., Williams, J.R., 1998. Large area hydrologic modeling and assessment part I: model development 1. JAWRA Journal of the American Water Resources Association, 34(1): 73-89.

Beck, H.E. et al., 2016. Global-scale regionalization of hydrologic model parameters. Water Resources Research, 52(5): 3599-3622. DOI:10.1002/2015wr018247

Beven, K., 2001. How far can we go in distributed hydrological modelling? Hydrology and Earth System Sciences, 5(1): 1-12. DOI:10.5194/hess-5-1-2001

Beven, K., 2007. Towards integrated environmental models of everywhere: uncertainty, data and modelling as a learning process. Hydrology and Earth System Sciences, 11(1): 460-467. DOI:DOI 10.5194/hess-11-460-2007

Beven, K., Binley, A., 1992. The Future of Distributed Models - Model Calibration and Uncertainty Prediction. Hydrological Processes, 6(3): 279-298. DOI:DOI 10.1002/hyp.3360060305

Bloschl, G., Sivapalan, M., 1995. Scale Issues in Hydrological Modeling - a Review. Hydrological Processes, 9(3-4): 251-290.

Cao, W., Bowden, W.B., Davie, T., Fenemor, A., 2006. Multi-variable and multi-site calibration and validation of SWAT in a large mountainous catchment with high spatial variability. Hydrological Processes, 20(5): 1057-1073. DOI:10.1002/hyp.5933

Chiang, L.C., Yuan, Y.P., Mehaffey, M., Jackson, M., Chaubey, I., 2014. Assessing SWAT's performance in the Kaskaskia River watershed as influenced by the number of calibration stations used. Hydrological Processes, 28(3): 676-687. DOI:10.1002/hyp.9589

Daggupati, P. et al., 2015. A Recommended Calibration and Validation Strategy for Hydrologic and Water Quality Models. Transactions of the Asabe, 58(6): 1705-1719. DOI:10.13031/trans.58.10712

Efstratiadis, A., Koutsoyiannis, D., 2010. One decade of multi-objective calibration approaches in hydrological modelling: a review. Hydrological Sciences Journal, 55(1): 58-78. DOI:10.1080/02626660903526292

Ehrhardt, S., Kumar, R., Fleckenstein, J.H., Attinger, S., Musolff, A., 2019. Trajectories of nitrate input and output in three nested catchments along a land use gradient. Hydrology and Earth System Sciences, 23(9): 3503-3524. DOI:10.5194/hess-23-3503-2019

Engel, B., Storm, D., White, M., Arnold, J., Arabi, M., 2007. A hydrologic/water quality model application protocol. Journal of the American Water Resources Association, 43(5): 1223-1236. DOI:10.1111/j.1752-1688.2007.00105.x

Franco, A.C.L., Oliveira, D.Y.d., Bonumá, N.B., 2020. Comparison of single-site, multi-site and multi-variable SWAT calibration strategies. Hydrological Sciences Journal, 65(14): 2376-2389. DOI:10.1080/02626667.2020.1810252

Ghaffar, S., Jomaa, S., Meon, G., Rode, M., 2021. Spatial validation of a semi-distributed hydrological nutrient transport model. Journal of Hydrology, 593: 125818. DOI:https://doi.org/10.1016/j.jhydrol.2020.125818

Gupta, H.V., Beven, K.J., Wagener, T., 2005. Model Calibration and Uncertainty Estimation, Encyclopedia of Hydrological Sciences. DOI:https://doi.org/10.1002/0470848944.hsa138

Hargreaves, G.H., Samani, Z.A., 1985. Reference Crop Evapotranspiration from Temperature. Applied Engineering in Agriculture, 1(2): 96-99. DOI:10.13031/2013.26773

Her, Y., Chaubey, I., 2015. Impact of the numbers of observations and calibration parameters on equifinality, model performance, and output and parameter uncertainty. Hydrological Processes, 29(19): 4220-4237. DOI:10.1002/hyp.10487

Hundecha, Y., Bárdossy, A., 2004. Modeling of the effect of land use changes on the runoff generation of a river basin through parameter regionalization of a watershed model. Journal of Hydrology, 292(1-4): 281-295. DOI:10.1016/j.jhydrol.2004.01.002

Jarvis, A., H.I. Reuter, A. Nelson, E. Guevara., 2008. Hole-filled SRTM for the globe Version 4, available from the CGIAR-CSI SRTM 90m Database http://srtm.csi.cgiar.org/, International Centre for Tropical Agriculture (CIAT).

Jiang, S., Jomaa, S., Büttner, O., Meon, G., Rode, M., 2015. Multi-site identification of a distributed hydrological nitrogen model using Bayesian uncertainty analysis. Journal of Hydrology, 529: 940-950. DOI:10.1016/j.jhydrol.2015.09.009

Jiang, S.Y. et al., 2019. Effects of stream nitrate data frequency on watershed model performance and prediction uncertainty. Journal of Hydrology, 569: 22-36. DOI:10.1016/j.jhydrol.2018.11.049

Khu, S.-T., Madsen, H., di Pierro, F., 2008. Incorporating multiple observations for distributed hydrologic model calibration: An approach using a multi-objective evolutionary algorithm and clustering. Advances in Water Resources, 31(10): 1387-1398. DOI:10.1016/j.advwatres.2008.07.011

Kunz, J.V., Annable, M.D., Rao, S., Rode, M., Borchardt, D., 2017. Hyporheic Passive Flux Meters Reveal Inverse Vertical Zonation and High Seasonality of Nitrogen Processing in an Anthropogenically Modified Stream (Holtemme, Germany). Water Resources Research, 53(12): 10155-10172. DOI:https://doi.org/10.1002/2017WR020709

Lerat, J. et al., 2012. Do internal flow measurements improve the calibration of rainfall-runoff models? Water Resources Research, 48(2). DOI:10.1029/2010wr010179

Leta, O.T., Griensven, A.v., Bauwens, W., 2017. Effect of Single and Multisite Calibration Techniques on the Parameter Estimation, Performance, and Output of a SWAT Model of a Spatially Heterogeneous Catchment. Journal of Hydrologic Engineering, 22(3): 05016036. DOI:doi:10.1061/(ASCE)HE.1943-5584.0001471

Li, X., Weller, D.E., Jordan, T.E., 2010. Watershed model calibration using multi-objective optimization and multi-site averaging. Journal of Hydrology, 380(3-4): 277-288. DOI:10.1016/j.jhydrol.2009.11.003

Lindström, G., Pers, C., Rosberg, J., Strömqvist, J., Arheimer, B., 2010. Development and testing of the HYPE (Hydrological Predictions for the Environment) water quality model for different spatial scales. Hydrology Research, 41(3-4): 295-319. DOI:10.2166/nh.2010.007

Merz, R., Blöschl, G., 2004. Regionalisation of catchment model parameters. Journal of Hydrology, 287(1-4): 95-123. DOI:10.1016/j.jhydrol.2003.09.028

Moriasi, D.N., Wilson, B.N., Douglas-Mankin, K.R., Arnold, J.G., Gowda, P.H., 2012. Hydrologic and Water Quality Models: Use, Calibration, and Validation. Transactions of the ASABE, 55(4): 1241-1247. DOI:10.13031/2013.42265

Morris, M.D., 1991. Factorial sampling plans for preliminary computational experiments. Technometrics, 33(2): 161-174.

Oudin, L., Andreassian, V., Perrin, C., Michel, C., Le Moine, N., 2008. Spatial proximity, physical similarity, regression and ungaged catchments: A comparison of regionalization approaches based on 913 French catchments. Water Resources Research, 44(3). DOI:Artn W03413

10.1029/2007wr006240

Parajka, J., Merz, R., Bloschl, G., 2005. A comparison of regionalisation methods for catchment model parameters. Hydrology and Earth System Sciences, 9(3): 157-171. DOI:DOI 10.5194/hess-9-157-2005

Parajka, J. et al., 2013. Comparative assessment of predictions in ungauged basins – Part 1: Runoff-hydrograph studies. Hydrology and Earth System Sciences, 17(5): 1783-1795. DOI:10.5194/hess-17-1783-2013

Pianosi, F., Sarrazin, F., Wagener, T., 2015. A Matlab toolbox for Global Sensitivity Analysis. Environ Modell Softw, 70: 80-85. DOI:10.1016/j.envsoft.2015.04.009

Pokhrel, P., Gupta, H.V., Wagener, T., 2008. A spatial regularization approach to parameter estimation for a distributed watershed model. Water Resources Research, 44(12). DOI:10.1029/2007wr006615

Refsgaard, J.C., 1997. Parameterisation, calibration and validation of distributed hydrological models. Journal of Hydrology, 198(1-4): 69-97. DOI:Doi 10.1016/S0022-1694(96)03329-X

Refsgaard, J.C. et al., 2016. Where are the limits of model predictive capabilities? Hydrological Processes, 30(26): 4956-4965. DOI:10.1002/hyp.11029

Samaniego, L., Kumar, R., Attinger, S., 2010. Multiscale parameter regionalization of a grid-based hydrologic model at the mesoscale. Water Resources Research, 46(5). DOI:10.1029/2008wr007327

Saraswat, D. et al., 2015. Hydrologic and Water Quality Models: Documentation and Reporting Procedures for Calibration, Validation, and Use. Transactions of the Asabe, 58(6): 1787-1797. DOI:10.13031/trans.57.10707

Shrestha, M.K., Recknagel, F., Frizenschaf, J., Meyer, W., 2016. Assessing SWAT models based on single and multi-site calibration for the simulation of flow and nutrient loads in the semi-arid Onkaparinga catchment in South Australia. Agricultural Water Management, 175: 61-71. DOI:10.1016/j.agwat.2016.02.009

Singh, R., Archfield, S.A., Wagener, T., 2014. Identifying dominant controls on hydrologic parameter transfer from gauged to ungauged catchments – A comparative hydrology approach. Journal of Hydrology, 517: 985-996. DOI:10.1016/j.jhydrol.2014.06.030

Tolson, B.A., Shoemaker, C.A., 2007. Dynamically dimensioned search algorithm for computationally efficient watershed model calibration. Water Resources Research, 43(1). DOI:Artn W01413

10.1029/2005wr004723

Vrugt, J.A., Diks, C.G.H., Gupta, H.V., Bouten, W., Verstraten, J.M., 2005. Improved treatment of uncertainty in hydrologic modeling: Combining the strengths of global optimization and data assimilation. Water Resources Research, 41(1). DOI:10.1029/2004wr003059

Vrugt, J.A., Gupta, H.V., Bouten, W., Sorooshian, S., 2003. A Shuffled Complex Evolution Metropolis algorithm for optimization and uncertainty assessment of hydrologic model parameters. Water Resources Research, 39(8). DOI:10.1029/2002wr001642

Vrugt, J.A., ter Braak, C.J.F., Clark, M.P., Hyman, J.M., Robinson, B.A., 2008. Treatment of input uncertainty in hydrologic modeling: Doing hydrology backward with Markov chain Monte Carlo simulation. Water Resources Research, 44(12). DOI:10.1029/2007wr006720

Wagener, T., Gupta, H.V., 2005. Model identification for hydrological forecasting under uncertainty. Stochastic Environmental Research and Risk Assessment, 19(6): 378-387. DOI:10.1007/s00477-005-0006-5

Wagener, T., McIntyre, N., Lees, M.J., Wheater, H.S., Gupta, H.V., 2003. Towards reduced uncertainty in conceptual rainfall-runoff modelling: dynamic identifiability analysis. Hydrological Processes, 17(2): 455-476. DOI:10.1002/hyp.1135

Wagener, T., Wheater, H.S., 2006. Parameter estimation and regionalization for continuous rainfall-runoff models including uncertainty. Journal of Hydrology, 320(1-2): 132-154. DOI:10.1016/j.jhydrol.2005.07.015

Wang, S. et al., 2012. Multi-site calibration, validation, and sensitivity analysis of the MIKE SHE Model for a large watershed in northern China. Hydrology and Earth System Sciences, 16(12): 4621-4632. DOI:10.5194/hess-16-4621-2012

Wellen, C., Kamran-Disfani, A.R., Arhonditsis, G.B., 2015. Evaluation of the current state of distributed watershed nutrient water quality modeling. Environ Sci Technol, 49(6): 3278-90. DOI:10.1021/es5049557

White, K.L., Chaubey, I., 2005. Sensitivity Analysis, Calibration, and Validations for a Multisite and Multivariable Swat Model. Journal of the American Water Resources Association, 41(5): 1077-1089. DOI:10.1111/j.1752-1688.2005.tb03786.x

Wollschläger, U. et al., 2016. The Bode hydrological observatory: a platform for integrated, interdisciplinary hydro-ecological research within the TERENO Harz/Central German Lowland Observatory. Environmental Earth Sciences, 76(1). DOI:10.1007/s12665-016-6327-5

Wu, L., Liu, X., Yang, Z., Yu, Y., Ma, X., 2022a. Effects of single- and multi-site calibration strategies on hydrological model performance and parameter sensitivity of large-scale semi-arid and semi-humid watersheds. Hydrological Processes, 36(6). DOI:10.1002/hyp.14616

Wu, S., Tetzlaff, D., Yang, X., Soulsby, C., 2022b. Disentangling the Influence of Landscape Characteristics, Hydroclimatic Variability and Land Management on Surface Water NO3-N Dynamics: Spatially Distributed Modeling Over 30 yr in a Lowland Mixed Land Use Catchment. Water Resources Research, 58(2). DOI:10.1029/2021wr030566

Yang, X., Jomaa, S., Buttner, O., Rode, M., 2019. Autotrophic nitrate uptake in river networks: A modeling approach using continuous high-frequency data. Water Res, 157: 258-268. DOI:10.1016/j.watres.2019.02.059

Yang, X. et al., 2018. A New Fully Distributed Model of Nitrate Transport and Removal at Catchment Scale. Water Resources Research. DOI:10.1029/2017wr022380

Yang, X., Rode, M., 2020. A Fully Distributed Catchment Nitrate Model - mHM-Nitrate v2.0. DOI:10.5281/ZENODO.3891629

Zhang, X., Srinivasan, R., Van Liew, M., 2008. Multi-Site Calibration of the SWAT Model for Hydrologic Modeling. Transactions of the ASABE, 51(6): 2039-2049. DOI:https://doi.org/10.13031/2013.25407

Zhou, X. et al., 2022. Exploring the relations between sequential droughts and stream nitrogen dynamics in central Germany through catchment-scale mechanistic modelling. Journal of Hydrology, 614: 128615. DOI:10.1016/j.jhydrol.2022.128615

2.8. Supplementary materials

Table S2.1. Description of calibrated parameters with their physical meaning, initial ranges and optimal values.

Process	Parameter	Description	Initial range	Optimal value
PET	pet1 (Shevenell, 1999)	Parameter for aspect correction of input potential evapotranspiration data	[6.99E-1, 1.30E+0]	1.093
Soil moisture	sm10 (Cosby et al., 1984)	Transfer function parameter used to calculate soil saturated hydraulic conductivity	[-1.20E+0, -2.85E-1]	-8.49E-1
	sm17 (Brooks and Corey, 1964)	Parameter that determines the relative contribution of precipitation or snowmelt to runoff	[1.00E+0, 4.00E+0]	1.71E+0
	sm4 (Cosby et al., 1984)	Pedotransfer function parameter used to calculate maximum soil moisture content	[6.46E-1, 9.51E-1]	9.12E-1
Percolation	pc1	Parameter used to calculate the percolation coefficient	[0.00E+0, 5.00E+1]	2.94E+1
Interflow	intfl1	Slow interflow storage capacity factor	[7.50E+1, 2.00E+2]	7.50E+1
	intfl4	Slow interflow recession coefficient	[1.00E+0, 3.00E+1]	2.99E+1
	intfl5	Slow interflow exponent coefficient	[5.00E-2, 2.99E-1]	5.01E-2
In-stream denitrification	deni_w	General parameter of in-stream denitrification rate (kg m^{-2} d^{-1})	[1.00E-8, 5.00E-2]	3.05E-4
Soil denitrification	deni_as	Soil denitrification rate on agricultural land (d^{-1})	[1.00E-8, 9.10E-3]	4.86E-3
	deni_s	Soil denitrification rate on non-agricultural land (d^{-1})	[1.00E-8, 1.10E-3]	1.09E-3
In-stream assimilation	pprt_aw	Primary production rate in agricultural streams (kg m^{-3} d^{-1})	[1.00E-8, 1.00E+0]	1.49E-1
	pprt_w	Primary production rate in non-agricultural streams (kg m^{-3} d^{-1})	[1.00E-8, 1.00E+0]	4.74E-3

Table S2.2. Catchment characteristics represented by 94 NO_3^- sampling locations.

Station ID	Area (km^2)	Number	NO_3^- (mg N L^{-1})	Precipitation (mm $year^{-1}$)
401005	80	15	2.8	538.6
410100	16.9	314	1.4	740.4
410101	119.78	99	0.8	1122.7
410102	7.19	141	1.5	810.7
410103	8.13	129	0.9	855.9
410106	19.2	97	1.3	866.3
410107	48.05	47	1.2	822.7
410108	1.36	23	1.2	868.9
410110	170.5	30	1.6	545.6
410120	105.67	210	1.7	628.2
410130	230.3	225	2	544.2
410145	131.52	53	2.3	514.6
410150	49.44	250	2.6	541.1
410160	59.15	333	3.5	512.3
410185	382.86	457	3.1	505.1
411059	14.74	12	1	1183.3
411060	1.58	190	0.6	849.3
411061	33.67	12	1.6	882.2
411062	0.7	30	1.3	667.2
411063	0.53	24	1.3	640
411070	28.19	65	2	652.2
411071	14.01	18	2.5	603.1
411080	29.99	194	3.3	630.9
411090	65.65	52	4	553.9
411091	1.05	52	3.6	522.8
411095	13.87	54	8.9	573.6
411096	26.51	23	10.7	563
411100	27.03	406	4.6	516.8
411104	7.3	10	1.3	814.6
411105	8.47	46	1	799.3
411106	0.37	39	2.4	757.4
411107	4.36	27	2.9	766.2
411108	6.9	16	1.9	813.6

411109	20.77	90	2	725
411111	0.83	16	1.3	725.1
411113	20.71	16	1.7	730.2
411114	2.2	22	1.7	677.2
411116	16.21	10	1.5	666.1
411120	2.81	16	2.5	649.5
411121	0.79	17	2.2	638.1
411130	11.29	185	1.5	677.2
411134	20.08	58	1.6	654.2
411145	43.42	34	1.7	601.6
411146	40.2	30	1.5	602.3
411153	22.6	10	2.6	545.31
411154	3.36	116	3.3	492
411156	5.69	16	2.8	494.1
411158	16.4	28	2.4	552.9
411160	58.08	72	3.8	538.1
411165	17.52	34	2.9	495.6
411169	146.2	14	3.1	510.4
411170	153.41	340	3.3	513.3
411171	3.13	90	2.6	499.4
411172	3.71	23	3.2	495.1
411186	9.54	20	4.7	567.4
411199	241.85	18	9.3	582.7
411200	284.55	138	5.8	582.5
411205	25.76	31	9.4	591.6
411210	150.84	83	5.4	559.7
411215	68.08	54	5.8	546.1
411220	24.93	155	4.5	542.7
411223	27.87	12	5.3	522.5
411225	1.66	37	4.7	547.3
411226	6.03	29	5.5	538
411240	0.61	11	4.4	524.4
411241	0.96	11	5	533.1
411261	24.4	46	1.6	763.8
411270	72.27	81	5.7	537.1
411300	37.4	138	2.3	836.5

411321	18.61	76	0.8	1209.9
411322	13.82	12	1.2	1401.9
411350	6.15	40	0.7	1228.6
411360	40.1	129	0.8	977.4
411370	11.56	36	2.7	771.7
411371	21.09	59	1.6	741.8
411809	7.28	47	2	727.7
411812	3.46	109	0.8	998.1
411813	10.95	64	1.4	896
411814	0.65	71	2.9	950.4
411870	4.77	33	2.8	719.4
411917	20.18	27	1.3	693.6
411925	9.89	22	2.4	644.1
413537	13.08	6	4.8	564.3
413539	17.5	20	17.2	536.3
413635	0.16	16	8.7	550.1
413636	8.35	23	10.6	554.4
414512	2.78	35	6.7	542.2
414513	50.39	103	7.9	544.4
414514	1.22	89	6.7	538.6
414515	16.7	118	7.2	558.5
414516	12.28	11	6.7	534
414535	6.24	133	8	518.7
414539	19.51	19	19.2	537.5
414545	5.96	17	7.9	548.2

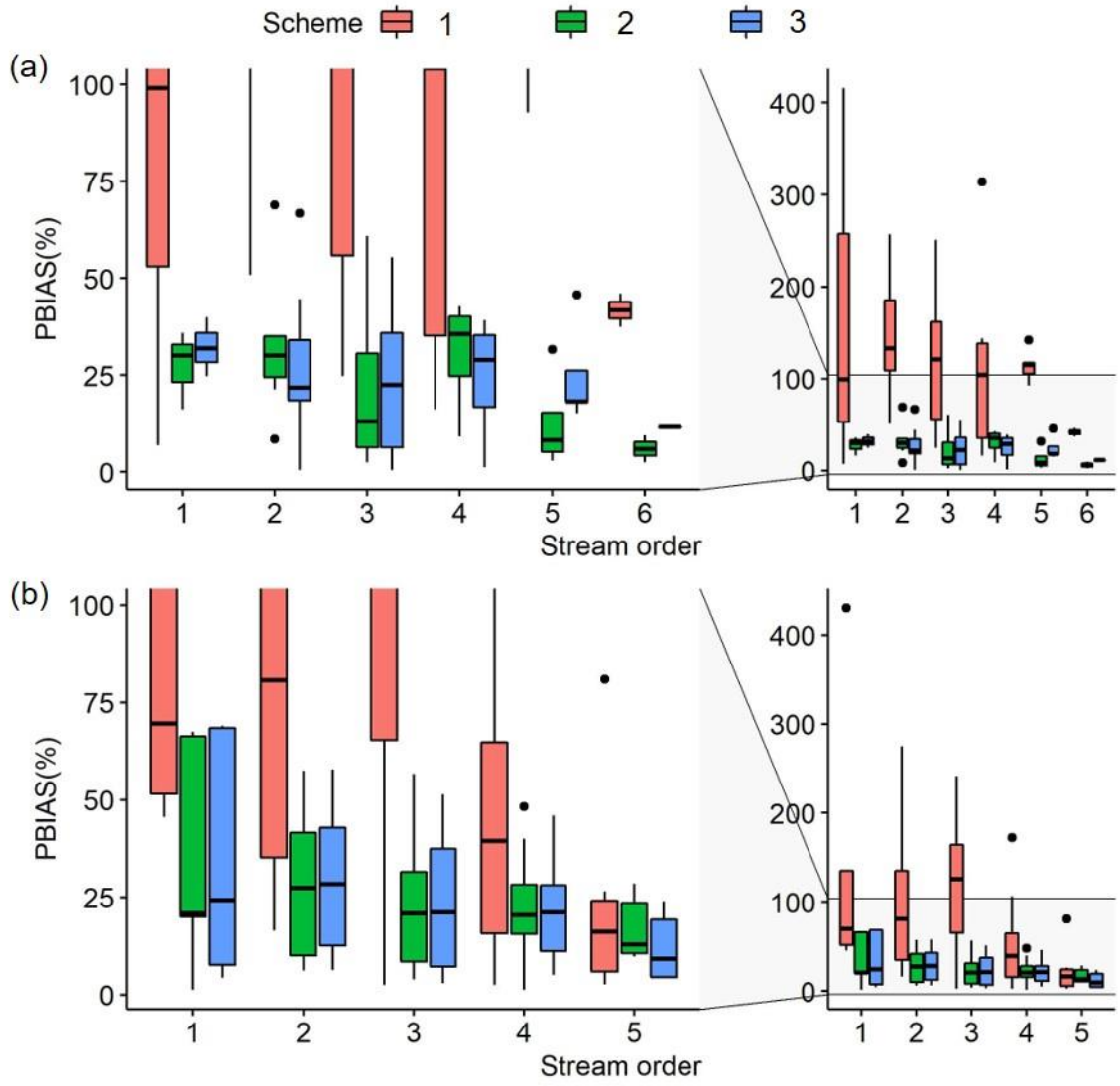

Figure S2.1. Model performance for NO_3^- concentration at each stream order at (a) arable- and (b) forest-dominated NO_3^- sampling locations at three calibration schemes.

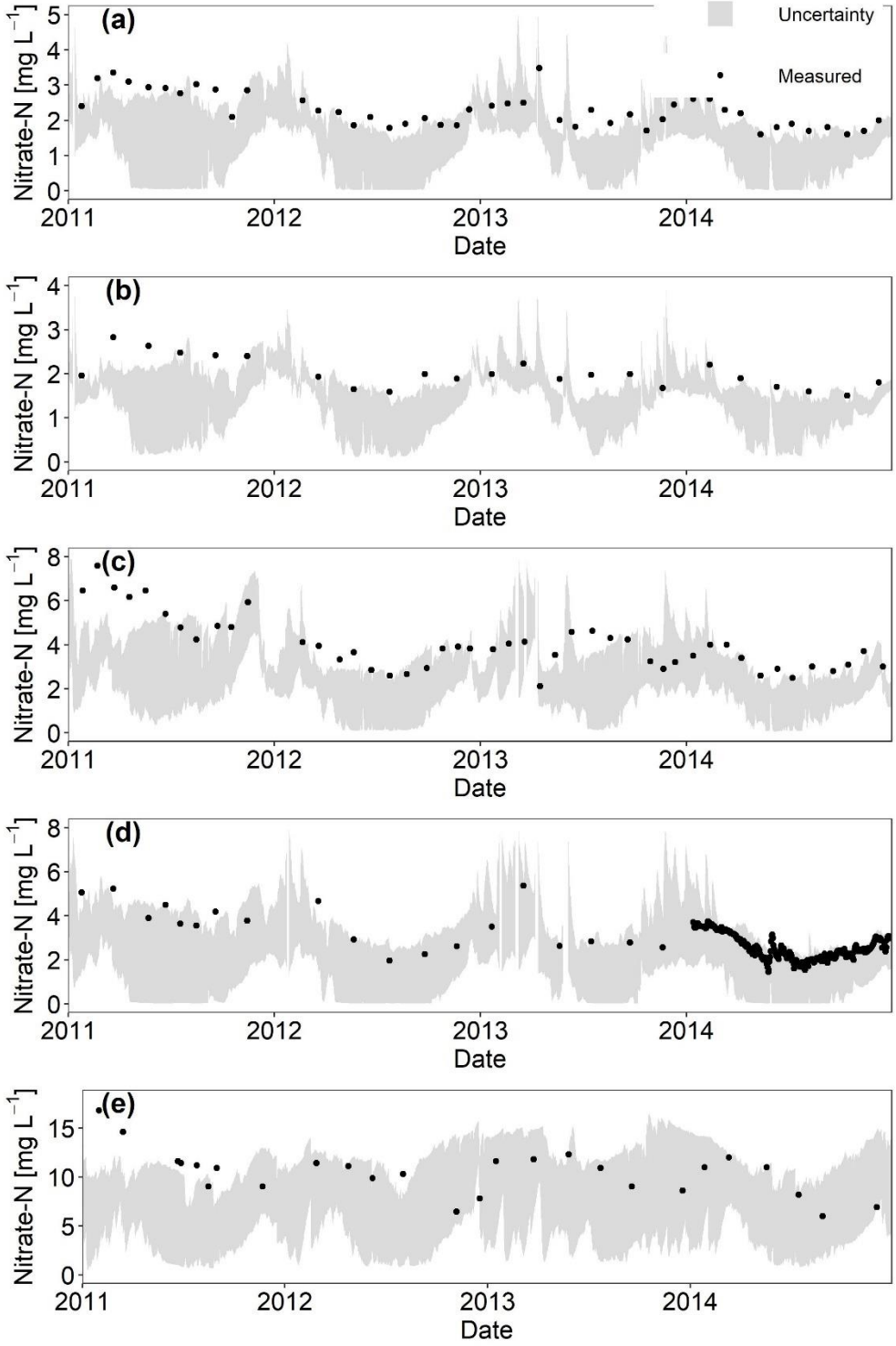

Figure S2.2. The 95% uncertainty boundaries of NO_3^- concentration at Scheme 3 at calibration station (a) Wegeleben, (b) Ditfurt, (c) Nienhagen, (d) Hadmersleben and (e) Peseckendorf.

Chapter 3: Exploring the relations between sequential droughts and stream nitrogen dynamics in central Germany through catchment-scale mechanistic modelling

Xiangqian Zhou[a,*], Seifeddine Jomaa[a], Xiaoqiang Yang[a] , Ralf Merz[b], Yanping Wang[c], Michael Rode[a,d]

[a]Department of Aquatic Ecosystem Analysis and Management, Helmholtz Centre for Environmental Research - UFZ, Magdeburg, Germany
[b]Department of Catchment Hydrology, Helmholtz Centre for Environmental Research - UFZHalle (Saale), Germany
[c]School of Geographical Science, Nantong University, Nantong, China
[d]Institute of Environmental Science and Geography, University of Potsdam, Potsdam-Golm, Germany
[*]Corresponding author: Xiangqian Zhou (xiangqian.zhou@ufz.de)

3.1. Abstract

Like many other regions in central Europe, Germany experienced sequential summer droughts from 2015-2018. As one of the environmental consequences, river nitrate concentrations have exhibited significant changes in many catchments. However, catchment nitrate responses to the changing weather conditions have not yet been mechanistically explored. Thus, a fully distributed, process-based catchment Nitrate model (mHM-Nitrate) was used to reveal the causal relations in the Bode catchment, of which river nitrate concentrations have experienced contrasting trends from upstream to downstream reaches. The model was evaluated using data from six gauging stations, reflecting different levels of runoff components and their associated nitrate-mixing from upstream to downstream. Results indicated that the mHM-Nitrate model reproduced dynamics of daily discharge and nitrate concentration well, with Nash-Sutcliffe Efficiency ≥ 0.73 for discharge and Kling-Gupta Efficiency ≥ 0.50 for nitrate concentration at most stations. Particularly, the spatially contrasting trends of nitrate concentration were successfully captured by the model. The decrease of nitrate concentration in the lowland area in drought years (2015-2018) was presumably due to (1) limited terrestrial export loading (ca. 40% lower than that of normal years 2004-2014), and (2) increased in-stream retention efficiency (20% higher in summer within the whole river network). From a mechanistic modelling perspective, this study provided insights into spatially heterogeneous flow and nitrate dynamics and effects of sequential droughts, which shed light on water-quality responses to future climate change, as droughts are projected to be more frequent.

Keywords:

Drought; Nitrate mixing; Catchment hydrology; Water quality model

Highlights:

- The model reproduces nitrate dynamics and trends under changing weather conditions.
- Nitrate dynamics show spatiotemporally varying responses to the sequential droughts.

- Soil export decreases while in-stream retention efficiency increases in droughts.

3.2. Introduction

Central Europe recently experienced sequential droughts in 2013, 2015, 2018 and 2019 (Hanel et al., 2018; Hari et al., 2020), and droughts are projected to become more frequent and severe in the future (Hari et al., 2020; Spinoni et al., 2018). In Germany, mean annual temperature increased by 1.5°C from 1881-2018, with ca. 0.3°C of that increase occurring from 2014-2018 (UBA, 2019). Using an ensemble of climate-change scenarios, Huang, Krysanova and Hattermann (2015) reported that most rivers in Germany will experience more frequent droughts.

Excess nitrogen (N) input to surface water due to intensive anthropogenic activities (e.g., fertiliser application from arable land, wastewater from urban and industrial areas) has caused widespread environmental problems in recent decades. Nitrate turnover processes at the catchment scale are expected to change due to climate change (Hesse and Krysanova, 2016; Mosley, 2015; Whitehead et al., 2009), especially due to an increase in drought events (Ballard, Sinha and Michalak, 2019; Zwolsman and van Bokhoven, 2007).

The influence of drought on N dynamics has received increasing attention in recent decades (e.g., Baldwin et al., 2005; Lutz et al., 2016; Mosley, 2015; van Vliet and Zwolsman, 2008; Whitehead et al., 2009; Yevenes, Figueroa and Parra, 2018; Zwolsman and van Bokhoven, 2007). Previous studies have reported decreasing nitrate concentration in response to drought, for example, in the Meuse River in western Europe (van Vliet and Zwolsman, 2008), which was attributed to less diffuse input during drought periods. During a drought in Chile from 2010-2015, Yevenes et al. (2018) found that nitrate concentration did not change in the upstream part of a study catchment but decreased downstream due to differences in discharge regime and nitrate sources from upstream to downstream. In line with these findings, numerous studies have reported that droughts can have spatiotemporally varying impacts on nitrate transport and transformation processes due to the heterogeneous changes in hydrological processes within catchments (e.g., Leitner et al., 2020; Lintern et al., 2018b; Lutz et al., 2016). These studies are generally based on data-driven and statistical analyses, but conclusions drawn from them are site-specific and often do not provide a full understanding of the factors that influence the effects of drought on nitrate dynamics and their spatial heterogeneity. Thus, it is crucial to identify the mechanisms that underlie water-quality trends under drought conditions to ensure future water quality and develop effective management strategies. Furthermore, the scientific understanding gained from analysing deterministic trends can help to predict future trends. However, how sequential droughts influence stream nitrate responses has not yet been mechanistically explored. Catchment-scale hydrological water-quality models are an alternative solution to identify the relations between changing weather conditions and changes in nitrate dynamics. These models can reproduce catchment nitrate dynamics and stream water concentrations well based on hydrological understanding, which can be transferred across catchments or climate conditions (Jiang, Jomaa and Rode, 2014; Wellen, Kamran-Disfani and Arhonditsis, 2015).

Process-based water-quality models are rarely used to investigate spatiotemporal effects of historical droughts on N concentrations at the catchment scale. One of the challenges is to adequately represent the catchment spatial heterogeneity and the complexity of nitrate dynamic

processes, which can become more important during droughts (Rode et al., 2010; Wellen, Kamran-Disfani and Arhonditsis, 2015). The fully distributed hydrological model mHM (Samaniego, Kumar and Attinger, 2010) introduces flexible multiscale catchment discretization and parameterization techniques. The mHM-Nitrate model was recently developed based on the hydrological mHM platform, including advanced descriptions of terrestrial and in-stream nitrate processes and consideration of agricultural management (Yang et al., 2018). The model has shown a robust ability to provide reliable, detailed information about terrestrial and in-stream nitrate dynamics (Yang et al., 2019; Yang et al., 2018; Yang, Jomaa and Rode, 2019). Thus, the model acts as a promising tool for mechanistic investigation of the impacts of drought on stream nitrate dynamics. In this study, we applied mHM-Nitrate to the Bode catchment (3200 km^2, central Germany; part of the German TERENO observatories). The catchment has large hydroclimatic, geophysical and landscape gradients and has experienced sequential droughts in recent years (2015-2018). The objectives of the study were to (i) simulate spatiotemporal nitrate dynamics in a mesoscale catchment with widely differing meteorological and land-use characteristics using the mHM-Nitrate model, (ii) evaluate mHM-Nitrate's ability to represent recent drought-induced trends in nitrate concentration and (iii) analyse mechanisms that influence spatiotemporally varying river nitrate concentrations under sequential droughts.

3.3. Materials and Methods

3.3.1. Study area

The Bode catchment is an intensively monitored and investigated mesoscale catchment in central Germany (Wollschläger et al., 2016) (Figure 3.1). The catchment includes the Harz Mountains in the southwest and lowland plains in the northeast. Elevation of the catchment ranges from 1142 m.a.s.l. at the Brocken (the highest peak of the Harz Mountains) to 70 m.a.s.l. in the lowland area. Along the elevation gradient, the catchment has large gradients of meteorological, land use, soil type and geological characteristics. Annual mean precipitation varies from more than 1500 mm at the Brocken to ca. 500 mm in the lowland (Wollschläger et al., 2016). Mean annual temperature is 9.5℃, with a minimum of -3.4℃ in January and a maximum of 19.6℃ in July (Wollschläger et al., 2016). The Bode catchment experienced sequential summer droughts from 2015-2018 according to the 3-month standardized precipitation evapotranspiration index (Vicente-Serrano, Begueria and Lopez-Moreno, 2010) (Figure S1). Land use in the mountain area is dominated by forest, with 10% pasture, 8% agriculture and 7% urban areas and lakes. The soil type in the Harz Mountains is dominated by Cambisols. Land use in the lowland area is dominated by agriculture (81%), whose main crops are winter wheat, winter barley, rapeseed and sugar beet; forest and pasture cover 7% and 3%, respectively; and urban areas and small lakes cover the remaining 9% (Figure 3.1b). Chernozems are the main soil type in the lowland area.

To classify typical landscape nitrate-leaching behaviour, five dominant soil classes were identified (Figure 3.1c) according to the United States Department of Agriculture classification by combining soil properties and land-use types: sandy, silt loam, silty clay loam and loam. Then, these classes on the soil texture map were intersected with the land-use map, and the

cells in which the area of the dominant soil-land-use class exceeded 80% of the cell's area were selected. Consequently, the lowland area was classified into Classes I-III, which represented the dominant loess area (silt loam soils), riverine area (loam soils) and highly sandy area (sandy soils), respectively. Two representative classes in the mountain area were selected: Class IV, which represented the mountain pasture area (silty clay loam soils), and Class V, which represented the mountain arable area (sandy soils).

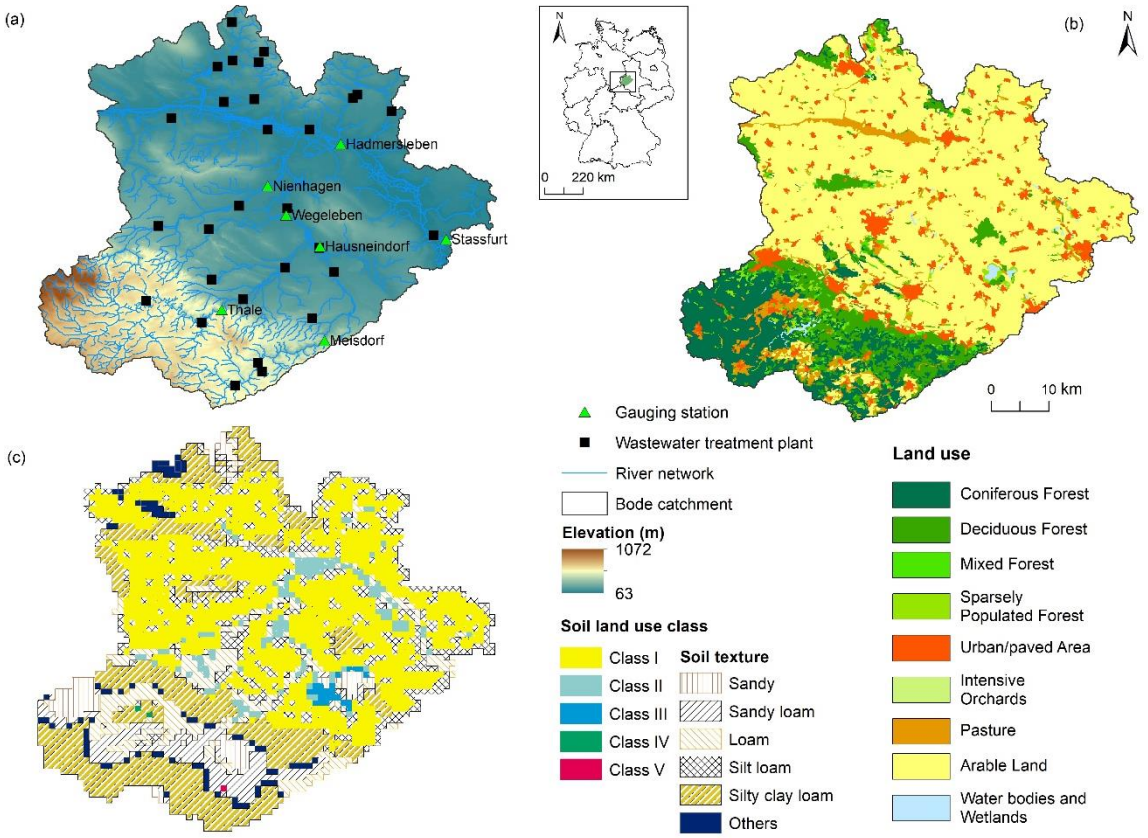

Figure 3.1. The Bode catchment: (a) geographical location of the gauging stations and wastewater treatment plants, (b) land use types and (c) five dominant soil-land-use classes.

3.3.2. Data availability

Meteorological data were derived from the German Weather Service (DWD), including daily precipitation and daily mean temperature from 2000-2018. To create the meteorological forcing inputs for the model, the DWD observations were spatially interpolated into 1 km × 1 km grid data, using the kriging method drifted by terrain elevation. This method considers the orographic effect on precipitation and temperature by using the elevation as an external variable for the interpolation (Hundecha and Bárdossy, 2004). Daily potential evapotranspiration data were calculated using the Hargreaves and Sammi (1985) method at the same spatial resolution.

A terrain elevation model was obtained from the Shuttle Radar Topography Mission (SRTM) sensor (Jarvis, 2008). The digitized geological map and soil map, both at a scale of 1:1,000,000, were obtained from the Federal Institute for Geosciences and Natural Resources (BGR) (https://produktcenter.bgr.de, last accessed 1 June 2020). Land-cover data were derived from CORINE Land Cover 10 ha (https://gdz.bkg.bund.de/index.php/default/open-data.html, last

accessed 1 June 2020). These datasets were resampled to a spatial resolution of 100 m × 100 m for model simulations.

Data on mineral fertiliser and manure application rates and times, as well as crop rotations on arable land, were obtained from the model configuration of Yang et al. (2018) and agricultural authorities (https://llg.sachsen-anhalt.de/llg/, last accessed 10 April 2020). The total amount of fertiliser (mineral fertiliser and manure) applied depended on crop type and was assumed to be applied evenly throughout the fertilisation period. The resolution of the crop-rotation map was set to that of the land-use map for technical simplification and due to the lack of detailed information. Point-source data were collected from Urban Wastewater Treatment Directive (UWWTD) sites for Germany (https://uwwtd.eu/Germany/uwwtps/treatment, last accessed 10 April 2020). Overall, 29 wastewater treatment plants (WWTPs) were considered (Figure 3.1a). The original point-source data were available only as of annual total N load, and thus daily mean values were used as model input. The percentage of point-source N load, which was calculated by dividing the annual total N load of the 29 WWTPs by the observed annual nitrate-N load at the catchment outlet station, equalled only 12% of the total N load in the Bode catchment during the study period.

Daily discharge at six gauging stations (Meisdorf, Hausneindorf, Wegeleben, Nienhagen, Hadmersleben and Stassfurt) was provided by the State Agency for Flood Protection and Water Management of Saxony-Anhalt (LHW) (http://gldweb.dhi-wasy.com/gld-portal/, last accessed 10 April 2020). Nitrate concentration was measured twice weekly to twice monthly from 2000-2009 by LHW (http://gldweb.dhi-wasy.com/gld-portal/, last accessed 10 April 2020) and daily from 2010-2018 by the Helmholtz Centre for Environmental Research – UFZ. Nitrate concentration observations were missing for 2015 and 2017-2018 at the Wegeleben station, and discharge observations were missing for 2017-2018 at the Nienhagen station (Figure 3.1a).

3.3.3. mHM-Nitrate model description

The mHM-Nitrate model is a grid-based catchment nitrate model that balances process complexity and model representation (Yang et al., 2018). Nitrate-process descriptions come mainly from the HYPE model (Lindström et al., 2010), with additional considerations of nitrate retention in deep groundwater, spatially distributed crop rotations and time-varying point-source inputs. The model includes the following hydrological processes: canopy interception, snow accumulation and melt, evapotranspiration, infiltration, soil moisture dynamics, runoff generation, percolation and flood routing along the river network. Nitrate processes are fully integrated into the hydrological cycling. Major N inputs include wet atmospheric deposition via precipitation, fertiliser and manure application and plant/crop residues. In each soil layer, four N pools are defined (i.e., active solid organic N, inactive solid organic N, dissolved organic N and dissolved inorganic N), along with soil N processes of denitrification, plant/crop uptake and transformations among the four N pools. In-stream N transformations include denitrification, primary production and mineralization. Governing equations of N transformations in the soil and the stream can be found in Supplementary material (Text S1). More detailed descriptions of the mHM-Nitrate model can be found in Yang et al. (2018), and source code can be found in Yang and Rode (2020).

3.3.4. Model calibration and performance measurements

The mHM-Nitrate model was set at a daily time step from 2000-2018 (2000-2003 was considered a warm-up period). We used daily discharge and nitrate concentration data from 2010-2014 as calibration data. The nitrate concentration data used to validate model predictions included twice weekly to twice monthly grab sampling data for 2004-2009 and daily data for 2015-2018. To minimize the influence of the Rappbode reservoir in the upper Bode River, observed reservoir outflow was used as the input flow when setting up the model.

Before calibrating the model, sensitivity analysis was performed to identify the most influential parameters using the Morris method (Morris, 1991). Parameter samples were generated using radial-based Latin-Hypercube sampling, and 200 trajectories were set to ensure convergence of the sensitivity analysis. Sensitivity indices (absolute mean (μ) and standard deviation (σ) of each parameter's elementary effect) were calculated using the SAFE tool (Sensitivity Analysis For Everybody, (Pianosi, Sarrazin and Wagener, 2015)). The sensitivity ranking was obtained by plotting μ vs. σ for all parameters; the more to the right and top of the plot a point is located, the more the parameter is influential and interrelated with other parameters, respectively. The Dynamically Dimensioned Search (DDS) method (Tolson and Shoemaker, 2007) was used to calibrate the most influential parameters, with 50,000 iterations as the terminal criterion. The detailed procedure of parameter sensitivity analysis and calibration can be found in Yang et al. (2018).

The multi-objective function for calibration consisted of multi-criteria, multi-site and multi-variable functions. We selected the Nash-Sutcliffe Efficiency (NSE) and the logarithm-transformed NSE (lnNSE) as objective criteria, in which the latter gives more weight to low values. The combined NSE and lnNSE as objective criteria increase the potential to find a robust parameter set for both high flow and low flow. In addition, six internal gauging stations were considered to calibrate discharge and nitrate concentrations simultaneously, with a weight-aggregated multi-variable function, as follows:

$$OF_{mutil-v} = min\{w_q OF^{q}_{mutil-s} + w_n OF^{n}_{mutil-s}\} \quad (1)$$

where $OF^{q}_{mutil-s}$ and $OF^{n}_{mutil-s}$ denote multi-site objective functions for discharge and nitrate concentration, respectively; and w_q= 0.9 and w_n= 0.1 denote weights for discharge and nitrate concentration objectives, respectively. Three goodness-of-fit metrics were used to evaluate model performance: NSE, Kling-Gupta Efficiency (KGE) and Percentage BIAS (PBIAS) (e.g., Gupta et al., 2009; Moriasi et al., 2015).

3.3.5. Trend analysis

Observed discharge and nitrate concentration time series at the six gauging stations were first aggregated into a monthly time step to minimize effects of different observation frequencies. Missing values in the observed nitrate time series were interpolated using the Kalman smoothing method in the R package *imputeTS* (version 4.0.2) (R Core Team., 2020). Each time series, Y_t (i.e., monthly nitrate or discharge) was analysed by using Mann-Kendall trend test,

which was performed using the mk.test function in the R package *trend* (version 1.1.4), then broken down into trend, seasonality and random components using the following equation:

$$Y_t = T_t + S_t + e_t \quad (2)$$

where T_t is the trend component, S_t is the seasonal component and e_t is a random component, which represents residuals.

The trend component was determined from a moving average with a symmetric window(Cleveland, 1990) using the STL function in the R package *stats* (version 4.0.2), which has been successfully used to analyse seasonal and long-term nitrate trends (Stow et al., 2014, 2015). The trends of monthly discharge and nitrate concentration were then normalized using min-max normalization.

3.4. Results

3.4.1. Sensitivity results

In this study, the mHM-Nitrate model included 72 parameters (61 for hydrological processes and 11 for nitrate processes). Simultaneous parameter sensitivity analysis showed that hydrological predictions were the most sensitive (Figure 3.2). Predictions of runoff were most sensitive to pet1 (the terrain-aspect correction of potential evapotranspiration), sm10 (the transfer function used to calculate soil saturated hydraulic conductivity) and sm17 (used to calculate the fraction of water that infiltrates through soil layers).

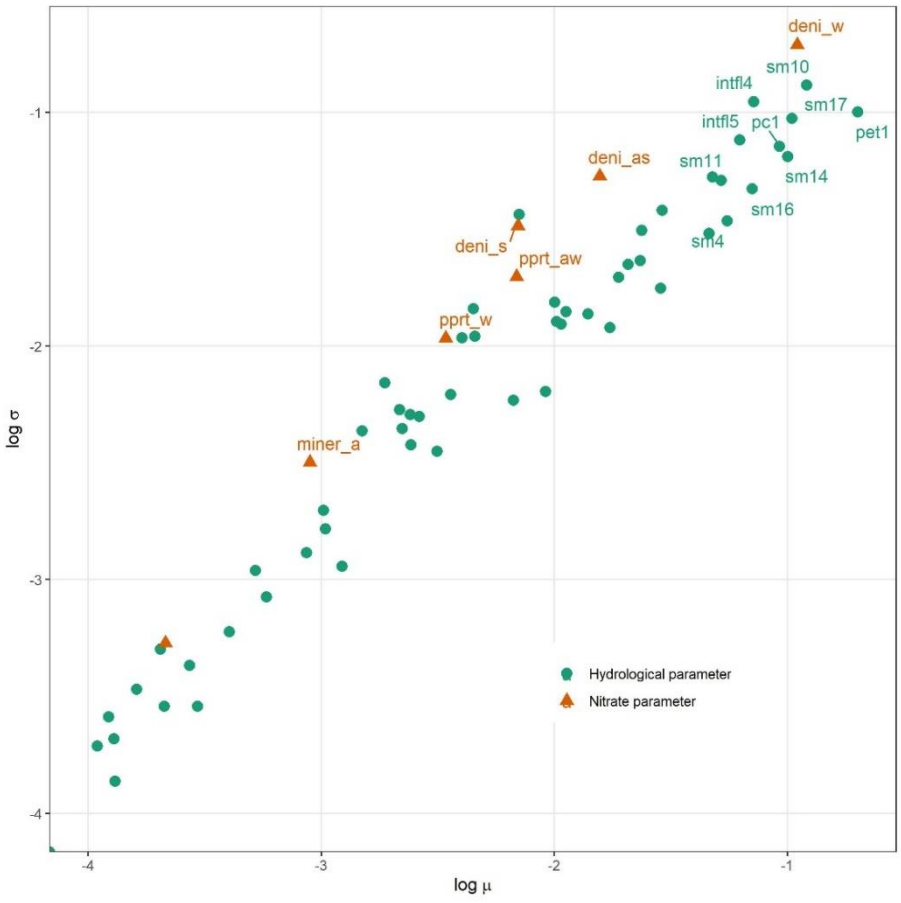

Figure 3.2. Simultaneous parameter sensitivity ranking of the 60 most influential parameters of the mHM-Nitrate model. The 16 labelled parameters (the top 10 hydrological and 6 nitrate parameters, respectively) are related to soil moisture (sm), evapotranspiration (pet), interflow generation (intfl), soil denitrification rates in the arable area (deni_as) and non-arable area (deni_s), mineralization rate in the arable area (miner_a), in-stream denitrification rates (deni_w) and in-stream primary production rate in the arable area (pprt_aw) and non-arable area (pprt_w). See Table 3.1 for additional definitions. The more a point is near the right and top of the plot, the more the parameter is influential and interrelated with other parameters, respectively. Note the log-log scales.

For nitrate submodel, the most sensitive parameters were the in-stream denitrification rate (deni_w) (for the entire Bode stream network) and two land-use parameters (deni_as and deni_s) (soil denitrification rate in the agricultural and non-agricultural areas, respectively) (Table 3.1). In line with the results of Yang et al. (2018) and Cuntz et al. (2015), the two most influential parameters for hydrological predictions were pet1 and sm10. Generally, the larger the associated flux, the more influential the parameter became (Cuntz et al., 2015). Because pet1 is directly related to evapotranspiration, which is the largest flux after precipitation in the water-balance equation, it was more influential in summer. Parameter sm10, a multiplier for saturated hydraulic conductivity, which influences the infiltration rate, became more influential during precipitation and snowmelt. The soil-moisture-related parameter sm17 was influential, but it was not for Yang et al. (2018), which indicates a larger influence of infiltration in the lowland part of the Bode catchment than in the Selke sub-catchment. Based on the sensitivity analysis, the top ten hydrological parameters and top five nitrate parameters were selected for model calibration.

Table 3.1. Description of parameters calibrated in the mHM-Nitrate model, their initial ranges and optimal values.

Process	Parameter	Description	Initial range	Optimal value
PET	pet1 (Shevenell, 1999)	Parameter for aspect correction of input potential evapotranspiration data	[6.99E-1, 1.30E+0]	9.80E-1
Soil moisture	sm10 (Cosby et al., 1984)	Transfer function parameter used to calculate soil saturated hydraulic conductivity	[-1.20E+0, -2.85E-1]	-8.42E-1
	sm17 (Brooks and Corey, 1964)	Parameter that determines the relative contribution of precipitation or snowmelt to runoff	[1.00E+0, 4.00E+0]	3.83E+0
	sm14 (Brooks and Corey, 1964)	Fraction of roots used to calculate actual evapotranspiration in forest areas	[9.00E-1, 9.99E-1]	9.73E-1
	sm16 (Brooks and Corey, 1964)	Fraction of roots used to calculate actual evapotranspiration in permeable areas	[1.00E-3, 8.99E-2]	5.63E-3
	sm4 (Cosby et al., 1984)	Pedotransfer function parameter used to calculate maximum soil moisture content	[6.46E-1, 9.51E-1]	9.44E-1
	sm11 (Cosby et al., 1984)	Pedotransfer function parameter used to calculate soil saturated hydraulic conductivity	[6.01E-3, 2.59E-2]	6.23E-3
Percolation	pc1	Parameter used to calculate the percolation coefficient	[0.00E+0, 5.00E+1]	1.44E+1
Interflow	intfl4	Slow interflow recession coefficient	[1.00E+0, 3.00E+1]	2.38E+1
	Intfl5	Slow interflow exponent coefficient	[5.00E-2, 2.99E-1]	5.55E-2
In-stream denitrification	deni_w	General parameter of in-stream denitrification rate (kg m^{-2} d^{-1})	[1.00E-8, 5.00E-2]	2.99E-4
Soil denitrification	deni_as	Soil denitrification rate on agricultural land (d^{-1})	[1.00E-8, 1.10E-1]	3.35E-3

	deni_s	Soil denitrification rate on non-agricultural land (d^{-1})	[1.00E-8, 1.10E-1]	5.50E-8
In-stream assimilation	pprt_aw	Primary production rate in agricultural streams (kg m^{-3} d^{-1})	[1.00E-8, 1.00E+0]	1.68E-1
	pprt_w	Primary production rate in non-agricultural streams (kg m^{-3} d^{-1})	[1.00E-8, 1.00E+0]	1.11E-1

3.4.2. Model performance

The mHM-Nitrate model reproduced the observed discharge and nitrate concentration at the six gauging stations reasonably well. Results for three typical gauging stations (Meisdorf, Hausneindorf and Stassfurt) are shown in this article, while those for other stations can be found in the Supplementary material. These three stations reflect different combinations of dominant land use and weather conditions from the upstream to downstream parts of the Bode catchment. Meisdorf represents a forest-dominated area, while Hausneindorf represents a mixture of forest and agricultural areas ranging from mountains to lowlands. In contrast, Stassfurt represents a lowland catchment with a mixture of forest and agricultural areas.

Daily discharge predictions (Figure 3.3) and goodness-of-fit metrics (Table 3.2) showed that mHM-Nitrate captured discharge dynamics well during both calibration (2010-2014) and validation (2004-2009 and 2015-2018) periods (lowest NSE of 0.76 and 0.73, respectively). The model performed worse for the forest area than for the mixture of forest and agricultural areas. For example, the Meisdorf station had the lowest performance during the calibration period (KGE and PBIAS of 0.64 and -14.1%, respectively) and the first validation period (2004-2009) (KGE and PBIAS of 0.66 and -17%, respectively). The model performed best for all stations during the second validation period (2015-2018) (lowest NSE and KGE of 0.83 and 0.91, respectively; largest PBIAS of 1.6%) (Figure 3.3, Table 3.2).

The model represented seasonal dynamics in observed nitrate concentrations well (Figure 3.3). Nitrate concentrations had similar seasonal patterns as discharge during the study period, which reflects their control by hydrological processes. In the forest area (Meisdorf station), the model captured long-term nitrate concentration dynamics (2004-2018) reasonably well (lowest KGE of 0.66 and largest PBIAS of 23.70%) (Table 3.2). Model performance decreased for mixed forest and agricultural areas, as indicated by the lowest KGE values for nitrate concentrations at the Hausneindorf and Nienhagen stations (0.21 and 0.59, respectively).

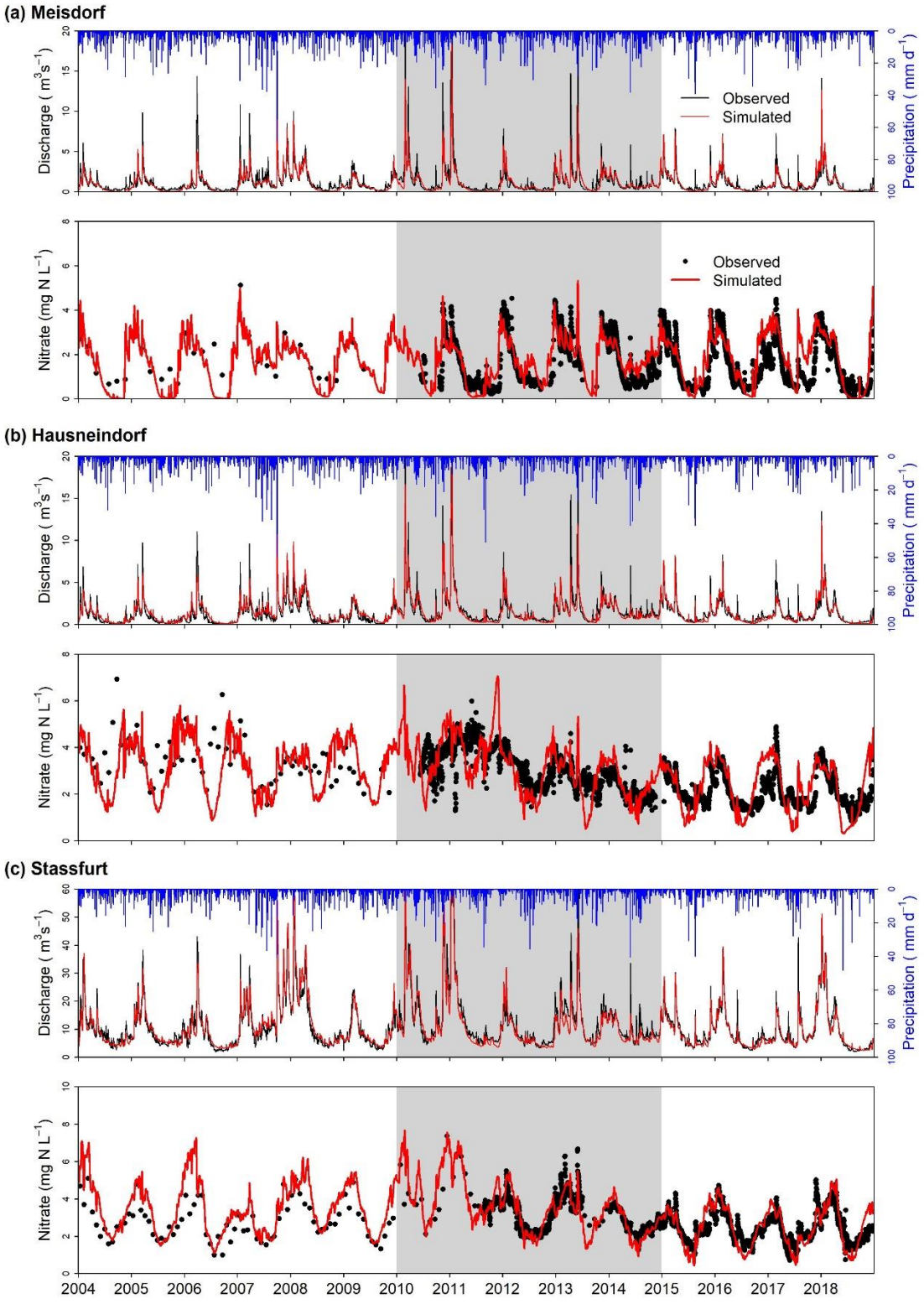

Figure 3.3. Observed and simulated daily discharge and nitrate concentration time series during the calibration (2010-2014) (shaded area) and validation period (2004-2009 and 2015-2018) at the three gauging stations: (a) Meisdorf, (b) Hausneindorf and (c) Stassfurt.

The model reproduced observed daily nitrate loads well for the Meisdorf, Hausneindorf and Stassfurt gauging stations, with the lowest coefficient of determination (R^2) of 0.73 (Figure S3.2). The model reproduced observed daily loads better for mixed forest and agricultural

areas, represented by the Hausneindorf and Stassfurt stations (R^2 of 0.83 and 0.85, respectively). The lower performance for simulated daily loads in the forest area (i.e., Meisdorf station) can be explained by underestimating discharge during high flow periods (Figure 3.3a), which resulted in underestimating daily nitrate loads (Figure S3.2a). Like simulated discharge, the daily load was reproduced best during the second validation period (2015-2018) (NSE ranged from 0.81-0.92 and PBIAS ranged from -2 to 9.6 among the six gauging stations (Table 3.2).

Table 3.2. Model evaluation metrics (Nash-Sutcliffe Efficiency (NSE), Kling-Gupta Efficiency (KGE) and Percentage BIAS (PBIAS) for daily discharge (Q), nitrate concentration (Nitrate) and nitrate load (Load = Nitrate × Q) at the Meisdorf, Hausneindorf, Wegeleben, Nienhagen, Hadmersleben and Stassfurt gauging stations during the calibration (2010-2014) and validation periods (2004-2009 and 2015-2018).

Station	Criterion	Calibration			Validation					
		2010-2014			2004-2009			2015-2018		
		Q	Nitrate	Load	Q	Nitrate	Load	Q	Nitrate	Load
Meisdorf	NSE	0.77	0.59	0.66	0.73	0.35	0.88	0.83	0.40	0.81
	KGE	0.64	0.72	0.56	0.66	0.68	0.66	0.91	0.66	0.81
	PBIAS	-14.10	12.30	-12.60	-17.00	-10.20	-20.30	1.60	23.70	9.60
Hausneindorf	NSE	0.85	-0.35	0.80	0.74	-0.84	0.82	0.86	-0.70	0.84
	KGE	0.85	0.42	0.89	0.76	0.21	0.82	0.91	0.27	0.87
	PBIAS	-8.10	-0.10	-1.30	15.50	-8.70	15.70	-5.10	9.00	1.00
Wegeleben	NSE	0.91	-0.39	0.74	0.94	0.08	0.89	0.93	-	-
	KGE	0.90	0.48	0.74	0.92	0.40	0.91	0.91	-	-
	PBIAS	-7.90	-12.00	-16.00	-4.60	-4.90	-4.10	-3.40	-	-
Nienhagen	NSE	0.76	0.15	0.90	0.76	-0.34	0.81	-	-1.59	-
	KGE	0.85	0.72	0.83	0.78	0.50	0.82	-	0.11	-
	PBIAS	2.90	-19.60	-13.30	19.90	-10.50	13.20	-	-9.20	-
Hadmersleben	NSE	0.87	0.67	0.88	0.93	0.65	0.93	0.94	0.25	0.92
	KGE	0.90	0.74	0.92	0.94	0.76	0.81	0.95	0.61	0.93
	PBIAS	-7.40	3.00	-5.50	1.90	19.10	17.30	-4.30	11.10	4.60
Stassfurt	NSE	0.86	0.65	0.80	0.90	0.23	0.81	0.94	0.44	0.92
	KGE	0.89	0.77	0.73	0.91	0.61	0.67	0.95	0.59	0.96
	PBIAS	-8.50	1.70	-14.20	4.00	22.10	25.00	-3.50	1.60	-2.00

3.4.3. Discharge and nitrate concentration trends

To evaluate further the ability of mHM-Nitrate to simulate spatiotemporal nitrate dynamics in the Bode catchment, the trends of monthly mean observed and simulated nitrate concentrations at the three gauging stations were examined. The three components of monthly mean observed nitrate concentration showed the influence of trend, seasonal and random effects (Figure S3.3). The model captured the observed normalized monthly trends of nitrate concentration well (Figure 3.4) (Spearman's correlation coefficient of 0.54, 0.83 and 0.82 for Meisdorf, Hausneindorf and Stassfurt, respectively ($p < 0.01$)), indicating that the model successfully represented temporal dynamics of nitrate concentration trends at the three gauging stations. In addition, during 2004-2018, nitrate concentration decreased significantly ($p<0.05$) at Hausneindorf but non-significant at the Meisdorf and Stassfurt stations (Table S3.1).

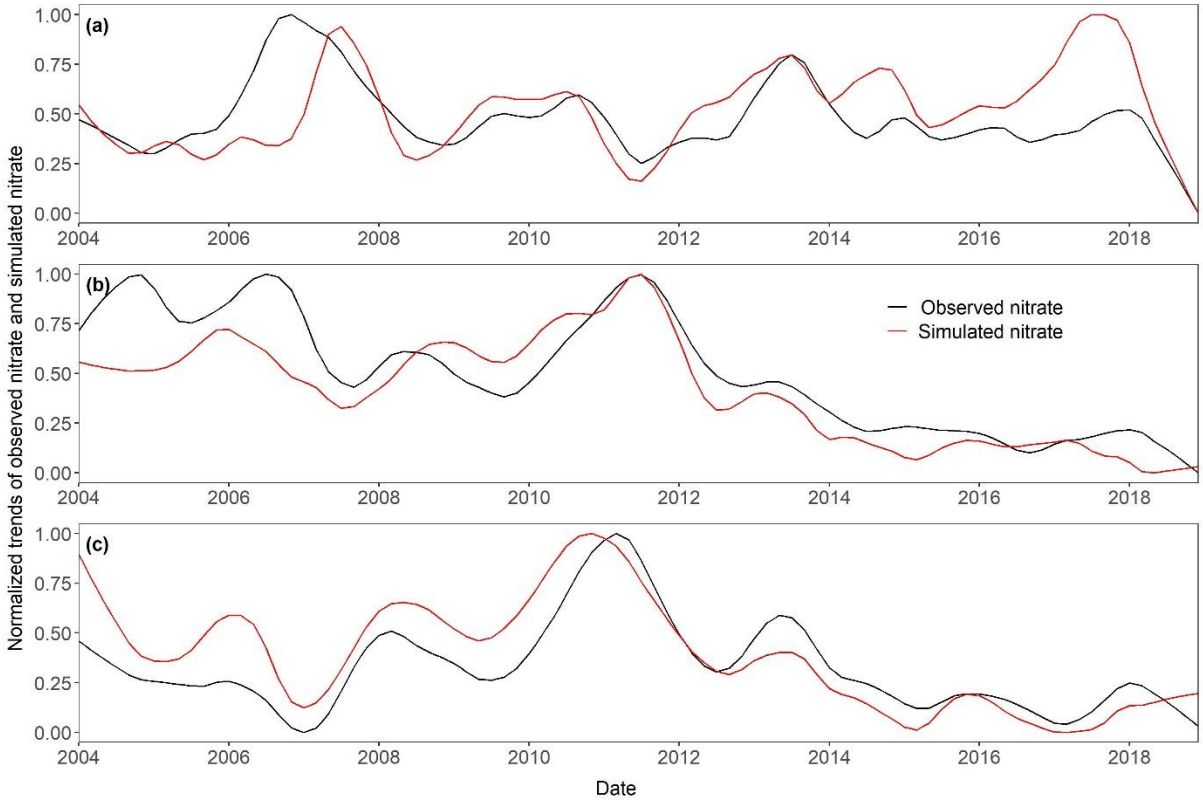

Figure 3.4. Normalized trends of monthly mean observed (aggregated from daily and monthly grab sampling data) nitrate concentration (black lines) and simulated (aggregated from daily mHM-Nitrate model results) nitrate concentration (red lines) from 2004-2018 at the gauging stations (a) Meisdorf, (b) Hausneindorf and (c) Stassfurt.

The trends of monthly mean observed discharge and nitrate concentration were normalized at the Meisdorf, Hausneindorf and Stassfurt gauging stations from 2004-2018. Normalized trends of the monthly mean observed discharge and nitrate concentration were strongly correlated at Meisdorf and Stassfurt from 2004-2018 (Spearman's correlation coefficient of 0.65 and 0.59, respectively ($p < 0.01$)) (Figure 3.5), which indicates that hydrology influenced nitrate concentration strongly.

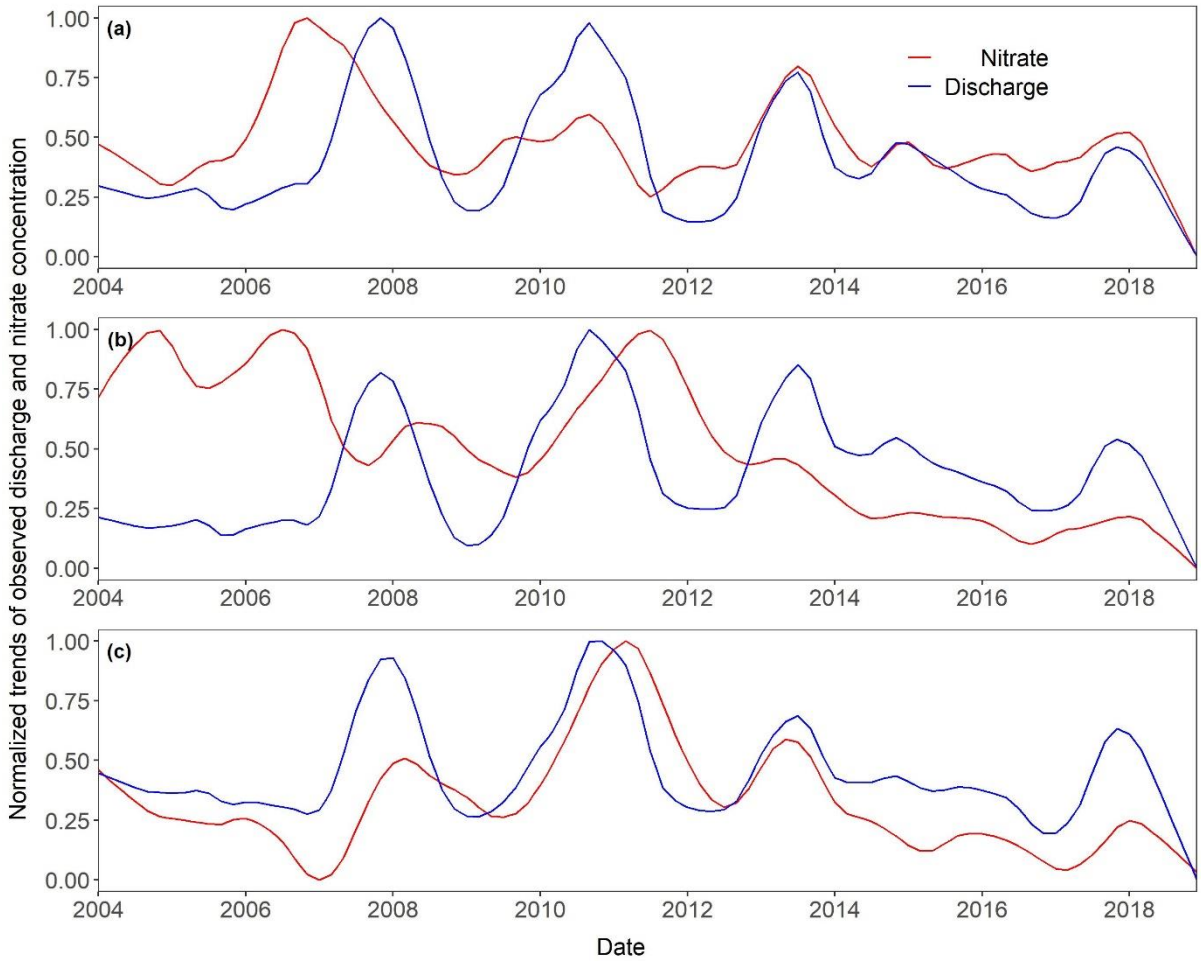

Figure 3.5. Normalized trends of monthly mean observed discharge (blue lines) and nitrate concentration (red lines) from 2004-2018 at the gauging stations (a) Meisdorf, (b) Hausneindorf and (c) Stassfurt.

3.4.4. Spatial heterogenous effects of drought on terrestrial nitrate export

The heterogeneous spatial changes in runoff components and thus nitrate concentrations (Figure S3.6) resulted in high spatial variability in nitrate load exported from the terrestrial compartment (Figure 3.6). The mean annual nitrate load in total runoff showed a spatial pattern that clearly depended on land use (Figure 3.6c), with the largest nitrate export from lowland agricultural area (Class I) and mountain pasture area (Class IV) (ca. 7 and 19 kg N ha^{-1} $year^{-1}$, respectively). The mean annual nitrate load in baseflow showed a similar spatial pattern (Figures 3.6b vs. 3.7c), with a mean of 5 and 6 kg N ha^{-1} $year^{-1}$ in Classes I and IV, respectively. In the 2015-2018 drought period, the nitrate load in total runoff decreased by a mean of 40% (Figure 3.6f), mainly due to the decreased nitrate export loads from interflow and baseflow in the lowland area (Figures 3.7d-e). For example, nitrate loads in interflow and baseflow decreased by 72% and 77%, respectively, in Class II, but they increased in baseflow by 16% in Class IV. The increased nitrate load of interflow, baseflow and total runoff in mountain area during the drought period were due to higher nitrate concentration in interflow, baseflow and total runoff in these areas (Figures S3.6n-p).

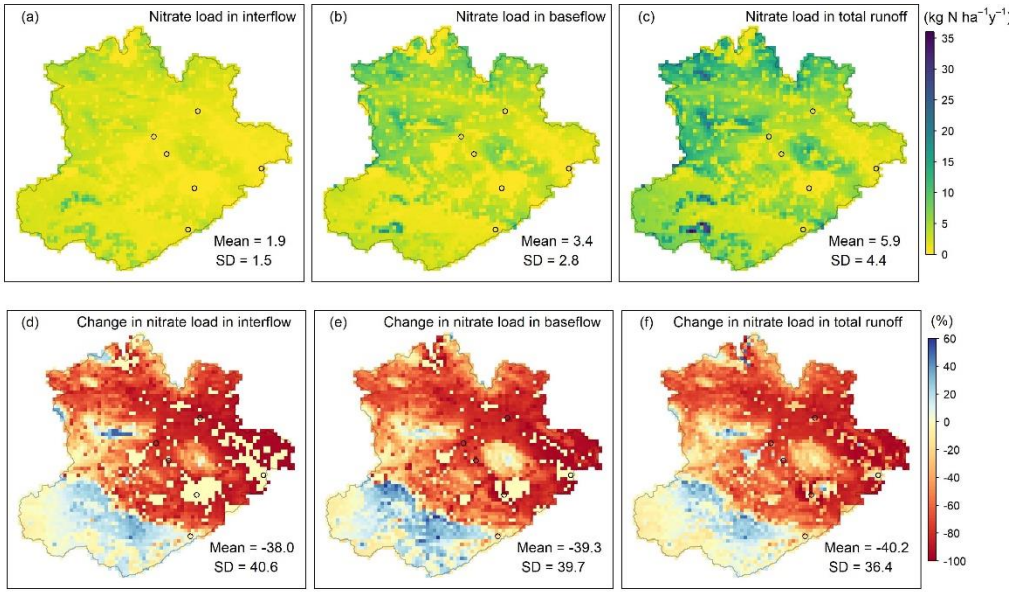

Figure 3.6. Spatial distribution of simulated (a-c) annual mean load of interflow, baseflow and total runoff from 2004-2014 and (d-f) the corresponding change from 2015-2018 compared to 2004-2014.

3.4.5. Drought effects on nitrate surplus among soil-land-use classes

To identify the internal processes that influence nitrate dynamics in the Bode catchment better, soil nitrate sources and sinks for the five soil-land-use classes were examined. For the agriculture-dominated lowland Classes I-III, the nitrate source was mainly fertiliser (including mineral fertiliser and mineralized organic manure), which decreased slightly (by 5%) during the drought period compared to the pre-drought period (Table 3.3). It is noteworthy that the decreased fertiliser is due to different crop rotations during the drought period compared to pre-drought period. Crop uptake was the main nitrate sink (83-90% of the total fertiliser amount) in Classes I-III, and it decreased slightly (ca. 10%) during the drought period compared to the pre-drought period. Soil denitrification, which can include denitrification in the upper groundwater when the water table is high, decreased considerably in Classes II and III (by 28% and 43%, respectively). This was likely due to lower soil moisture induced by drought in the lowland, which decreased crop uptake and soil denitrification during the drought period. Terrestrial export also decreased greatly in Classes I-III. Therefore, soil N surplus, which equals input (total fertiliser amount and precipitation deposition) minus output (crop/plant uptake) was higher in Classes I-II (4.4 and 3.1 kg N ha^{-1} y^{-1}, respectively) during the drought period than the pre-drought period, indicating that more nitrate was stored in the soil in the lowland area during the drought period.

In the mountain area, nitrate sources and sinks in Classes IV and V responded differently to drought than these of Classes I-III (Table 3.3). The total amount of fertiliser in Classes IV and V remained relatively constant during the drought period. Class IV had the lowest soil denitrification among the five classes, perhaps due to lower total fertiliser amount and lower temperature in mountain pastures. In addition, soil denitrification and terrestrial export in Classes IV and V did not change during the 2015-2018 drought period compared to the 2004-2014 period, which indicates that drought had less effect in the mountain area.

Table 3.3. Nitrate balances (mean ± standard deviation) in the five soil-land-use classes during the 2004-2014 pre-drought period and, in parentheses, their corresponding values in the 2015-2018 drought period.

Nitrate balances	Soil-land-use classes					
(kg N ha^{-1} y^{-1})	I	II	III	IV	V*	Catchment mean
Total fertiliser amount	172.5 ± 8.2 (163.1 ± 7.7)	168.8 ± 10.0 (159.6 ± 9.4)	170.5 ± 9.2 (161.3 ± 8.7)	63.8 ± 16.4 (64.2 ± 16.9)	158.3 (163.5)	113.0 ± 69.8 (107.4 ± 65.6)
Precipitation deposition	11.7 ± 0.6 (9.9 ± 1.1)	11.2 ± 0.5 (9.2 ± 0.9)	11.0 ± 0.2 (8.7 ± 0.3)	17.7 ± 0.4 (16.7 ± 0.4)	14.7 (13.7)	13.2 ± 3.3 (11.5 ± 3.4)
Crop/plant uptake	142.8 ± 6.8 (127.2 ± 6.9)	142.6 ± 8.0 (128.3 ± 8.0)	154.1 ± 6.6 (143.6 ± 7.6)	39.8 ± 17.6 (37.3 ± 15.8)	121.2 (106.4)	96.4 ± 55.2 (86.7 ± 49.0)
Soil denitrification	34.2 ± 3.3 (28.1 ± 5.6)	32.5 ± 4.5 (23.4 ± 5.3)	21.0 ± 4.4 (12.8 ± 2.0)	2.5 ± 3.5 (2.6 ± 3.7)	24.0 (25.0)	20.3 ± 15.2 (16.7 ± 13.0)
Terrestrial export	7.2 ± 3.6 (3.2 ± 3.2)	4.0 ± 2.6 (1.2 ± 1.8)	0.3 ± 0.2 (0.02 ± 0.02)	19.4 ± 3.5 (20.3 ± 2.3)	12.1 (13.5)	6.0 ± 4.1 (3.7 ± 3.7)

*Note that for Class V only one grid was selected.

3.4.6. Drought effects on in-stream nitrate retention

Annual and seasonal mean lateral nitrate loading from terrestrial to streams decreased during the drought period compared to the pre-drought period, except for the streams upstream of Meisdorf (Table 3.4). Lateral nitrate loading reduced by 41% and 44% in summer and autumn within the whole river network; meanwhile, in-stream retention amount decreased by 20% and 16%, respectively, plausibly due to smaller stream benthic area and lower nitrate concentrations during the drought period. Lateral nitrate loading reduced more than that of in-stream retention during the drought period, and this likely resulted in a higher in-stream retention efficiency (Table 3.4).

Table 3.4. Seasonal and annual mean values of nitrate loading and in-stream retention at station Meisdorf (Meis), Hausneindorf (Haus) and Stassfurt (Stass) during the 2004-2014 pre-drought period and, in parentheses, their corresponding values in the 2015-2018 drought period.

	Winter			Spring			Summer			Autumn			Annual		
Load/In-stream retention (kg N d^{-1})	Meis	Haus	Stass	Meis	Haus	Stass	Meis	Haus	Stass	Meis	Haus	Stass	Meis	Haus	Stass
Load	423.3	837.8	7848.9	317.8	730.0	6947.1	103.0	299.9	2972.9	126.3	332.0	3324.3	229.5	539.0	5249.5
	(554.7)	(746.1)	(5529.2)	(303.2)	(468.8)	(4044.1)	(56.2)	(157.6)	(1758.5)	(91.7)	(178.5)	(1853.8)	(238.3)	(375.2)	(3233.8)
Retention	5.7	19.1	211.5	35.3	117.1	1232	33.7	143.0	1671.4	16.2	61.3	728.4	22.4	83.9	947.7
	(8.9)	(25.8)	(267.2)	(39.2)	(113.6)	(1124.5)	(28.1)	(98.5)	(1332.4)	(16.0)	(50.4)	(615.2)	(22.7)	(71.1)	(823.4)
Percentage of retention	1.4	2.3	2.7	11.1	16.0	17.7	32.7	47.7	56.2	12.8	18.5	21.9	9.8	15.6	18.1
(%)	(1.6)	(3.5)	(4.8)	(12.9)	(24.2)	(27.8)	(50.0)	(62.5)	(75.8)	(17.5)	(28.2)	(33.2)	(9.5)	(18.9)	(25.5)

Note. The load was the sum of model-simulated total terrestrial loads from the drainage area upstream of each station, and in-stream retention was the sum of net assimilation uptake and denitrification amount from the stream network upstream of each station.

3.5. Discussion

3.5.1. Model performance evaluation

The mHM-Nitrate model reproduced the observed discharge throughout the Bode catchment well (mean NSE of 0.85 and PBIAS $\leq \pm 20\%$), according to guidelines for evaluating the performance of catchment simulations (Moriasi et al., 2015). This accuracy is similar to those of previous simulations of the study area (e.g., Mueller et al., 2016; Nguyen et al., 2021; Yang et al., 2018). Comparing the three representative gauging stations, the performance at the Meisdorf station was relatively low, as indicated by lower NSE and KGE (Table 3.1), perhaps due to underestimating peak flow events and the high sensitivity of NSE to extreme values (e.g., Krause, Boyle and Bäse, 2005). Similarly, the low KGE was likely due to underestimating high flow values in 2010, 2013 and 2014 (Figure 3.3a). The model may have underestimated peak flow events because of the inaccurately measured precipitation and the lower density of meteorological stations. Specifically, daily precipitation is not sufficiently precise to represent a detailed discharge response, especially in the headwater of the Bode catchment (due to high heterogeneity in precipitation), where many storm events last only a few hours. Moreover, the spatial coverage of the meteorological stations decreased significantly during the recent period, especially in the mountain area of the catchment. For example, the number of precipitation gauging stations in the Selke sub-catchment decreased from 16 to only 8 after 2004 (Yang et al., 2018). Generally, the decrease in detailed precipitation records decreased performance in predicting discharge in the headwater area, which is known for its high spatiotemporal variability in precipitation due to the varying elevation. Therefore, the less accurate precipitation inputs from the lower station density could explain the slight underestimate of water balance at Meisdorf (PBIAS of -14% and -17% for the calibration and first validation period, respectively). However, the model slightly overestimated the water balance for the Hausneindorf station during the first validation period (Table 3.2). Jiang, Jomaa and Rode (2014) and Winter et al. (2021) stated that water from the lower Selke River was abstracted to fill pit lakes from 1998-2009 at a rate of 3.1 million m^3 $year^{-1}$, which was ca. 8% of the mean annual stream flow from 2004-2009. Although the water balance remained overestimated after considering this abstraction, these overestimates occurred mainly during the low-flow period and were acceptable when the corresponding runoff depth was considered (i.e., the largest PBIAS of 15.5% at Hausneindorf corresponded to a runoff depth of only 12.8 mm/year).

The model can represent observed nitrate concentrations well for several reasons. First, its flexible structure ensures sufficient spatial representation of catchment heterogeneity as well as of spatiotemporal variability in meteorological inputs (Kumar, Samaniego and Attinger, 2010; Samaniego, Kumar and Attinger, 2010; Yang et al., 2018). In addition, it can adequately represent the diffuse source inputs and turnover (i.e., agricultural practices, crop rotation and plant uptake) and point-source contributions (input time series can be added at the real stream locations) at the resolution of the input data, which increases the model's ability to represent spatial variability in nitrate sources (Yang et al., 2018). Selecting an appropriate calibration period under varying conditions (i.e., not at steady-state equilibrium) is crucial for model training and refinement of internal processes. For example, during the calibration period, 2011

was a wetter year, while 2012 was a drier year. Thus, selecting a calibration period that encompasses varying hydrological conditions helps activate all model components. This approach agrees with Engel et al. (2007), who suggested that both calibration and validation periods should have high and low flows to increase a model's robustness. Together, these characteristics helped to identify model parameters better and reliably estimate nitrate contributions from different runoff components, which is crucial for representing nitrate concentrations spatiotemporally in the entire Bode catchment.

The most influential nitrate sub-model parameter was related to in-stream denitrification, while in the study of Yang et al. (2018), which focused more on upstream catchments, the most influential parameter was related to soil denitrification. This is presumably due to the larger total stream benthic areas for the Bode catchment, which is in line with Yang et al. (2019) who found that there is a significant relationship between stream benthic area and in-stream denitrification rate, reflecting the relative importance of in-stream processes increases with increasing catchment size. The slightly lower performance of mHM-Nitrate at the Hausneindorf station than at the other stations was likely due to the lack of detailed time series of point sources from urban areas during the low-flow period, especially in the initial period of operation of the WWTPs, as they started to function properly only in 2007 (Yang et al., 2018). The high nitrate concentrations during summers before 2007 (Figure 3.3b) were likely due to the untreated point sources, as discussed by Yang et al. (2018). After 2007, the model captured dynamics of nitrate concentration well at Hausneindorf. In addition, some houses (mainly summer houses) in the Selke sub-catchment are not connected to the sewage system, which generates additional unknown point sources and decreases model performance under low-flow conditions. The lack of detailed spatial cropping information for the entire Bode catchment and the need to rely on only rough survey information might introduce uncertainty. Based on the uncertainty analysis at the Selke sub-catchment by Yang et al. (2018) using the MCMC-based DREAM tool (ter Braak and Vrugt, 2008; Vrugt, 2016), the simulations uncertainty of discharge and nitrate concentration were well constrained and in line with the DDS calibration results. Nevertheless, mHM-Nitrate successfully identified decreasing trends in observed nitrate concentrations at the Hausneindorf and Stassfurt lowland stations (Figures 3 and 4).

3.5.2. Explaining changes in nitrate concentration during drought years

Recent droughts (2015-2018) in the Bode catchment provided an opportunity to investigate the internal processes that influence nitrate dynamics under changing weather conditions at the catchment scale. Observed nitrate concentration showed a decreasing trend in lowland agricultural areas (i.e., Hausneindorf and Stassfurt stations) but not significant in the mountain forest area (i.e., Meisdorf station) (Figure 3.4). Results suggested that the influence of drought on nitrate concentration could be explained by (i) spatiotemporal differences in hydrological response and (ii) its associated effects on soil and in-stream nitrate processes during the 2015-2018 drought period compared to the 2004-2014 pre-drought period.

Seasonal total runoff decreased in the entire Bode catchment during the drought period (Figures S7m-p). The decrease was larger in the lowland area, due to the combined effects of meteorology and soil properties. Annual precipitation in the 2015-2018 drought period did not differ greatly from that in long-term historical records (1971-2000) from DWD. When

considering the temporal distribution of precipitation, however, precipitation decreased greatly in winter and spring in the lowland agricultural area during the drought period, especially in Class II (by 25% and 30%, respectively) (Figures S7a-b). Soil moisture decreased continuously in all seasons and was not replenished during the rewetting seasons due to reduced precipitation in the lowland area (Figures S7i-l). In addition, the modeled soil moisture of the third layer in Classes (I-III) showed a significant decline during the drought period (Figure S3.8).

Consequently, this process could decrease unsaturated zone storage and groundwater recharge during the drought period. This further explains the decrease in mean annual interflow, baseflow and total runoff in the lowland area during the 2015-2018 drought period compared to 2004-2014. Furthermore, the decrease in soil moisture content may have decreased hydrological connectivity between hillslope and streams during the drought period (Figures S6f-h), thus increasing the potential for soil profiles to become disconnected from the stream channel and shallow groundwater (Davis et al., 2014; Outram et al., 2016). In contrast, total runoff in the mountain area decreased only slightly during the drought period, perhaps due to seasonal precipitation and slightly decreased soil moisture content there (Figure S3.7). This result agrees with other studies that reported that flatter and less forested catchments are more vulnerable to long-term drought (Saft et al., 2015).

The large decrease in nitrate concentration in the lowland area during the drought period, represented by the Hausneindorf and Stassfurt stations (Figures 4b-c), was plausible because the decrease in total runoff in Classes I-III greatly reduced soil nitrate export to surface water (Figures 3.7d-f, Table 3.3). This indicates that nitrate became transport-limited in the lowland area during the drought period. In addition, upstream discharge with low nitrate concentration could dilute downstream nitrate concentration during the drought period. Furthermore, drought increased water temperatures, and longer water residence time in summer could have stimulated in-stream uptake and denitrification efficiency (Table 3.4) (Hosen et al., 2019). Therefore, the combined effects of terrestrial export load and in-stream processes could explain the decrease of in-stream nitrate concentrations in lowland areas (e.g., at the Hausneindorf and Stassfurt stations in Figures 3.4b-c). In contrast, nitrate concentration in the mountain forest-dominated area showed a constant pattern during the drought period compared to the pre-drought period, as reflected by the Meisdorf station (Figures 3a and 4a). This pattern could have occurred because the nitrate source in the mountain forest-dominated area comes mainly from patches of agricultural area, which decreased slightly during the drought period in Class IV (Table 3.3). Although total runoff increased in the mountain area in winter during the drought period, in-stream nitrate concentrations were similar to those during the pre-drought period (Figures S3.7m vs. 3.3a). In addition, in-stream retention in winter was low and did not influence nitrate concentration, which indicated that nitrate could be supply-limited in the mountain area.

Previous studies have reported a decrease in stream nitrate concentrations during droughts (e.g., van Vliet and Zwolsman, 2008; Yevenes, Figueroa and Parra, 2018). They also explained the decrease in nitrate concentration by less diffuse supply based on empirical relations between nitrate concentration and discharge. Our study confirmed this explanation by simulating a large decrease in soil nitrate export in the lowland area during the drought period (Figure 3.6).

3.6. Conclusion

Varying spatial trends in nitrate concentration under drought conditions were observed in the Bode catchment in central Germany. To explain the mechanisms that influence the changes in trends, calibrated mHM-Nitrate model outputs and internal processes were compared between a drought period (2015-2018) and a pre-drought period (2004-2014). Results indicated that nitrate export from the terrestrial compartment greatly decreased while in-stream retention efficiency increased during the drought periods, which could result in the decrease of in-stream nitrate concentration in the lowland area of the Bode catchment. In contrast, nitrate export and in-stream retention efficiency in the upper mountain area of the catchment changed little. Therefore, nitrate concentrations remained relatively constant in the drought and pre-drought periods. Results suggested that during the drought periods, nitrate was mainly stored in the soil rather than mobilized or transported, especially in the lowland area of the catchment. This study assessed the model's ability to represent nitrate concentrations under varying weather conditions, which could be used to study the effects of climate change. The Bode catchment is a typical mesoscale catchment in central Europe, in which the headwater is a mountain area with high precipitation, and the lowland is an agricultural area with relatively low precipitation. We expect that catchments with landscape and climate conditions similar to those of the Bode catchment (i.e., wet mountain areas and dry lowland areas) are highly vulnerable to changing weather conditions. This study showed that droughts have heterogeneous spatial effects on hydrology and water-quality responses. Therefore, water managers should specifically consider this spatial heterogeneity when managing future droughts.

Acknowledgements

X. Zhou is funded by the Chinese Scholarship Council (CSC). We thank the German Weather Service (DWD), Federal Institute for Geosciences and Natural Resources (BGR) and State Agency for Flood Protection and Water Management of Saxony-Anhalt (LHW) for providing meteorological, geological and discharge and water-quality data, respectively. The high-frequency nitrate-concentration data were provided by the TERENO (Terrestrial Environment Observatories) project.

Data Availability Statement

The model code of mHM-Nitrate is publicly available at https://zenodo.org/record/3891629.

3.7. References

Abbaspour, K.C., Yang, J., Maximov, I., Siber, R., Bogner, K., Mieleitner, J., Zobrist, J. and Srinivasan, R. 2007. Modelling hydrology and water quality in the pre-alpine/alpine Thur watershed using SWAT. Journal of Hydrology 333(2-4), 413-430.

Abdelwahab, O.M.M., Bingner, R.L., Milillo, F. and Gentile, F. 2016. Evaluation of Alternative Management Practices With the AnnAGNPS Model in the Carapelle Watershed. Soil Science 181(7), 293-305.

Agency, E.E. (2018) European waters — assessment of status and pressures 2018.

Ahmadi, M., Arabi, M., Ascough, J.C., Fontane, D.G. and Engel, B.A. 2014. Toward improved calibration of watershed models: Multisite multiobjective measures of information. Environ Modell Softw 59, 135-145.

Ajami, N.K., Duan, Q. and Sorooshian, S. 2007. An integrated hydrologic Bayesian multimodel combination framework: Confronting input, parameter, and model structural uncertainty in hydrologic prediction. Water Resources Research 43(1).

Alexander, R.B., Bohlke, J.K., Boyer, E.W., David, M.B., Harvey, J.W., Mulholland, P.J., Seitzinger, S.P., Tobias, C.R., Tonitto, C. and Wollheim, W.M. 2009. Dynamic modeling of nitrogen losses in river networks unravels the coupled effects of hydrological and biogeochemical processes. Biogeochemistry 93(1-2), 91-116.

Alexander, R.B., Smith, R.A. and Schwarz, G.E. 2000. Effect of stream channel size on the delivery of nitrogen to the Gulf ofMexico. nature 403, 758.

Andersson, L., Rosberg, J., Pers, B.C., Olsson, J. and Arheimer, B. 2005. Estimating Catchment Nutrient Flow with the HBV-NP Model: Sensitivity To Input Data. AMBIO: A Journal of the Human Environment 34(7), 521-532.

Arango, C.P., Tank, J.L., Johnson, L.T. and Hamilton, S.K. 2008. Assimilatory uptake rather than nitrification and denitrification determines nitrogen removal patterns in streams of varying land use. Limnology and Oceanography 53(6), 2558-2572.

Arheimer, B., Andréasson, J., Fogelberg, S., Johnsson, H., Pers, C.B. and Persson, K. 2005. Climate Change Impact on Water Quality: Model Results from Southern Sweden. AMBIO: A Journal of the Human Environment 34(7), 559-566.

Arnold 1998. LARGE AREA HYDROLOGIC MODELING AND ASSESSMENT. Journal of the American Water Resources Association.

Arnold, J.G., Moriasi, D.N., Gassman, P.W., Abbaspour, K.C., White, M.J., Srinivasan, R., Santhi, C., Harmel, R.D., van Griensven, A., Van Liew, M.W., Kannan, N. and Jha, M.K. 2012. Swat: Model Use, Calibration, and Validation. Transactions of the Asabe 55(4), 1491-1508.

Arnold, J.G., Srinivasan, R., Muttiah, R.S. and Williams, J.R. 1998. Large area hydrologic modeling and assessment part I: model development 1. JAWRA Journal of the American Water Resources Association 34(1), 73-89.

B. Duda, P., R. Hummel, P., S. Donigian Jr, A. and C. Imhoff, J. 2012. BASINS/HSPF: Model Use, Calibration, and Validation. Transactions of the ASABE 55(4), 1523-1547.

Baffaut, C., Dabney, S.M., Smolen, M.D., Youssef, M.A., Bonta, J.V., Chu, M.L., Guzman, J.A., Shedekar, V.S., Jha, M.K. and Arnold, J.G. 2015. Hydrologic and water quality modeling: Spatial and temporal considerations. Transactions of the ASABE 58(6), 1661-1680.

Baker, D.W., Bledsoe, B.P. and Price, J.M. 2012. Stream nitrate uptake and transient storage over a gradient of geomorphic complexity, north-central Colorado, USA. Hydrological Processes 26(21), 3241-3252.

Baldwin, D.S., Rees, G.N., Mitchell, A.M. and Watson, G. 2005. Spatial and temporal variability of nitrogen dynamics in an upland stream before and after a drought. Marine and Freshwater Research 56(4), 457-464.

Ballard, T.C., Sinha, E. and Michalak, A.M. 2019. Long-Term Changes in Precipitation and Temperature Have Already Impacted Nitrogen Loading. Environ Sci Technol 53(9), 5080-5090.

Bandini, F., Olesen, D., Jakobsen, J., Kittel, C.M.M., Wang, S., Garcia, M. and Bauer-Gottwein, P. 2018. Technical note: Bathymetry observations of inland water bodies using a tethered single-beam sonar controlled by an unmanned aerial vehicle. Hydrology and Earth System Sciences 22(8), 4165-4181.

Baron, J.S., Hall, E.K., Nolan, B.T., Finlay, J.C., Bernhardt, E.S., Harrison, J.A., Chan, F. and Boyer, E.W. 2012. The interactive effects of excess reactive nitrogen and climate change on aquatic ecosystems and water resources of the United States. Biogeochemistry 114(1-3), 71-92.

Beck, H.E., van Dijk, A.I.J.M., de Roo, A., Miralles, D.G., McVicar, T.R., Schellekens, J. and Bruijnzeel, L.A. 2016. Global-scale regionalization of hydrologic model parameters. Water Resources Research 52(5), 3599-3622.

Bergström, S. (1976) Development and application of a conceptual runoff model for Scandinavian catchments.

Bergström, S., Lindström, G. and Pettersson, A. 2002. Multi-variable parameter estimation to increase confidence in hydrological modelling. Hydrological Processes 16(2), 413-421.

Beusen, A.H.W., Bouwman, A.F., Van Beek, L.P.H., Mogollón, J.M. and Middelburg, J.J. 2016. Global riverine N and P transport to ocean increased during the 20th century despite increased retention along the aquatic continuum. Biogeosciences 13(8), 2441-2451.

Beven, K. 1993. Prophecy, Reality and Uncertainty in Distributed Hydrological Modeling. Advances in Water Resources 16(1), 41-51.

Beven, K. 2001. How far can we go in distributed hydrological modelling? Hydrology and Earth System Sciences 5(1), 1-12.

Beven, K. 2006. A manifesto for the equifinality thesis. Journal of Hydrology 320(1-2), 18-36.

Beven, K. 2007. Towards integrated environmental models of everywhere: uncertainty, data and modelling as a learning process. Hydrology and Earth System Sciences 11(1), 460-467.

Beven, K. and Binley, A. 1992. The Future of Distributed Models - Model Calibration and Uncertainty Prediction. Hydrological Processes 6(3), 279-298.

Beven, K. and Freer, J. 2001. Equifinality, data assimilation, and uncertainty estimation in mechanistic modelling of complex environmental systems using the GLUE methodology. Journal of Hydrology 249(1-4), 11-29.

Bicknell, B.R. 1997. Hydrological Simulation Program—FORTRAN User's Manual for Version 11.

Bingner, R.L., Theurer, F.D. and Yuan, Y. 2003. AnnAGNPS technical processes. USDA-ARS. National Sedimentation Laboratory.

Bloschl, G. and Sivapalan, M. 1995. Scale Issues in Hydrological Modeling - a Review. Hydrological Processes 9(3-4), 251-290.

Breuer, L., VachÉ, K.B., Julich, S. and Frede, H.-G. 2008. Current concepts in nitrogen dynamics for mesoscale catchments. Hydrological Sciences Journal 53(5), 1059-1074.

Brooks, R.H. and Corey, A.T. 1964. Hydraulic properties of porous media. Hydrology papers (Colorado State University); no. 3.

Bukaveckas, P.A. 2007. Effects of channel restoration on water velocity, transient storage, and nutrient uptake in a channelized stream. Environ Sci Technol 41(5), 1570-1576.

Cao, W., Bowden, W.B., Davie, T. and Fenemor, A. 2006. Multi-variable and multi-site calibration and validation of SWAT in a large mountainous catchment with high spatial variability. Hydrological Processes 20(5), 1057-1073.

Cardenas, M.B. 2009. A model for lateral hyporheic flow based on valley slope and channel sinuosity. Water Resources Research 45(1).

Carvalho, L., Mackay, E.B., Cardoso, A.C., Baattrup-Pedersen, A., Birk, S., Blackstock, K.L., Borics, G., Borja, A., Feld, C.K., Ferreira, M.T., Globevnik, L., Grizzetti, B., Hendry, S., Hering, D., Kelly, M., Langaas, S., Meissner, K., Panagopoulos, Y., Penning, E., Rouillard, J., Sabater, S., Schmedtje, U., Spears, B.M., Venohr, M., van de Bund, W. and Solheim, A.L. 2019. Protecting and restoring Europe's waters: An analysis of the future development needs of the Water Framework Directive. Science of The Total Environment 658, 1228-1238.

Chen, Q., Wu, W., Blanckaert, K., Ma, J. and Huang, G. 2012. Optimization of water quality monitoring network in a large river by combining measurements, a numerical model and matter-element analyses. J Environ Manage 110, 116-124.

Chiang, L.C., Yuan, Y.P., Mehaffey, M., Jackson, M. and Chaubey, I. 2014. Assessing SWAT's performance in the Kaskaskia River watershed as influenced by the number of calibration stations used. Hydrological Processes 28(3), 676-687.

Cleveland, R.B., Cleveland, W. S., McRae, J. E., & Terpenning, I. J. 1990. STL: A seasonal-trend decomposition procedure based on loess. Journal of Official Statistics 6.

Cosby, B.J., Hornberger, G.M., Clapp, R.B. and Ginn, T.R. 1984. A Statistical Exploration of the Relationships of Soil-Moisture Characteristics to the Physical-Properties of Soils. Water Resources Research 20(6), 682-690.

Craig, L.S., Palmer, M.A., Richardson, D.C., Filoso, S., Bernhardt, E.S., Bledsoe, B.P., Doyle, M.W., Groffman, P.M., Hassett, B.A., Kaushal, S.S., Mayer, P.M., Smith, S.M. and Wilcock, P.R. 2008. Stream restoration strategies for reducing river nitrogen loads. Frontiers in Ecology and the Environment 6(10), 529-538.

Creed, I.F. and Beall, F.D. 2009. Distributed topographic indicators for predicting nitrogen export from headwater catchments. Water Resources Research 45(10).

Cuntz, M., Mai, J., Zink, M., Thober, S., Kumar, R., Schäfer, D., Schrön, M., Craven, J., Rakovec, O., Spieler, D., Prykhodko, V., Dalmasso, G., Musuuza, J., Langenberg, B., Attinger, S. and Samaniego, L. 2015. Computationally inexpensive identification of noninformative model parameters by sequential screening. Water Resources Research 51(8), 6417-6441.

Daggupati, P., Pai, N., Ale, S., Douglas-Mankin, K.R., Zeckoski, R.W., Jeong, J., Parajuli, P.B., Saraswat, D. and Youssef, M.A. 2015. A Recommended Calibration and Validation Strategy for Hydrologic and Water Quality Models. Transactions of the Asabe 58(6), 1705-1719.

Dal Molin, M., Schirmer, M., Zappa, M. and Fenicia, F. 2020. Understanding dominant controls on streamflow spatial variability to set up a semi-distributed hydrological model: the case study of the Thur catchment. Hydrology and Earth System Sciences 24(3), 1319-1345.

Davis, C.A., Ward, A.S., Burgin, A.J., Loecke, T.D., Riveros-Iregui, D.A., Schnoebelen, D.J., Just, C.L., Thomas, S.A., Weber, L.J. and St. Clair, M.A. 2014. Antecedent Moisture Controls on Stream Nitrate Flux in an Agricultural Watershed. Journal of Environmental Quality 43(4), 1494-1503.

Dembélé, M., Ceperley, N., Zwart, S.J., Salvadore, E., Mariethoz, G. and Schaefli, B. 2020a. Potential of satellite and reanalysis evaporation datasets for hydrological modelling under various model calibration strategies. Advances in Water Resources 143.

Dembélé, M., Hrachowitz, M., Savenije, H.H.G., Mariéthoz, G. and Schaefli, B. 2020b. Improving the Predictive Skill of a Distributed Hydrological Model by Calibration on Spatial Patterns With Multiple Satellite Data Sets. Water Resources Research 56(1).

Demirel, M.C., Mai, J., Mendiguren, G., Koch, J., Samaniego, L. and Stisen, S. 2018. Combining satellite data and appropriate objective functions for improved spatial pattern performance of a distributed hydrologic model. Hydrology and Earth System Sciences 22(2), 1299-1315.

Djodjic, F., Bieroza, M. and Bergstrom, L. 2021. Land use, geology and soil properties control nutrient concentrations in headwater streams. Sci Total Environ 772, 145108.

Doyle, M.W., Stanley, E.H. and Harbor, J.M. 2003. Hydrogeomorphic controls on phosphorus retention in streams. Water Resources Research 39(6).

Duan, Q.Y., Sorooshian, S. and Gupta, V. 1992. Effective and Efficient Global Optimization for Conceptual Rainfall-Runoff Models. Water Resources Research 28(4), 1015-1031.

Duethmann, D., Peters, J., Blume, T., Vorogushyn, S. and Güntner, A. 2014. The value of satellite-derived snow cover images for calibrating a hydrological model in snow-dominated catchments in Central Asia. Water Resources Research 50(3), 2002-2021.

Dupas, R., Jomaa, S., Musolff, A., Borchardt, D. and Rode, M. 2016. Disentangling the influence of hydroclimatic patterns and agricultural management on river nitrate dynamics from sub-hourly to decadal time scales. Sci Total Environ 571, 791-800.

EEA (2018) European waters -- Assessment of status and pressures 2018,Rep. No 7/2018, Copenhagen,Denmark. https://www.eea.europa.eu/publications/state-of-water.

Efstratiadis, A. and Koutsoyiannis, D. 2010. One decade of multi-objective calibration approaches in hydrological modelling: a review. Hydrological Sciences Journal 55(1), 58-78.

Ehrhardt, S., Kumar, R., Fleckenstein, J.H., Attinger, S. and Musolff, A. 2019. Trajectories of nitrate input and output in three nested catchments along a land use gradient. Hydrology and Earth System Sciences 23(9), 3503-3524.

Engel, B., Storm, D., White, M., Arnold, J. and Arabi, M. 2007. A hydrologic/water quality model application protocol. Journal of the American Water Resources Association 43(5), 1223-1236.

Ensign, S.H. and Doyle, M.W. 2006. Nutrient spiraling in streams and river networks. Journal of Geophysical Research: Biogeosciences 111(G4).

EU 2000 Directive 2000/60/EC of the European Parliament and of the Council of 23 October 2000 establishing a framework for Community action in the field of water policy, p. 2000.

European Commission 1991a Council Directive 91/271/EEC of 21 May 1991 concerning urban waste-water treatment.

European Commission 1991b Council Directive 91/676/EEC of 12 December 1991 concerning the protection of waters against pollution caused by nitrates from agricultural sources.

Finger, D., Pellicciotti, F., Konz, M., Rimkus, S. and Burlando, P. 2011. The value of glacier mass balance, satellite snow cover images, and hourly discharge for improving the performance of a physically based distributed hydrological model. Water Resources Research 47(7).

Franco, A.C.L., Oliveira, D.Y.d. and Bonumá, N.B. 2020. Comparison of single-site, multi-site and multi-variable SWAT calibration strategies. Hydrological Sciences Journal 65(14), 2376-2389.

Fu, B., Horsburgh, J.S., Jakeman, A.J., Gualtieri, C., Arnold, T., Marshall, L., Green, T.R., Quinn, N.W.T., Volk, M., Hunt, R.J., Vezzaro, L., Croke, B.F.W., Jakeman, J.D., Snow, V. and Rashleigh, B. 2020. Modeling Water Quality in Watersheds: From Here to the Next Generation. Water Resour Res 56(11).

Fu, B., Merritt, W.S., Croke, B.F.W., Weber, T.R. and Jakeman, A.J. 2019. A review of catchment-scale water quality and erosion models and a synthesis of future prospects. Environ Modell Softw 114, 75-97.

Futter, M.N., Erlandsson, M.A., Butterfield, D., Whitehead, P.G., Oni, S.K. and Wade, A.J. 2014. PERSiST: a flexible rainfall-runoff modelling toolkit for use with the INCA family of models. Hydrology and Earth System Sciences 18(2), 855-873.

Gao, H., Sabo, J.L., Chen, X., Liu, Z., Yang, Z., Ren, Z. and Liu, M. 2018. Landscape heterogeneity and hydrological processes: a review of landscape-based hydrological models. Landscape Ecology 33(9), 1461-1480.

Gassman, P.W., Reyes, M.R., Green, C.H. and Arnold, J.G. 2007. The soil and water assessment tool: historical development, applications, and future research directions. Transactions of the ASABE 50(4), 1211-1250.

Gavahi, K., Abbaszadeh, P., Moradkhani, H., Zhan, X. and Hain, C. 2020. Multivariate Assimilation of Remotely Sensed Soil Moisture and Evapotranspiration for Drought Monitoring. Journal of Hydrometeorology 21(10), 2293-2308.

Ghaffar, S., Jomaa, S., Meon, G. and Rode, M. 2021. Spatial validation of a semi-distributed hydrological nutrient transport model. Journal of Hydrology 593, 125818.

Gomez-Velez, J.D. and Harvey, J.W. 2014. A hydrogeomorphic river network model predicts where and why hyporheic exchange is important in large basins. Geophysical Research Letters 41(18), 6403-6412.

Gomez-Velez, J.D., Harvey, J.W., Cardenas, M.B. and Kiel, B. 2015. Denitrification in the Mississippi River network controlled by flow through river bedforms. Nature Geoscience 8(12), 941-945.

Gomez-Velez, J.D., Wilson, J.L., Cardenas, M.B. and Harvey, J.W. 2017. Flow and Residence Times of Dynamic River Bank Storage and Sinuosity-Driven Hyporheic Exchange. Water Resources Research 53(10), 8572-8595.

Gomez, J.D., Wilson, J.L. and Cardenas, M.B. 2012. Residence time distributions in sinuosity-driven hyporheic zones and their biogeochemical effects. Water Resources Research 48(9).

Götzinger, J. and Bárdossy, A. 2007. Comparison of four regionalisation methods for a distributed hydrological model. Journal of Hydrology 333(2-4), 374-384.

Grimm, N.B., Gergel, S.E., McDowell, W.H., Boyer, E.W., Dent, C.L., Groffman, P., Hart, S.C., Harvey, J., Johnston, C., Mayorga, E., McClain, M.E. and Pinay, G. 2003. Merging aquatic and terrestrial perspectives of nutrient biogeochemistry. Oecologia 137(4), 485-501.

Groffman, P.M., Altabet, M.A., Bohlke, J.K., Butterbach-Bahl, K., David, M.B., Firestone, M.K., Giblin, A.E., Kana, T.M., Nielsen, L.P. and Voytek, M.A. 2006. Methods for measuring denitrification: diverse approaches to a difficult problem. Ecol Appl 16(6), 2091-2122.

Gucker, B. and Boechat, I.G. 2004. Stream morphology controls ammonium retention in tropical headwaters. Ecology 85(10), 2818-2827.

Guidicelli, M., Gugerli, R., Gabella, M., Marty, C. and Salzmann, N. 2021. Continuous Spatio-Temporal High-Resolution Estimates of SWE Across the Swiss Alps – A Statistical Two-Step Approach for High-Mountain Topography. Frontiers in Earth Science 9.

Gupta, H.V., Beven, K.J. and Wagener, T. (2005) Encyclopedia of Hydrological Sciences.

Gupta, H.V., Kling, H., Yilmaz, K.K. and Martinez, G.F. 2009. Decomposition of the mean squared error and NSE performance criteria: Implications for improving hydrological modelling. Journal of Hydrology 377(1-2), 80-91.

Gupta, H.V., Sorooshian, S. and Yapo, P.O. 1998. Toward improved calibration of hydrologic models: Multiple and noncommensurable measures of information. Water Resources Research 34(4), 751-763.

Gupta, H.V., Sorooshian, S. and Yapo, P.O. 1999. Status of Automatic Calibration for Hydrologic Models: Comparison with Multilevel Expert Calibration. Journal of Hydrologic Engineering 4(2), 135-143.

Gupta, H.V., Wagener, T. and Liu, Y. 2008. Reconciling theory with observations: elements of a diagnostic approach to model evaluation. Hydrological Processes 22(18), 3802-3813.

Hall, R.O., Bernhardt, E.S. and Likens, G.E. 2002. Relating nutrient uptake with transient storage in forested mountain streams. Limnology and Oceanography 47(1), 255-265.

Han, E., Merwade, V. and Heathman, G.C. 2012. Implementation of surface soil moisture data assimilation with watershed scale distributed hydrological model. Journal of Hydrology 416-417, 98-117.

Hanel, M., Rakovec, O., Markonis, Y., Maca, P., Samaniego, L., Kysely, J. and Kumar, R. 2018. Revisiting the recent European droughts from a long-term perspective. Sci Rep 8(1), 9499.

Hargreaves, G.H. and Samani, Z.A. 1985. Reference Crop Evapotranspiration from Temperature. Applied Engineering in Agriculture 1(2), 96-99.

Hari, V., Rakovec, O., Markonis, Y., Hanel, M. and Kumar, R. 2020. Increased future occurrences of the exceptional 2018-2019 Central European drought under global warming. Sci Rep 10(1), 12207.

Helton, A.M., Hall, R.O. and Bertuzzo, E. 2018. How network structure can affect nitrogen removal by streams. Freshwater Biology 63(1), 128-140.

Hensley, R.T. and Cohen, M.J. 2020. Nitrate depletion dynamics and primary production in riverine benthic chambers. Freshwater Science 39(1), 169-182.

Hensley, R.T., Cohen, M.J. and Korhnak, L.V. 2014. Inferring nitrogen removal in large rivers from high-resolution longitudinal profiling. Limnology and Oceanography 59(4), 1152-1170.

Her, Y. and Chaubey, I. 2015. Impact of the numbers of observations and calibration parameters on equifinality, model performance, and output and parameter uncertainty. Hydrological Processes 29(19), 4220-4237.

Hesse, C. and Krysanova, V. 2016. Modeling Climate and Management Change Impacts on Water Quality and In-Stream Processes in the Elbe River Basin. Water 8(2).

Heuvelmans, G., Muys, B. and Feyen, J. 2004. Evaluation of hydrological model parameter transferability for simulating the impact of land use on catchment hydrology. Physics and Chemistry of the Earth, Parts A/B/C 29(11-12), 739-747.

Homyak, P.M., Allison, S.D., Huxman, T.E., Goulden, M.L. and Treseder, K.K. 2017. Effects of Drought Manipulation on Soil Nitrogen Cycling: A Meta-Analysis. Journal of Geophysical Research: Biogeosciences 122(12), 3260-3272.

Horn, A.L., Rueda, F.J., Hörmann, G. and Fohrer, N. 2004. Implementing river water quality modelling issues in mesoscale watershed models for water policy demands—an overview on current concepts, deficits, and future tasks. Physics and Chemistry of the Earth, Parts A/B/C 29(11-12), 725-737.

Hosen, J.D., Aho, K.S., Appling, A.P., Creech, E.C., Fair, J.H., Hall, R.O., Kyzivat, E.D., Lowenthal, R.S., Matt, S., Morrison, J., Saiers, J.E., Shanley, J.B., Weber, L.C., Yoon, B. and Raymond, P.A. 2019. Enhancement of primary production during drought in a temperate watershed is greater in larger rivers than headwater streams. Limnology and Oceanography 64(4), 1458-1472.

Howarth, R., Swaney, D., Billen, G., Garnier, J., Hong, B., Humborg, C., Johnes, P., Mörth, C.-M. and Marino, R. 2012. Nitrogen fluxes from the landscape are controlled by net anthropogenic nitrogen inputs and by climate. Frontiers in Ecology and the Environment 10(1), 37-43.

Huang, S., Krysanova, V. and Hattermann, F. 2015. Projections of climate change impacts on floods and droughts in Germany using an ensemble of climate change scenarios. Regional Environmental Change 15(3), 461-473.

Hundecha, Y. and Bárdossy, A. 2004. Modeling of the effect of land use changes on the runoff generation of a river basin through parameter regionalization of a watershed model. Journal of Hydrology 292(1-4), 281-295.

Immerzeel, W.W. and Droogers, P. 2008. Calibration of a distributed hydrological model based on satellite evapotranspiration. Journal of Hydrology 349(3-4), 411-424.

Jakeman, A.J. and Hornberger, G.M. 1993. How Much Complexity Is Warranted in a Rainfall-Runoff Model. Water Resources Research 29(8), 2637-2649.

Jarvie, H.P., Sharpley, A.N., Kresse, T., Hays, P.D., Williams, R.J., King, S.M. and Berry, L.G. 2018. Coupling High-Frequency Stream Metabolism and Nutrient Monitoring to Explore Biogeochemical Controls on Downstream Nitrate Delivery. Environ Sci Technol 52(23), 13708-13717.

Jarvis, A., H.I. Reuter, A. Nelson, E. Guevara. 2008 Hole-filled SRTM for the globe Version 4, available from the CGIAR-CSI SRTM 90m Database http://srtm.csi.cgiar.org/.

Jiang, S., Jomaa, S., Büttner, O., Meon, G. and Rode, M. 2015. Multi-site identification of a distributed hydrological nitrogen model using Bayesian uncertainty analysis. Journal of Hydrology 529, 940-950.

Jiang, S.Y., Jomaa, S. and Rode, M. 2014. Modelling inorganic nitrogen leaching in nested mesoscale catchments in central Germany. Ecohydrology 7(5), 1345-1362.

Jiang, S.Y., Zhang, Q., Werner, A.D., Wellen, C., Jomaa, S., Zhu, Q.D., Büttner, O., Meon, G. and Rode, M. 2019. Effects of stream nitrate data frequency on watershed model performance and prediction uncertainty. Journal of Hydrology 569, 22-36.

Jones, C.S., Kim, S.-w., Wilton, T.F., Schilling, K.E. and Davis, C.A. 2018. Nitrate uptake in an agricultural stream estimated from high-frequency, in-situ sensors. Environmental Monitoring and Assessment 190(4).

Kasvi, E., Salmela, J., Lotsari, E., Kumpula, T. and Lane, S.N. 2019. Comparison of remote sensing based approaches for mapping bathymetry of shallow, clear water rivers. Geomorphology 333, 180-197.

Kaushal, S.S., Groffman, P.M., Mayer, P.M., Striz, E. and Gold, A.J. 2008. Effects of stream restoration on denitrification in an urbanizing watershed. Ecol Appl 18(3), 789-804.

Khalil, B. and Ouarda, T.B.M.J. 2009. Statistical approaches used to assess and redesign surface water-quality-monitoring networks. Journal of Environmental Monitoring 11(11).

Khu, S.-T., Madsen, H. and di Pierro, F. 2008. Incorporating multiple observations for distributed hydrologic model calibration: An approach using a multi-objective evolutionary algorithm and clustering. Advances in Water Resources 31(10), 1387-1398.

Kiel, B.A. and Bayani Cardenas, M. 2014. Lateral hyporheic exchange throughout the Mississippi River network. Nature Geoscience 7(6), 413-417.

Klocker, C.A., Kaushal, S.S., Groffman, P.M., Mayer, P.M. and Morgan, R.P. 2009. Nitrogen uptake and denitrification in restored and unrestored streams in urban Maryland, USA. Aquatic Sciences 71(4), 411-424.

Kochendorfer, J., Rasmussen, R., Wolff, M., Baker, B., Hall, M.E., Meyers, T., Landolt, S., Jachcik, A., Isaksen, K., Braekkan, R. and Leeper, R. 2017. The quantification and correction of wind-induced precipitation measurement errors. Hydrology and Earth System Sciences 21(4), 1973-1989.

Kong, X., Ghaffar, S., Determann, M., Friese, K., Jomaa, S., Mi, C., Shatwell, T., Rinke, K. and Rode, M. 2022. Reservoir water quality deterioration due to deforestation emphasizes the indirect effects of global change. Water Res 221.

Krause, P., Boyle, D.P. and Bäse, F. 2005. Comparison of different efficiency criteria for hydrological model assessment. Advances in Geosciences 5, 89-97.

Kumar, R., Samaniego, L. and Attinger, S. 2010. The effects of spatial discretization and model parameterization on the prediction of extreme runoff characteristics. Journal of Hydrology 392(1-2), 54-69.

Kunz, J.V., Annable, M.D., Rao, S., Rode, M. and Borchardt, D. 2017a. Hyporheic Passive Flux Meters Reveal Inverse Vertical Zonation and High Seasonality of Nitrogen Processing in an Anthropogenically Modified Stream (Holtemme, Germany). Water Resources Research 53(12), 10155-10172.

Kunz, J.V., Hensley, R., Brase, L., Borchardt, D. and Rode, M. 2017b. High frequency measurements of reach scale nitrogen uptake in a fourth order river with contrasting hydromorphology and variable water chemistry (Weiße Elster, Germany). Water Resources Research 53(1), 328-343.

Kyllmar, K., Forsberg, L.S., Andersson, S. and Mårtensson, K. 2014. Small agricultural monitoring catchments in Sweden representing environmental impact. Agriculture, Ecosystems & Environment 198, 25-35.

Ladrera, R., Belmar, O., Tomas, R., Prat, N. and Canedo-Arguelles, M. 2019. Agricultural impacts on streams near Nitrate Vulnerable Zones: A case study in the Ebro basin, Northern Spain. PLoS One 14(11), e0218582.

Lei, C., Wagner, P.D. and Fohrer, N. 2021. Effects of land cover, topography, and soil on stream water quality at multiple spatial and seasonal scales in a German lowland catchment. Ecological Indicators 120.

Leitner, S., Dirnbock, T., Kobler, J. and Zechmeister-Boltenstern, S. 2020. Legacy effects of drought on nitrate leaching in a temperate mixed forest on karst. J Environ Manage 262, 110338.

Lerat, J., Andréassian, V., Perrin, C., Vaze, J., Perraud, J.M., Ribstein, P. and Loumagne, C. 2012. Do internal flow measurements improve the calibration of rainfall-runoff models? Water Resources Research 48(2).

Leta, O.T., Griensven, A.v. and Bauwens, W. 2017a. Effect of Single and Multisite Calibration Techniques on the Parameter Estimation, Performance, and Output of a SWAT Model of a Spatially Heterogeneous Catchment. Journal of Hydrologic Engineering 22(3), 05016036.

Leta, O.T., van Griensven, A. and Bauwens, W. 2017b. Effect of Single and Multisite Calibration Techniques on the Parameter Estimation, Performance, and Output of a SWAT Model of a Spatially Heterogeneous Catchment. Journal of Hydrologic Engineering 22(3), 05016036.

Lettenmaier, D.P., Alsdorf, D., Dozier, J., Huffman, G.J., Pan, M. and Wood, E.F. 2015. Inroads of remote sensing into hydrologic science during the WRR era. Water Resources Research 51(9), 7309-7342.

Li, L., Sullivan, P.L., Benettin, P., Cirpka, O.A., Bishop, K., Brantley, S.L., Knapp, J.L.A., Meerveld, I., Rinaldo, A., Seibert, J., Wen, H. and Kirchner, J.W. 2020. Toward catchment hydro-biogeochemical theories. WIREs Water 8(1).

Li, X., Weller, D.E. and Jordan, T.E. 2010. Watershed model calibration using multi-objective optimization and multi-site averaging. Journal of Hydrology 380(3-4), 277-288.

Lin, L., Davis, L., Cohen, S., Chapman, E. and Edmonds, J.W. 2016. The influence of geomorphic unit spatial distribution on nitrogen retention and removal in a large river. Ecological Modelling 336, 26-35.

Lin, L., Reisinger, A.J., Rosi, E.J., Groffman, P.M. and Band, L.E. 2021. Evaluating Instream Restoration Effectiveness in Reducing Nitrogen Export from an Urban Catchment with a Data-Model Approach. JAWRA Journal of the American Water Resources Association 57(3), 449-473.

Lindstrom, G., Johansson, B., Persson, M., Gardelin, M. and Bergstrom, S. 1997. Development and test of the distributed HBV-96 hydrological model. Journal of Hydrology 201(1-4), 272-288.

Lindström, G., Pers, C., Rosberg, J., Strömqvist, J. and Arheimer, B. 2010. Development and testing of the HYPE (Hydrological Predictions for the Environment) water quality model for different spatial scales. Hydrology Research 41(3-4), 295-319.

Lindström, G., Rosberg, J. and Arheimer, B. 2005. Parameter Precision in the HBV-NP Model and Impacts on Nitrogen Scenario Simulations in the Rönneå River, Southern Sweden. AMBIO: A Journal of the Human Environment 34(7), 533-537.

Lintern, A., Webb, J.A., Ryu, D., Liu, S., Bende-Michl, U., Waters, D., Leahy, P., Wilson, P. and Western, A.W. 2018a. Key factors influencing differences in stream water quality across space. Wiley Interdisciplinary Reviews: Water 5(1).

Lintern, A., Webb, J.A., Ryu, D., Liu, S., Waters, D., Leahy, P., Bende-Michl, U. and Western, A.W. 2018b. What Are the Key Catchment Characteristics Affecting Spatial Differences in Riverine Water Quality? Water Resources Research 54(10), 7252-7272.

Liu, J., Zhang, L., Zhang, Y., Hong, H. and Deng, H. 2008. Validation of an agricultural non-point source (AGNPS) pollution model for a catchment in the Jiulong River watershed, China. J Environ Sci (China) 20(5), 599-606.

Lohse, K.A., Brooks, P.D., McIntosh, J.C., Meixner, T. and Huxman, T.E. 2009. Interactions Between Biogeochemistry and Hydrologic Systems. Annual Review of Environment and Resources 34(1), 65-96.

Lutz, S.R., Mallucci, S., Diamantini, E., Majone, B., Bellin, A. and Merz, R. 2016. Hydroclimatic and water quality trends across three Mediterranean river basins. Sci Total Environ 571, 1392-1406.

McDonnell, J.J., Sivapalan, M., Vaché, K., Dunn, S., Grant, G., Haggerty, R., Hinz, C., Hooper, R., Kirchner, J., Roderick, M.L., Selker, J. and Weiler, M. 2007. Moving beyond heterogeneity and process complexity: A new vision for watershed hydrology. Water Resources Research 43(7).

McMillan, H.K. 2021. A review of hydrologic signatures and their applications. WIREs Water 8(1), e1499.

Merz, R. and Blöschl, G. 2004. Regionalisation of catchment model parameters. Journal of Hydrology 287(1-4), 95-123.

Merz, R., Parajka, J. and Blöschl, G. 2011. Time stability of catchment model parameters: Implications for climate impact analyses. Water Resources Research 47(2).

Michaelides, S., Levizzani, V., Anagnostou, E., Bauer, P., Kasparis, T. and Lane, J.E. 2009. Precipitation: Measurement, remote sensing, climatology and modeling. Atmospheric Research 94(4), 512-533.

Moriasi, D.N., Gitau, M.W., Pai, N. and Daggupati, P. 2015. Hydrologic and Water Quality Models: Performance Measures and Evaluation Criteria. Transactions of the Asabe 58(6), 1763-1785.

Moriasi, D.N., Wilson, B.N., Douglas-Mankin, K.R., Arnold, J.G. and Gowda, P.H. 2012. Hydrologic and Water Quality Models: Use, Calibration, and Validation. Transactions of the Asabe 55(4), 1241-1247.

Morris, M.D. 1991. Factorial sampling plans for preliminary computational experiments. Technometrics 33(2), 161-174.

Mosley, L.M. 2015. Drought impacts on the water quality of freshwater systems; review and integration. Earth-Science Reviews 140, 203-214.

Mueller, C., Zink, M., Samaniego, L., Krieg, R., Merz, R., Rode, M. and Knoller, K. 2016. Discharge Driven Nitrogen Dynamics in a Mesoscale River Basin As Constrained by Stable Isotope Patterns. Environ Sci Technol 50(17), 9187-9196.

Muleta, M.K. 2012. Model Performance Sensitivity to Objective Function during Automated Calibrations. Journal of Hydrologic Engineering 17(6), 756-767.

Mulholland, P.J., Hall Jr, R.O., Sobota, D.J., Dodds, W.K., Findlay, S.E., Grimm, N.B., Hamilton, S.K., McDowell, W.H., O'Brien, J.M. and Tank, J.L. 2009. Nitrate removal in stream ecosystems measured by 15N addition experiments: denitrification. Limnology and Oceanography 54(3), 666-680.

Mulholland, P.J., Helton, A.M., Poole, G.C., Hall, R.O., Hamilton, S.K., Peterson, B.J., Tank, J.L., Ashkenas, L.R., Cooper, L.W., Dahm, C.N., Dodds, W.K., Findlay, S.E., Gregory, S.V., Grimm, N.B., Johnson, S.L., McDowell, W.H., Meyer, J.L., Valett, H.M., Webster, J.R., Arango, C.P., Beaulieu, J.J., Bernot, M.J., Burgin, A.J., Crenshaw, C.L., Johnson, L.T., Niederlehner, B.R., O'Brien, J.M., Potter, J.D., Sheibley, R.W., Sobota, D.J. and Thomas, S.M. 2008. Stream denitrification across biomes and its response to anthropogenic nitrate loading. Nature 452(7184), 202-205.

Mulholland, P.J. and Webster, J.R. 2010. Nutrient dynamics in streams and the role of J-NABS. J N Am Benthol Soc 29(1), 100-117.

Newcomer Johnson, T., Kaushal, S., Mayer, P., Smith, R. and Sivirichi, G. 2016. Nutrient Retention in Restored Streams and Rivers: A Global Review and Synthesis. Water 8(4).

Nguyen, T.V., Kumar, R., Lutz, S.R., Musolff, A., Yang, J. and Fleckenstein, J.H. 2021. Modeling Nitrate Export From a Mesoscale Catchment Using StorAge Selection Functions. Water Resources Research 57(2).

Onderka, M., Wrede, S., Rodný, M., Pfister, L., Hoffmann, L. and Krein, A. 2012. Hydrogeologic and landscape controls of dissolved inorganic nitrogen (DIN) and dissolved silica (DSi) fluxes in heterogeneous catchments. Journal of Hydrology 450-451, 36-47.

Opdyke, M.R., David, M.B. and Rhoads, B.L. 2006. Influence of geomorphological variability in channel characteristics on sediment denitrification in agricultural streams. J Environ Qual 35(6), 2103-2112.

Oudin, L., Andreassian, V., Perrin, C., Michel, C. and Le Moine, N. 2008. Spatial proximity, physical similarity, regression and ungaged catchments: A comparison of regionalization approaches based on 913 French catchments. Water Resources Research 44(3).

Outram, F.N., Cooper, R.J., Sünnenberg, G., Hiscock, K.M. and Lovett, A.A. 2016. Antecedent conditions, hydrological connectivity and anthropogenic inputs: Factors affecting nitrate and phosphorus transfers to agricultural headwater streams. Science of The Total Environment 545-546, 184-199.

Pander, J., Mueller, M., Knott, J., Egg, L. and Geist, J. 2017. Is it Worth the Money? The Functionality of Engineered Shallow Stream Banks as Habitat for Juvenile Fishes in Heavily Modified Water Bodies. River Research and Applications 33(1), 63-72.

Parajka, J. and Blöschl, G. 2008. The value of MODIS snow cover data in validating and calibrating conceptual hydrologic models. Journal of Hydrology 358(3-4), 240-258.

Parajka, J., Merz, R. and Bloschl, G. 2005. A comparison of regionalisation methods for catchment model parameters. Hydrology and Earth System Sciences 9(3), 157-171.

Parajka, J., Viglione, A., Rogger, M., Salinas, J.L., Sivapalan, M. and Blöschl, G. 2013. Comparative assessment of predictions in ungauged basins – Part 1: Runoff-hydrograph studies. Hydrology and Earth System Sciences 17(5), 1783-1795.

Parajuli, P.B., Nelson, N.O., Frees, L.D. and Mankin, K.R. 2009. Comparison of AnnAGNPS and SWAT model simulation results in USDA-CEAP agricultural watersheds in south-central Kansas. Hydrological Processes 23(5), 748-763.

Pianosi, F., Beven, K., Freer, J., Hall, J.W., Rougier, J., Stephenson, D.B. and Wagener, T. 2016. Sensitivity analysis of environmental models: A systematic review with practical workflow. Environ Modell Softw 79, 214-232.

Pianosi, F., Sarrazin, F. and Wagener, T. 2015. A Matlab toolbox for Global Sensitivity Analysis. Environ Modell Softw 70, 80-85.

Pinay, G., Peiffer, S., De Dreuzy, J.-R., Krause, S., Hannah, D.M., Fleckenstein, J.H., Sebilo, M., Bishop, K. and Hubert-Moy, L. 2015. Upscaling Nitrogen Removal Capacity from Local Hotspots to Low Stream Orders' Drainage Basins. Ecosystems 18(6), 1101-1120.

Pokhrel, P., Gupta, H.V. and Wagener, T. 2008. A spatial regularization approach to parameter estimation for a distributed watershed model. Water Resources Research 44(12).

R Core Team. 2020 R: A Language and Environment for Statistical Computing. Vienna, Austria: R Foundation for Statistical Computing. Available online: http://www.R-project.org/ (accessed on 09 September 2020).

Rajib, A., Evenson, G.R., Golden, H.E. and Lane, C.R. 2018. Hydrologic model predictability improves with spatially explicit calibration using remotely sensed evapotranspiration and biophysical parameters. J Hydrol (Amst) 567, 668-683.

Rajib, M.A., Merwade, V. and Yu, Z. 2016. Multi-objective calibration of a hydrologic model using spatially distributed remotely sensed/in-situ soil moisture. Journal of Hydrology 536, 192-207.

Rathjens, H. and Oppelt, N. 2012. SWATgrid: An interface for setting up SWAT in a grid-based discretization scheme. Computers & Geosciences 45, 161-167.

Rathjens, H., Oppelt, N., Bosch, D.D., Arnold, J.G. and Volk, M. 2015. Development of a grid-based version of the SWAT landscape model. Hydrological Processes 29(6), 900-914.

Refsgaard, J.C. 1997. Parameterisation, calibration and validation of distributed hydrological models. Journal of Hydrology 198(1-4), 69-97.

Refsgaard, J.C., Højberg, A.L., He, X., Hansen, A.L., Rasmussen, S.H. and Stisen, S. 2016. Where are the limits of model predictive capabilities? Hydrological Processes 30(26), 4956-4965.

Rode, M., Arhonditsis, G., Balin, D., Kebede, T., Krysanova, V., van Griensven, A. and van der Zee, S.E.A.T.M. 2010. New challenges in integrated water quality modelling. Hydrological Processes 24(24), 3447-3461.

Rode, M. and Lindenschmidt, K.E. 2001. Distributed sediment and phosporus transport modeling on a medium sized catchment in Central Germany. Phys Chem Earth Pt B 26(7-8), 635-640.

Rode, M., Wade, A.J., Cohen, M.J., Hensley, R.T., Bowes, M.J., Kirchner, J.W., Arhonditsis, G.B., Jordan, P., Kronvang, B., Halliday, S.J., Skeffington, R.A., Rozemeijer, J.C., Aubert, A.H., Rinke, K. and Jomaa, S. 2016. Sensors in the Stream: The High-Frequency Wave of the Present. Environ Sci Technol 50(19), 10297-10307.

Ruiz, L., Abiven, S., Durand, P., Martin, C., Vertès, F. and Beaujouan, V. 2002. Effect on nitrate concentration in stream water of agricultural practices in small catchments in Brittany: I. Annual nitrogen budgets. Hydrology and Earth System Sciences 6(3), 497-506.

Saft, M., Western, A.W., Zhang, L., Peel, M.C. and Potter, N.J. 2015. The influence of multiyear drought on the annual rainfall-runoff relationship: An Australian perspective. Water Resources Research 51(4), 2444-2463.

Samaniego, L., Kumar, R. and Attinger, S. 2010. Multiscale parameter regionalization of a grid-based hydrologic model at the mesoscale. Water Resources Research 46(5).

Samaniego, L., Kumar, R., Thober, S., Rakovec, O., Zink, M., Wanders, N., Eisner, S., Schmied, H.M., Sutanudjaja, E.H., Warrach-Sagi, K. and Attinger, S. 2017. Toward seamless hydrologic predictions across spatial scales. Hydrology and Earth System Sciences 21(9), 4323-4346.

Saraswat, D., Frankenberg, J.R., Pai, N., Ale, S., Daggupati, P., Douglas-Mankin, K.R. and Youssef, M.A. 2015. Hydrologic and Water Quality Models: Documentation and Reporting Procedures for Calibration, Validation, and Use. Transactions of the Asabe 58(6), 1787-1797.

Shevenell, L. 1999. Regional potential evapotranspiration in arid climates based on temperature, topography and calculated solar radiation. Hydrological Processes 13(4), 577-596.

Shrestha, M.K., Recknagel, F., Frizenschaf, J. and Meyer, W. 2016. Assessing SWAT models based on single and multi-site calibration for the simulation of flow and nutrient loads in the semi-arid Onkaparinga catchment in South Australia. Agricultural Water Management 175, 61-71.

Singh, R., Archfield, S.A. and Wagener, T. 2014. Identifying dominant controls on hydrologic parameter transfer from gauged to ungauged catchments – A comparative hydrology approach. Journal of Hydrology 517, 985-996.

Singh, S.K. and Bárdossy, A. 2012. Calibration of hydrological models on hydrologically unusual events. Advances in Water Resources 38, 81-91.

Singh, V.P. and Woolhiser, D.A. 2002. Mathematical Modeling of Watershed Hydrology. Journal of Hydrologic Engineering 7(4), 270-292.

Song, X., Zhang, J., Zhan, C., Xuan, Y., Ye, M. and Xu, C. 2015. Global sensitivity analysis in hydrological modeling: Review of concepts, methods, theoretical framework, and applications. Journal of Hydrology 523, 739-757.

Spinoni, J., Vogt, J.V., Naumann, G., Barbosa, P. and Dosio, A. 2018. Will drought events become more frequent and severe in Europe? International Journal of Climatology 38(4), 1718-1736.

Sprague, L.A. 2005. Drought effects on water quality in the South Platte River Basin, Colorado. Journal of the American Water Resources Association 41(1), 11-24.

Stanley, E.H. and Doyle, M.W. 2002. A geomorphic perspective on nutrient retention following dam removal. Bioscience 52(8), 693-701.

Stisen, S., Koch, J., Sonnenborg, T.O., Refsgaard, J.C., Bircher, S., Ringgaard, R. and Jensen, K.H. 2018. Moving beyond run-off calibration-Multivariable optimization of a surface-subsurface-atmosphere model. Hydrological Processes 32(17), 2654-2668.

Stow, C.A., Cha, Y., Johnson, L.T., Confesor, R. and Richards, R.P. 2015. Long-Term and Seasonal Trend Decomposition of Maumee River Nutrient Inputs to Western Lake Erie. Environmental Science & Technology 49(6), 3392-3400.

Stow, C.A., Dyble, J., Kashian, D.R., Johengen, T.H., Winslow, K.P., Peacor, S.D., Francoeur, S.N., Burtner, A.M., Palladino, D., Morehead, N., Gossiaux, D., Cha, Y., Qian, S.S. and Miller, D. 2014. Phosphorus targets and eutrophication objectives in Saginaw Bay: A 35year assessment. Journal of Great Lakes Research 40, 4-10.

Strobl, R.O. and Robillard, P.D. 2008. Network design for water quality monitoring of surface freshwaters: a review. J Environ Manage 87(4), 639-648.

Suddick, E.C., Whitney, P., Townsend, A.R. and Davidson, E.A. 2012. The role of nitrogen in climate change and the impacts of nitrogen–climate interactions in the United States: foreword to thematic issue. Biogeochemistry 114(1-3), 1-10.

Tank, J.L., Rosi-Marshall, E.J., Baker, M.A. and Hall, R.O. 2008. Are Rivers Just Big Streams? A Pulse Method to Quantify Nitrogen Demand in a Large River. Ecology 89(10), 2935-2945.

Tatariw, C., Chapman, E.L., Sponseller, R.A., Mortazavi, B. and Edmonds, J.W. 2013. Denitrification in a large river: consideration of geomorphic controls on microbial activity and community structure. Ecology 94(10), 2249-2262.

ter Braak, C.J.F. and Vrugt, J.A. 2008. Differential Evolution Markov Chain with snooker updater and fewer chains. Statistics and Computing 18(4), 435-446.

Thiemann, M., Trosset, M., Gupta, H. and Sorooshian, S. 2001. Bayesian recursive parameter estimation for hydrologic models. Water Resources Research 37(10), 2521-2535.

Tian, F., Hu, H., Lei, Z. and Sivapalan, M. 2006. Extension of the Representative Elementary Watershed approach for cold regions via explicit treatment of energy related processes. Hydrology and Earth System Sciences 10(5), 619-644.

Tolson, B.A. and Shoemaker, C.A. 2007. Dynamically dimensioned search algorithm for computationally efficient watershed model calibration. Water Resources Research 43(1).
UBA (2019) 2019 Monitoring Report on the German Strategy for Adaptation to Climate Change,https://www.umweltbundesamt.de/en/publikationen/2019-monitoring-report.
van Vliet, M.T.H. and Zwolsman, J.J.G. 2008. Impact of summer droughts on the water quality of the Meuse river. Journal of Hydrology 353(1-2), 1-17.
Veraart, A.J., Audet, J., Dimitrov, M.R., Hoffmann, C.C., Gillissen, F. and de Klein, J.J.M. 2014. Denitrification in restored and unrestored Danish streams. Ecological Engineering 66, 129-140.
Vicente-Serrano, S.M., Begueria, S. and Lopez-Moreno, J.I. 2010. A Multiscalar Drought Index Sensitive to Global Warming: The Standardized Precipitation Evapotranspiration Index. Journal of Climate 23(7), 1696-1718.
Vrugt, J.A. 2016. Markov chain Monte Carlo simulation using the DREAM software package: Theory, concepts, and MATLAB implementation. Environ Modell Softw 75, 273-316.
Vrugt, J.A., Diks, C.G.H., Gupta, H.V., Bouten, W. and Verstraten, J.M. 2005. Improved treatment of uncertainty in hydrologic modeling: Combining the strengths of global optimization and data assimilation. Water Resources Research 41(1).
Vrugt, J.A., Gupta, H.V., Bouten, W. and Sorooshian, S. 2003. A Shuffled Complex Evolution Metropolis algorithm for optimization and uncertainty assessment of hydrologic model parameters. Water Resources Research 39(8).
Vrugt, J.A., ter Braak, C.J.F., Clark, M.P., Hyman, J.M. and Robinson, B.A. 2008. Treatment of input uncertainty in hydrologic modeling: Doing hydrology backward with Markov chain Monte Carlo simulation. Water Resources Research 44(12).
Wade, A.J., Durand, P., Beaujouan, V., Wessel, W.W., Raat, K.J., Whitehead, P.G., Butterfield, D., Rankinen, K. and Lepisto, A. 2002. A nitrogen model for European catchments: INCA, new model structure and equations. Hydrology and Earth System Sciences 6(3), 559-582.
Wagener, T. and Gupta, H.V. 2005. Model identification for hydrological forecasting under uncertainty. Stochastic Environmental Research and Risk Assessment 19(6), 378-387.
Wagener, T., McIntyre, N., Lees, M.J., Wheater, H.S. and Gupta, H.V. 2003. Towards reduced uncertainty in conceptual rainfall-runoff modelling: dynamic identifiability analysis. Hydrological Processes 17(2), 455-476.
Wagener, T., Sivapalan, M., Troch, P. and Woods, R. 2007. Catchment Classification and Hydrologic Similarity. Geography Compass 1(4), 901-931.
Wagener, T. and Wheater, H.S. 2006. Parameter estimation and regionalization for continuous rainfall-runoff models including uncertainty. Journal of Hydrology 320(1-2), 132-154.
Wagenschein, D. and Rode, M. 2008. Modelling the impact of river morphology on nitrogen retention—A case study of the Weisse Elster River (Germany). Ecological Modelling 211(1-2), 224-232.
Wang, S., Zhang, Z., Sun, G., Strauss, P., Guo, J., Tang, Y. and Yao, A. 2012. Multi-site calibration, validation, and sensitivity analysis of the MIKE SHE Model for a large watershed in northern China. Hydrology and Earth System Sciences 16(12), 4621-4632.
Wellen, C., Kamran-Disfani, A.R. and Arhonditsis, G.B. 2015. Evaluation of the current state of distributed watershed nutrient water quality modeling. Environ Sci Technol 49(6), 3278-3290.
White, K.L. and Chaubey, I. 2005. Sensitivity Analysis, Calibration, and Validations for a Multisite and Multivariable Swat Model. Journal of the American Water Resources Association 41(5), 1077-1089.
Whitehead, P., Wilson, E. and Butterfield, D. 1998. A semi-distributed ntegrated itrogen model for multiple source assessment in tchments (INCA): Part I — model structure and process equations. Science of The Total Environment 210-211, 547-558.

Whitehead, P.G., Wilby, R.L., Battarbee, R.W., Kernan, M. and Wade, A.J. 2009. A review of the potential impacts of climate change on surface water quality. Hydrological Sciences Journal 54(1), 101-123.

Whitehead, P.G., Wilby, R.L., Butterfield, D. and Wade, A.J. 2006. Impacts of climate change on in-stream nitrogen in a lowland chalk stream: an appraisal of adaptation strategies. Sci Total Environ 365(1-3), 260-273.

Winter, C., Lutz, S.R., Musolff, A., Kumar, R., Weber, M. and Fleckenstein, J.H. 2021. Disentangling the Impact of Catchment Heterogeneity on Nitrate Export Dynamics From Event to Long-Term Time Scales. Water Resources Research 57(1).

Wohl, E., Lane, S.N. and Wilcox, A.C. 2015. The science and practice of river restoration. Water Resources Research 51(8), 5974-5997.

Wollheim, W.M., Mulukutla, G.K., Cook, C. and Carey, R.O. 2017. Aquatic Nitrate Retention at River Network Scales Across Flow Conditions Determined Using Nested In Situ Sensors. Water Resources Research 53(11), 9740-9756.

Wollheim, W.M., Peterson, B.J., Deegan, L.A., Hobbie, J.E., Hooker, B., Bowden, W.B., Edwardson, K.J., Arscott, D.B., Hershey, A.E. and Finlay, J. 2001. Influence of stream size on ammonium and suspended particulate nitrogen processing. Limnology and Oceanography 46(1), 1-13.

Wollheim, W.M., Peterson, B.J., Thomas, S.M., Hopkinson, C.H. and Vörösmarty, C.J. 2008a. Dynamics of N removal over annual time periods in a suburban river network. Journal of Geophysical Research 113(G3).

Wollheim, W.M., Vörösmarty, C.J., Bouwman, A.F., Green, P., Harrison, J., Linder, E., Peterson, B.J., Seitzinger, S.P. and Syvitski, J.P.M. 2008b. Global N removal by freshwater aquatic systems using a spatially distributed, within-basin approach. Global Biogeochemical Cycles 22(2), n/a-n/a.

Wollheim, W.M., Vörösmarty, C.J., Peterson, B.J., Seitzinger, S.P. and Hopkinson, C.S. 2006. Relationship between river size and nutrient removal. Geophysical Research Letters 33(6).

Wollschläger, U., Attinger, S., Borchardt, D., Brauns, M., Cuntz, M., Dietrich, P., Fleckenstein, J.H., Friese, K., Friesen, J., Harpke, A., Hildebrandt, A., Jäckel, G., Kamjunke, N., Knöller, K., Kögler, S., Kolditz, O., Krieg, R., Kumar, R., Lausch, A., Liess, M., Marx, A., Merz, R., Mueller, C., Musolff, A., Norf, H., Oswald, S.E., Rebmann, C., Reinstorf, F., Rode, M., Rink, K., Rinke, K., Samaniego, L., Vieweg, M., Vogel, H.-J., Weitere, M., Werban, U., Zink, M. and Zacharias, S. 2016. The Bode hydrological observatory: a platform for integrated, interdisciplinary hydro-ecological research within the TERENO Harz/Central German Lowland Observatory. Environmental Earth Sciences 76(1).

Wu, L., Liu, X., Yang, Z., Yu, Y. and Ma, X. 2022a. Effects of single- and multi-site calibration strategies on hydrological model performance and parameter sensitivity of large-scale semi-arid and semi-humid watersheds. Hydrological Processes 36(6).

Wu, S., Tetzlaff, D., Yang, X. and Soulsby, C. 2022b. Disentangling the Influence of Landscape Characteristics, Hydroclimatic Variability and Land Management on Surface Water NO3-N Dynamics: Spatially Distributed Modeling Over 30 yr in a Lowland Mixed Land Use Catchment. Water Resources Research 58(2).

Yang, X., Jomaa, S., Buttner, O. and Rode, M. 2019a. Autotrophic nitrate uptake in river networks: A modeling approach using continuous high-frequency data. Water Res 157, 258-268.

Yang, X., Jomaa, S., Zink, M., Fleckenstein, J.H., Borchardt, D. and Rode, M. 2018. A New Fully Distributed Model of Nitrate Transport and Removal at Catchment Scale. Water Resources Research.

Yang, X. and Rode, M. 2020 A Fully Distributed Catchment Nitrate Model - mHM-Nitrate v2.0.

Yang, X.Q., Jomaa, S. and Rode, M. 2019b. Sensitivity Analysis of Fully Distributed Parameterization Reveals Insights Into Heterogeneous Catchment Responses for Water Quality Modeling. Water Resources Research 55(12), 10935-10953.

Ye, S., Covino, T.P., Sivapalan, M., Basu, N.B., Li, H.-Y. and Wang, S.-W. 2012. Dissolved nutrient retention dynamics in river networks: A modeling investigation of transient flows and scale effects. Water Resources Research 48(6).

Ye, S., Reisinger, A.J., Tank, J.L., Baker, M.A., Hall, R.O., Rosi, E.J. and Sivapalan, M. 2017. Scaling Dissolved Nutrient Removal in River Networks: A Comparative Modeling Investigation. Water Resources Research 53(11), 9623-9641.

Yen, H., Wang, X., Fontane, D.G., Harmel, R.D. and Arabi, M. 2014. A framework for propagation of uncertainty contributed by parameterization, input data, model structure, and calibration/validation data in watershed modeling. Environ Modell Softw 54, 211-221.

Yevenes, M.A., Figueroa, R. and Parra, O. 2018. Seasonal drought effects on the water quality of the Biobio River, Central Chile. Environ Sci Pollut Res Int 25(14), 13844-13856.

Young 1989. AGNPS: A Non-Point-Source Pollution Model for Evaluating Agricultural Watersheds.

Yuan, L., Sinshaw, T. and Forshay, K.J. 2020. Review of Watershed-Scale Water Quality and Nonpoint Source Pollution Models. Geosciences 10(1).

Zhang, L., Zhao, Y., Ma, Q., Wang, P., Ge, Y. and Yu, W. 2021. A parallel computing-based and spatially stepwise strategy for constraining a semi-distributed hydrological model with streamflow observations and satellite-based evapotranspiration. Journal of Hydrology 599.

Zhang, X., Srinivasan, R. and Van Liew, M. 2008. Multi-Site Calibration of the SWAT Model for Hydrologic Modeling. Transactions of the ASABE 51(6), 2039-2049.

Zhou, X., Jomaa, S., Yang, X., Merz, R., Wang, Y. and Rode, M. 2022. Exploring the relations between sequential droughts and stream nitrogen dynamics in central Germany through catchment-scale mechanistic modelling. Journal of Hydrology 614, 128615.

Zwolsman, J.J.G. and van Bokhoven, A.J. 2007. Impact of summer droughts on water quality of the Rhine River - a preview of climate change? Water Science and Technology 56(4), 45-55.

3.8. Supplementary materials

Text S3.1.: governing equations of nitrogen processes in the mHM-Nitrate modelS3.1.1. In the terrestrial phase

(1) Degradation from inactive soild organic nitrogen pool (humus_N) to active soild organic nitrogen pool (fast_N)

$$\text{degradN} = \text{pardegradN} * \text{fct\_temp} * \text{fct\_sm} * \text{humus\_N} / \text{DT}$$

$$\text{humus\_N} = \text{humus\_N} - \text{degradN}$$

$$\text{fast\_N} = \text{fast\_N} + \text{degradN}$$

(2) Mineralization from fast_N and dissolved organic nitrogen pool (diss_ON), respectively, to dissolved inorganic nitrogen pool (diss_IN)

$$\text{mineraN} = \text{parmineraN} * \text{fct\_temp} * \text{fct\_sm} * \text{fast\_N} / \text{DT}$$

$$\text{mineraN2} = \text{parmineraN} * \text{fct\_temp} * \text{fct\_sm} * \text{diss\_ON} / \text{DT}$$

$$\text{fast\_N} = \text{fast\_N} - \text{mineraN}$$

$$\text{diss\_ON} = \text{diss\_ON} - \text{mineraN2}$$

$$\text{diss\_IN} = \text{diss\_IN} + \text{mineraN} + \text{mineraN2}$$

(3) Dissolution from fast_N to diss_ON

$$\text{dissolN} = \text{pardissolN} * \text{fct\_temp} * \text{fct\_sm} * \text{fast\_N} / \text{DT}$$

$$\text{fast\_N} = \text{fast\_N} - \text{dissolN}$$

$$\text{diss\_ON} = \text{diss\_ON} + \text{dissolN}$$

where degradN is degradation amount (mg N m^{-2}), mineraN and mineraN2 are mineralization amount (mg N m^{-2}), dissolN is dissolution amount (mg N m^{-2}), pardegradN, parmineraN and pardissolN is landuse dependent degradation rate, mineralization rate and dissolution rate, respectively (d^{-1}); fct_temp and fct_sm is common function that represent impacts of soil temperature and soil moisture, respectively, DT = model timestep (h)/24.

(4) Soil denitrification

$$\text{denitri\_s} = \text{deni\_s} * \text{fct\_temp} * \text{fct\_sm} * \text{fct\_conc} * \text{diss\_IN} / \text{DT}$$

$$\text{diss\_IN} = \text{diss\_IN} - \text{denitri\_s}$$

where denitri_s is denitrified nitrate amount (mg N m^{-2}), deni_s is soil denitrification rate (d^{-1}); fct_temp, fct_sm and fct_conc represent functions of impacts of soil temperature, soil moisture and nitrate concentration, respectively.

(5) Plant/crop uptake

Potential uptake (uptk_max) is based on the logistic plant/crop growth function from SOILN model in HYPE.

$$\text{uptk} = \min\left(\text{uptk\_max}, \left(1 - \frac{\text{wp}}{\text{SM}}\right) * \text{diss\_IN}\right)$$

$$\text{diss\_IN} = \text{diss\_IN} - \text{uptk}$$

where uptk is uptake amount (mg N m^{-2}), wp is wilting point, SM is soil moisture.

S3.1.2. In-stream phase

(1) In-stream denitrification (denitri_w)

$$denitri\_w = deni\_w * f_{temp} * f_{conc} * A/DT$$

$$DIN = DIN - denitri\_w$$

where DIN is dissolved inorganic nitrogen pool in water; $deni_w$ is in-stream denitrification rate (mg N m^{-2} d^{-1}); f_{temp} and f_{conc} represent function of stream water temperature and nitrate concentration impacts, respectively, on in-stream denitrification; A is stream benthic area (m^{-2}).

(2) Instream primary uptake (assim) and mineralization are inverse transformation between DIN and dissolved inorganic nitrogen pool (DON) in water

$$assim = pprt * f_{temp1} * f_{temp2} * f_{light} * d * A/DT$$

$$DON = DON + assim$$

where DON is dissolved organic nitrogen pool in water; pprt is in-stream primary production rate (mg N m^{-3} d^{-1}); f_{temp1} , f_{temp2} and f_{light} represent function of water temperature and light effects, respectively, on primary production (Yang et al., 2019); d is the water depth (m). f_{temp1} is only depend on the water temperature, f_{temp2} determines which one is dominate between primary production and mineralization (Lindström et al., 2010).

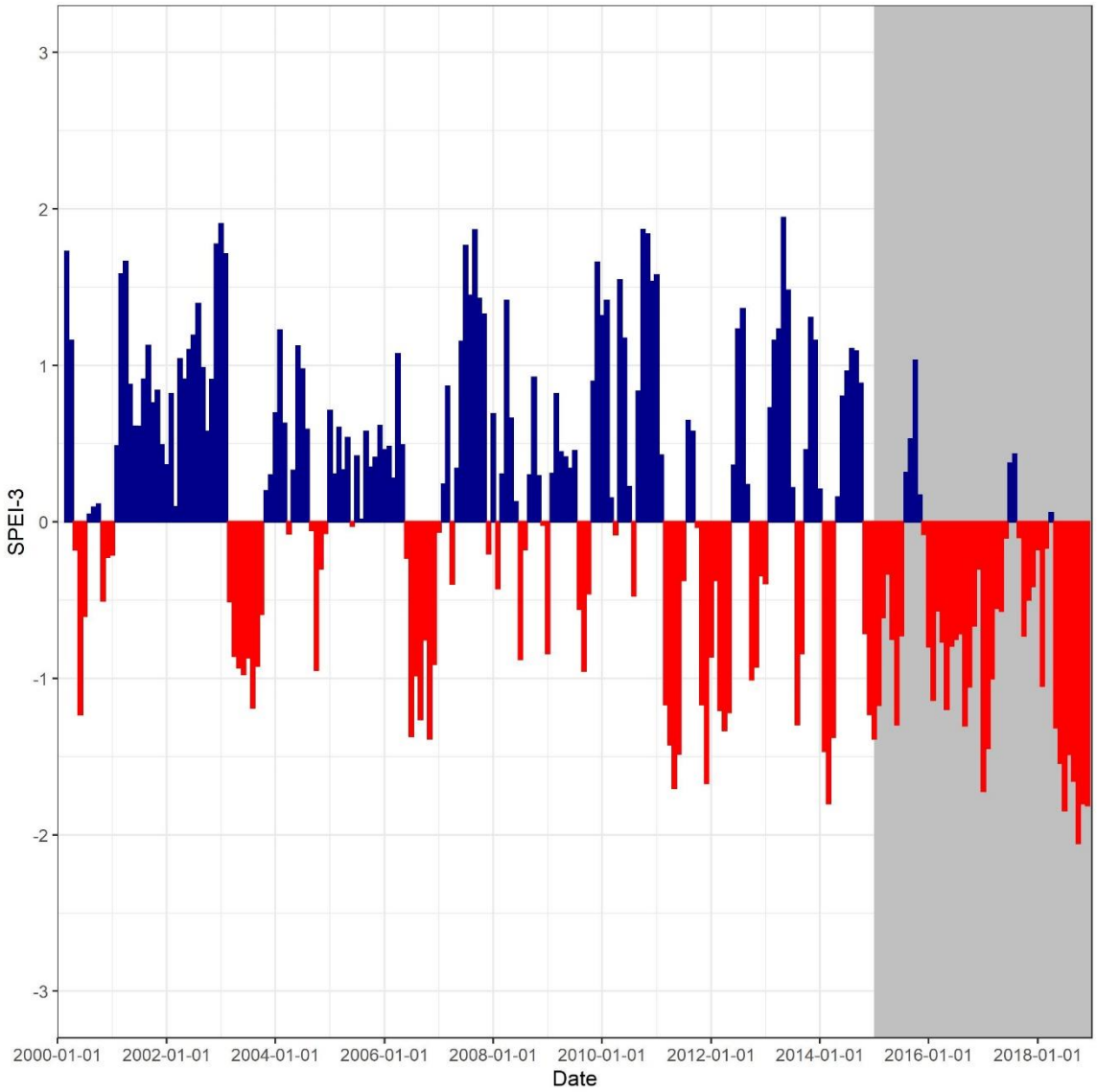

Figure S3.1. The SPEI values on a 3-month time scale during 2000-2018 at the gauging station Stassfurt.

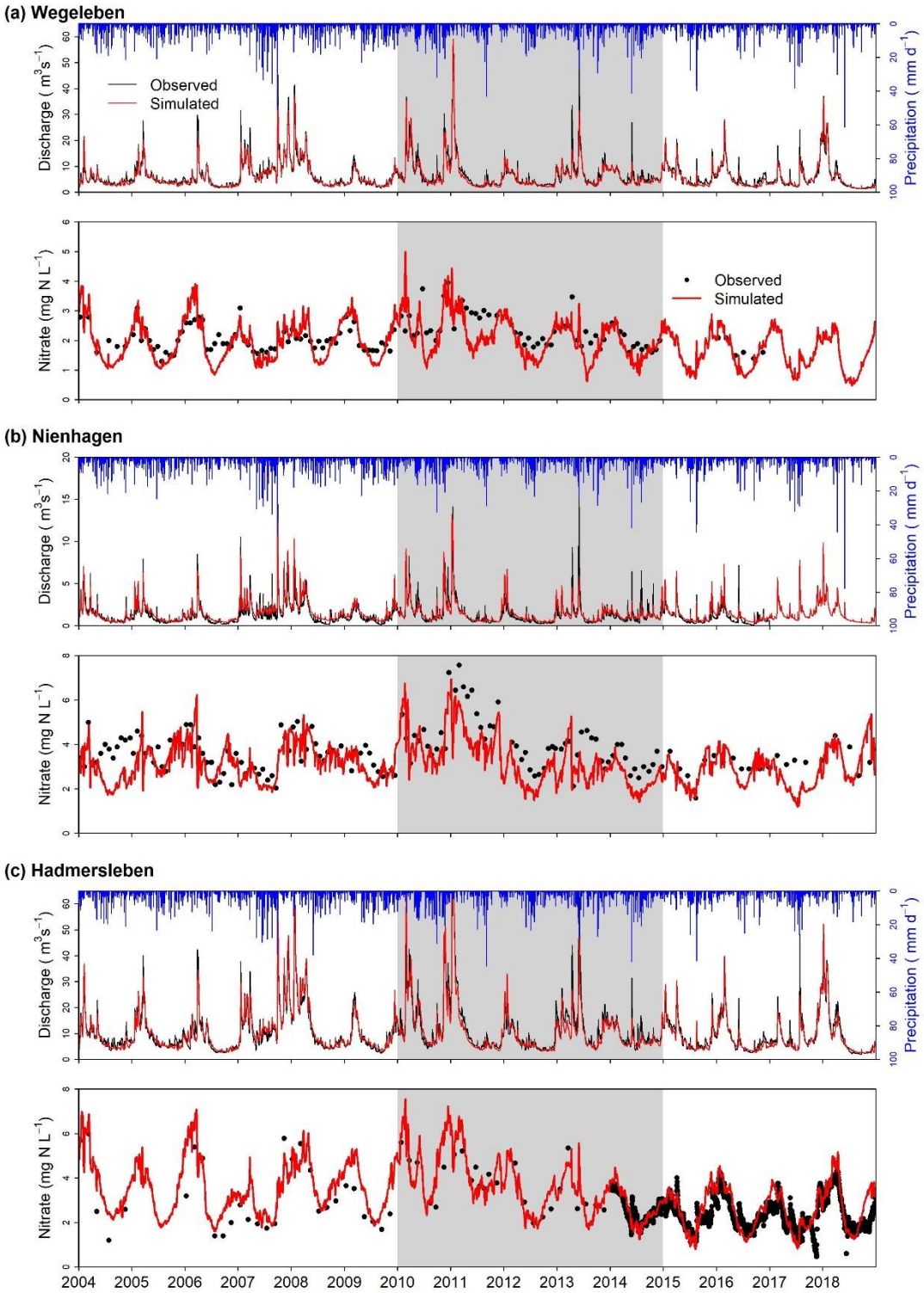

Figure S3.2. Observed and simulated daily discharge and nitrate concentration time series during calibration (2010-2014) and validation periods (2004-2009 and 2015-2018) for the (a) Wegeleben, (b) Nienhagen and (c) Hadmersleben gauging stations.

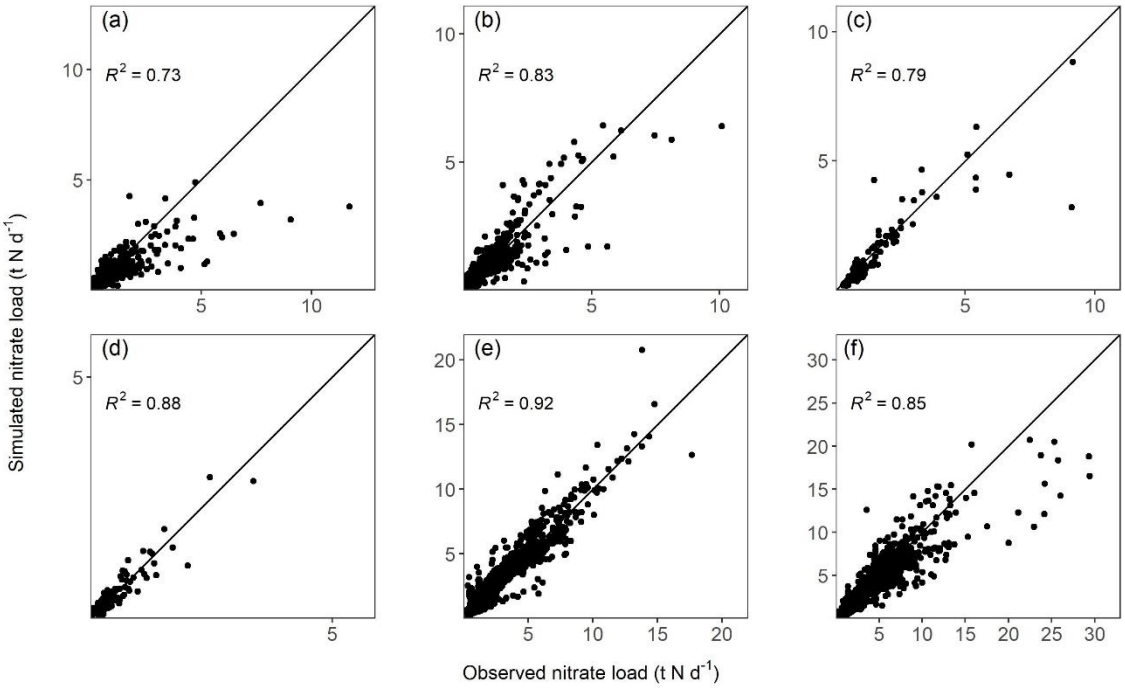

Figure S3.3. Observed and simulated daily nitrate loads during the model simulation period (2004-2018) for the (a) Meisdorf, (b) Hausneindorf, (c) Wegeleben, (d) Nienhagen, (e) Hadmersleben and (f) Stassfurt gauging stations.

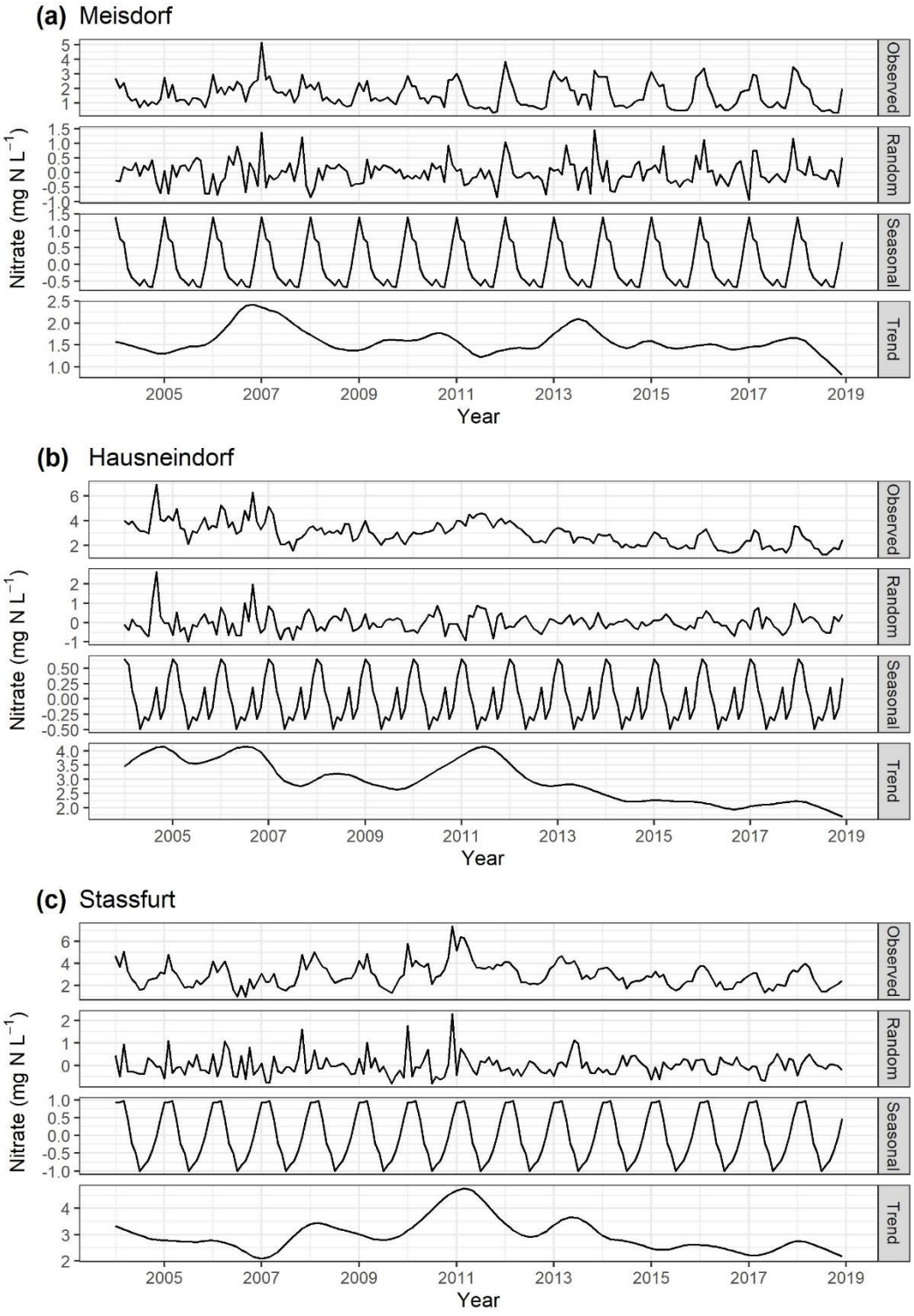

Figure S3.4. Monthly observed nitrate concentration and its three components (random, seasonal and trend) from 2004-2018 for the (a) Meisdorf, (b) Hausneindorf and (c) Stassfurt gauging stations.

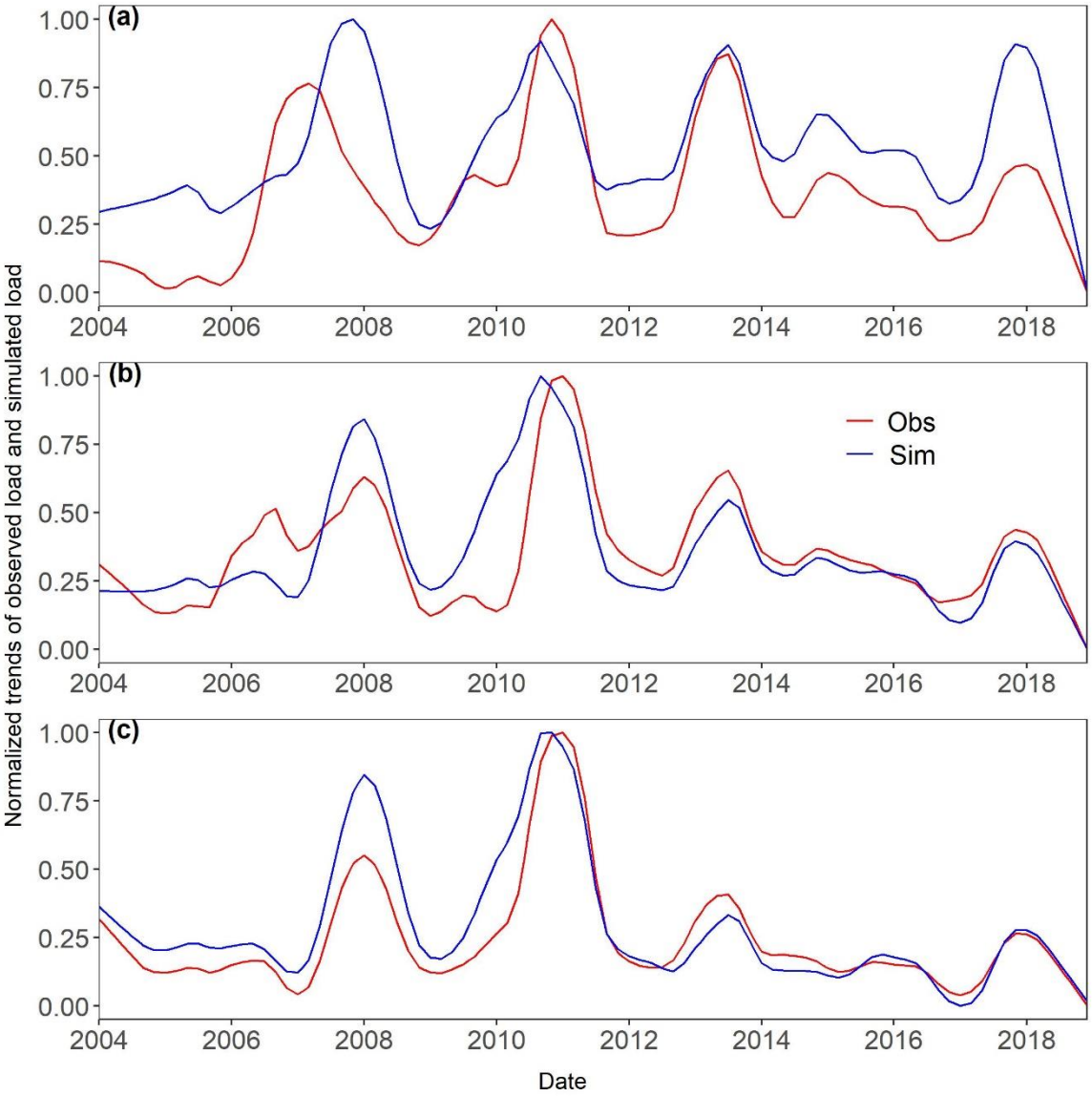

Figure S3.5. Normalized trends of monthly observed (red lines) and simulated nitrate load (blue lines) during 2004-2018 at the gauging stations (a) Meisdorf, (b) Hausneindorf and (c) Stassfurt.

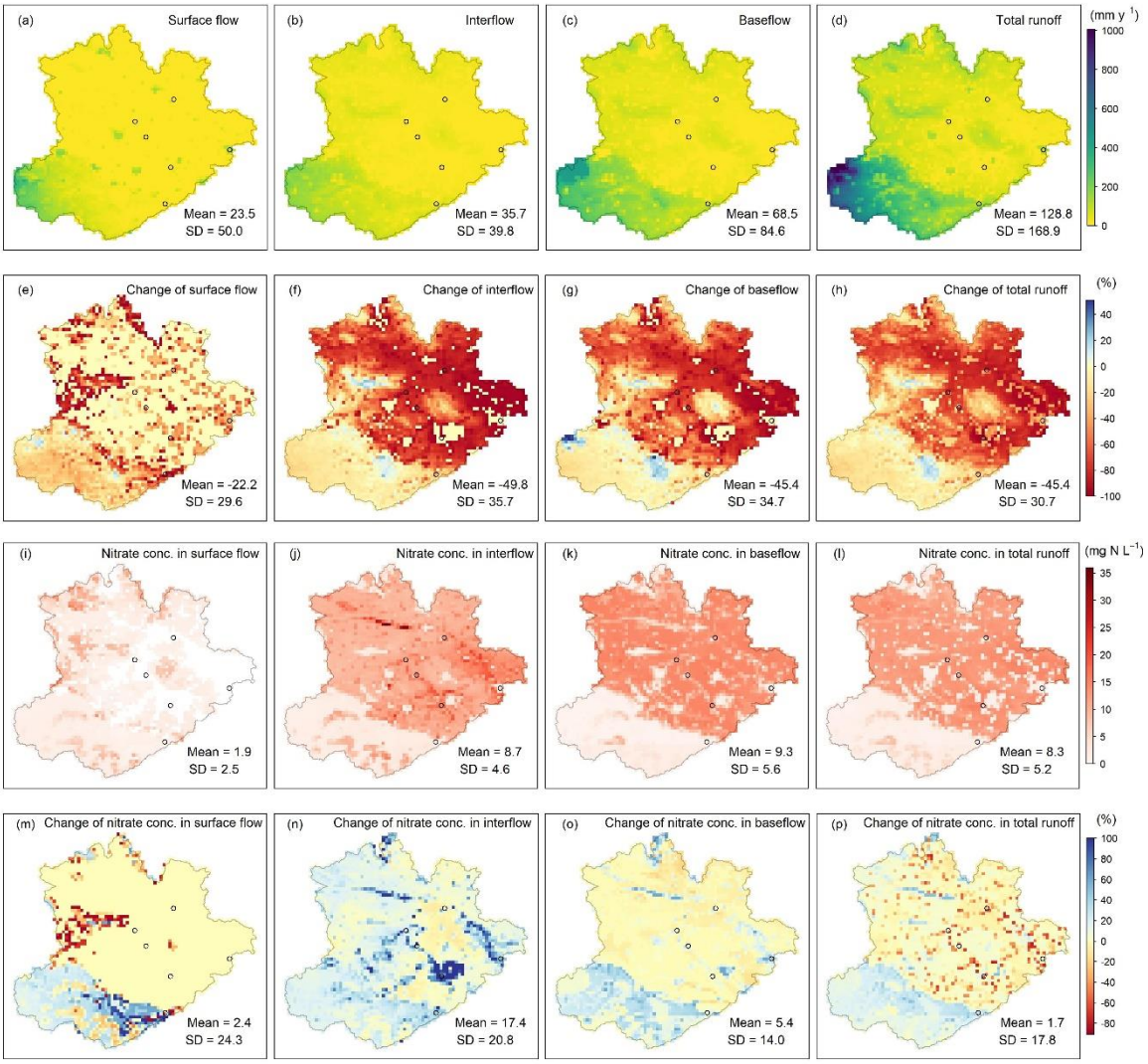

Figure S3.6. Spatial distribution of simulated (a-d) annual mean total runoff and its three components from 2004-2014 and (e-h) the corresponding change from 2015-2018 compared to 2004-2014. Spatial distribution of simulated (i-l) annual mean nitrate concentrations in total runoff and its components from 2004-2014 and (m-p) the corresponding change from 2015-2018 compared to 2004-2014. SD represents the standard deviation.

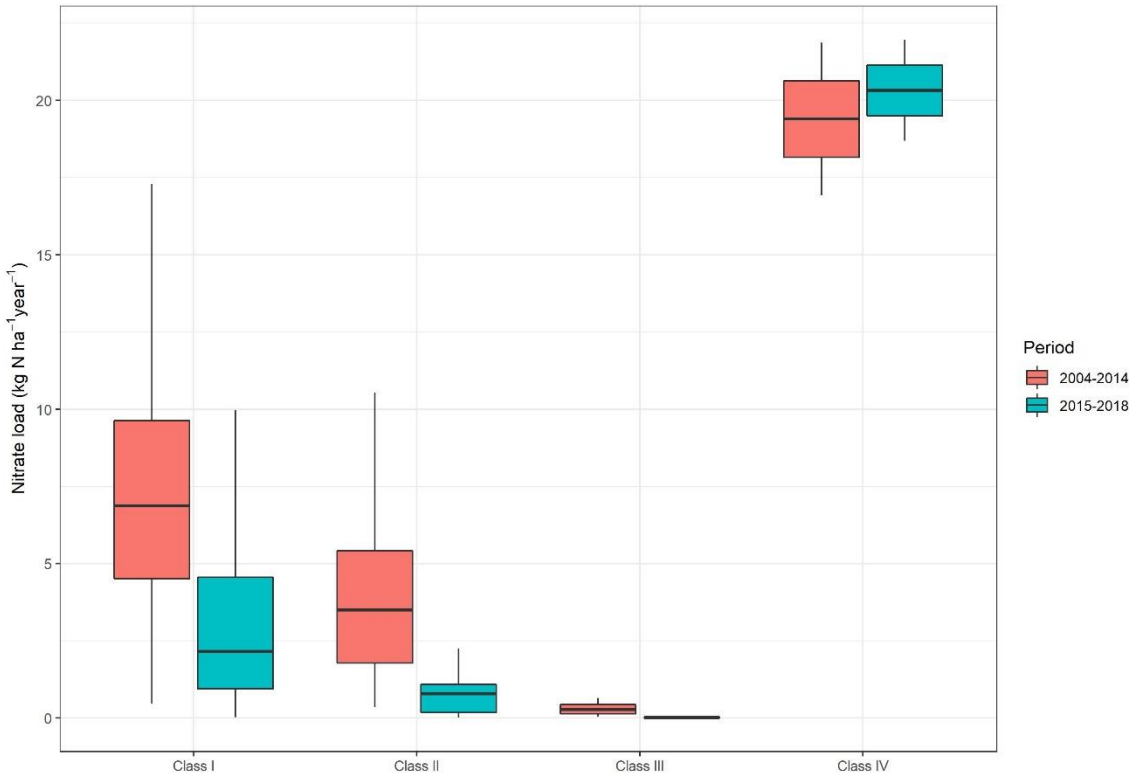

Figure S3.7. Mean annual terrestrial nitrate export load in four soil-land-use classes during the pre-drought period (2004-2014) and the drought period (2015-2018).

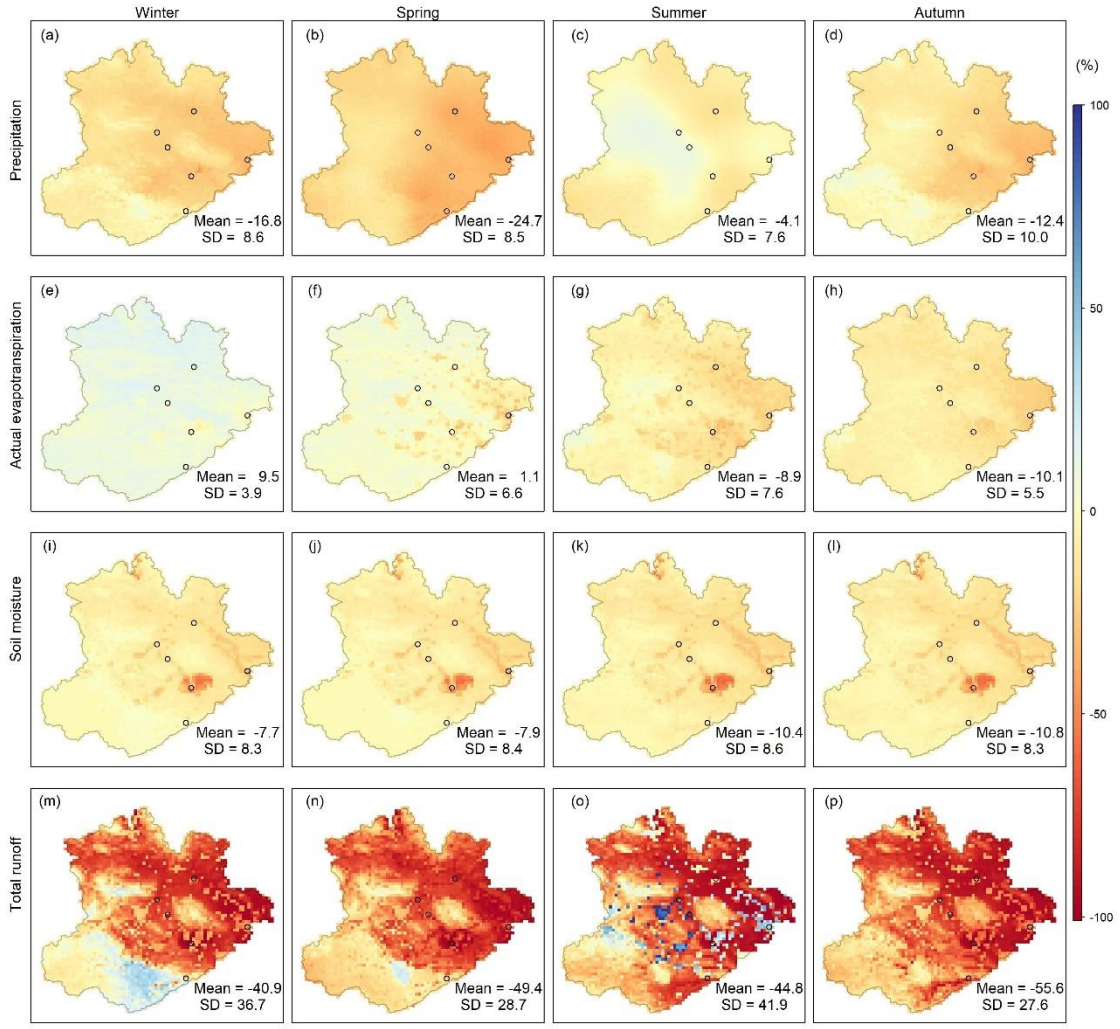

Figure S3.8. Spatial distributions of the difference in mean seasonal precipitation, actual evapotranspiration, soil moisture content and total runoff in the drought period (2015-2018) compared to the reference period (2004-2014).

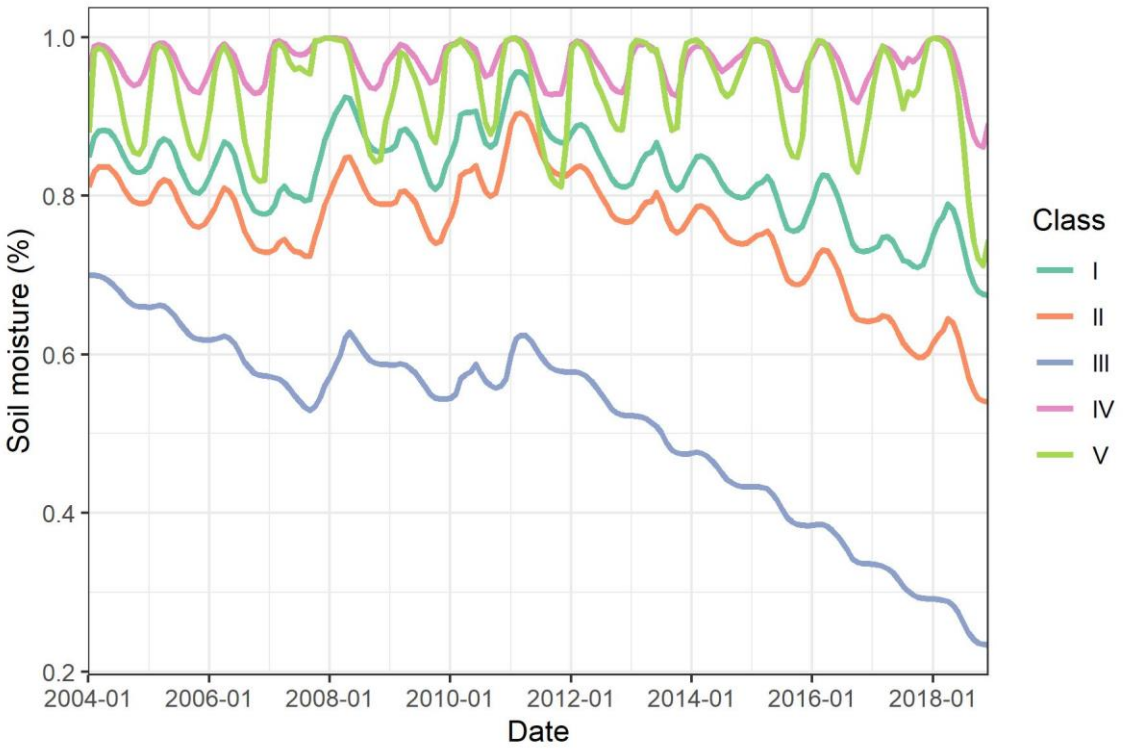

Figure S3.9. Dynamics of modeled soil moisture (%) of the third layer in the five soil-land-use classes (I-V) during 2004-2018.

Table S3.1. Mann-Kendall test of nitrate concentration at three gauging stations in 2004-2018.

Station	MK test	Winter	Spring	Summer	Autumn
Meisdorf	τ	-0.1282	-0.2564	-0.3590	-0.1026
	p-value	0.5830	0.2464	0.0995	0.6693
Hausneindorf	τ	**-0.5897****	**-0.5385***	**-0.6667****	**-0.8462****
	p-value	0.0060	0.0124	0.0019	0.0001
Stassfurt	τ	-0.2381	-0.1810	-0.0476	-0.2381
	p-value	0.2350	0.3731	0.8431	0.2350

* indicates significant trend at 0.05 level, ** indicates significant trend at 0.01 level.

Table S3.2. Crop data for different crop types at the Bode catchment. Fertiliser amount (*frtn*, kg ha^{-1} y^{-1}), day number of fertiliser application (*frtday*), fraction of fertiliser that is tilled down to second soil layer (*frtdown*), fertiliser period (*frtperiod*), plants residue amount (*resn*, kg ha^{-1} y^{-1}) added to the soil N pool, day number of plants residue application (*resday*), fraction of plants residue that is tilled down to second soil layer (*resdown*), fraction of plants residue that are added to active solid organic soil N pool.

Crop_id	crop_name	frtn	frtday	frtdown	frtperiod	resn	resday	resdown	resfast
1	winter_wheat_lw	173	110	0.08	60	19.6	260	0.2	0.8
2	winter_barley	133	97	0.1	60	13	262	0.2	0.6
3	sugarbeets	89	123	0.1	60	15.2	270	0.2	0.6
4	rapeseed	181	97	0.1	60	20	262	0.2	0.6
5	inte_grass	54	120	0.2	60	0	290	0.3	0.8
6	exte_grass	20	100	0.1	60	0	300	0.2	0.6
7	forest	0	130	0	60	15	290	0.3	0.1
8	winter_wheat_up	158	110	0.08	60	19.6	260	0.2	0.8
9	triticale	105	104	0.1	60	19.5	87	0.2	0.6

Chapter 4: Stream restoration can reduce nitrate levels in agricultural landscapes

Xiangqian Zhou[a,*], Seifeddine Jomaa[a], Xiaoqiang Yang[a] , Ralf Merz[b], Yanping Wang[c], Michael Rode[a,d,*]

[a]Department of Aquatic Ecosystem Analysis and Management, Helmholtz Centre for Environmental Research - UFZ, Magdeburg, Germany
[b]Department of Catchment Hydrology, Helmholtz Centre for Environmental Research - UFZ, Halle (Saale), Germany
[c]School of Geographical Science, Nantong University, Nantong, China
[d]Institute of Environmental Science and Geography, University of Potsdam, Potsdam-Golm, Germany
*Corresponding authors: Xiangqian Zhou (xiangqian.zhou@ufz.de), Michael Rode (michael. rode@ufz.de)

4.1. Abstract

The EU Water Framework Directive (WFD) has emphasized that altered stream/river morphology and diffuse pollution are the two major pressures faced by European water bodies at catchment scales. Increasing efforts have been directed toward restoration to meet WFD standards for ecological health, but this work has achieved limited success. One challenge is that little is known about how morphological changes (i.e., re-meandering) may affect nitrate retention within whole stream networks. We investigated this issue in the well-monitored Bode catchment (3,200 km^2) in central Germany. First, we implemented a fully distributed process-based mHM-Nitrate model, exploring its performance over the period from 2015 to 2018. Second, we simulated the effects of restoring more natural stream morphology (i.e., increasing sinuosity) on nitrate retention. The mHM-Nitrate model performed well in replicating daily discharge and nitrate concentrations (median Kling-Gupta values of 0.78 and 0.74, respectively). Within the stream network, mean and standard deviation (SD) of gross nitrate retention efficiency was 5.1±0.61% and 74.7±23.2% in the winter and summer, respectively; this measure took into account both denitrification and assimilatory uptake. In the summer, the denitrification rate was about two times higher in a lowland sub-catchment dominated by agricultural lands than in a mountainous sub-catchment dominated by forested areas (median ± SD of 204±22.6 and 102±22.1 mg N m^{-2} d^{-1}, respectively). Similarly, in the same season, the assimilatory uptake rate was approximately five times higher in streams surrounded by lowland agricultural areas than in streams in higher-elevation, forested areas (median ± SD of 200±27.1 and 39.1±8.7 mg N m^{-2} d^{-1}, respectively). This suggests that restoration strategies targeted at lowland agricultural areas may have a greater potential for increasing nitrate retention. In our simulation, restoring stream sinuosity was found to increase net nitrate retention efficiency by up to 25.4±5.3%; greater effects were seen in small streams. Taken together, our results indicate that restoration efforts should consider augmenting stream sinuosity to increase nitrate retention and decrease nitrate concentrations at the catchment scale.

Keywords:

River restoration; sinuosity; mHM-Nitrate model; stream denitrification; assimilatory uptake

Highlights:

- The simulated denitrification rate and assimilatory uptake rate are higher in agricultural than in forest areas.
- Increasing stream sinuosity due to stream restauration improves net nitrate retention efficiency more in small streams than in large streams.
- Small streams in agricultural areas should be given priority in restoration efforts.

4.2. Introduction

Excess nitrogen in surface waters represents a major threat to aquatic ecosystems (Birgand et al., 2007). In streams, inorganic nitrogen largely occurs in the form of nitrate (NO_3^-), a highly water soluble ion that can easily enter streams and rivers from both diffuse and point sources. To reduce NO_3^- levels in Europe's streams and rivers, extensive management strategies have been deployed over the past three decades (European Commission, 1991a; European Commission, 1991b). Their success remains limited, as around 60% of Europe's surface water bodies still have not achieved good ecological status (European Environment Agency,2018). The EU Water Framework Directive (WFD) has emphasized that, in Europe, altered stream/river morphology and diffuse pollution are two key pressures acting on water bodies at the catchment scale (Carvalho et al., 2019). For example, more than 37% of Germany's rivers are classified as heavily modified, as a result of channelization or straightening (Pander et al., 2017). The loss of stream bottoms has shortened water residence times and limited hyporheic exchanges, resulting in lower levels of nutrient retention and greater rates of downstream transport (Baker, Bledsoe and Price, 2012; Doyle, Stanley and Harbor, 2003; Gucker and Boechat, 2004; Opdyke, David and Rhoads, 2006). Attention has turned to stream restoration as a management tool for increasing nitrate retention (Craig et al., 2008; Newcomer Johnson et al., 2016; Wohl, Lane and Wilcox, 2015). Multiple techniques have been tested out in headwater streams and large lowland rivers (Flávio et al., 2017), such as re-meandering (Lorenz, Jahnig and Hering, 2009; Pedersen, Kristensen and Friberg, 2014) and reconnecting streams with floodplains (Roley, Tank and Williams, 2012) and ponds (Passy et al., 2012) in agricultural zones.

Within streams, nitrate retention is the result of temporary retention by plants (i.e., assimilatory uptake) and permanent removal by bacteria (i.e., denitrification) (Groffman et al., 2009; Ye et al., 2012). In general, stream restoration is thought to promote both processes (assimilatory

uptake: Huang et al. 2022; denitrification: Craig et al., 2008). To date, research has largely focused on the effects of re-meandering at the reach scale and has found contrasting results (Bukaveckas, 2007; Craig et al., 2008; Kaushal et al., 2008; Klocker et al., 2009; Lin et al., 2021; Veraart et al., 2014; Wagenschein and Rode, 2008). For example, denitrification was seen to be higher in restored streams (i.e., after reconnection with floodplains) than in unrestored streams (Kaushal et al., 2008; Roley, Tank and Williams, 2012). Furthermore, restored reaches may display higher levels of gross primary productivity and ecosystem respiration (Kupilas et al., 2017). In contrast, Klocker et al. (2009) found no difference in denitrification rates between restored and unrestored streams, and Veraart et al. (2014) observed that denitrification rates were highly variable: for some streams, rates were significantly higher in unrestored versus restored sections, while, in other streams, rates did not vary among sections. The researchers attributed these results to differences in hydrological conditions and levels of sedimentary organic matter. Thus, we presently have a limited understanding of how restoration could affect nitrate retention at broader scales.

Within stream networks, nitrate retention is shaped by complex interactions between hydrological, geomorphological, and biogeochemical processes (Ensign and Doyle, 2006; Yang et al., 2019; Ye et al., 2012). While the effects of hydrological and biogeochemical processes have been explored to some degree (Alexander et al., 2009; Covino, McGlynn and Baker, 2010; Marcé et al., 2018), there has been no systemic research on networks with contrasting morphologies and, more notably, on the effects of restoration efforts (i.e., re-meandering). This gap in knowledge likely results from three key challenges. First, it is difficult to disentangle how nitrate retention is affected by geomorphology versus other factors (e.g., discharge, NO_3^- concentration) (Lin et al., 2016). Second, we lack detailed historical information on stream morphology (i.e., natural conditions) within catchments (Guzelj, Hauer and Egger, 2020). Third, uncertainty arises when attempts are made to parse out the influences

of lateral terrestrial flows versus in-stream processes (Helton, Hall and Bertuzzo, 2018; Helton et al., 2011).

Scenario analysis holds promise for addressing these challenges because it can be implemented by combining fully distributed catchment modeling with detailed spatiotemporal data from monitoring programs. In particular, simulations can explore how re-meandering could affect nitrate retention at the network scale. Recently, Yang et al. (2018) developed a fully distributed grid-based hydrological nitrate model (mHM-Nitrate) that can provide detailed spatial information on terrestrial nitrate inputs within stream networks. This model has successfully described terrestrial and aquatic processes (i.e., assimilatory uptake) (Yang et al., 2019) across different catchments (Wu et al., 2022b; Yang et al., 2018; Zhou et al., 2022). In addition, researchers have been extensively characterizing the denitrification rates associated with different land-use types (Böhlke et al., 2009; Mulholland et al., 2009). This has yielded abundant opportunities for evaluating how morphological changes in streams can spatially and temporally impact nitrate transport and retention.

Here, we looked at how stream morphology affects spatiotemporal nitrate retention dynamics within a stream network—the Bode catchment in central Germany. To this end, we used the mHM-nitrate model, which can handle large gradients in catchment characteristics. More specifically, we aimed to i) evaluate the reliability of the model simulation by assessing assimilatory uptake and denitrification throughout the entire catchment before evaluating stream restoration scenarios ; ii) characterize spatiotemporal variability in retention dynamics and identify the key factors at play in two sub-catchments to inform stream restoration measures; and iii) simulate the effects of re-meandering on nitrate concentrations and retention efficiency for a stream network.

4.3. Study area and methods

4.3.1. Study area

Covering around 3,200 km^2 in central Germany, the Bode catchment is closely monitored and thus serves as a rich source of hydrological and hydrochemical data (Mueller et al., 2016; Wollschläger et al., 2016). The catchment extends from the Harz Mountains, a low, rocky mountain range, to the northeastern lowlands of central Germany. Annual precipitation follows an elevational gradient within the catchment, ranging from more than 1,500 mm in the upper Harz Mountains to less than 500 mm in the vast lowland plains (Figure 4.1a). Mean annual air temperature ranges from 5 °C at Brocken, the mountain's highest peak, to 9.5 °C in eastern Magdeburg Börde (Wollschläger et al., 2016). The Harz Mountains have steep slopes with shallow, less fertile soils that are predominantly covered by forests. All agricultural activity is associated with the region's plateaus and lower-elevation areas. Within the catchment, 66% of the land is arable; 26% is forested or composed of semi-natural habitat; 7% is urban or dedicated to open-cast mining; and 1% is covered by water bodies and wetlands (CORINE 2012 land cover map, https://gdz.bkg.bund.de/index.php/default/open-data.html, last accessed 1 June 2020; Figure 4.1b).

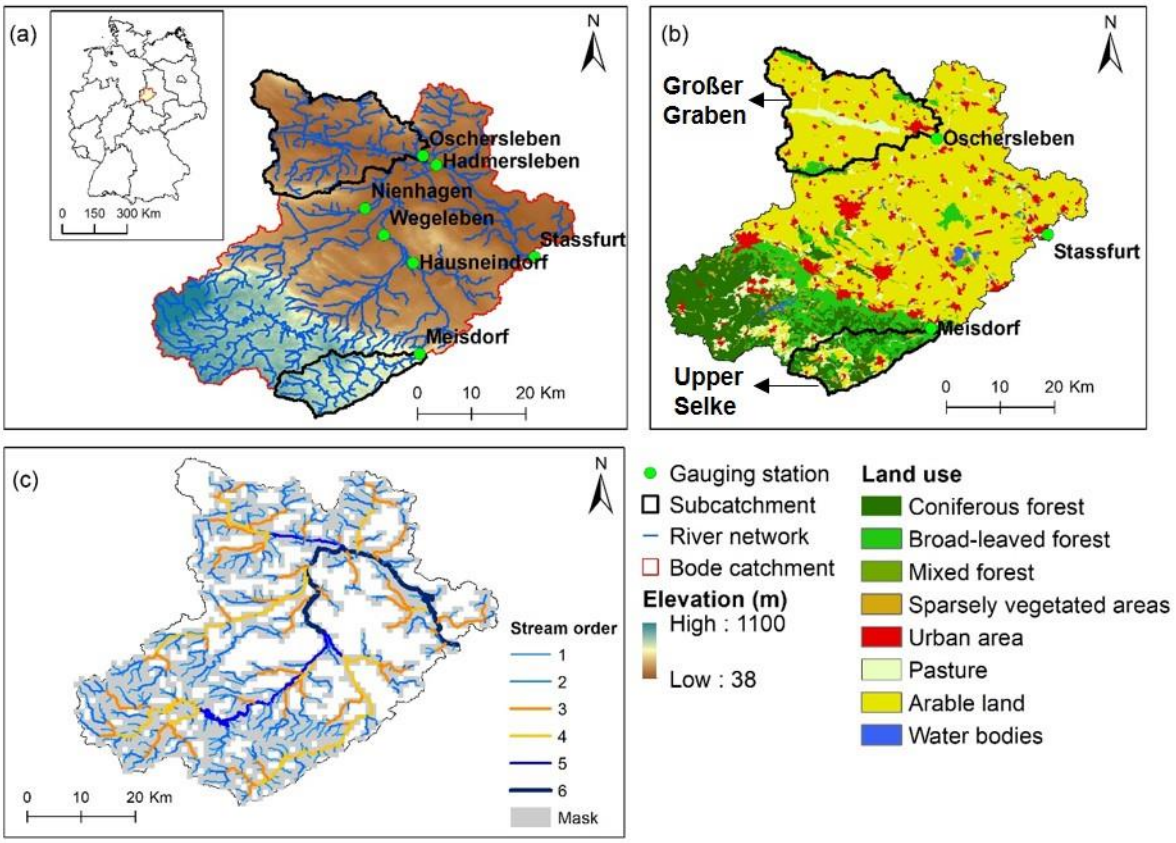

Figure 4.1. Bode catchment: (a) elevational map showing the gauging stations, (b) land use map and two sub-catchments, and (c) stream order obtained from the mHM-Nitrate model (1-km routing grid) with a stream mask derived from the observed network.

We chose two sub-catchments with different representative landscapes to investigate retention processes in greater detail. Upper Selke is a sub-catchment located in the Harz Mountains (Meisdorf outlet; Figure 4.1); it is dominated by forests (73% of 177.7 km^2) and contains natural streams. Großer Graben is a sub-catchment in the intensively farmed lowlands (Oschersleben outlet; Figure 4.1); it is dominated by arable land (87.4% of 435.4 km^2) and contains heavily modified streams (Figure 4.1b).

About 80% of the lowland stream network is heavily modified or completely changed (State Agency for Flood Protection and Water Management of Saxony-Anhalt, LHW; http://gldweb.dhi-wasy.com/gld-portal/, last accessed 10 April 2020; Figure S4.1). Stream order analysis showed that there were two times more streams in Großer Graben than in Upper Selke (Table S4.1), the result of artificial drainage in the former. Additionally, the total stream

length in Großer Graben was twice that in Upper Selke, except in the case of 1st-order streams (Table S4.1). Small streams (1^{st}–3^{rd} order) accounted for a high percentage of total stream length: 81% and 88% in Großer Graben and Upper Selke, respectively.

Mean daily nitrate concentrations (data collected at 15-min intervals) were available for the Meisdorf, Hausneindorf, Hadmersleben, and Stassfurt stations (Helmholtz Centre for Environmental Research – UFZ; Rode et al., 2016a). Monthly and biweekly nitrate data (obtained via grab samples) were available for the Wegeleben, Nienhagen, and Oschersleben stations (LHW, http://gldweb.dhi-wasy.com/gld-portal/, last accessed 10 April 2020). Daily discharge data were available for all seven stations (LHW, http://gldweb.dhi-wasy.com/gld-portal/, last accessed 10 April 2020). Monthly nitrate concentrations were available for the Wegeleben and Nienhagen stations between 2007 and 2014. For the Wegeleben station, nitrate concentrations were unavailable in 2015 and between 2017 and 2018. However, they were available at two-month intervals at the Nienhagen station from 2015 to 2018 and at monthly intervals at the Oschersleben station from 2010 to 2018.

4.3.2. mHM-Nitrate model

The mHM-Nitrate model is a fully distributed process-based model of nitrate dynamics at the catchment scale (Yang et al., 2018). It was developed from the mesoscale Hydrological Model (Samaniego, Kumar and Attinger, 2010) and the Hydrological Predictions for the Environment model (Lindström et al., 2010). The mHM-Nitrate model simultaneously characterizes the hydrological and nitrate processes associated with terrestrial and stream environments for individual grid cells using a daily time step. For the terrestrial environment, the model considers the following key hydrological processes: interception, snow accumulation, snow melting, evapotranspiration, infiltration, groundwater recharge, and runoff generation. The nitrate processes considered are the sources of nitrate (i.e., wet atmospheric deposition, application of fertilizer and manure, and presence of plant/crop residues), transports (i.e.,

infiltration through multiple soil layers and percolation to the deep groundwater layer), sinks (i.e., denitrification and uptake by plants/crops), and transformation among the four nitrogen pools (i.e., dissolved inorganic nitrogen, dissolved organic nitrogen, active solid organic nitrogen, and inactive solid organic nitrogen) for each soil layer. The quantity of mineral and manure fertilizers applied was dependent on the crop type, and it was assumed that they were applied uniformly throughout the fertilization period. The State agricultural authority provided information on the rates and dates of fertilization. The fertiliser amount at 1 km resolution was calculated by adding the amount of fertiliser for each crop type in the 1 km grid. The wet atmospheric deposition amount was determined by multiplying the amount of rainfall by the concentration of nitrate in the rainfall. Wet deposition is considered as total nitrogen including NO_3, NH_4 as well as NO_2. Dry deposition is a minor contributor to total N deposition, which was measured at less than 10% of total atmospheric N deposition. For the stream environment, the model considered nitrate transformation (i.e., denitrification, assimilatory uptake, and remineralization) for each reach. More detailed descriptions of the mHM-Nitrate model can be found in Yang et al. (2018) and Yang et al. (2019); the source code can be found in Yang and Rode (2020).

Gross nitrate assimilatory uptake within streams (F_{assim}; kg N d^{-1}) was calculated using the new regionalization approach proposed by Yang et al. (2019):

$$F_{assim} = U_{assim} \times f_L \times W \times L \times H \times \Delta t \qquad (1)$$

where U_{assim} is the assimilatory uptake rate (mg N m^{-3} d^{-1}); $f_L \in$ [0,1] is a light availability coefficient that reflects the combined impact of global radiation and riparian shading on assimilatory uptake; and W, L, H are stream width (m), length (m), and depth (m), respectively.

Net assimilatory uptake within streams (F_{net}; kg N d^{-1}) was calculated by subtracting remineralization from gross assimilatory uptake (Yang et al., 2019), which was determined by multiplying gross assimilatory uptake and a temperature factor (f_T),

$$F_{net} = F_{assim} \times f_T \times f_{net} \quad (2)$$

$$f_T = \frac{T}{20} \times \frac{T_{10} - T_{20}}{5} \quad (3)$$

where $f_{net} \in [0,1]$ is a land-use coefficient that reflects the fraction of gross assimilatory uptake; T is water temperature (°C); and T_{10} and T_{20} are mean water temperature at 10 and 20 days, respectively.

The amount of denitrification within streams (F_{den}; kg N d^{-1}) was calculated based on the relationship between the denitrification rate and nitrate concentrations:

$$F_{den} = U_{den} * W * L \quad (4)$$

$$U_{den} = U_{max} * \frac{C_{NO_3^-}}{C_{NO_3^-} + ks} * f_{temp} \quad (5)$$

$$f_{temp} = \begin{cases} 0 & , \quad T < 0 \\ \frac{T}{5} \times 2^{\frac{T-20}{10}}, & 0 < T < 5 \\ 2^{\frac{T-20}{10}}, & T > 5 \end{cases} \quad (6)$$

where U_{max} is the maximum potential denitrification rate (mg N m^{-2} d^{-1}) and U_{den} is the denitrification rate (mg N m^{-2} d^{-1}) adjusted for $C_{NO_3^-}$ (nitrate concentration; mg N L^{-1}) and ks (nitrate concentration at half saturation; mg N L^{-1}). The latter has a default value of 1.5 mg N L^{-1} in the mHM-Nitrate model (Yang et al., 2018).

The net nitrate retention efficiency (Eff_{net}) of a stream is the amount of nitrate retained by net assimilatory uptake and denitrification (sum of F_{den} and F_{net}) divided by the total nitrate input load (L_{input}; the sum of lateral terrestrial imports and upstream loads). The gross nitrate retention efficiency (Eff_{gross}) for a stream is the amount of nitrate retained by gross

assimilatory uptake and denitrification (sum of F_{den} and F_{assim}) divided by the total nitrate input load (L_{input}) (Wollheim et al., 2008a).

In previous studies using the mHM-Nitrate model, stream networks were generated using the digital elevation model (DEM), and nitrate retention processes within streams (both assimilatory uptake and denitrification) were considered for all reaches (i.e., grid cells). This approach may generate a high degree of uncertainty around retention levels because of the uncertainty around the quantity of benthic surface area within the stream network. Thus, we employed a high-resolution digital elevation model (DEM; 25×25 m) in combination with the observed stream network (LHW, http://gldweb.dhi-wasy.com/gld-portal/, last accessed 10 April 2020) (Figure 4.1c) to generate a more representative model stream network.

To this end, we first created a fishnet grid polygon with a routing resolution of 1×1 km using the Create Fishnet tool in the Data Management Toolbox in ArcMap 10.8. Second, the fishnet polygon was transposed onto the observed stream network (Figure 4.1c). If the real stream occurred within a grid cell of the fishnet polygon, the grid cell was assigned a value of 1; if not, the grid cell was assigned a value of 0. Third, the fishnet was converted to raster using the Polygon to Raster tool in the Conversion Toolbox and exported into an ASCII file using the Raster to ASCII tool, also in the Conversion Toolbox. Fourth, the ASCII file was imported into the mHM-Nitrate model, where the routing source code was modified to consider an additional routing mask—representing the observed stream network. Stream retention processes were only activated within the routing mask (Figure 4.1c).

4.4.3. Model setup

We only briefly summarize the setup of the mHM-Nitrate model for the Bode catchment because it is described in detail elsewhere (Zhou et al., 2022). The data used for setup are listed in Table 4.1. The model was run using daily time steps over the period from 2006 to 2018. It was calibrated using data from 2010 to 2014. The results were validated using data from 2015

to 2018, namely discharge and nitrate concentrations at seven gauging stations that reflected key features of the Bode catchment (e.g., land use, stream order, and nitrate concentration). To model processes within terrestrial and stream environments, the grid resolution was set to 1 km. To calibrate the model, we used sensitivity analysis to identify the 15 most sensitive parameters—the top 10 hydrological parameters and the top 5 nitrate parameters (Table 4.2). The latter were the stream denitrification rate, the soil denitrification rate in arable and non-arable areas, and the assimilatory uptake rate within streams in arable and non-arable areas. The range for the assimilatory uptake rate (100–500 mg N m^{-2} d^{-1}) was defined using high-frequency sensor measurements from previous research (Rode et al., 2016a; Yang et al., 2019). The range for the stream denitrification rate (10–700 mg N m^{-2} d^{-1}) was defined using studies on lowland streams in central Germany (Huang, Borchardt and Rode, 2022; Kunz et al., 2017a; Kunz et al., 2017c; Zhang et al., 2023).

Table 4.1. Data used to set up the model in the Bode catchment.

Data Type	Resolution	Time Period	Source
Meteorological Data (Precipitation, mean, minimum and maximum temperature)	1 km × 1 km, daily	2006-2018	German Weather Service (https://opendata.dwd.de/climate_environment/CDC/observations_germany/climate/daily/, last accessed 1 June 2020)
Digital Elevation Model (DEM)	25 m × 25 m	-	Shuttle Radar Topography Mission (SRTM) DEM (https://earthexplorer.usgs.gov/, last accessed 1 June 2020)
Geological Map	1:1,000,000	-	Federal Institute for Geosciences and Natural Resources (https://produktcenter.bgr.de, last accessed 1 June 2020)
Soil Map	1:1,000,000	-	Federal Institute for Geosciences and Natural Resources (https://produktcenter.bgr.de, last accessed 1 June 2020)
Land use/ land cover Data	25 m × 25 m	-	CORINE Land Cover 10 ha (https://gdz.bkg.bund.de/index.php/default/open-data.html, last accessed 1 June 2020)
Mineral Fertilizer and Manure Application Rates	-	-	State agricultural authority (https://llg.sachsen-anhalt.de/llg/, last accessed 10 April 2020)
Crop Rotations	25 m × 25 m	-	State agricultural authority (https://llg.sachsen-anhalt.de/llg/, last accessed 10 April 2020)
Point-source Data	-	-	Urban Wastewater Treatment Directive (https://uwwtd.eu/Germany/uwwtps/treatment, last accessed 10 April 2020)
Discharge Data	daily	2006-2018	State Agency for Flood Protection and Water Management of Saxony-Anhalt (LHW) (http://gldweb.dhi-wasy.com/gld-portal/, last accessed 10 April 2020)

Data Type	Resolution	Time Period	Source
Nitrate Concentration Data	monthly to twice monthly, daily	2006-2018	LHW (http://gldweb.dhi-wasy.com/gld-portal/, last accessed 10 April 2020) and the Helmholtz Centre for Environmental Research – UFZ

Table 4.2. Description of parameters calibrated in the mHM-Nitrate model, their initial ranges and optimal values.

Process	Parameter	Description	Initial range	Optimal value
PET	pet1 (Shevenell, 1999)	Parameter for aspect correction of input potential evapotranspiration data	[6.99E-1, 1.30E+0]	9.91E-1
Soil moisture	sm10 (Cosby et al., 1984)	Transfer function parameter used to calculate soil saturated hydraulic conductivity	[-1.20E+0, -2.85E-1]	-5.76E-1
	sm17 (Brooks and Corey, 1964)	Parameter that determines the relative contribution of precipitation or snowmelt to runoff	[1.00E+0, 4.00E+0]	2.45E+0
	sm14 (Brooks and Corey, 1964)	Fraction of roots used to calculate actual evapotranspiration in forest areas	[9.00E-1, 9.99E-1]	9.69E-1
	sm16 (Brooks and Corey, 1964)	Fraction of roots used to calculate actual evapotranspiration in permeable areas	[1.00E-3, 8.99E-2]	1.33E-2
	sm4 (Cosby et al., 1984)	Pedotransfer function parameter used to calculate maximum soil moisture content	[6.46E-1, 9.51E-1]	9.47E-1
	sm11 (Cosby et al., 1984)	Pedotransfer function parameter used to calculate soil saturated hydraulic conductivity	[6.01E-3, 2.59E-2]	6.23E-3
Percolation	pc1	Parameter used to calculate the percolation coefficient	[0.00E+0, 5.00E+1]	4.99E+1
Interflow	intfl4	Slow interflow recession coefficient	[1.00E+0, 3.00E+1]	2.87E+1
	Intfl5	Slow interflow exponent coefficient	[5.00E-2, 2.99E-1]	5.40E-2
In-stream denitrification	deni_w	General parameter of in-stream denitrification rate (kg m^{-2} d^{-1})	[1.00E-8, 5.00E-2]	3.28E-4
Soil denitrification	deni_as	Soil denitrification rate on agricultural land (d^{-1})	[1.00E-8, 1.10E+1]	6.57E-3
	deni_s	Soil denitrification rate on non-agricultural land (d^{-1})	[1.00E-8, 1.10E+1]	1.09E-8
In-stream assimilation	pprt_aw	Primary production rate in agricultural streams (kg m^{-3} d^{-1})	[1.00E-8, 1.00E+0]	1.46E-2
	pprt_w	Primary production rate in non-agricultural streams (kg m^{-3} d^{-1})	[1.00E-8, 1.00E+0]	1.02E-1

4.3.4. Simulating stream restoration

We designed a model scenario to explore the effects of stream sinuosity on nitrate retention. It simulated a situation in which the current stream network had been restored, such that its

sinuosity was greater than that seen in networks of channelized streams. Stream sinuosity (S_n) in each grid cell was calculated by dividing stream length (determined from LHW data) by thalweg length (determined using the DEM). We estimated the sinuosity of natural streams using a series of equations. First, we calculated stream power (SP; kg m s^{-3}) in each grid cell as follows (Rhoads, 2010):

$$SP = \rho g Q S \quad (7)$$

where ρ is water density (1,000 kg m^{-3}), g is the gravitational acceleration (9.8 m s^{-2}), Q is the discharge rate (m^3 s^{-1}), and S is the channel slope.

Second, we calculated natural stream sinuosity for the grid cells in which stream power was greater than 10 kg m s^{-3}. We drew on the work of Harnischmacher (2007), which showed that the sinuosity of lowland streams was correlated with stream power when stream power was between 10 and 100 kg m s^{-3} (correlation coefficient = 0.946, p=0.001). This analysis used data for 11 undisturbed stream sections that served as references; these streams displayed similar geological conditions to natural streams in the lower Bode catchment (Harnischmacher, 2007). Sinuosity (S_n) was calculated as follows:

$$S_n = 0.043 + log_{10}^{SP} \quad (8)$$

For grid cells in which stream power was less than 10 kg m s^{-3}, we calculated natural stream sinuosity by estimating mean potential sinuosity based on stream type (Briem, Spitzer and Schrenk, 2003; Ministerium für Umwelt und Naturschutz Landwirtschaft und Verbraucherschutz des Landes Nordrhein-Westfalen, 2010). The lowlands of the Bode catchment are largely characterized by small loess and loam-dominated rivers (Type 18) (Figure S4.2), and potential natural sinuosity within the entire stream network ranges from 1.01 to 2.0, depending on stream type (Table S4.2). To simplify our calculations, we used the mean potential natural sinuosity for each stream type. Finally, we only focused on simulating the

restoration of streams in arable areas, since the streams in forested areas were less affected by human activity (Figure S4.1). The riparian zone was sufficiently large in the lowland arable areas to allow for increases in stream sinuosity.

In the baseline scenario (i.e., the actual state of the Bode stream network), stream sinuosity was low (mean = 1.04 for 1st–3rd order streams and mean = 1.07 for 4th–6th order streams; Table 4.3). However, there was a certain degree of variability (range: 1.00–2.73), with high levels of sinuosity seen exclusively in very short stream sections (Figure S4.3a). In the restoration scenario, mean sinuosity increased by 0.35 relative to the baseline, with the biggest augmentation seen in 6th-order streams (Table 4.3 and Figure S4.3b).

The effects of stream restoration were simulated over the validation period because the years between 2015 and 2022 were relatively dry and warm (Zhou et al., 2022), which likely represents future conditions under climate change (Huang, Krysanova and Hattermann, 2015).

Table 4.3. Stream sinuosity range (and mean) for each stream order in the baseline and restoration scenarios.

Stream order	Sinuosity	
	Baseline	Restoration
1st	1.00–2.53 (1.03)	1.00–2.53 (1.30)
2nd	1.00–2.60 (1.04)	1.00–2.60 (1.34)
3rd	1.00–2.28 (1.04)	1.00–2.53 (1.44)
4th	1.00–2.73 (1.06)	1.00–3.11 (1.50)
5th	1.00–2.09 (1.08)	1.00–2.54 (1.29)
6th	1.00–2.65 (1.07)	1.00–3.62 (1.55)

4.4. Results

4.4.1. Model performance

The mHM-Nitrate model generally performed well when simulating discharge, nitrate concentrations, and nitrate loads at the seven gauging stations (Figures 4.2 and S4.4-S4.5 and Table 4.4). Nash-Sutcliffe efficiency (NSE) values of discharge exceeded 0.75 and 0.78 for the

calibration and validation periods, respectively, except for Nienhagen station (Table 4.4). The lowest model performance for discharge occurred at Nienhagen station with the NSE values of 0.72 and 0.37 for the calibration and validation periods, respectively. The seasonal dynamics of nitrate concentrations were relatively well represented at all seven gauging stations (Figures 2 and S4). The NSE values for nitrate concentration ranged from -0.56 to 0.54 and from -0.46 to 0.63 for the calibration and validation periods, respectively (Table 4.4). For the validation period, the ranges of Kling-Gupta efficiency (KGE) were 0.52–0.93, 0.22–0.80, and 0.60–0.91 for discharge, nitrate concentrations, and nitrate loads, respectively (Table 4.4). The model did overestimate nitrate concentrations at the Oschersleben station (Figure 4.2d) for the whole modeling period (2010–2018); percent bias (PBIAS) was 11.0% and 28.8% for the calibration and validation periods, respectively. In contrast, in the calibration periods, the model underestimated nitrate concentrations at other six gauging stations with the PBIAS values ranging from -23.2% to -6.4%. Despite these discrepancies, nitrate loads were accurately estimated at all seven stations during both the calibration and validation periods (PBIAS range = -18.7–23.2%).

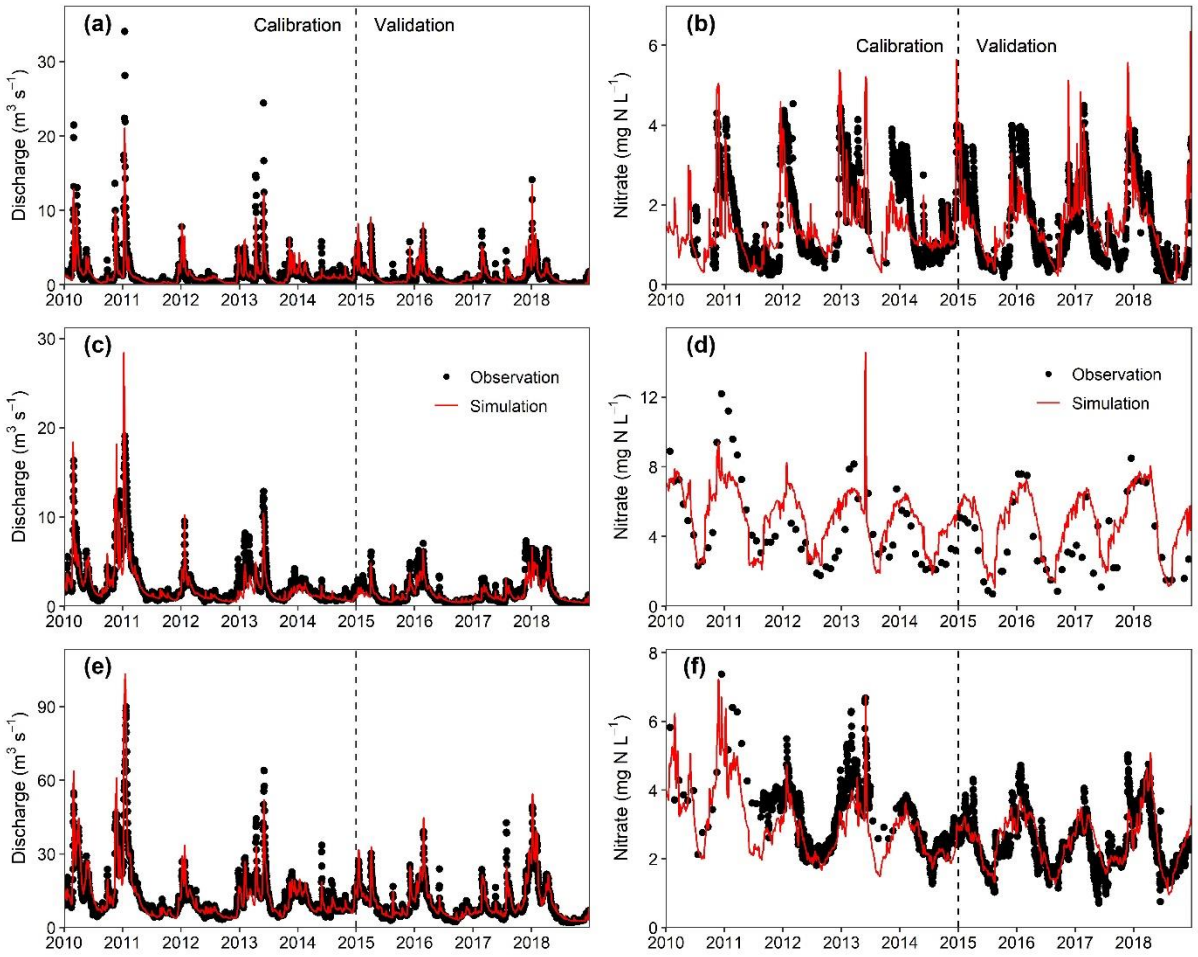

Figure 4.2. Performance of the mHM-Nitrate model: discharge and nitrate concentrations at (a-b) Meisdorf, (c-d) Oschersleben, and (e-f) Stassfurt during the calibration period (2010–2014) and validation period (2015–2018).

Table 4.4. Model evaluation metrics for daily discharge (Q; $m^3 s^{-1}$), nitrate concentrations (mg N L^{-1}), and nitrate loads (kg N d^{-1}) at the seven gauging stations during the calibration and validation periods. Metric abbreviations: NSE = Nash-Sutcliffe efficiency, KGE = Kling-Gupta efficiency, and PBIAS = percent bias.

Station	Metric	Calibration (2010–2014)			Validation (2015–2018)		
		Q	**NO_3^-**	**Load**	**Q**	**NO_3^-**	**Load**
Meisdorf	NSE	0.84	0.48	0.67	0.78	0.60	0.72
	KGE	0.77	0.70	0.74	0.71	0.76	0.82
	PBIAS	4.10	-6.40	-3.60	23.8	4.10	11.8
Hausneindorf	NSE	0.85	-0.56	0.68	0.82	0.42	0.77
	KGE	0.87	0.44	0.75	0.78	0.72	0.83
	PBIAS	11.1	-21.4	4.40	16.2	3.30	12.4
Wegeleben	NSE	0.93	-0.36	0.79	0.93	-	-
	KGE	0.96	0.58	0.72	0.88	-	-
	PBIAS	-0.50	-17.0	-16.2	3.30	-	-
Nienhagen	NSE	0.72	-0.08	0.75	0.37	-0.46	0.77
	KGE	0.80	0.50	0.78	0.52	0.22	0.70

Station	Metric	Calibration (2010–2014)			Validation (2015–2018)		
		Q	**NO_3^-**	**Load**	**Q**	**NO_3^-**	**Load**
	PBIAS	13.3	-23.2	-15.5	36.1	-2.40	23.2
Oschersleben	NSE	0.75	0.54	0.65	0.80	0.41	0.78
	KGE	0.85	0.60	0.61	0.71	0.61	0.60
	PBIAS	-8.70	11.0	-13.3	-8.30	28.8	-10.7
Hadmersleben	NSE	0.87	0.52	0.85	0.93	0.61	0.93
	KGE	0.89	0.66	0.79	0.93	0.80	0.91
	PBIAS	0.80	-8.30	-8.50	4.80	6.30	5.80
Stassfurt	NSE	0.85	0.50	0.82	0.92	0.63	0.91
	KGE	0.87	0.71	0.72	0.91	0.80	0.91
	PBIAS	0.50	-13.7	-18.7	6.20	2.60	3.10

4.4.2. Spatiotemporal dynamics of nitrate retention

4.4.2.1. Annual and seasonal nitrate retention in the Bode catchment

The mHM-Nitrate model suggested that the Bode stream network experienced the highest total nitrate input loads (L_{input}) in the winter from 2015 to 2018 (annual mean ± standard deviation (SD) = 3.68±0.12 kg N ha^{-1} y^{-1}; Table 4.5). For this same period, annual net and gross nitrate retention efficiency (Eff_{net} and Eff_{gross}) were 12.9±0.64% and 24.6±1.56%, respectively (Table 4.5). Both peaked in the summer (37.3±11.4% and 74.7±23.2%, respectively), which is when input loads were lowest and assimilatory uptake and denitrification were highest. In contrast, the two types of efficiency had lower values in the winter and spring (Table 4.5). Within the stream network, the assimilatory uptake rate (U_{assim}) reached its greatest value in the spring and summer (105±62.4 and 134 79.4 mg N m^{-2} d^{-1}, respectively), while the denitrification rate (U_{den}) was highest in the summer and autumn (158±64.6 and 117±56.0 mg N m^{-2} d^{-1}, respectively; Table 4.5).

Table 4.5. Variables describing mean±SD annual and seasonal nitrate input loads and retention for the entire stream network from 2015–2018. Variable values were estimated using the mHM-Nitrate model; the only exception was L_{obs}, which was calculated from the observed data. Abbreviations: L_{input} = total nitrate input load; L_{obs} = observed exported nitrate load; L_{out} = estimated exported nitrate load; F_{assim} = amount of gross assimilatory uptake; U_{assim} = assimilatory uptake rate; F_{den} = amount of denitrification; U_{den} = denitrification rate; Eff_{net} = net nitrate retention efficiency; and Eff_{gross} = gross nitrate retention efficiency.

Variable	Winter	Spring	Summer	Autumn	Annual

L_{input} (kg N ha^{-1} season^{-1}/ kg N ha^{-1} y^{-1})	1.49±1.05	1.06±0.49	0.52±0.31	0.56±0.49	3.68±0.12
L_{obs} (kg N ha^{-1} y^{-1})	1.47±0.27	0.97±0.30	0.32±0.17	0.38±0.20	3.14±0.23
L_{out} (kg N ha^{-1} y^{-1})	1.44±0.26	1.09±0.30	0.34±0.14	0.40±0.21	3.27±0.26
F_{assim} (kg N d^{-1})	58.1±55.4	502±185	553±111	164±102	321±243
U_{assim} (mg N m^{-2} d^{-1})	12.7±13.8	105±62.4	134±79.4	45.9±39.3	74.7±72.5
F_{den} (kg N d^{-1})	170±96.2	321±147.0	537±61.3	362±96.7	348±166
U_{den} (mg N m^{-2} d^{-1})	45.4±34.2	77.1±46.7	158±64.6	117±56.0	99.5±66.6
Eff_{net} (%)	3.8±0.39	10.3±1.25	37.3±11.4	26.6±13.9	12.9±0.64
Eff_{gross} (%)	5.1±0.61	26.2±3.34	74.7±23.2	38.9±20.9	24.6±1.56

4.4.2.2. Nitrate retention within two representative sub-catchments

For the period from 2015 to 2018, we investigated nitrate retention within two sub-catchments—Upper Selke and Großer Graben. They were chosen because they represented certain landscape profiles within the Bode catchment (Figure 4.1). To characterize daily rates of denitrification (U_{den}) and assimilatory uptake (U_{assim}), we determined the median values for all the streams in the network. Both rates were highly variable among seasons and years in the two sub-catchments (Figure 4.3).

At the annual scale, the denitrification rate (U_{den}) was nearly two times higher in Großer Graben than in Upper Selke (126±61.6 vs. 69.1±36.5 mg N m^{-2} d^{-1}, respectively; Table 4.6). Seasonally, U_{den} was high in the summer and autumn and low in the spring and winter in both sub-catchments (Figure 4.3 and Table 4.6). Furthermore, there was seemingly an influence of land-use type. In the summer, U_{den} was two-fold greater in Großer Graben (median±SD = 204±22.6 mg N m^{-2} d^{-1}), which is dominated by arable land, than in Upper Selke, which is dominated by forests (median±SD = 102±22.1 mg N m^{-2} d^{-1}).

At the annual scale, the assimilatory uptake rate (U_{assim}) was more than three times higher in Großer Graben than in Upper Selke (102±77.5 vs. 27.6±24.3 mg N m^{-2} d^{-1}, respectively; Table 4.6). This rate was also high in the spring and summer and low in the autumn and winter in both sub-catchments (Figure 4.3 and Table 4.6). In the summer, the U_{assim} was five times greater in Großer Graben than in Upper Selke (median ± SD = 200 ± 27.1 vs. 39.1 ± 8.7 mg N m^{-2} d^{-1}, respectively). In Upper Selke, it always peaked in April and then rapidly decreased (Figure 4.3a).

Compared to assimilatory uptake, denitrification accounted for a higher proportion of gross nitrate uptake in Upper Selke than in Großer Graben across all seasons, except for the spring (range in Upper Selke: 72–88% vs. Großer Graben: 51–87%; Table 4.6). A similar pattern was seen at the annual scale (Upper Selke: 71% vs. Großer Graben: 55%; Table 4.6).

Gross nitrate retention efficiency (Eff_{gross}) demonstrated clear annual and seasonal patterns in both sub-catchments (Figure 4.4); high values of Eff_{gross} were seen during low-flow periods in the summer and autumn (Table 4.6). It decreased rapidly in July 2017 at Großer Graben and Upper Selke, the result of peak flow events causing high nitrate loads in streams (Figures 4.2a and 4.2c). At the annual scale, gross efficiency displayed a similar median value in both sub-catchments (Upper Selke: 26.0±22.4% and Großer Graben: 35.2±31.7%). In the summer, the median was higher for Großer Graben than for Upper Selke (82.2±23.3% vs. 58.8±17.4%, respectively). It is worth noting that the sub-catchments had similar median benthic surface areas in the summer (Großer Graben: 0.28 km^2 and Upper Selke: 0.24 km^2).

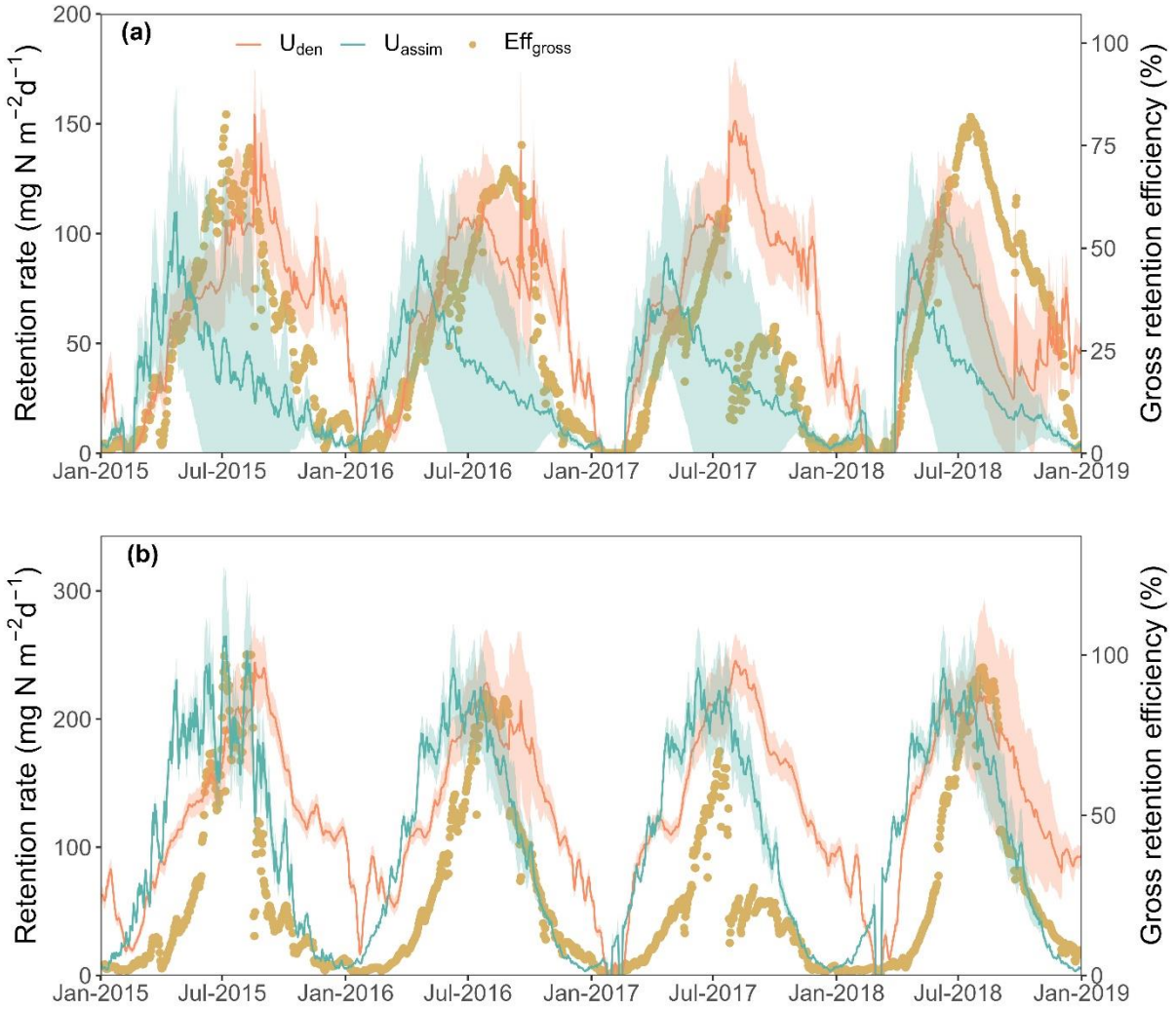

Figure 4.3. Daily median± SD denitrification rates, gross assimilation rates, and gross nitrate retention efficiencies in the sub-catchments of (a) Upper Selke and (b) Großer Graben from 2015 to 2018.

Table 4.6. Median ± SD daily denitrification rates, assimilatory uptake rates, and gross nitrate retention efficiency at seasonal and annual scales in the Upper Selke and Großer Graben sub-catchments from 2015 to 2018. Abbreviations: U_{den} = denitrification rate; U_{assim} = assimilatory uptake rate; and Eff_{gross} = gross nitrate retention efficiency.

Variable	Sub-catchment	Winter	Spring	Summer	Autumn	Annual
U_{den}	Upper Selke	25.9 ± 22.8	61.8 ± 28.1	102 ± 22.1	81.1 ± 25.6	69.1 ± 36.5
(mg N m^{-2} d^{-1})	Großer Graben	70.3 ± 33.3	111 ± 41.3	204 ± 22.6	149 ± 34.8	126 ± 61.6
U_{assim}	Upper Selke	5.0 ± 8.4	63.9 ± 22.7	39.1 ± 8.7	18.3 ± 6.1	27.6 ± 24.3
(mg N m^{-2} d^{-1})	Großer Graben	9.9 ± 14.7	149 ± 51.1	200 ± 27.1	56.8 ± 40.6	102 ± 77.5
Eff_{gross} (%)	Upper Selke	2.0 ± 3.7	22.7 ± 14.0	58.8 ± 17.4	29.3 ± 17.2	26.0 ± 22.4
	Großer Graben	5.4 ± 7.0	22.0 ± 17.2	82.2 ± 23.3	42.6 ± 30.4	35.2 ± 31.7

4.4.2.3. Spatiotemporal patterns in nitrate retention efficiency

We plotted accumulated net retention efficiency (ANRE) along an upstream to downstream gradient for the two main stems of the Upper Selke and Großer Graben sub-catchments (Figure

4.4: heatmap; Figure S4.6: stream networks). ANRE is the ratio between total nitrate retention within streams and the total nitrate input load attributable to terrestrial sources. Spatiotemporal patterns in ANRE varied with catchment size, which increased from headwater to outlet. Dynamics were similar across seasons and years in both sub-catchments: ANRE was higher in the summer and autumn but lower in the winter and spring (Figure 4.4). ANRE remained high (>60%) between late June and late November of 2018 in Upper Selke and between late July and early December of 2018 in Großer Graben, periods of drought in the sub-catchments. Between 2015 and 2018, ANRE hit its minimum value in the summer of 2017, due to peak flows in July 2017 (Figure 4.4 and Figures 4.2a and 4.2c).

However, some differences were apparent between the two sub-catchments for the period between 2015 and 2018. In Upper Selke, which is dominated by forests, ANRE was lowest in headwater streams, as a result of their low assimilatory uptake rates (U_{assim}) and denitrification rates (U_{den}) (Figure 4.4a). In contrast, in streams near the outlet (<36 km away), ANRE reached high values (>60%) during the summer and autumn (Figure 4.4a). In Großer Graben, which is dominated by arable land, ANRE was highest in headwater streams, which experienced lower total nitrate input loads (L_{input}) than higher order streams (Figure 4.4b). In this sub-catchment, high ANRE values (>60%) only occurred in headwater streams that were about 40 km upstream from the outlet (Figure 4.4b).

In Upper Selke, there was a correlation between ANRE values in the summer and catchment size (Figure 4.4a). This pattern could have two explanations: 1) the relative surface area covered by forest increased from upstream to downstream and 2) there is a positive correlation between nitrate retention and benthic surface area. In the summer of 2018, ANRE was lower in the sub-catchment's middle region, namely in streams located 24.8 and 18.0 km from the outlet (Meisdorf station, Figure 4.4). Such was due to the large nitrate input loads (L_{input}) from nearby arable land (Figure S4.6a). Similarly, ANRE was dramatically lower in intermediate

sections of Großer Graben (Figure 4.4b) because of the large nitrate input loads (L_{input}) from tributaries that joined the main network stem around 38.9 and 25.5 km from the outlet.

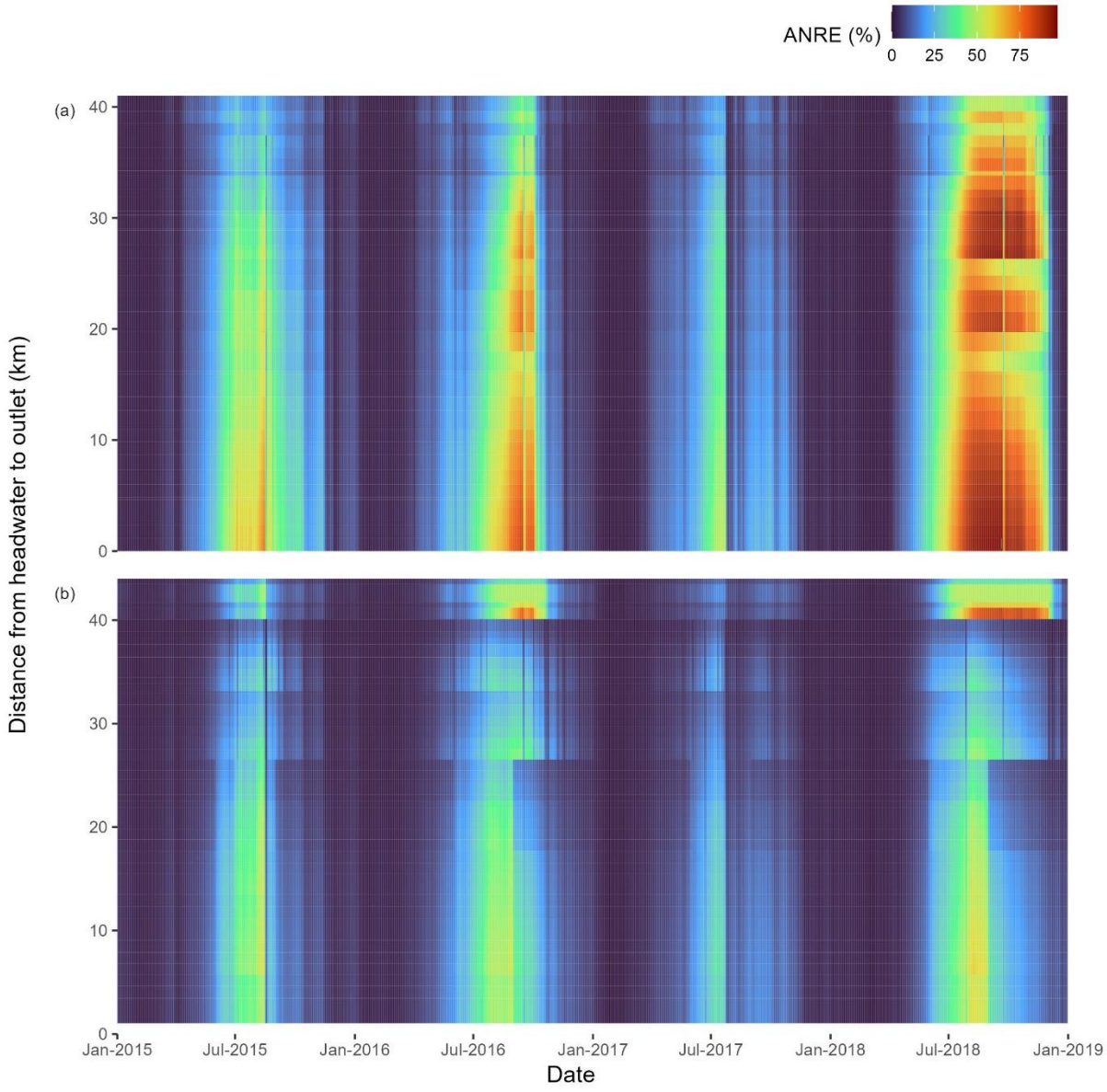

Figure 4.4. Patterns of accumulated net retention efficiency (ANRE) in the (a) Upper Selke and (b) Großer Graben sub-catchments. The y-axis depicts the direction of flow (headwater to outlet = top to bottom), while the x-axis depicts changes over time.

4.4.3. Simulated effects of stream restoration

In the baseline scenario, summer net nitrate retention efficiency (Eff_{net}) was slightly higher in streams in forested areas versus agricultural areas (median ± SD = 6.2 ± 13.9% vs. 3.9 ± 10.3%, respectively). Within areas with similar land use, this variable had larger values in small

streams than in large streams. For example, in the summer in Großer Graben, the values of Eff_{net} ranged from 0.1 to 34.0% for 1st–3rd order streams and from 0.1 to 2.0% for 4th–5th order streams (Figure 4.5a). The Eff_{net} values of small streams varied more than that of large streams, as demonstrated by the standard deviation values of Eff_{net} of 3.3-9.1% for 1st–3rd order streams and 0.3-0.5% for 4th–5th order streams in Großer Graben (Figure S4.7a).In the restoration scenario, in the summer, greater improvements in net retention efficiency were seen for small streams in Großer Graben (1st–3rd order streams: increase of 0.1–16.8%, 4th–5th order streams: increase of 0–11.8%) (Figure 4.5b). The most dramatic increase (median ± SD = 25.4±5.3%) was seen for a 1st-order stream (Figure 4.5b).

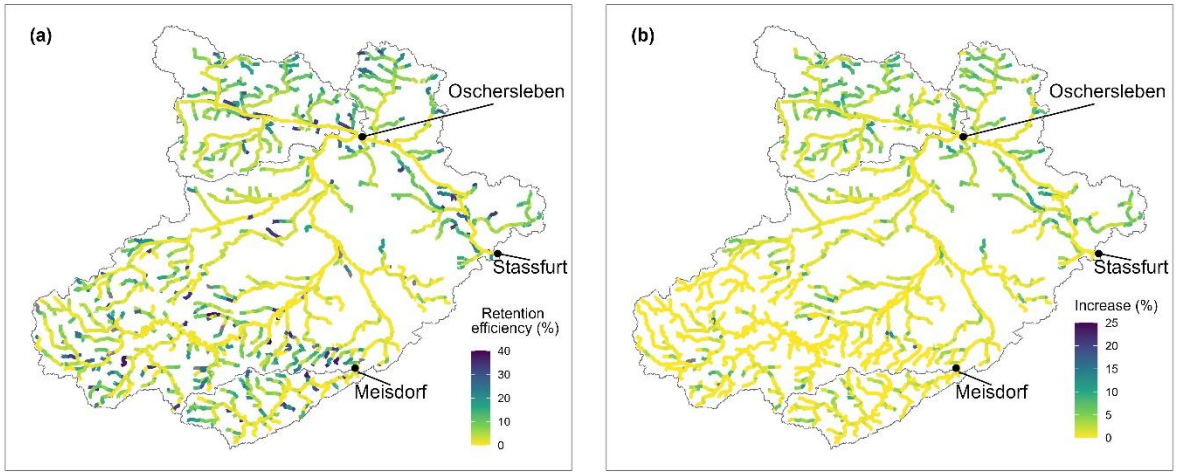

Figure 4.5. Spatial patterns of median net nitrate retention efficiency in the summer in the (a) baseline scenario and (b) in the restoration scenario (% increase over baseline).

In the baseline scenario, within areas with similar land use, mean summer nitrate concentrations were higher in small streams (1st–3rd order) than in large streams (4th–6th order) (Figure 4.6a). For instance, in Großer Graben, the range for small streams was 3.3–4.8 mg N L^{-1}, while the range for large streams was 2.3–2.6 mg N L^{-1}. Additionally, these concentrations were also higher in small streams found in lowland agricultural areas (range = 0.9–17.0 mg N L^{-1}) than in small streams in mountainous areas (range = 0.6–5.2 mg N L^{-1}) (Figure 4.6a). In the restoration scenario, nitrate concentrations declined more sharply in the former than in the latter

areas; the largest decrease occurred in the tributaries of the lower Bode river (-1.3 mg N L^{-1}; Figure 4.6b). In lowland areas, summer nitrate concentrations dropped more for large streams (4^{th}–6^{th} order) than for small streams (1^{st}–3^{rd} order) (Figures 4.6b and S4.7b). For example, in Großer Graben, these concentrations declined by 0.1–0.3 mg N L^{-1} and 0.3-0.5 mg N L^{-1} for small and large streams, respectively.

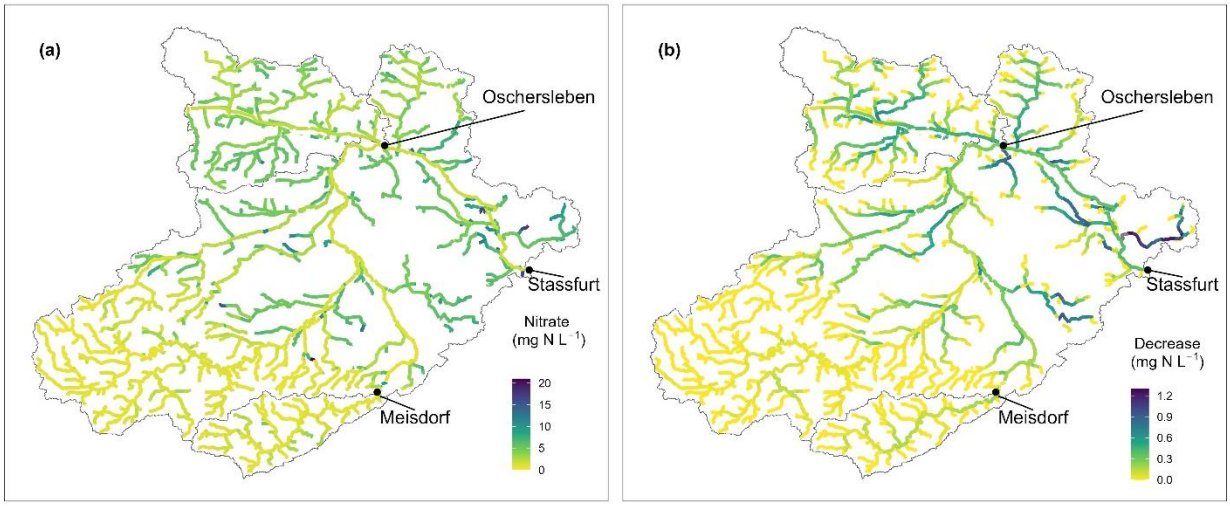

Figure 4.6. Spatial patterns of mean summer nitrate concentrations in the a) baseline scenario and (b) in the restoration scenario (absolute decrease from baseline).

4.5. Discussion

4.5.1. Model performance evaluation

In this study, we investigated the potential effects of stream restoration on nitrate retention dynamics via a combined approach. We utilized the detailed monitoring data available for the Bode catchment in a well-calibrated, process-based mHM-Nitrate model to explore network-scale patterns. According to established criteria for evaluating watershed model performance (Moriasi et al., 2015; Moriasi et al., 2012), the mHM-Nitrate model generally performed well in capturing the dynamics of both discharge and nitrate concentrations. Although the model struggled somewhat with discharge at the Meisdorf and Nienhagen stations (PBIAS: 23.8% and 36.1%, respectively; Table 4.4), the absolute differences between the observed and

estimated values were small (Meisdorf: 36.1 mm $year^{-1}$ and Nienhagen: 23.5 mm $year^{-1}$). Nitrate concentrations were overestimated at the Oschersleben station for the entire modeling period (2010–2018) because discharge and nitrate concentrations were overestimated (PBIAS: 26.8% and 18.4%, respectively) in the summer during the validation period. The differences corresponded to 3.34 mm $year^{-1}$ and 0.31 mg N L^{-1}, respectively. Conversely, nitrate concentrations at other six gauging stations were underestimated in the calibration period, particularly during 2011 and 2012. This discrepancy may be attributed to the underestimation of interflow, leading to a reduced amount of nitrate being carried to the river during the aforementioned years (Figures S4.4b, S4.4d, S4.4f and S4.4k). The variability in model performance across different sub-catchments can be attributed to various factors. These include the sub-catchment characteristics such as soil type, topography and precipitation patterns, which can influence the hydrological and water quality processes. For instance, Jiang et al. (2014) found that the contribution of interflow decreases from mountainous areas to lowland areas due to variations in topography and soil type. In hilly areas with rapid hydrological processes and shallow nitrate storage, nitrate is rapidly transported to streams, whereas in lowland areas, it is less rapidly transported to streams as baseflow contribution increases. In addition, the high percentage of urban areas with a low number of precipitation stations at the Holtemme sub-catchment (Nienhagen as the outlet) can impact the accuracy of the model. The discharge at the Nienhagen station is also heavily affected by weirs (Kunz et al., 2017b). According to Yang et al. (2018), who conducted an uncertainty analysis in the Selke sub-catchment using the MCMC-based DREAM tool (ter Braak and Vrugt, 2008; Vrugt, 2016), the uncertainty in simulations regarding discharge and nitrate concentration was effectively limited. A detailed discussion of model performance for the Bode catchment is provided by Zhou et al. (2022).

4.5.2. Modeling nitrate retention processes in stream networks

The mHM-Nitrate model estimated that, in the summer, daily denitrification rates (U_{den}) ranged from 100.9 to 198.5 mg N m^{-2} d^{-1} (mean ± SD = 151.1 ± 19.1 mg N m^{-2} d^{-1} for the entire stream network). These figures fit with those obtained by Mulholland et al. (2009), who used ^{15}N isotope analysis to estimate daily denitrification rates (U_{den}) at the reach scale. They found that values ranged from 0 to 220.1 mg N m^{-2} d^{-1} for small streams in areas with different land uses and climatic conditions. Using a reach-scale N_2 method on N-enriched streams, Böhlke et al. (2009) estimated that daily denitrification rates (U_{den}) in the Iroquois River basin (USA) ranged from 48.4 to 677.0 mg N m^{-2} d^{-1}; stream nitrate concentrations were similar between their study and ours. In addition, Zhang et al. (2023) used high-frequency measurements to quantify daily denitrification rates (U_{den}) in the summer in the lower Bode River. These observed values fell between 72.3 and 253.0 mg N m^{-2} d^{-1} and were thus reasonably similar to our model's estimated values of 81.8 to 188.2 mg N m^{-2} d^{-1} for the same reaches.

The model estimated that daily assimilatory uptake rates (U_{assim}) were 27.6 ± 24.3 and 102.0 ± 77.5 mg N m^{-2} d^{-1} for streams in forested and agricultural areas, respectively (Table 4.6). Using high-frequency measurements, Rode et al. (2016a) found maximum daily assimilatory uptake rates in a Selke sub-catchment (streams in forested areas: 97.5 mg N m^{-2} d^{-1} and streams in agricultural areas: 270 mg N m^{-2} d^{-1}) that are consistent with our results (Figure 4.3 and Table 4.6). Applying the same model to the Selke catchment, Yang et al. (2019) reported values ($mean \pm SD$) of 86.4 ± 1.9 mg N m^{-2} d^{-1} for streams in forested areas and 18.8 ± 6.2 mg N m^{-2} d^{-1} for streams in agricultural areas. Kunz et al. (2017c) determined that mean daily assimilatory uptake rates (U_{assim}) were 120 mg N m^{-2} d^{-1} and 239 mg N m^{-2} d^{-1} for channelized and natural streams, respectively. This work took place in the lowlands associated with the Weiße Elster River, which is near to our study area and thus provides additional support for the reliability of our model's estimates.

4.5.3. Relationships between catchment characteristics and nitrate retention

Nitrate retention is determined by both denitrification and assimilatory uptake (U_{den} and U_{assim}). These variables displayed pronounced seasonal variability among different land-use categories (Figure 4.3). Denitrification (U_{den}) was higher in the summer and autumn and lower in the spring and winter for both sub-catchments. This pattern matches those seen in previous studies (Alexander et al., 2009; Wollheim et al., 2008a), where retention dynamics were correlated with nitrate concentrations and temperature. This seasonality could also be related to levels of sediment and dissolved oxygen (Christensen et al., 1990; Inwood, Tank and Bernot, 2005; Uusheimo et al., 2018) and to levels of organic carbon (Arango et al., 2007; Comer-Warner et al., 2020; Tatariw et al., 2013). However, we were unable to include these variables in our mHM-Nitrate model because the lack of observed data made it impossible to construct empirical equations that would have allowed us to scale up to the entire stream network.

From 2015 to 2018, denitrification rates (U_{den}) were higher in Großer Graben than in Upper Selke across all seasons (Figure 4.3 and Table 4.6). This pattern likely resulted from the higher $nitrate^-$ concentrations and water temperatures in Großer Graben, a sub-catchment dominated by agricultural activity. Our findings concur with those of past studies (Böhlke et al. (2009); Inwood, Tank and Bernot (2007); Mulholland et al. (2008)), which observed that denitrification rates (U_{den}) were positively correlated with nitrate concentrations across land use types.

Assimilatory uptake rates (U_{assim}) were similarly higher in Großer Graben than in Upper Selke across all seasons (Figure 4.3 and Table 4.6). These results align with those of previous research that utilized high-frequency measurements (Rode et al. 2016) and that applied the mHM-Nitrate model to the Selke catchment (Yang et al., 2019a). The latter two studies reported that assimilatory uptake (U_{assim}) occurred at a higher rate in streams in open-canopy environments (i.e., agricultural areas) versus closed-canopy environments (i.e., forests). Arango et al. (2008) found similar results. The assimilatory uptake of nitrate is mainly controlled by primary

productivity (Heffernan and Cohen, 2010; Roberts and Mulholland, 2007), which is affected by light, a resource whose availability is higher in agricultural versus forested areas (Yang et al., 2019). The standard deviation of U_{assim} is higher in Upper Selke compared to Großer Graben (Figure 4.3a vs 4.3b), which could be attributed to the diverse shading effects. This diversity in shading effects is likely due to the more heterogeneous land use in Upper Selke compared to Großer Graben (Figure S4.6). Denitrification always peaked after assimilatory uptake, in the second half of July and August. This pattern likely arises because denitrification is more sensitive to water temperature, while assimilatory uptake is more sensitive to light availability (Heffernan and Cohen, 2010, Kunz et al. 2017b). Dynamics were consistent across streams and years.

Although the rates of both processes varied in space and time for the two sub-catchments, denitrification surpassed assimilatory uptake across all seasons, except for spring. Our observation fits with the work by Böhlke, Harvey and Voytek (2004), who noted that denitrification accounted for more than 50% of gross nitrate uptake in a stream with high nitrate concentrations (i.e., occurring in an agricultural area). Similarly, Potter et al. (2010) reported that denitrification accounted for 1–97% of gross nitrate uptake and that this figure exceeded 35% for five out of the nine streams studied. Kunz et al. (2017c) found that, in July, the denitrification rate was about five times higher than the assimilatory uptake rate in a natural reach of the Weiße Elster River. In contrast, Mulholland et al. (2008) indicated that denitrification made a relatively limited contribution (16%) to gross nitrate uptake (mainly in low-nitrate streams); Ribot, von Schiller and Martí (2017) arrived at a figure of 0.15%. These low values may have resulted from specific site conditions. They were obtained using $^{15}NO_3^-$ tracers that were added to streams with low nitrate concentrations. It appears that denitrification makes a greater contribution to total nitrate uptake when nitrate concentrations are higher.

Upper Selke and Großer Graben likely had similar temporal patterns of gross nitrate retention efficiency and ANRE (Figures 4.3 and 4.4) because of similarities in interactions among land use, nitrate concentrations, temperature, and discharge. Both variables had low values in the winter and spring due to elevated terrestrial inputs during high flow periods, and seasonally low water temperatures resulted in reduced rates of assimilatory uptake and denitrification (Alexander et al., 2009). Terrestrial inputs likely had more influence on the above temporal dynamics because they were an order of magnitude larger. While terrestrial inputs were higher in Großer Graben than Upper Selke, median gross nitrate retention efficiency in the summer was higher in Großer Graben than Upper Selke (Table 4.6), a pattern that can be explained by the former's higher rates of assimilatory uptake and denitrification. The sub-catchments displayed significantly different spatial patterns of ANRE (Figure 4.4). ANRE was low in Upper Selke headwaters because assimilatory uptake and denitrification were low (Figure 4.4a); it was higher in Großer Graben headwaters than downstream reaches (Figure 4.4b) because the elevated nitrate levels caused by terrestrial inputs in the downstream reaches far exceeded the amounts of nitrate removed by assimilatory uptake and denitrification. This suggests that the stream has a greater capacity to remove nitrate in headwaters in Großer Graben. This information can be used to prioritize restoration efforts in areas where the ARNE is high. Furthermore, this result indicates that land use around the nitrate source (e.g., arable land) can strongly influence retention efficiency at the network scale. Previous research arrived at a similar conclusion: land use, and notably the location of arable lands within catchments, can strongly affect the nitrate removal and export from the catchment (Casquin et al., 2021; Dupas et al., 2019; Mineau, Wollheim and Stewart, 2015).

4.5.4. Potential effects of restoring sinuosity on nitrate retention

In our baseline scenario, summer net nitrate retention efficiency was higher in streams in forested versus agricultural areas (Figure 4.5a). Indeed, in the latter, retention capacity was

overwhelmed by large nitrate inputs from terrestrial sources. Adjusting for stream length, net nitrate retention efficiency per km was lower for large than small streams (Figure 4.5a), as seen in previous studies (Wollheim et al., 2008a; Wollheim et al., 2006). This suggests that restoration efforts aimed at reducing nitrate concentrations in large streams may need to focus on other strategies beyond increasing stream length. These strategies could include creating wetlands or other riparian buffer zones, or reducing nutrient inputs from upstream and terrestrial sources.

Our restoration scenario specifically explored the effects of increasing stream sinuosity. It found that in areas with arable land, the changes to stream morphology increased net nitrate retention efficiency more in the lowlands than in the mountains (Figure 4.5b); in the latter area, small streams already display pronounced meandering (Figure S4.3). As stream length increased, so did the benthic surface areas, also augmenting retention. These gains have also been observed at the reach scale in prior research (Wagenschein and Rode, 2008). While the study found greater improvements in net retention efficiency for small streams in the summer, the magnitude of the improvements varied widely between different stream orders and even within the same stream order (Figure 4.5b). Restoration efforts should be designed and implemented with caution, considering the uncertainties in the accuracy of the model simulation. The effectiveness of restoration efforts can be influenced by a range of factors, including the specific characteristics of the stream and surrounding landscape, the type and intensity of land use in the watershed, and the timing and duration of restoration activities. It is important to acknowledge and account for uncertainties when designing and implementing stream restoration projects. This can be done by conducting thorough assessments of the site, monitoring the effectiveness of restoration efforts over time, and using adaptive management strategies to adjust restoration approaches as needed (Convertino et al., 2013).

Furthermore, in our restoration scenario, net nitrate retention efficiency improved more for small streams (1^{st}–3^{rd} order) than for large streams (4^{th}–6^{th} order), as seen in Großer Graben (Figure 5b). This pattern emerges because terrestrial nitrate input greatly exceeds nitrate retention in larger streams, which suggests that increasing sinuosity could have a greater impact on retention efficiency in small streams. This indicates that small streams may play a more significant role in reducing nitrate pollution in downstream watersheds. This is because small streams are typically more reactive and have higher surface area to volume ratios (Ensign and Doyle, 2006; Wollheim et al., 2006), which allows for greater contact between water and sediment, promoting denitrification and other processes that remove nitrate from the water. Across the entire stream network, increased sinuosity more dramatically reduced nitrate concentrations in large streams than in small streams (Figure 4.6b), likely because large streams have experienced cumulative downstream retention and harbor larger benthic surface areas (Alexander et al., 2009). Consequently, restoration regimes that increase sinuosity could be powerfully deployed in small streams in agricultural areas, acting to increase nitrate retention efficiency and decrease nitrate transport downstream.

Our study adds to research looking at how alterations in stream morphology could affect nitrate retention dynamics. Past work has shown that re-meandering can induce transient storage, which impacts the denitrification rate (Baker, Bledsoe and Price, 2012; Opdyke, David and Rhoads, 2006). Such may result mechanistically from lower flow velocities and higher water residence times in the hyporheic zone (Bukaveckas, 2007; Gomez, Wilson and Cardenas, 2012; Pinay et al., 2009; Zarnetske et al., 2011). Additionally, denitrification could experience greater increase in vertical hyporheic zones compared to meanders because vertical exchanges beneath stream bedforms are considerably more pronounced than are lateral exchanges through stream bars and meander banks (Gomez-Velez and Harvey, 2014; Gomez-Velez et al., 2015). Modifications to stream morphology can directly or indirectly affect nutrient dynamics by

increasing spatiotemporal variability in the composition and activity of aquatic communities (Lin et al., 2016). However, it is hard to arrive at any generalizations because we continue to lack field studies comparing denitrification rates in modified versus natural streams—data that are essential for model parameterization. We have interpreted our results conservatively because we did not explicitly establish any links between these processes and natural stream morphology, which shapes rates of nitrate uptake in the stream bed.

4.5.5. Implications for stream restoration

Although stream restoration projects are abundant, they often focus on the reach scale (Newcomer Johnson et al., 2016). This study highlights the need for developing methods that act at the network scale, such as increasing stream sinuosity. In our simulation, increasing stream sinuosity improved nitrate retention efficiency more in streams in agricultural areas (Großer Graben) than in streams in forested areas (Upper Selke). Moreover, this strategy more dramatically reduced nitrate concentrations in large streams than in small streams because of the accumulative retention in the upper streams. This finding indicates that restoration efforts should prioritize small streams in highly polluted, agricultural areas, such as our study area in the lowlands of central Germany.

Encouraging investment in stream restoration (e.g., re-meandering) can be challenging for two key reasons: first, it is costly and technically difficult and, second, the benefits are only significant during periods of low flow and low terrestrial inputs. Realistically, stream restoration alone cannot reduce nitrate concentrations to desired levels. Instead, systems exploiting a combination of terrestrial and stream-targeted measurements could be used to effectively and sustainably manage river basins (Lammers and Bledsoe, 2017). However, we must first conduct further research on how such combined measurements can affect nitrate retention at the stream network scale.

4.6. Conclusion

In this study, we used observed data from Germany's Bode catchment in combination with a fully distributed process-based mHM-Nitrate model to investigate how re-meandering could affect nitrate retention dynamics within a heavily modified stream network. There was pronounced spatiotemporal variability in rates of assimilatory uptake and denitrification within stream networks with different land-use types and morphological characteristics. Both rates were higher in streams in more agricultural versus more forested areas. At the network scale, increased stream sinuosity had a greater positive impact on nitrate retention efficiency in small streams. However, nitrate concentrations decreased more dramatically in large streams due to accumulative retention in upper streams. Our findings underscore that major benefits could arise from re-meandering small streams in agricultural areas. It is important to acknowledge that our stream restoration regime was somewhat simplified—we increased sinuosity without considering the resulting effects on rates of nitrate denitrification and assimilatory uptake. Thus, this work is a conservative first step along a lengthy research pathway. For example, future research should explore whether nitrate retention efficiency could be enhanced even more by combining stream-based strategies (e.g., re-meandering, improved floodplain connectivity) with land-based strategies (e.g., buffer strips, construction of wetlands).

Our results highlight the dominant role of denitrification in gross nitrate uptake across all seasons (excluding the spring). They also showed that, regardless of stream size or nearby land use, the denitrification rate always peaked after the assimilatory uptake rate, in the second half of July and August.

Taken together, our findings suggest that stream restoration efforts should prioritize small streams in highly polluted, agricultural areas. To optimally design restoration strategies, we must characterize denitrification and assimilatory uptake rates in stream networks in the field before and after restoration; these data could then be used in distributed hydrological water

quality models (such as an mHM-Nitrate model) to further improve understanding of these dynamics.

Acknowledgements

X. Zhou is funded by the Chinese Scholarship Council (CSC). We thank the German Weather Service (DWD), Federal Institute for Geosciences and Natural Resources (BGR) and State Agency for Flood Protection and Water Management of Saxony-Anhalt (LHW) for providing meteorological, geological and discharge and water-quality data, respectively. The high-frequency nitrate-concentration data were provided by the TERENO (Terrestrial Environment Observatories) project.

4.7. References

Abbaspour, K.C. et al., 2007. Modelling hydrology and water quality in the pre-alpine/alpine Thur watershed using SWAT. Journal of Hydrology, 333(2-4): 413-430. DOI:10.1016/j.jhydrol.2006.09.014

Abdelwahab, O.M.M., Bingner, R.L., Milillo, F., Gentile, F., 2016. Evaluation of Alternative Management Practices With the AnnAGNPS Model in the Carapelle Watershed. Soil Science, 181(7): 293-305. DOI:10.1097/ss.0000000000000162

Agency, E.E., 2018. European waters — assessment of status and pressures 2018.

Ahmadi, M., Arabi, M., Ascough, J.C., Fontane, D.G., Engel, B.A., 2014. Toward improved calibration of watershed models: Multisite multiobjective measures of information. Environ Modell Softw, 59: 135-145. DOI:10.1016/j.envsoft.2014.05.012

Ajami, N.K., Duan, Q., Sorooshian, S., 2007. An integrated hydrologic Bayesian multimodel combination framework: Confronting input, parameter, and model structural uncertainty in hydrologic prediction. Water Resources Research, 43(1). DOI:10.1029/2005wr004745

Alexander, R.B. et al., 2009. Dynamic modeling of nitrogen losses in river networks unravels the coupled effects of hydrological and biogeochemical processes. Biogeochemistry, 93(1-2): 91-116. DOI:10.1007/s10533-008-9274-8

Alexander, R.B., Smith, R.A., Schwarz, G.E., 2000. Effect of stream channel size on the delivery of nitrogen to the Gulf ofMexico. nature, 403: 758.

Andersson, L., Rosberg, J., Pers, B.C., Olsson, J., Arheimer, B., 2005. Estimating Catchment Nutrient Flow with the HBV-NP Model: Sensitivity To Input Data. AMBIO: A Journal of the Human Environment, 34(7): 521-532. DOI:10.1579/0044-7447-34.7.521

Arango, C.P., Tank, J.L., Johnson, L.T., Hamilton, S.K., 2008. Assimilatory uptake rather than nitrification and denitrification determines nitrogen removal patterns in streams of varying land use. Limnology and Oceanography, 53(6): 2558-2572. DOI:DOI 10.4319/lo.2008.53.6.2558

Arango, C.P., Tank, J.L., Schaller, J.L., Royer, T.V., Bernot, M.J., David, M.B., 2007. Benthic organic carbon influences denitrification in streams with high nitrate concentration. Freshwater Biology, 52(7): 1210-1222. DOI:10.1111/j.1365-2427.2007.01758.x

Arheimer, B., Andréasson, J., Fogelberg, S., Johnsson, H., Pers, C.B., Persson, K., 2005. Climate Change Impact on Water Quality: Model Results from Southern Sweden. AMBIO: A Journal of the Human Environment, 34(7): 559-566. DOI:10.1579/0044-7447-34.7.559

Arnold, 1998. LARGE AREA HYDROLOGIC MODELING AND ASSESSMENT. Journal of the American Water Resources Association.

Arnold, J.G. et al., 2012. Swat: Model Use, Calibration, and Validation. Transactions of the Asabe, 55(4): 1491-1508.

Arnold, J.G., Srinivasan, R., Muttiah, R.S., Williams, J.R., 1998. Large area hydrologic modeling and assessment part I: model development 1. JAWRA Journal of the American Water Resources Association, 34(1): 73-89.

B. Duda, P., R. Hummel, P., S. Donigian Jr, A., C. Imhoff, J., 2012. BASINS/HSPF: Model Use, Calibration, and Validation. Transactions of the ASABE, 55(4): 1523-1547. DOI:https://doi.org/10.13031/2013.42261

Baffaut, C. et al., 2015. Hydrologic and water quality modeling: Spatial and temporal considerations. Transactions of the ASABE, 58(6): 1661-1680. DOI:10.13031/trans.58.10714

Baker, D.W., Bledsoe, B.P., Price, J.M., 2012. Stream nitrate uptake and transient storage over a gradient of geomorphic complexity, north-central Colorado, USA. Hydrological Processes, 26(21): 3241-3252. DOI:10.1002/hyp.8385

Baldwin, D.S., Rees, G.N., Mitchell, A.M., Watson, G., 2005. Spatial and temporal variability of nitrogen dynamics in an upland stream before and after a drought. Marine and Freshwater Research, 56(4): 457-464. DOI:10.1071/Mf04189

Ballard, T.C., Sinha, E., Michalak, A.M., 2019. Long-Term Changes in Precipitation and Temperature Have Already Impacted Nitrogen Loading. Environ Sci Technol, 53(9): 5080-5090. DOI:10.1021/acs.est.8b06898

Bandini, F. et al., 2018. Technical note: Bathymetry observations of inland water bodies using a tethered single-beam sonar controlled by an unmanned aerial vehicle. Hydrology and Earth System Sciences, 22(8): 4165-4181. DOI:10.5194/hess-22-4165-2018

Baron, J.S. et al., 2012. The interactive effects of excess reactive nitrogen and climate change on aquatic ecosystems and water resources of the United States. Biogeochemistry, 114(1-3): 71-92. DOI:10.1007/s10533-012-9788-y

Beck, H.E. et al., 2016. Global-scale regionalization of hydrologic model parameters. Water Resources Research, 52(5): 3599-3622. DOI:10.1002/2015wr018247

Bergström, S., 1976. Development and application of a conceptual runoff model for Scandinavian catchments.

Bergström, S., Lindström, G., Pettersson, A., 2002. Multi-variable parameter estimation to increase confidence in hydrological modelling. Hydrological Processes, 16(2): 413-421. DOI:10.1002/hyp.332

Beusen, A.H.W., Bouwman, A.F., Van Beek, L.P.H., Mogollón, J.M., Middelburg, J.J., 2016. Global riverine N and P transport to ocean increased during the 20th century despite increased retention along the aquatic continuum. Biogeosciences, 13(8): 2441-2451. DOI:10.5194/bg-13-2441-2016

Beven, K., 1993. Prophecy, Reality and Uncertainty in Distributed Hydrological Modeling. Advances in Water Resources, 16(1): 41-51. DOI:Doi 10.1016/0309-1708(93)90028-E

Beven, K., 2001. How far can we go in distributed hydrological modelling? Hydrology and Earth System Sciences, 5(1): 1-12. DOI:10.5194/hess-5-1-2001

Beven, K., 2006. A manifesto for the equifinality thesis. Journal of Hydrology, 320(1-2): 18-36. DOI:10.1016/j.jhydrol.2005.07.007

Beven, K., 2007. Towards integrated environmental models of everywhere: uncertainty, data and modelling as a learning process. Hydrology and Earth System Sciences, 11(1): 460-467. DOI:DOI 10.5194/hess-11-460-2007

Beven, K., Binley, A., 1992. The Future of Distributed Models - Model Calibration and Uncertainty Prediction. Hydrological Processes, 6(3): 279-298. DOI:DOI 10.1002/hyp.3360060305

Beven, K., Freer, J., 2001. Equifinality, data assimilation, and uncertainty estimation in mechanistic modelling of complex environmental systems using the GLUE methodology. Journal of Hydrology, 249(1-4): 11-29. DOI:Doi 10.1016/S0022-1694(01)00421-8

Beven, K.J., 2000. Uniqueness of place and process representations in hydrological modelling. Hydrol. Earth Syst. Sci., 4(2): 203-213. DOI:10.5194/hess-4-203-2000

Bicknell, B.R., 1997. Hydrological Simulation Program—FORTRAN User's Manual for Version 11.

Bingner, R.L., Theurer, F.D., Yuan, Y., 2003. AnnAGNPS technical processes. USDA-ARS. National Sedimentation Laboratory.

Birgand, F., Skaggs, R.W., Chescheir, G.M., Gilliam, J.W., 2007. Nitrogen Removal in Streams of Agricultural Catchments—A Literature Review. Critical Reviews in Environmental Science and Technology, 37(5): 381-487. DOI:10.1080/10643380600966426

Birkel, C., Soulsby, C., Tetzlaff, D., 2014. Integrating parsimonious models of hydrological connectivity and soil biogeochemistry to simulate stream DOC dynamics. Journal of Geophysical Research: Biogeosciences, 119(5): 1030-1047. DOI:https://doi.org/10.1002/2013JG002551

Bloschl, G., Sivapalan, M., 1995. Scale Issues in Hydrological Modeling - a Review. Hydrological Processes, 9(3-4): 251-290.

Böhlke, J.K. et al., 2009. Multi-scale measurements and modeling of denitrification in streams with varying flow and nitrate concentration in the upper Mississippi River basin, USA. Biogeochemistry, 93(1-2): 117-141. DOI:10.1007/s10533-008-9282-8

Böhlke, J.K., Harvey, J.W., Voytek, M.A., 2004. Reach-scale isotope tracer experiment to quantify denitrification and related processes in a nitrate-rich stream, midcontinent United States. Limnology and Oceanography, 49(3): 821-838. DOI:10.4319/lo.2004.49.3.0821

Breuer, L., VachÉ, K.B., Julich, S., Frede, H.-G., 2008. Current concepts in nitrogen dynamics for mesoscale catchments. Hydrological Sciences Journal, 53(5): 1059-1074. DOI:10.1623/hysj.53.5.1059

Briem, E., Spitzer, A., Schrenk, G., 2003. Gewässerlandschaften der Bundesrepublik Deutschland. WASSERWIRTSCHAFT, 94: 58-62. DOI:10.1007/BF03252330

Brooks, R.H., Corey, A.T., 1964. Hydraulic properties of porous media. Hydrology papers (Colorado State University); no. 3.

Bukaveckas, P.A., 2007. Effects of channel restoration on water velocity, transient storage, and nutrient uptake in a channelized stream. Environ Sci Technol, 41(5): 1570-6.

Cao, W., Bowden, W.B., Davie, T., Fenemor, A., 2006. Multi-variable and multi-site calibration and validation of SWAT in a large mountainous catchment with high spatial variability. Hydrological Processes, 20(5): 1057-1073. DOI:10.1002/hyp.5933

Cardenas, M.B., 2009. A model for lateral hyporheic flow based on valley slope and channel sinuosity. Water Resources Research, 45(1). DOI:10.1029/2008wr007442

Carvalho, L. et al., 2019. Protecting and restoring Europe's waters: An analysis of the future development needs of the Water Framework Directive. Science of The Total Environment, 658: 1228-1238. DOI:10.1016/j.scitotenv.2018.12.255

Casquin, A., Dupas, R., Gu, S., Couic, E., Gruau, G., Durand, P., 2021. The influence of landscape spatial configuration on nitrogen and phosphorus exports in agricultural catchments. Landscape Ecology, 36(12): 3383-3399. DOI:10.1007/s10980-021-01308-5

Chen, Q., Wu, W., Blanckaert, K., Ma, J., Huang, G., 2012. Optimization of water quality monitoring network in a large river by combining measurements, a numerical model and matter-element analyses. J Environ Manage, 110: 116-24. DOI:10.1016/j.jenvman.2012.05.024

Chiang, L.C., Yuan, Y.P., Mehaffey, M., Jackson, M., Chaubey, I., 2014. Assessing SWAT's performance in the Kaskaskia River watershed as influenced by the number of calibration stations used. Hydrological Processes, 28(3): 676-687. DOI:10.1002/hyp.9589

Christensen, P.B., Nielsen, L.P., Sørensen, J., Revsbech, N.P., 1990. Denitrification in nitrate-rich streams: Diurnal and seasonal variation related to benthic oxygen metabolism. Limnology and Oceanography, 35(3): 640-651. DOI:https://doi.org/10.4319/lo.1990.35.3.0640

Chuan-zhe, L., 2010. Effect of calibration data series length on performance and optimal parameters of hydrological model. DOI:10.3882/j.issn.1674-2370.2010.04.002

Cleveland, R.B., Cleveland, W. S., McRae, J. E., & Terpenning, I. J., 1990. STL: A seasonal-trend decomposition procedure based on loess. Journal of Official Statistics, 6.

Comer-Warner, S.A. et al., 2020. Seasonal variability of sediment controls of nitrogen cycling in an agricultural stream. Biogeochemistry, 148(1): 31-48. DOI:10.1007/s10533-020-00644-z

Conover, W.J., 1999. Practical nonparametric statistics, 350. john wiley & sons.

Convertino, M. et al., 2013. Enhanced adaptive management: integrating decision analysis, scenario analysis and environmental modeling for the Everglades. Sci Rep, 3: 2922. DOI:10.1038/srep02922

Cosby, B.J., Hornberger, G.M., Clapp, R.B., Ginn, T.R., 1984. A Statistical Exploration of the Relationships of Soil-Moisture Characteristics to the Physical-Properties of Soils. Water Resources Research, 20(6): 682-690. DOI:DOI 10.1029/WR020i006p00682

Covino, T., McGlynn, B., Baker, M., 2010. Separating physical and biological nutrient retention and quantifying uptake kinetics from ambient to saturation in successive mountain stream reaches. Journal of Geophysical Research, 115(G4). DOI:10.1029/2009jg001263

Craig, L.S. et al., 2008. Stream restoration strategies for reducing river nitrogen loads. Frontiers in Ecology and the Environment, 6(10): 529-538. DOI:10.1890/070080

Creed, I.F., Beall, F.D., 2009. Distributed topographic indicators for predicting nitrogen export from headwater catchments. Water Resources Research, 45(10). DOI:10.1029/2008wr007285

Cuntz, M. et al., 2015. Computationally inexpensive identification of noninformative model parameters by sequential screening. Water Resources Research, 51(8): 6417-6441. DOI:10.1002/2015wr016907

Daggupati, P. et al., 2015. A Recommended Calibration and Validation Strategy for Hydrologic and Water Quality Models. Transactions of the Asabe, 58(6): 1705-1719. DOI:10.13031/trans.58.10712

Dal Molin, M., Schirmer, M., Zappa, M., Fenicia, F., 2020. Understanding dominant controls on streamflow spatial variability to set up a semi-distributed hydrological model: the case study of the Thur catchment. Hydrology and Earth System Sciences, 24(3): 1319-1345. DOI:10.5194/hess-24-1319-2020

Davis, C.A. et al., 2014. Antecedent Moisture Controls on Stream Nitrate Flux in an Agricultural Watershed. Journal of Environmental Quality, 43(4): 1494-1503. DOI:10.2134/jeq2013.11.0438

Dembélé, M., Ceperley, N., Zwart, S.J., Salvadore, E., Mariethoz, G., Schaefli, B., 2020a. Potential of satellite and reanalysis evaporation datasets for hydrological modelling under various model calibration strategies. Advances in Water Resources, 143. DOI:10.1016/j.advwatres.2020.103667

Dembélé, M., Hrachowitz, M., Savenije, H.H.G., Mariéthoz, G., Schaefli, B., 2020b. Improving the Predictive Skill of a Distributed Hydrological Model by Calibration on Spatial Patterns With Multiple Satellite Data Sets. Water Resources Research, 56(1). DOI:10.1029/2019wr026085

Demirel, M.C., Mai, J., Mendiguren, G., Koch, J., Samaniego, L., Stisen, S., 2018. Combining satellite data and appropriate objective functions for improved spatial pattern performance of a distributed hydrologic model. Hydrology and Earth System Sciences, 22(2): 1299-1315. DOI:10.5194/hess-22-1299-2018

Djodjic, F., Bieroza, M., Bergstrom, L., 2021. Land use, geology and soil properties control nutrient concentrations in headwater streams. Sci Total Environ, 772: 145108. DOI:10.1016/j.scitotenv.2021.145108

Doyle, M.W., Stanley, E.H., Harbor, J.M., 2003. Hydrogeomorphic controls on phosphorus retention in streams. Water Resources Research, 39(6). DOI:Artn 1147

10.1029/2003wr002038

Duan, Q.Y., Sorooshian, S., Gupta, V., 1992. Effective and Efficient Global Optimization for Conceptual Rainfall-Runoff Models. Water Resources Research, 28(4): 1015-1031. DOI:Doi 10.1029/91wr02985

Duethmann, D., Peters, J., Blume, T., Vorogushyn, S., Güntner, A., 2014. The value of satellite-derived snow cover images for calibrating a hydrological model in snow-dominated catchments in Central Asia. Water Resources Research, 50(3): 2002-2021. DOI:https://doi.org/10.1002/2013WR014382

Dupas, R., Abbott, B.W., Minaudo, C., Fovet, O., 2019. Distribution of Landscape Units Within Catchments Influences Nutrient Export Dynamics. Frontiers in Environmental Science, 7. DOI:10.3389/fenvs.2019.00043

Dupas, R., Jomaa, S., Musolff, A., Borchardt, D., Rode, M., 2016. Disentangling the influence of hydroclimatic patterns and agricultural management on river nitrate dynamics from sub-hourly to decadal time scales. Sci Total Environ, 571: 791-800. DOI:10.1016/j.scitotenv.2016.07.053

EEA, 2018. European waters -- Assessment of status and pressures 2018. Rep. No 7/2018, European Environment Agency, Copenhagen,Denmark.

Efstratiadis, A., Koutsoyiannis, D., 2010. One decade of multi-objective calibration approaches in hydrological modelling: a review. Hydrological Sciences Journal, 55(1): 58-78. DOI:10.1080/02626660903526292

Ehrhardt, S., Kumar, R., Fleckenstein, J.H., Attinger, S., Musolff, A., 2019. Trajectories of nitrate input and output in three nested catchments along a land use gradient. Hydrology and Earth System Sciences, 23(9): 3503-3524. DOI:10.5194/hess-23-3503-2019

Engel, B., Storm, D., White, M., Arnold, J., Arabi, M., 2007. A hydrologic/water quality model application protocol. Journal of the American Water Resources Association, 43(5): 1223-1236. DOI:10.1111/j.1752-1688.2007.00105.x

Ensign, S.H., Doyle, M.W., 2006. Nutrient spiraling in streams and river networks. Journal of Geophysical Research: Biogeosciences, 111(G4). DOI:10.1029/2005jg000114

EU, 2000. Directive 2000/60/EC of the European Parliament and of the Council of 23 October 2000 establishing a framework for Community action in the field of water policy, Official journal of the European communities, pp. 2000.

European Commission, 1991a. Council Directive 91/271/EEC of 21 May 1991 concerning urban waste-water treatment.

European Commission, 1991b. Council Directive 91/676/EEC of 12 December 1991 concerning the protection of waters against pollution caused by nitrates from agricultural sources.

Faramarzi, M. et al., 2015. Setting up a hydrological model of Alberta: Data discrimination analyses prior to calibration. Environ Modell Softw, 74: 48-65. DOI:10.1016/j.envsoft.2015.09.006

Finger, D., Pellicciotti, F., Konz, M., Rimkus, S., Burlando, P., 2011. The value of glacier mass balance, satellite snow cover images, and hourly discharge for improving the performance of a physically based distributed hydrological model. Water Resources Research, 47(7). DOI:https://doi.org/10.1029/2010WR009824

Flávio, H.M., Ferreira, P., Formigo, N., Svendsen, J.C., 2017. Reconciling agriculture and stream restoration in Europe: A review relating to the EU Water Framework Directive. Science of The Total Environment, 596-597: 378-395. DOI:10.1016/j.scitotenv.2017.04.057

Franco, A.C.L., Oliveira, D.Y.d., Bonumá, N.B., 2020. Comparison of single-site, multi-site and multi-variable SWAT calibration strategies. Hydrological Sciences Journal, 65(14): 2376-2389. DOI:10.1080/02626667.2020.1810252

Fu, B. et al., 2020. Modeling Water Quality in Watersheds: From Here to the Next Generation. Water Resour Res, 56(11). DOI:10.1029/2020wr027721

Fu, B., Merritt, W.S., Croke, B.F.W., Weber, T.R., Jakeman, A.J., 2019. A review of catchment-scale water quality and erosion models and a synthesis of future prospects. Environ Modell Softw, 114: 75-97. DOI:10.1016/j.envsoft.2018.12.008

Futter, M.N., Erlandsson, M.A., Butterfield, D., Whitehead, P.G., Oni, S.K., Wade, A.J., 2014. PERSiST: a flexible rainfall-runoff modelling toolkit for use with the INCA family of models. Hydrology and Earth System Sciences, 18(2): 855-873. DOI:10.5194/hess-18-855-2014

Gao, H., Hrachowitz, M., Sriwongsitanon, N., Fenicia, F., Gharari, S., Savenije, H.H.G., 2016. Accounting for the influence of vegetation and landscape improves model transferability in a tropical savannah region. Water Resources Research, 52(10): 7999-8022. DOI:10.1002/2016wr019574

Gao, H. et al., 2018. Landscape heterogeneity and hydrological processes: a review of landscape-based hydrological models. Landscape Ecology, 33(9): 1461-1480. DOI:10.1007/s10980-018-0690-4

Gassman, P.W., Reyes, M.R., Green, C.H., Arnold, J.G., 2007. The soil and water assessment tool: historical development, applications, and future research directions. Transactions of the ASABE, 50(4): 1211-1250.

Gavahi, K., Abbaszadeh, P., Moradkhani, H., Zhan, X., Hain, C., 2020. Multivariate Assimilation of Remotely Sensed Soil Moisture and Evapotranspiration for Drought Monitoring. Journal of Hydrometeorology, 21(10): 2293-2308. DOI:10.1175/jhm-d-20-0057.1

Ghaffar, S., Jomaa, S., Meon, G., Rode, M., 2021. Spatial validation of a semi-distributed hydrological nutrient transport model. Journal of Hydrology, 593: 125818. DOI:https://doi.org/10.1016/j.jhydrol.2020.125818

Gomez-Velez, J.D., Harvey, J.W., 2014. A hydrogeomorphic river network model predicts where and why hyporheic exchange is important in large basins. Geophysical Research Letters, 41(18): 6403-6412. DOI:10.1002/2014gl061099

Gomez-Velez, J.D., Harvey, J.W., Cardenas, M.B., Kiel, B., 2015. Denitrification in the Mississippi River network controlled by flow through river bedforms. Nature Geoscience, 8(12): 941-945. DOI:10.1038/ngeo2567

Gomez-Velez, J.D., Wilson, J.L., Cardenas, M.B., Harvey, J.W., 2017. Flow and Residence Times of Dynamic River Bank Storage and Sinuosity-Driven Hyporheic Exchange. Water Resources Research, 53(10): 8572-8595. DOI:10.1002/2017wr021362

Gomez, J.D., Wilson, J.L., Cardenas, M.B., 2012. Residence time distributions in sinuosity-driven hyporheic zones and their biogeochemical effects. Water Resources Research, 48(9). DOI:10.1029/2012wr012180

Götzinger, J., Bárdossy, A., 2007. Comparison of four regionalisation methods for a distributed hydrological model. Journal of Hydrology, 333(2-4): 374-384. DOI:10.1016/j.jhydrol.2006.09.008

Grimm, N.B. et al., 2003. Merging aquatic and terrestrial perspectives of nutrient biogeochemistry. Oecologia, 137(4): 485-501. DOI:10.1007/s00442-003-1382-5

Groffman, P.M. et al., 2006. Methods for measuring denitrification: diverse approaches to a difficult problem. Ecol Appl, 16(6): 2091-122. DOI:10.1890/1051-0761(2006)016[2091:mfmdda]2.0.co;2

Groffman, P.M. et al., 2009. Challenges to incorporating spatially and temporally explicit phenomena (hotspots and hot moments) in denitrification models. Biogeochemistry, 93(1-2): 49-77. DOI:10.1007/s10533-008-9277-5

Gucker, B., Boechat, I.G., 2004. Stream morphology controls ammonium retention in tropical headwaters. Ecology, 85(10): 2818-2827. DOI:Doi 10.1890/04-0171

Guidicelli, M., Gugerli, R., Gabella, M., Marty, C., Salzmann, N., 2021. Continuous Spatio-Temporal High-Resolution Estimates of SWE Across the Swiss Alps – A Statistical Two-Step Approach for High-Mountain Topography. Frontiers in Earth Science, 9. DOI:10.3389/feart.2021.664648

Gupta, H.V., Beven, K.J., Wagener, T., 2005. Model Calibration and Uncertainty Estimation, Encyclopedia of Hydrological Sciences. DOI:https://doi.org/10.1002/0470848944.hsa138

Gupta, H.V., Kling, H., Yilmaz, K.K., Martinez, G.F., 2009. Decomposition of the mean squared error and NSE performance criteria: Implications for improving hydrological modelling. Journal of Hydrology, 377(1-2): 80-91. DOI:10.1016/j.jhydrol.2009.08.003

Gupta, H.V., Sorooshian, S., Yapo, P.O., 1998. Toward improved calibration of hydrologic models: Multiple and noncommensurable measures of information. Water Resources Research, 34(4): 751-763. DOI:10.1029/97wr03495

Gupta, H.V., Sorooshian, S., Yapo, P.O., 1999. Status of Automatic Calibration for Hydrologic Models: Comparison with Multilevel Expert Calibration. Journal of Hydrologic Engineering, 4(2): 135-143. DOI:doi:10.1061/(ASCE)1084-0699(1999)4:2(135)

Gupta, H.V., Wagener, T., Liu, Y., 2008. Reconciling theory with observations: elements of a diagnostic approach to model evaluation. Hydrological Processes, 22(18): 3802-3813. DOI:10.1002/hyp.6989

Guzelj, M., Hauer, C., Egger, G., 2020. The third dimension in river restoration: how anthropogenic disturbance changes boundary conditions for ecological mitigation. Sci Rep, 10(1): 13106. DOI:10.1038/s41598-020-69796-0

Hall, R.O., Bernhardt, E.S., Likens, G.E., 2002. Relating nutrient uptake with transient storage in forested mountain streams. Limnology and Oceanography, 47(1): 255-265. DOI:DOI 10.4319/lo.2002.47.1.0255

Han, E., Merwade, V., Heathman, G.C., 2012. Implementation of surface soil moisture data assimilation with watershed scale distributed hydrological model. Journal of Hydrology, 416-417: 98-117. DOI:10.1016/j.jhydrol.2011.11.039

Hanel, M. et al., 2018. Revisiting the recent European droughts from a long-term perspective. Sci Rep, 8(1): 9499. DOI:10.1038/s41598-018-27464-4

Hargreaves, G.H., Samani, Z.A., 1985. Reference Crop Evapotranspiration from Temperature. Applied Engineering in Agriculture, 1(2): 96-99. DOI:10.13031/2013.26773

Hari, V., Rakovec, O., Markonis, Y., Hanel, M., Kumar, R., 2020. Increased future occurrences of the exceptional 2018-2019 Central European drought under global warming. Sci Rep, 10(1): 12207. DOI:10.1038/s41598-020-68872-9

Harnischmacher, S., 2007. Thresholds in small rivers? Hypotheses developed from fluvial morphological research in western Germany. Geomorphology, 92(3-4): 119-133. DOI:10.1016/j.geomorph.2006.07.036

Heffernan, J.B., Cohen, M.J., 2010. Direct and indirect coupling of primary production and diel nitrate dynamics in a subtropical spring-fed river. Limnology and Oceanography.

Helton, A.M., Hall, R.O., Bertuzzo, E., 2018. How network structure can affect nitrogen removal by streams. Freshwater Biology, 63(1): 128-140. DOI:10.1111/fwb.12990

Helton, A.M. et al., 2011. Thinking outside the channel: modeling nitrogen cycling in networked river ecosystems. Frontiers in Ecology and the Environment, 9(4): 229-238. DOI:10.1890/080211

Hensley, R.T., Cohen, M.J., 2020. Nitrate depletion dynamics and primary production in riverine benthic chambers. Freshwater Science, 39(1): 169-182. DOI:10.1086/707650

Hensley, R.T., Cohen, M.J., Korhnak, L.V., 2014. Inferring nitrogen removal in large rivers from high-resolution longitudinal profiling. Limnology and Oceanography, 59(4): 1152-1170. DOI:10.4319/lo.2014.59.4.1152

Her, Y., Chaubey, I., 2015. Impact of the numbers of observations and calibration parameters on equifinality, model performance, and output and parameter uncertainty. Hydrological Processes, 29(19): 4220-4237. DOI:10.1002/hyp.10487

Hesse, C., Krysanova, V., 2016. Modeling Climate and Management Change Impacts on Water Quality and In-Stream Processes in the Elbe River Basin. Water, 8(2). DOI:10.3390/w8020040

Heuvelmans, G., Muys, B., Feyen, J., 2004. Evaluation of hydrological model parameter transferability for simulating the impact of land use on catchment hydrology. Physics and Chemistry of the Earth, Parts A/B/C, 29(11-12): 739-747. DOI:10.1016/j.pce.2004.05.002

Homyak, P.M., Allison, S.D., Huxman, T.E., Goulden, M.L., Treseder, K.K., 2017. Effects of Drought Manipulation on Soil Nitrogen Cycling: A Meta-Analysis. Journal of Geophysical Research: Biogeosciences, 122(12): 3260-3272. DOI:10.1002/2017jg004146

Horn, A.L., Rueda, F.J., Hörmann, G., Fohrer, N., 2004. Implementing river water quality modelling issues in mesoscale watershed models for water policy demands—an overview on current concepts, deficits, and future tasks. Physics and Chemistry of the Earth, Parts A/B/C, 29(11-12): 725-737. DOI:10.1016/j.pce.2004.05.001

Hosen, J.D. et al., 2019. Enhancement of primary production during drought in a temperate watershed is greater in larger rivers than headwater streams. Limnology and Oceanography, 64(4): 1458-1472. DOI:10.1002/lno.11127

Howarth, R. et al., 2012. Nitrogen fluxes from the landscape are controlled by net anthropogenic nitrogen inputs and by climate. Frontiers in Ecology and the Environment, 10(1): 37-43. DOI:10.1890/100178

Huang, J., Borchardt, D., Rode, M., 2022. How do inorganic nitrogen processing pathways change quantitatively at daily, seasonal, and multiannual scales in a large agricultural stream? Hydrol. Earth Syst. Sci., 26(22): 5817-5833. DOI:10.5194/hess-26-5817-2022

Huang, S., Krysanova, V., Hattermann, F., 2015. Projections of climate change impacts on floods and droughts in Germany using an ensemble of climate change scenarios. Regional Environmental Change, 15(3): 461-473. DOI:10.1007/s10113-014-0606-z

Hundecha, Y., Bárdossy, A., 2004. Modeling of the effect of land use changes on the runoff generation of a river basin through parameter regionalization of a watershed model. Journal of Hydrology, 292(1-4): 281-295. DOI:10.1016/j.jhydrol.2004.01.002

Immerzeel, W.W., Droogers, P., 2008. Calibration of a distributed hydrological model based on satellite evapotranspiration. Journal of Hydrology, 349(3-4): 411-424. DOI:10.1016/j.jhydrol.2007.11.017

Inwood, S.E., Tank, J.L., Bernot, M.J., 2005. Patterns of denitrification associated with land use in 9 midwestern headwater streams. J N Am Benthol Soc, 24(2): 227-245. DOI:Doi 10.1899/04-032.1

Inwood, S.E., Tank, J.L., Bernot, M.J., 2007. Factors controlling sediment denitrification in midwestern streams of varying land use. Microb Ecol, 53(2): 247-58. DOI:10.1007/s00248-006-9104-2

Jakeman, A.J., Hornberger, G.M., 1993. How Much Complexity Is Warranted in a Rainfall-Runoff Model. Water Resources Research, 29(8): 2637-2649. DOI:Doi 10.1029/93wr00877

Jarvie, H.P. et al., 2018. Coupling High-Frequency Stream Metabolism and Nutrient Monitoring to Explore Biogeochemical Controls on Downstream Nitrate Delivery. Environ Sci Technol, 52(23): 13708-13717. DOI:10.1021/acs.est.8b03074

Jarvis, A., H.I. Reuter, A. Nelson, E. Guevara., 2008. Hole-filled SRTM for the globe Version 4, available from the CGIAR-CSI SRTM 90m Database http://srtm.csi.cgiar.org/, International Centre for Tropical Agriculture (CIAT).

Jiang, S., Jomaa, S., Büttner, O., Meon, G., Rode, M., 2015. Multi-site identification of a distributed hydrological nitrogen model using Bayesian uncertainty analysis. Journal of Hydrology, 529: 940-950. DOI:10.1016/j.jhydrol.2015.09.009

Jiang, S.Y., Jomaa, S., Rode, M., 2014. Modelling inorganic nitrogen leaching in nested mesoscale catchments in central Germany. Ecohydrology, 7(5): 1345-1362. DOI:10.1002/eco.1462

Jiang, S.Y. et al., 2019. Effects of stream nitrate data frequency on watershed model performance and prediction uncertainty. Journal of Hydrology, 569: 22-36. DOI:10.1016/j.jhydrol.2018.11.049

Jones, C.S., Kim, S.-w., Wilton, T.F., Schilling, K.E., Davis, C.A., 2018. Nitrate uptake in an agricultural stream estimated from high-frequency, in-situ sensors. Environmental Monitoring and Assessment, 190(4). DOI:10.1007/s10661-018-6599-1

Karimi, P., Bastiaanssen, W.G.M., 2015. Spatial evapotranspiration, rainfall and land use data in water accounting – Part 1: Review of the accuracy of the remote sensing data. Hydrology and Earth System Sciences, 19(1): 507-532. DOI:10.5194/hess-19-507-2015

Kasvi, E., Salmela, J., Lotsari, E., Kumpula, T., Lane, S.N., 2019. Comparison of remote sensing based approaches for mapping bathymetry of shallow, clear water rivers. Geomorphology, 333: 180-197. DOI:10.1016/j.geomorph.2019.02.017

Kaushal, S.S., Groffman, P.M., Mayer, P.M., Striz, E., Gold, A.J., 2008. Effects of stream restoration on denitrification in an urbanizing watershed. Ecol Appl, 18(3): 789-804. DOI:10.1890/07-1159.1

Khorashadi Zadeh, F., Nossent, J., Woldegiorgis, B.T., Bauwens, W., van Griensven, A., 2019. Impact of measurement error and limited data frequency on parameter estimation and uncertainty quantification. Environ Modell Softw, 118: 35-47. DOI:https://doi.org/10.1016/j.envsoft.2019.03.022

Khu, S.-T., Madsen, H., di Pierro, F., 2008. Incorporating multiple observations for distributed hydrologic model calibration: An approach using a multi-objective evolutionary algorithm and clustering. Advances in Water Resources, 31(10): 1387-1398. DOI:10.1016/j.advwatres.2008.07.011

Kiel, B.A., Bayani Cardenas, M., 2014. Lateral hyporheic exchange throughout the Mississippi River network. Nature Geoscience, 7(6): 413-417. DOI:10.1038/ngeo2157

Kirchner, J.W., Feng, X., Neal, C., Robson, A.J., 2004. The fine structure of water-quality dynamics: the(high-frequency) wave of the future. Hydrological Processes, 18(7): 1353-1359. DOI:10.1002/hyp.5537

Klocker, C.A., Kaushal, S.S., Groffman, P.M., Mayer, P.M., Morgan, R.P., 2009. Nitrogen uptake and denitrification in restored and unrestored streams in urban Maryland, USA. Aquatic Sciences, 71(4): 411-424. DOI:10.1007/s00027-009-0118-y

Kochendorfer, J. et al., 2017. The quantification and correction of wind-induced precipitation measurement errors. Hydrology and Earth System Sciences, 21(4): 1973-1989. DOI:10.5194/hess-21-1973-2017

Kong, X. et al., 2022. Reservoir water quality deterioration due to deforestation emphasizes the indirect effects of global change. Water Res, 221. DOI:10.1016/j.watres.2022.118721

Krabbenhoft, C.A. et al., 2022. Assessing placement bias of the global river gauge network. Nat Sustain, 5(7): 586-592. DOI:10.1038/s41893-022-00873-0

Krause, P., Boyle, D.P., Bäse, F., 2005. Comparison of different efficiency criteria for hydrological model assessment. Advances in Geosciences, 5: 89-97. DOI:10.5194/adgeo-5-89-2005

Kumar, R., Samaniego, L., Attinger, S., 2010. The effects of spatial discretization and model parameterization on the prediction of extreme runoff characteristics. Journal of Hydrology, 392(1-2): 54-69. DOI:10.1016/j.jhydrol.2010.07.047

Kunz, J.V. et al., 2017a. Quantifying nutrient fluxes with a new hyporheic passive flux meter (HPFM). Biogeosciences, 14(3): 631-649. DOI:10.5194/bg-14-631-2017

Kunz, J.V., Annable, M.D., Rao, S., Rode, M., Borchardt, D., 2017b. Hyporheic Passive Flux Meters Reveal Inverse Vertical Zonation and High Seasonality of Nitrogen Processing in an Anthropogenically Modified Stream (Holtemme, Germany). Water Resources Research, 53(12): 10155-10172. DOI:https://doi.org/10.1002/2017WR020709

Kunz, J.V., Hensley, R., Brase, L., Borchardt, D., Rode, M., 2017c. High frequency measurements of reach scale nitrogen uptake in a fourth order river with contrasting hydromorphology and variable water chemistry (Weiße Elster, Germany). Water Resources Research, 53(1): 328-343. DOI:10.1002/2016wr019355

Kupilas, B., Hering, D., Lorenz, A.W., Knuth, C., Gücker, B., 2017. Hydromorphological restoration stimulates river ecosystem metabolism. Biogeosciences, 14(7): 1989-2002. DOI:10.5194/bg-14-1989-2017

Kyllmar, K., Forsberg, L.S., Andersson, S., Mårtensson, K., 2014. Small agricultural monitoring catchments in Sweden representing environmental impact. Agriculture, Ecosystems & Environment, 198: 25-35. DOI:10.1016/j.agee.2014.05.016

Ladrera, R., Belmar, O., Tomas, R., Prat, N., Canedo-Arguelles, M., 2019. Agricultural impacts on streams near Nitrate Vulnerable Zones: A case study in the Ebro basin, Northern Spain. PLoS One, 14(11): e0218582. DOI:10.1371/journal.pone.0218582

Lammers, R.W., Bledsoe, B.P., 2017. What role does stream restoration play in nutrient management? Critical Reviews in Environmental Science and Technology, 47(6): 335-371. DOI:10.1080/10643389.2017.1318618

Lei, C., Wagner, P.D., Fohrer, N., 2021. Effects of land cover, topography, and soil on stream water quality at multiple spatial and seasonal scales in a German lowland catchment. Ecological Indicators, 120. DOI:10.1016/j.ecolind.2020.106940

Leitner, S., Dirnbock, T., Kobler, J., Zechmeister-Boltenstern, S., 2020. Legacy effects of drought on nitrate leaching in a temperate mixed forest on karst. J Environ Manage, 262: 110338. DOI:10.1016/j.jenvman.2020.110338

Lerat, J. et al., 2012. Do internal flow measurements improve the calibration of rainfall-runoff models? Water Resources Research, 48(2). DOI:10.1029/2010wr010179

Leta, O.T., Griensven, A.v., Bauwens, W., 2017. Effect of Single and Multisite Calibration Techniques on the Parameter Estimation, Performance, and Output of a SWAT Model of a Spatially Heterogeneous Catchment. Journal of Hydrologic Engineering, 22(3): 05016036. DOI:doi:10.1061/(ASCE)HE.1943-5584.0001471

Leta, O.T., van Griensven, A., Bauwens, W., 2017. Effect of Single and Multisite Calibration Techniques on the Parameter Estimation, Performance, and Output of a SWAT Model of a Spatially Heterogeneous Catchment. Journal of Hydrologic Engineering, 22(3): 05016036. DOI:Artn 05016036

10.1061/(Asce)He.1943-5584.0001471

Lettenmaier, D.P., Alsdorf, D., Dozier, J., Huffman, G.J., Pan, M., Wood, E.F., 2015. Inroads of remote sensing into hydrologic science during the WRR era. Water Resources Research, 51(9): 7309-7342. DOI:10.1002/2015wr017616

Li, L. et al., 2020. Toward catchment hydro-biogeochemical theories. WIREs Water, 8(1). DOI:10.1002/wat2.1495

Li, X., Weller, D.E., Jordan, T.E., 2010. Watershed model calibration using multi-objective optimization and multi-site averaging. Journal of Hydrology, 380(3-4): 277-288. DOI:10.1016/j.jhydrol.2009.11.003

Lin, L., Davis, L., Cohen, S., Chapman, E., Edmonds, J.W., 2016. The influence of geomorphic unit spatial distribution on nitrogen retention and removal in a large river. Ecological Modelling, 336: 26-35. DOI:10.1016/j.ecolmodel.2016.05.018

Lin, L., Reisinger, A.J., Rosi, E.J., Groffman, P.M., Band, L.E., 2021. Evaluating Instream Restoration Effectiveness in Reducing Nitrogen Export from an Urban Catchment with a Data-Model Approach. JAWRA Journal of the American Water Resources Association, 57(3): 449-473. DOI:10.1111/1752-1688.12922

Lindstrom, G., Johansson, B., Persson, M., Gardelin, M., Bergstrom, S., 1997. Development and test of the distributed HBV-96 hydrological model. Journal of Hydrology, 201(1-4): 272-288. DOI:Doi 10.1016/S0022-1694(97)00041-3

Lindström, G., Pers, C., Rosberg, J., Strömqvist, J., Arheimer, B., 2010. Development and testing of the HYPE (Hydrological Predictions for the Environment) water quality model for different spatial scales. Hydrology Research, 41(3-4): 295-319. DOI:10.2166/nh.2010.007

Lindström, G., Rosberg, J., Arheimer, B., 2005. Parameter Precision in the HBV-NP Model and Impacts on Nitrogen Scenario Simulations in the Rönneå River, Southern Sweden. AMBIO: A Journal of the Human Environment, 34(7): 533-537. DOI:10.1579/0044-7447-34.7.533

Lintern, A. et al., 2018a. Key factors influencing differences in stream water quality across space. Wiley Interdisciplinary Reviews: Water, 5(1). DOI:10.1002/wat2.1260

Lintern, A. et al., 2018b. What Are the Key Catchment Characteristics Affecting Spatial Differences in Riverine Water Quality? Water Resources Research, 54(10): 7252-7272. DOI:10.1029/2017wr022172

Liu, J., Zhang, L., Zhang, Y., Hong, H., Deng, H., 2008. Validation of an agricultural non-point source (AGNPS) pollution model for a catchment in the Jiulong River watershed, China. J Environ Sci (China), 20(5): 599-606. DOI:10.1016/s1001-0742(08)62100-2

Lohse, K.A., Brooks, P.D., McIntosh, J.C., Meixner, T., Huxman, T.E., 2009. Interactions Between Biogeochemistry and Hydrologic Systems. Annual Review of Environment and Resources, 34(1): 65-96. DOI:10.1146/annurev.environ.33.031207.111141

Lorenz, A.W., Jahnig, S.C., Hering, D., 2009. Re-meandering German lowland streams: qualitative and quantitative effects of restoration measures on hydromorphology and macroinvertebrates. Environ Manage, 44(4): 745-54. DOI:10.1007/s00267-009-9350-4

Lute, A.C., Luce, C.H., 2017. Are Model Transferability And Complexity Antithetical? Insights From Validation of a Variable-Complexity Empirical Snow Model in Space and Time. Water Resources Research, 53(11): 8825-8850. DOI:https://doi.org/10.1002/2017WR020752

Lutz, S.R., Mallucci, S., Diamantini, E., Majone, B., Bellin, A., Merz, R., 2016. Hydroclimatic and water quality trends across three Mediterranean river basins. Sci Total Environ, 571: 1392-406. DOI:10.1016/j.scitotenv.2016.07.102

Marcé, R., von Schiller, D., Aguilera, R., Martí, E., Bernal, S., 2018. Contribution of Hydrologic Opportunity and Biogeochemical Reactivity to the Variability of Nutrient Retention in River Networks. Global Biogeochemical Cycles, 32(3): 376-388. DOI:10.1002/2017gb005677

McDonnell, J.J. et al., 2007. Moving beyond heterogeneity and process complexity: A new vision for watershed hydrology. Water Resources Research, 43(7). DOI:10.1029/2006wr005467

McMillan, H.K., 2021. A review of hydrologic signatures and their applications. WIREs Water, 8(1): e1499. DOI:https://doi.org/10.1002/wat2.1499

Merz, R., Blöschl, G., 2004. Regionalisation of catchment model parameters. Journal of Hydrology, 287(1-4): 95-123. DOI:10.1016/j.jhydrol.2003.09.028

Merz, R., Parajka, J., Blöschl, G., 2011. Time stability of catchment model parameters: Implications for climate impact analyses. Water Resources Research, 47(2). DOI:10.1029/2010wr009505

Michaelides, S., Levizzani, V., Anagnostou, E., Bauer, P., Kasparis, T., Lane, J.E., 2009. Precipitation: Measurement, remote sensing, climatology and modeling. Atmospheric Research, 94(4): 512-533. DOI:10.1016/j.atmosres.2009.08.017

Mineau, M.M., Wollheim, W.M., Stewart, R.J., 2015. An index to characterize the spatial distribution of land use within watersheds and implications for river network nutrient removal and export. Geophysical Research Letters, 42(16): 6688-6695. DOI:10.1002/2015gl064965

Ministerium für Umwelt und Naturschutz Landwirtschaft und Verbraucherschutz des Landes Nordrhein-Westfalen, 2010. Richtlinie für die Entwicklung naturnaher Fließgewässer in Nordrhein-Westfalen: Ausbau und Unterhaltung, Düsseldorf

Moriasi, D.N., Gitau, M.W., Pai, N., Daggupati, P., 2015. Hydrologic and Water Quality Models: Performance Measures and Evaluation Criteria. Transactions of the Asabe, 58(6): 1763-1785. DOI:10.13031/trans.58.10715

Moriasi, D.N., Wilson, B.N., Douglas-Mankin, K.R., Arnold, J.G., Gowda, P.H., 2012. Hydrologic and Water Quality Models: Use, Calibration, and Validation. Transactions of the ASABE, 55(4): 1241-1247. DOI:10.13031/2013.42265

Morris, M.D., 1991. Factorial sampling plans for preliminary computational experiments. Technometrics, 33(2): 161-174.

Mosley, L.M., 2015. Drought impacts on the water quality of freshwater systems; review and integration. Earth-Science Reviews, 140: 203-214. DOI:10.1016/j.earscirev.2014.11.010

Mueller, C. et al., 2016. Discharge Driven Nitrogen Dynamics in a Mesoscale River Basin As Constrained by Stable Isotope Patterns. Environ Sci Technol, 50(17): 9187-96. DOI:10.1021/acs.est.6b01057

Muleta, M.K., 2012. Model Performance Sensitivity to Objective Function during Automated Calibrations. Journal of Hydrologic Engineering, 17(6): 756-767. DOI:10.1061/(Asce)He.1943-5584.0000497

Mulholland, P.J. et al., 2009. Nitrate removal in stream ecosystems measured by 15N addition experiments: denitrification. Limnology and Oceanography, 54(3): 666-680.

Mulholland, P.J. et al., 2008. Stream denitrification across biomes and its response to anthropogenic nitrate loading. Nature, 452(7184): 202-5. DOI:10.1038/nature06686

Mulholland, P.J., Webster, J.R., 2010. Nutrient dynamics in streams and the role of J-NABS. J N Am Benthol Soc, 29(1): 100-117. DOI:10.1899/08-035.1

Neal, C. et al., 2012. High-frequency water quality time series in precipitation and streamflow: from fragmentary signals to scientific challenge. Sci Total Environ, 434: 3-12. DOI:10.1016/j.scitotenv.2011.10.072

Newcomer Johnson, T., Kaushal, S., Mayer, P., Smith, R., Sivirichi, G., 2016. Nutrient Retention in Restored Streams and Rivers: A Global Review and Synthesis. Water, 8(4). DOI:10.3390/w8040116

Nguyen, T.V., Kumar, R., Lutz, S.R., Musolff, A., Yang, J., Fleckenstein, J.H., 2021. Modeling Nitrate Export From a Mesoscale Catchment Using StorAge Selection Functions. Water Resources Research, 57(2). DOI:10.1029/2020wr028490

Nijzink, R.C. et al., 2018. Constraining Conceptual Hydrological Models With Multiple Information Sources. Water Resources Research, 54(10): 8332-8362. DOI:10.1029/2017wr021895

Onderka, M., Wrede, S., Rodný, M., Pfister, L., Hoffmann, L., Krein, A., 2012. Hydrogeologic and landscape controls of dissolved inorganic nitrogen (DIN) and dissolved silica (DSi) fluxes in heterogeneous catchments. Journal of Hydrology, 450-451: 36-47. DOI:10.1016/j.jhydrol.2012.05.035

Opdyke, M.R., David, M.B., Rhoads, B.L., 2006. Influence of geomorphological variability in channel characteristics on sediment denitrification in agricultural streams. J Environ Qual, 35(6): 2103-12. DOI:10.2134/jeq2006.0072

Orth, R., Staudinger, M., Seneviratne, S.I., Seibert, J., Zappa, M., 2015. Does model performance improve with complexity? A case study with three hydrological models. Journal of Hydrology, 523: 147-159. DOI:10.1016/j.jhydrol.2015.01.044

Oudin, L., Andreassian, V., Perrin, C., Michel, C., Le Moine, N., 2008a. Spatial proximity, physical similarity, regression and ungaged catchments: A comparison of regionalization approaches based on 913 French catchments. Water Resources Research, 44(3). DOI:Artn W03413

10.1029/2007wr006240

Oudin, L., Andréassian, V., Perrin, C., Michel, C., Le Moine, N., 2008b. Spatial proximity, physical similarity, regression and ungaged catchments: A comparison of regionalization approaches based on 913 French catchments. Water Resources Research, 44(3). DOI:10.1029/2007wr006240

Outram, F.N., Cooper, R.J., Sünnenberg, G., Hiscock, K.M., Lovett, A.A., 2016. Antecedent conditions, hydrological connectivity and anthropogenic inputs: Factors affecting nitrate and phosphorus transfers to agricultural headwater streams. Science of The Total Environment, 545-546: 184-199. DOI:https://doi.org/10.1016/j.scitotenv.2015.12.025

Outram, F.N. et al., 2014. High-frequency monitoring of nitrogen and phosphorus response in three rural catchments to the end of the 2011–2012 drought in England. Hydrology and Earth System Sciences, 18(9): 3429-3448. DOI:10.5194/hess-18-3429-2014

Pander, J., Mueller, M., Knott, J., Egg, L., Geist, J., 2017. Is it Worth the Money? The Functionality of Engineered Shallow Stream Banks as Habitat for Juvenile Fishes in Heavily Modified Water Bodies. River Research and Applications, 33(1): 63-72. DOI:10.1002/rra.3065

Parajka, J., Blöschl, G., 2008. The value of MODIS snow cover data in validating and calibrating conceptual hydrologic models. Journal of Hydrology, 358(3-4): 240-258. DOI:10.1016/j.jhydrol.2008.06.006

Parajka, J., Merz, R., Bloschl, G., 2005. A comparison of regionalisation methods for catchment model parameters. Hydrology and Earth System Sciences, 9(3): 157-171. DOI:DOI 10.5194/hess-9-157-2005

Parajka, J., Viglione, A., Rogger, M., Salinas, J.L., Sivapalan, M., Blöschl, G., 2013. Comparative assessment of predictions in ungauged basins – Part 1: Runoff-hydrograph studies. Hydrology and Earth System Sciences, 17(5): 1783-1795. DOI:10.5194/hess-17-1783-2013

Parajuli, P.B., Nelson, N.O., Frees, L.D., Mankin, K.R., 2009. Comparison of AnnAGNPS and SWAT model simulation results in USDA-CEAP agricultural watersheds in south-central Kansas. Hydrological Processes, 23(5): 748-763. DOI:10.1002/hyp.7174

Passy, P., Garnier, J., Billen, G., Fesneau, C., Tournebize, J., 2012. Restoration of ponds in rural landscapes: modelling the effect on nitrate contamination of surface water (the Seine River Basin, France). Sci Total Environ, 430: 280-90. DOI:10.1016/j.scitotenv.2012.04.035

Pedersen, M.L., Kristensen, K.K., Friberg, N., 2014. Re-meandering of lowland streams: will disobeying the laws of geomorphology have ecological consequences? PLoS One, 9(9): e108558. DOI:10.1371/journal.pone.0108558

Perrin, C., Michel, C., Andréassian, V., 2001. Does a large number of parameters enhance model performance? Comparative assessment of common catchment model structures on 429 catchments. Journal of Hydrology, 242(3): 275-301. DOI:https://doi.org/10.1016/S0022-1694(00)00393-0

Pianosi, F. et al., 2016. Sensitivity analysis of environmental models: A systematic review with practical workflow. Environ Modell Softw, 79: 214-232. DOI:10.1016/j.envsoft.2016.02.008

Pianosi, F., Sarrazin, F., Wagener, T., 2015. A Matlab toolbox for Global Sensitivity Analysis. Environ Modell Softw, 70: 80-85. DOI:10.1016/j.envsoft.2015.04.009

Pinay, G., O'Keefe, T.C., Edwards, R.T., Naiman, R.J., 2009. Nitrate removal in the hyporheic zone of a salmon river in Alaska. River Research and Applications, 25(4): 367-375. DOI:https://doi.org/10.1002/rra.1164

Pokhrel, P., Gupta, H.V., Wagener, T., 2008. A spatial regularization approach to parameter estimation for a distributed watershed model. Water Resources Research, 44(12). DOI:10.1029/2007wr006615

Potter, J.D., McDowell, W.H., Merriam, J.L., Peterson, B.J., Thomas, S.M., 2010. Denitrification and total nitrate uptake in streams of a tropical landscape. Ecol Appl, 20(8): 2104-15. DOI:10.1890/09-1110.1

Pottgiesser, T., Sommerhäuser, M., 2004. Die Fließgewässertypologie Deutschlands: System der Gewässertypen und Steckbriefe zu den Referenzbedingungen, Handbuch Angewandte Limnologie. ecomed Verlagsgesellschaft: Landsberg/Lech, Germany.

R Core Team., 2020. R: A Language and Environment for Statistical Computing. Vienna, Austria: R Foundation for Statistical Computing. Available online: http://www.R-project.org/ (accessed on 09 September 2020).

Rajib, A., Evenson, G.R., Golden, H.E., Lane, C.R., 2018. Hydrologic model predictability improves with spatially explicit calibration using remotely sensed evapotranspiration and biophysical parameters. J Hydrol (Amst), 567: 668-683. DOI:10.1016/j.jhydrol.2018.10.024

Rajib, M.A., Merwade, V., Yu, Z., 2016. Multi-objective calibration of a hydrologic model using spatially distributed remotely sensed/in-situ soil moisture. Journal of Hydrology, 536: 192-207. DOI:10.1016/j.jhydrol.2016.02.037

Rathjens, H., Oppelt, N., 2012. SWATgrid: An interface for setting up SWAT in a grid-based discretization scheme. Computers & Geosciences, 45: 161-167. DOI:10.1016/j.cageo.2011.11.004

Rathjens, H., Oppelt, N., Bosch, D.D., Arnold, J.G., Volk, M., 2015. Development of a grid-based version of the SWAT landscape model. Hydrological Processes, 29(6): 900-914. DOI:10.1002/hyp.10197

Refsgaard, J.C., 1997. Parameterisation, calibration and validation of distributed hydrological models. Journal of Hydrology, 198(1-4): 69-97. DOI:Doi 10.1016/S0022-1694(96)03329-X

Refsgaard, J.C., Højberg, A.L., He, X., Hansen, A.L., Rasmussen, S.H., Stisen, S., 2016. Where are the limits of model predictive capabilities? Hydrological Processes, 30(26): 4956-4965. DOI:10.1002/hyp.11029

Refsgaard, J.C., Stisen, S., Koch, J., 2022. Hydrological process knowledge in catchment modelling – Lessons and perspectives from 60 years development. Hydrological Processes, 36(1). DOI:10.1002/hyp.14463

Reisinger, A.J., Tank, J.L., Hoellein, T.J., Hall, R.O., 2016. Sediment, water column, and open-channel denitrification in rivers measured using membrane-inlet mass spectrometry. J Geophys Res-Biogeo, 121(5): 1258-1274. DOI:10.1002/2015jg003261

Reisinger, A.J., Tank, J.L., Rosi-Marshall, E.J., Hall, R.O., Baker, M.A., 2015. The varying role of water column nutrient uptake along river continua in contrasting landscapes. Biogeochemistry, 125(1): 115-131. DOI:10.1007/s10533-015-0118-z

Rhoads, B.L., 2010. Stream Power Terminology. The Professional Geographer, 39(2): 189-195. DOI:10.1111/j.0033-0124.1987.00189.x

Ribot, M., von Schiller, D., Martí, E., 2017. Understanding pathways of dissimilatory and assimilatory dissolved inorganic nitrogen uptake in streams. Limnology and Oceanography, 62(3): 1166-1183. DOI:10.1002/lno.10493

Roberts, B.J., Mulholland, P.J., 2007. In-stream biotic control on nutrient biogeochemistry in a forested stream, West Fork of Walker Branch. Journal of Geophysical Research: Biogeosciences, 112(G4). DOI:https://doi.org/10.1029/2007JG000422

Rode, M. et al., 2010. New challenges in integrated water quality modelling. Hydrological Processes, 24(24): 3447-3461. DOI:10.1002/hyp.7766

Rode, M., Halbedel Nee Angelstein, S., Anis, M.R., Borchardt, D., Weitere, M., 2016a. Continuous In-Stream Assimilatory Nitrate Uptake from High-Frequency Sensor Measurements. Environ Sci Technol, 50(11): 5685-94. DOI:10.1021/acs.est.6b00943

Rode, M., Lindenschmidt, K.E., 2001. Distributed sediment and phosporus transport modeling on a medium sized catchment in Central Germany. Phys Chem Earth Pt B, 26(7-8): 635-640. DOI:Doi 10.1016/S1464-1909(01)00061-2

Rode, M., Osenbrück, K., Shrestha, R.R., 2013. Assessment of catchment response and calibration of a hydrological model using high-frequency discharge–nitrate concentration data. Hydrology Research, 44(6): 995-1012. DOI:10.2166/nh.2013.087

Rode, M. et al., 2016b. Sensors in the Stream: The High-Frequency Wave of the Present. Environ Sci Technol, 50(19): 10297-10307. DOI:10.1021/acs.est.6b02155

Roley, S.S., Tank, J.L., Williams, M.A., 2012. Hydrologic connectivity increases denitrification in the hyporheic zone and restored floodplains of an agricultural stream. Journal of Geophysical Research: Biogeosciences, 117(G3). DOI:10.1029/2012JG001950

Ruiz, L., Abiven, S., Durand, P., Martin, C., Vertès, F., Beaujouan, V., 2002. Effect on nitrate concentration in stream water of agricultural practices in small catchments in Brittany: I. Annual nitrogen budgets. Hydrology and Earth System Sciences, 6(3): 497-506. DOI:10.5194/hess-6-497-2002

Rusjan, S., Brilly, M., Mikoš, M., 2008. Flushing of nitrate from a forested watershed: An insight into hydrological nitrate mobilization mechanisms through seasonal high-frequency stream nitrate dynamics. Journal of Hydrology, 354(1-4): 187-202. DOI:10.1016/j.jhydrol.2008.03.009

Saft, M., Western, A.W., Zhang, L., Peel, M.C., Potter, N.J., 2015. The influence of multiyear drought on the annual rainfall-runoff relationship: An Australian perspective. Water Resources Research, 51(4): 2444-2463. DOI:10.1002/2014wr015348

Samaniego, L., Kumar, R., Attinger, S., 2010. Multiscale parameter regionalization of a grid-based hydrologic model at the mesoscale. Water Resources Research, 46(5). DOI:10.1029/2008wr007327

Samaniego, L. et al., 2017. Toward seamless hydrologic predictions across spatial scales. Hydrology and Earth System Sciences, 21(9): 4323-4346. DOI:10.5194/hess-21-4323-2017

Saraswat, D. et al., 2015. Hydrologic and Water Quality Models: Documentation and Reporting Procedures for Calibration, Validation, and Use. Transactions of the Asabe, 58(6): 1787-1797. DOI:10.13031/trans.57.10707

Savenije, H.H.G., 2001. Equifinality, a blessing in disguise? Hydrological Processes, 15(14): 2835-2838. DOI:10.1002/hyp.494

Schoups, G., van de Giesen, N.C., Savenije, H.H.G., 2008. Model complexity control for hydrologic prediction. Water Resources Research, 44(12). DOI:10.1029/2008wr006836

Seibert, J., Staudinger, M., van Meerveld, H.J., 2019. Validation and Over-Parameterization—Experiences from Hydrological Modeling. In: Beisbart, C., Saam, N.J. (Eds.), Computer Simulation Validation: Fundamental Concepts, Methodological Frameworks, and Philosophical Perspectives. Springer International Publishing, Cham, pp. 811-834. DOI:10.1007/978-3-319-70766-2_33

Shevenell, L., 1999. Regional potential evapotranspiration in arid climates based on temperature, topography and calculated solar radiation. Hydrological Processes, 13(4): 577-596. DOI:Doi 10.1002/(Sici)1099-1085(199903)13:4<577::Aid-Hyp757>3.0.Co;2-P

Shrestha, M.K., Recknagel, F., Frizenschaf, J., Meyer, W., 2016. Assessing SWAT models based on single and multi-site calibration for the simulation of flow and nutrient loads in the semi-arid Onkaparinga catchment in South Australia. Agricultural Water Management, 175: 61-71. DOI:10.1016/j.agwat.2016.02.009

Singh, R., Archfield, S.A., Wagener, T., 2014. Identifying dominant controls on hydrologic parameter transfer from gauged to ungauged catchments – A comparative hydrology approach. Journal of Hydrology, 517: 985-996. DOI:10.1016/j.jhydrol.2014.06.030

Singh, S.K., Bárdossy, A., 2012. Calibration of hydrological models on hydrologically unusual events. Advances in Water Resources, 38: 81-91. DOI:10.1016/j.advwatres.2011.12.006

Singh, V.P., Woolhiser, D.A., 2002. Mathematical Modeling of Watershed Hydrology. Journal of Hydrologic Engineering, 7(4): 270-292. DOI:doi:10.1061/(ASCE)1084-0699(2002)7:4(270)

Song, X., Zhang, J., Zhan, C., Xuan, Y., Ye, M., Xu, C., 2015. Global sensitivity analysis in hydrological modeling: Review of concepts, methods, theoretical framework, and applications. Journal of Hydrology, 523: 739-757. DOI:10.1016/j.jhydrol.2015.02.013

Spinoni, J., Vogt, J.V., Naumann, G., Barbosa, P., Dosio, A., 2018. Will drought events become more frequent and severe in Europe? International Journal of Climatology, 38(4): 1718-1736. DOI:10.1002/joc.5291

Sprague, L.A., 2005. Drought effects on water quality in the South Platte River Basin, Colorado. Journal of the American Water Resources Association, 41(1): 11-24. DOI:DOI 10.1111/j.1752-1688.2005.tb03713.x

Stanley, E.H., Doyle, M.W., 2002. A geomorphic perspective on nutrient retention following dam removal. Bioscience, 52(8): 693-701. DOI:Doi 10.1641/0006-3568(2002)052[0693:Agponr]2.0.Co;2

Stisen, S. et al., 2018. Moving beyond run-off calibration-Multivariable optimization of a surface-subsurface-atmosphere model. Hydrological Processes, 32(17): 2654-2668. DOI:10.1002/hyp.13177

Stow, C.A., Cha, Y., Johnson, L.T., Confesor, R., Richards, R.P., 2015. Long-Term and Seasonal Trend Decomposition of Maumee River Nutrient Inputs to Western Lake Erie. Environmental Science & Technology, 49(6): 3392-3400. DOI:10.1021/es5062648

Stow, C.A. et al., 2014. Phosphorus targets and eutrophication objectives in Saginaw Bay: A 35year assessment. Journal of Great Lakes Research, 40: 4-10. DOI:https://doi.org/10.1016/j.jglr.2013.10.003

Suddick, E.C., Whitney, P., Townsend, A.R., Davidson, E.A., 2012. The role of nitrogen in climate change and the impacts of nitrogen–climate interactions in the United States: foreword to thematic issue. Biogeochemistry, 114(1-3): 1-10. DOI:10.1007/s10533-012-9795-z

Tank, J.L., Rosi-Marshall, E.J., Baker, M.A., Hall, R.O., 2008. Are Rivers Just Big Streams? A Pulse Method to Quantify Nitrogen Demand in a Large River. Ecology, 89(10): 2935-2945.

Tatariw, C., Chapman, E.L., Sponseller, R.A., Mortazavi, B., Edmonds, J.W., 2013. Denitrification in a large river: consideration of geomorphic controls on microbial activity and community structure. Ecology, 94(10): 2249-62.

ter Braak, C.J.F., Vrugt, J.A., 2008. Differential Evolution Markov Chain with snooker updater and fewer chains. Statistics and Computing, 18(4): 435-446. DOI:10.1007/s11222-008-9104-9

Thiemann, M., Trosset, M., Gupta, H., Sorooshian, S., 2001. Bayesian recursive parameter estimation for hydrologic models. Water Resources Research, 37(10): 2521-2535. DOI:10.1029/2000wr900405

Tian, F., Hu, H., Lei, Z., Sivapalan, M., 2006. Extension of the Representative Elementary Watershed approach for cold regions via explicit treatment of energy related processes. Hydrology and Earth System Sciences, 10(5): 619-644. DOI:DOI 10.5194/hess-10-619-2006

Tolson, B.A., Shoemaker, C.A., 2007. Dynamically dimensioned search algorithm for computationally efficient watershed model calibration. Water Resources Research, 43(1). DOI:Artn W01413

10.1029/2005wr004723

Tran, Q.Q., De Niel, J., Willems, P., 2018. Spatially Distributed Conceptual Hydrological Model Building: A Generic Top-Down Approach Starting From Lumped Models. Water Resources Research, 54(10): 8064-8085. DOI:https://doi.org/10.1029/2018WR023566

UBA, 2019. 2019 Monitoring Report on the German Strategy for Adaptation to Climate Change.

Ullrich, A., Volk, M., 2010. Influence of different nitrate-N monitoring strategies on load estimation as a base for model calibration and evaluation. Environ Monit Assess, 171(1-4): 513-27. DOI:10.1007/s10661-009-1296-8

Uusheimo, S., Tulonen, T., Aalto, S.L., Arvola, L., 2018. Mitigating agricultural nitrogen load with constructed ponds in northern latitudes: A field study on sedimental denitrification rates. Agriculture, Ecosystems & Environment, 261: 71-79. DOI:https://doi.org/10.1016/j.agee.2018.04.002

van Vliet, M.T.H., Zwolsman, J.J.G., 2008. Impact of summer droughts on the water quality of the Meuse river. Journal of Hydrology, 353(1-2): 1-17. DOI:10.1016/j.jhydrol.2008.01.001

Veraart, A.J., Audet, J., Dimitrov, M.R., Hoffmann, C.C., Gillissen, F., de Klein, J.J.M., 2014. Denitrification in restored and unrestored Danish streams. Ecological Engineering, 66: 129-140. DOI:10.1016/j.ecoleng.2013.07.068

Vicente-Serrano, S.M., Begueria, S., Lopez-Moreno, J.I., 2010. A Multiscalar Drought Index Sensitive to Global Warming: The Standardized Precipitation Evapotranspiration Index. Journal of Climate, 23(7): 1696-1718. DOI:10.1175/2009jcli2909.1

Vrugt, J.A., 2016. Markov chain Monte Carlo simulation using the DREAM software package: Theory, concepts, and MATLAB implementation. Environ Modell Softw, 75: 273-316. DOI:10.1016/j.envsoft.2015.08.013

Vrugt, J.A., Diks, C.G.H., Gupta, H.V., Bouten, W., Verstraten, J.M., 2005. Improved treatment of uncertainty in hydrologic modeling: Combining the strengths of global optimization and data assimilation. Water Resources Research, 41(1). DOI:10.1029/2004wr003059

Vrugt, J.A., Gupta, H.V., Bouten, W., Sorooshian, S., 2003. A Shuffled Complex Evolution Metropolis algorithm for optimization and uncertainty assessment of hydrologic model parameters. Water Resources Research, 39(8). DOI:10.1029/2002wr001642

Vrugt, J.A., ter Braak, C.J.F., Clark, M.P., Hyman, J.M., Robinson, B.A., 2008. Treatment of input uncertainty in hydrologic modeling: Doing hydrology backward with Markov chain Monte Carlo simulation. Water Resources Research, 44(12). DOI:10.1029/2007wr006720

Wade, A.J. et al., 2002. A nitrogen model for European catchments: INCA, new model structure and equations. Hydrology and Earth System Sciences, 6(3): 559-582. DOI:DOI 10.5194/hess-6-559-2002

Wade, A.J., Jackson, B.M., Butterfield, D., 2008. Over-parameterised, uncertain 'mathematical marionettes' - how can we best use catchment water quality models? An example of an 80-year catchment-scale nutrient balance. Sci Total Environ, 400(1-3): 52-74. DOI:10.1016/j.scitotenv.2008.04.030

Wagener, T., Gupta, H.V., 2005. Model identification for hydrological forecasting under uncertainty. Stochastic Environmental Research and Risk Assessment, 19(6): 378-387. DOI:10.1007/s00477-005-0006-5

Wagener, T., McIntyre, N., Lees, M.J., Wheater, H.S., Gupta, H.V., 2003. Towards reduced uncertainty in conceptual rainfall-runoff modelling: dynamic identifiability analysis. Hydrological Processes, 17(2): 455-476. DOI:10.1002/hyp.1135

Wagener, T., Sivapalan, M., Troch, P., Woods, R., 2007. Catchment Classification and Hydrologic Similarity. Geography Compass, 1(4): 901-931. DOI:10.1111/j.1749-8198.2007.00039.x

Wagener, T., Wheater, H.S., 2006. Parameter estimation and regionalization for continuous rainfall-runoff models including uncertainty. Journal of Hydrology, 320(1-2): 132-154. DOI:10.1016/j.jhydrol.2005.07.015

Wagenschein, D., Rode, M., 2008. Modelling the impact of river morphology on nitrogen retention—A case study of the Weisse Elster River (Germany). Ecological Modelling, 211(1-2): 224-232. DOI:10.1016/j.ecolmodel.2007.09.009

Wagner, P.D., Waske, B., 2016. Importance of spatially distributed hydrologic variables for land use change modeling. Environ Modell Softw, 83: 245-254. DOI:https://doi.org/10.1016/j.envsoft.2016.06.005

Wang, S. et al., 2012. Multi-site calibration, validation, and sensitivity analysis of the MIKE SHE Model for a large watershed in northern China. Hydrology and Earth System Sciences, 16(12): 4621-4632. DOI:10.5194/hess-16-4621-2012

Wellen, C., Kamran-Disfani, A.R., Arhonditsis, G.B., 2015. Evaluation of the current state of distributed watershed nutrient water quality modeling. Environ Sci Technol, 49(6): 3278-90. DOI:10.1021/es5049557

White, K.L., Chaubey, I., 2005. Sensitivity Analysis, Calibration, and Validations for a Multisite and Multivariable Swat Model. Journal of the American Water Resources Association, 41(5): 1077-1089. DOI:10.1111/j.1752-1688.2005.tb03786.x

Whitehead, P., Wilson, E., Butterfield, D., 1998. A semi-distributed ntegrated itrogen model for multiple source assessment in tchments (INCA): Part I — model structure and process equations. Science of The Total Environment, 210-211: 547-558. DOI:10.1016/s0048-9697(98)00037-0

Whitehead, P.G., Wilby, R.L., Battarbee, R.W., Kernan, M., Wade, A.J., 2009. A review of the potential impacts of climate change on surface water quality. Hydrological Sciences Journal, 54(1): 101-123. DOI:10.1623/hysj.54.1.101

Whitehead, P.G., Wilby, R.L., Butterfield, D., Wade, A.J., 2006. Impacts of climate change on in-stream nitrogen in a lowland chalk stream: an appraisal of adaptation strategies. Sci Total Environ, 365(1-3): 260-73. DOI:10.1016/j.scitotenv.2006.02.040

Winter, C., Lutz, S.R., Musolff, A., Kumar, R., Weber, M., Fleckenstein, J.H., 2021. Disentangling the Impact of Catchment Heterogeneity on Nitrate Export Dynamics From Event to Long-Term Time Scales. Water Resources Research, 57(1). DOI:10.1029/2020wr027992

Wohl, E., Lane, S.N., Wilcox, A.C., 2015. The science and practice of river restoration. Water Resources Research, 51(8): 5974-5997. DOI:10.1002/2014wr016874

Wollheim, W.M., Mulukutla, G.K., Cook, C., Carey, R.O., 2017. Aquatic Nitrate Retention at River Network Scales Across Flow Conditions Determined Using Nested In Situ Sensors. Water Resources Research, 53(11): 9740-9756. DOI:10.1002/2017wr020644

Wollheim, W.M. et al., 2001. Influence of stream size on ammonium and suspended particulate nitrogen processing. Limnology and Oceanography, 46(1): 1-13. DOI:DOI 10.4319/lo.2001.46.1.0001

Wollheim, W.M., Peterson, B.J., Thomas, S.M., Hopkinson, C.H., Vörösmarty, C.J., 2008a. Dynamics of N removal over annual time periods in a suburban river network. Journal of Geophysical Research, 113(G3). DOI:10.1029/2007jg000660

Wollheim, W.M. et al., 2008b. Global N removal by freshwater aquatic systems using a spatially distributed, within-basin approach. Global Biogeochemical Cycles, 22(2): n/a-n/a. DOI:10.1029/2007gb002963

Wollheim, W.M., Vörösmarty, C.J., Peterson, B.J., Seitzinger, S.P., Hopkinson, C.S., 2006. Relationship between river size and nutrient removal. Geophysical Research Letters, 33(6). DOI:10.1029/2006gl025845

Wollschläger, U. et al., 2016. The Bode hydrological observatory: a platform for integrated, interdisciplinary hydro-ecological research within the TERENO Harz/Central German Lowland Observatory. Environmental Earth Sciences, 76(1). DOI:10.1007/s12665-016-6327-5

Wu, H., Chen, B., Ye, X., Guo, H., Meng, X., Zhang, B., 2021. An improved calibration and uncertainty analysis approach using a multicriteria sequential algorithm for hydrological modeling. Sci Rep, 11(1): 16954. DOI:10.1038/s41598-021-96250-6

Wu, L., Liu, X., Yang, Z., Yu, Y., Ma, X., 2022a. Effects of single- and multi-site calibration strategies on hydrological model performance and parameter sensitivity of large-scale semi-arid and semi-humid watersheds. Hydrological Processes, 36(6). DOI:10.1002/hyp.14616

Wu, S., Tetzlaff, D., Yang, X., Soulsby, C., 2022b. Disentangling the Influence of Landscape Characteristics, Hydroclimatic Variability and Land Management on Surface Water NO3-N Dynamics: Spatially Distributed Modeling Over 30 yr in a Lowland Mixed Land Use Catchment. Water Resources Research, 58(2). DOI:10.1029/2021wr030566

Xu, X., Li, J., Tolson, B.A., 2014. Progress in integrating remote sensing data and hydrologic modeling. Progress in Physical Geography: Earth and Environment, 38(4): 464-498. DOI:10.1177/0309133314536583

Yang, X., Jomaa, S., Buttner, O., Rode, M., 2019. Autotrophic nitrate uptake in river networks: A modeling approach using continuous high-frequency data. Water Res, 157: 258-268. DOI:10.1016/j.watres.2019.02.059

Yang, X., Jomaa, S., Zink, M., Fleckenstein, J.H., Borchardt, D., Rode, M., 2018. A New Fully Distributed Model of Nitrate Transport and Removal at Catchment Scale. Water Resources Research. DOI:10.1029/2017wr022380

Yang, X., Rode, M., 2020. A Fully Distributed Catchment Nitrate Model - mHM-Nitrate v2.0. DOI:10.5281/ZENODO.3891629

Yang, X.Q., Jomaa, S., Rode, M., 2019. Sensitivity Analysis of Fully Distributed Parameterization Reveals Insights Into Heterogeneous Catchment Responses for Water Quality Modeling. Water Resources Research, 55(12): 10935-10953. DOI:10.1029/2019wr025575

Ye, S., Covino, T.P., Sivapalan, M., Basu, N.B., Li, H.-Y., Wang, S.-W., 2012. Dissolved nutrient retention dynamics in river networks: A modeling investigation of transient flows and scale effects. Water Resources Research, 48(6). DOI:10.1029/2011wr010508

Ye, S. et al., 2017. Scaling Dissolved Nutrient Removal in River Networks: A Comparative Modeling Investigation. Water Resources Research, 53(11): 9623-9641. DOI:10.1002/2017wr020858

Yen, H., Wang, X., Fontane, D.G., Harmel, R.D., Arabi, M., 2014. A framework for propagation of uncertainty contributed by parameterization, input data, model structure, and calibration/validation data in watershed modeling. Environ Modell Softw, 54: 211-221. DOI:10.1016/j.envsoft.2014.01.004

Yevenes, M.A., Figueroa, R., Parra, O., 2018. Seasonal drought effects on the water quality of the Biobio River, Central Chile. Environ Sci Pollut Res Int, 25(14): 13844-13856. DOI:10.1007/s11356-018-1415-6

Young, 1989. AGNPS: A Non-Point-Source Pollution Model for Evaluating Agricultural Watersheds.

Yuan, L., Sinshaw, T., Forshay, K.J., 2020. Review of Watershed-Scale Water Quality and Nonpoint Source Pollution Models. Geosciences, 10(1). DOI:10.3390/geosciences10010025

Zarnetske, J.P., Haggerty, R., Wondzell, S.M., Baker, M.A., 2011. Dynamics of nitrate production and removal as a function of residence time in the hyporheic zone. Journal of Geophysical Research, 116(G1). DOI:10.1029/2010jg001356

Zhang, L., Zhao, Y., Ma, Q., Wang, P., Ge, Y., Yu, W., 2021. A parallel computing-based and spatially stepwise strategy for constraining a semi-distributed hydrological model with streamflow observations and satellite-based evapotranspiration. Journal of Hydrology, 599. DOI:10.1016/j.jhydrol.2021.126359

Zhang, X., Srinivasan, R., Van Liew, M., 2008. Multi-Site Calibration of the SWAT Model for Hydrologic Modeling. Transactions of the ASABE, 51(6): 2039-2049. DOI:https://doi.org/10.13031/2013.25407

Zhang, X., Yang, X., Hensley, R., Lorke, A., Rode, M., 2023. Disentangling In-Stream Nitrate Uptake Pathways Based on Two-Station High-Frequency Monitoring in High-Order Streams. Water Resources Research, 59(3): e2022WR032329. DOI:10.1029/2022wr032329

Zhou, X., Jomaa, S., Yang, X., Merz, R., Wang, Y., Rode, M., 2022. Exploring the relations between sequential droughts and stream nitrogen dynamics in central Germany through catchment-scale mechanistic modelling. Journal of Hydrology, 614: 128615. DOI:10.1016/j.jhydrol.2022.128615

Zwolsman, J.J.G., van Bokhoven, A.J., 2007. Impact of summer droughts on water quality of the Rhine River - a preview of climate change? Water Science and Technology, 56(4): 45-55. DOI:10.2166/wst.2007.535

4.8. Supplementary materials

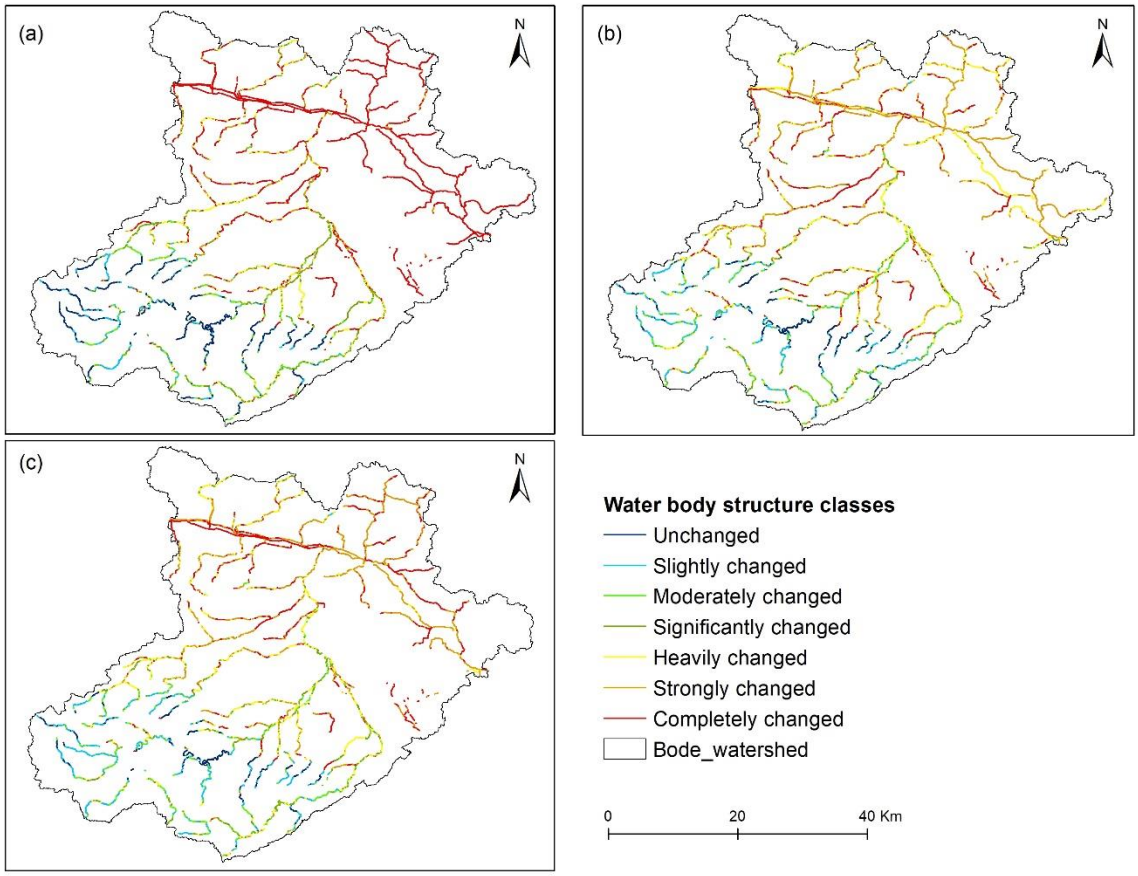

Figure S4.1. Classification of quality of the (a) longitudinal profile, (b) bank structure and (c) overall water body structure of the Bode river network.

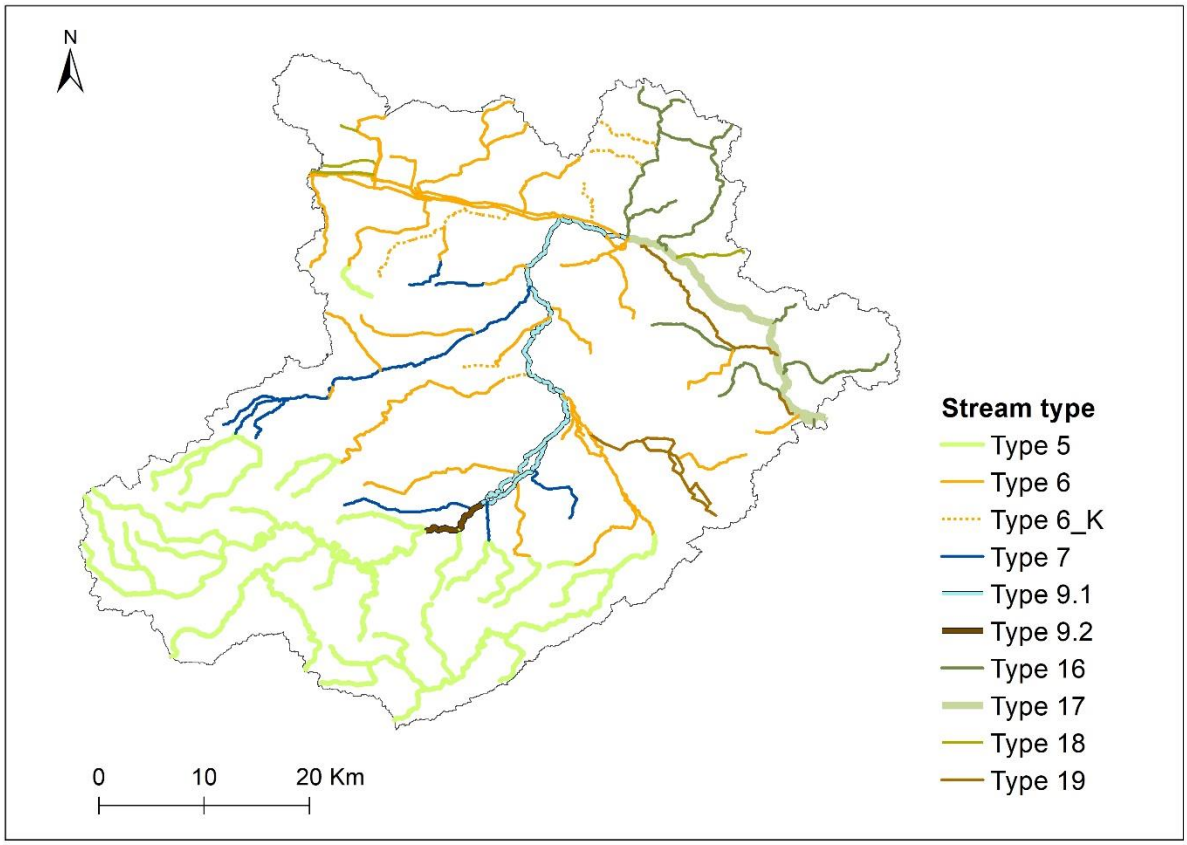

Figure S4.2. Stream types of the Bode river network according to the WFD classification river typology (Pottgiesser and Sommerhäuser, 2004). The description of stream types in are given in Table S2.

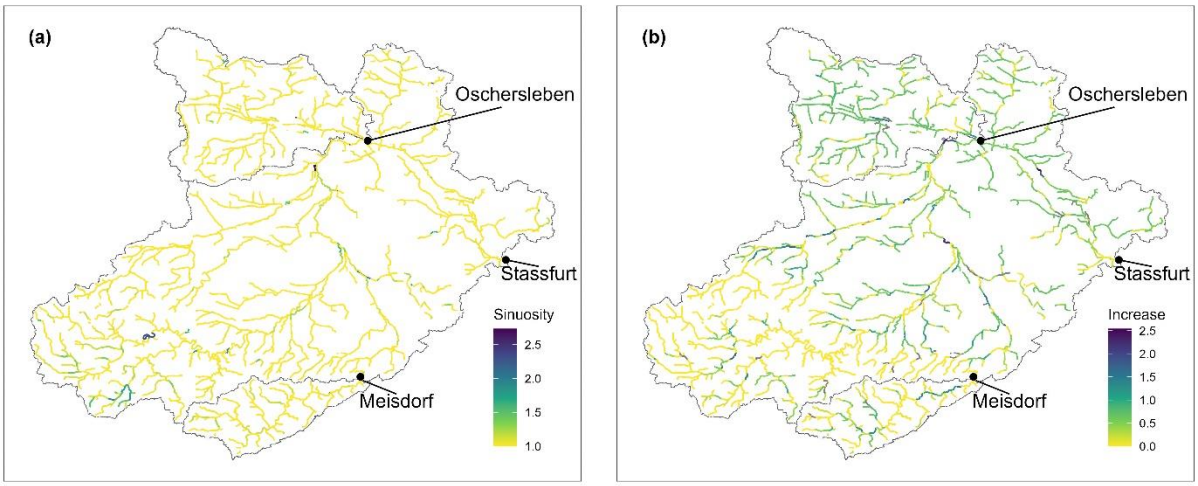

Figure S4.3. Spatial distribution of (a) river sinuosity at baseline and (b) the increase of sinuosity under scenario compared to baseline.

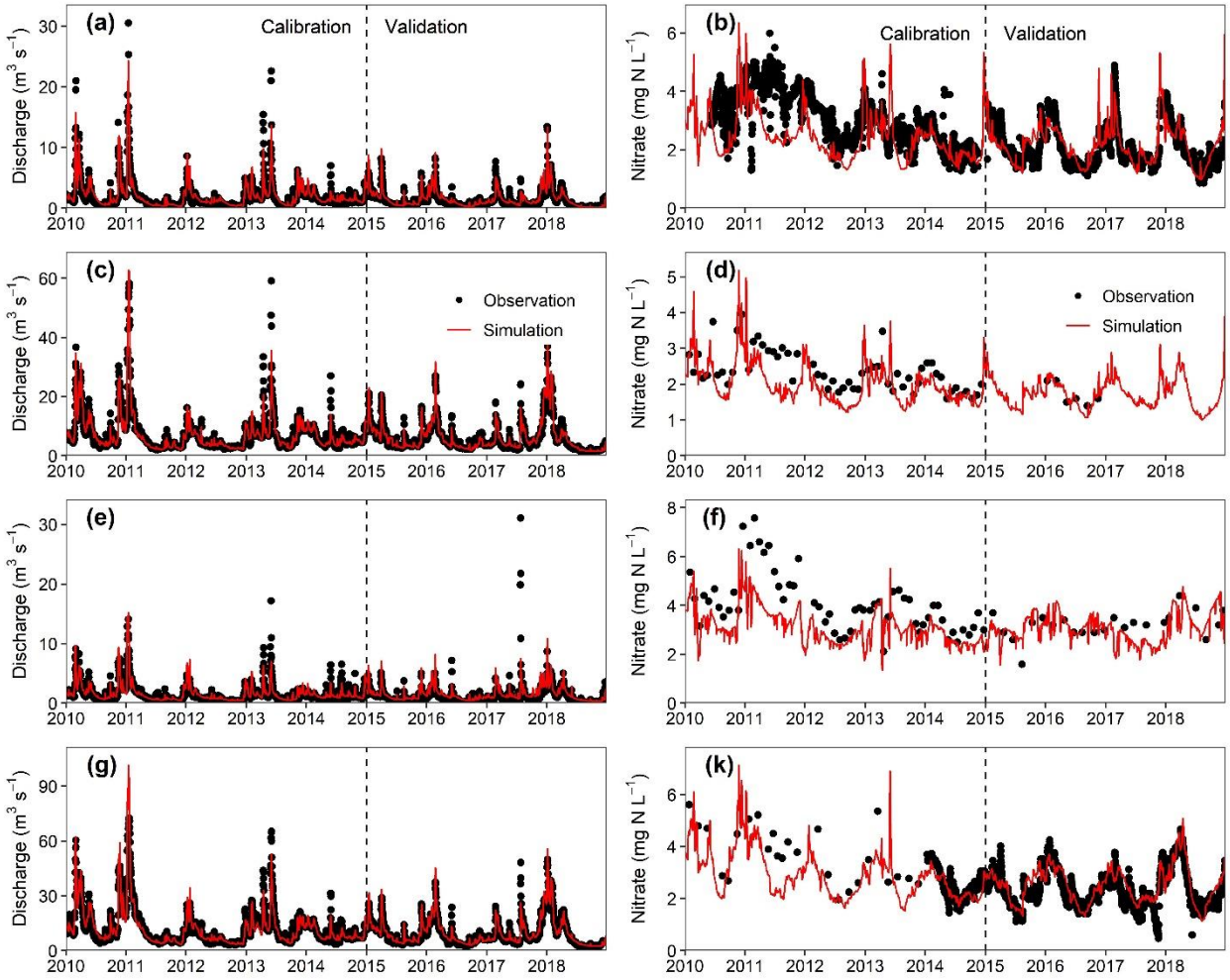

Figure S4.4. The mHM-Nitrate model performances of discharge and nitrate concentration at (a-b) Hausneindorf, (c-d) Wegeleben, (e-f) Nienhagen and (g-k) Hadmersleben in the calibration period (2010-2014) and validation period (2015-2018).

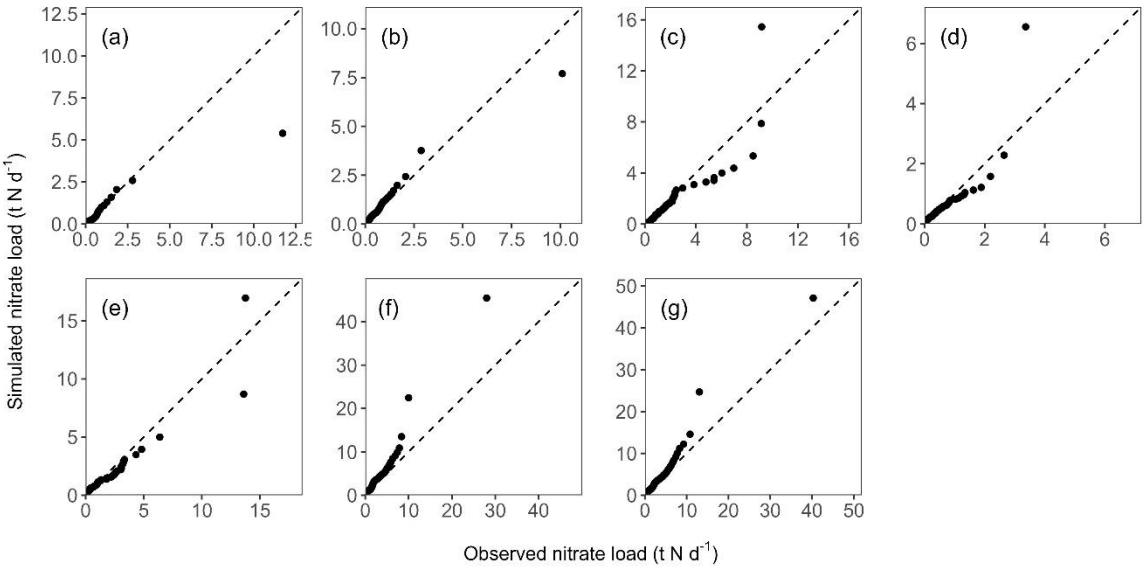

Figure S4.5. The mHM-Nitrate model simulated nitrate load compared to observed nitrate load during 2010-2018 at gauging stations (a) Meisdorf, (b) Hausneindorf, (c) Wegeleben, (d) Nienhagen, (e) Oschersleben, (f) Hadmersleben and (g) Stassfurt.

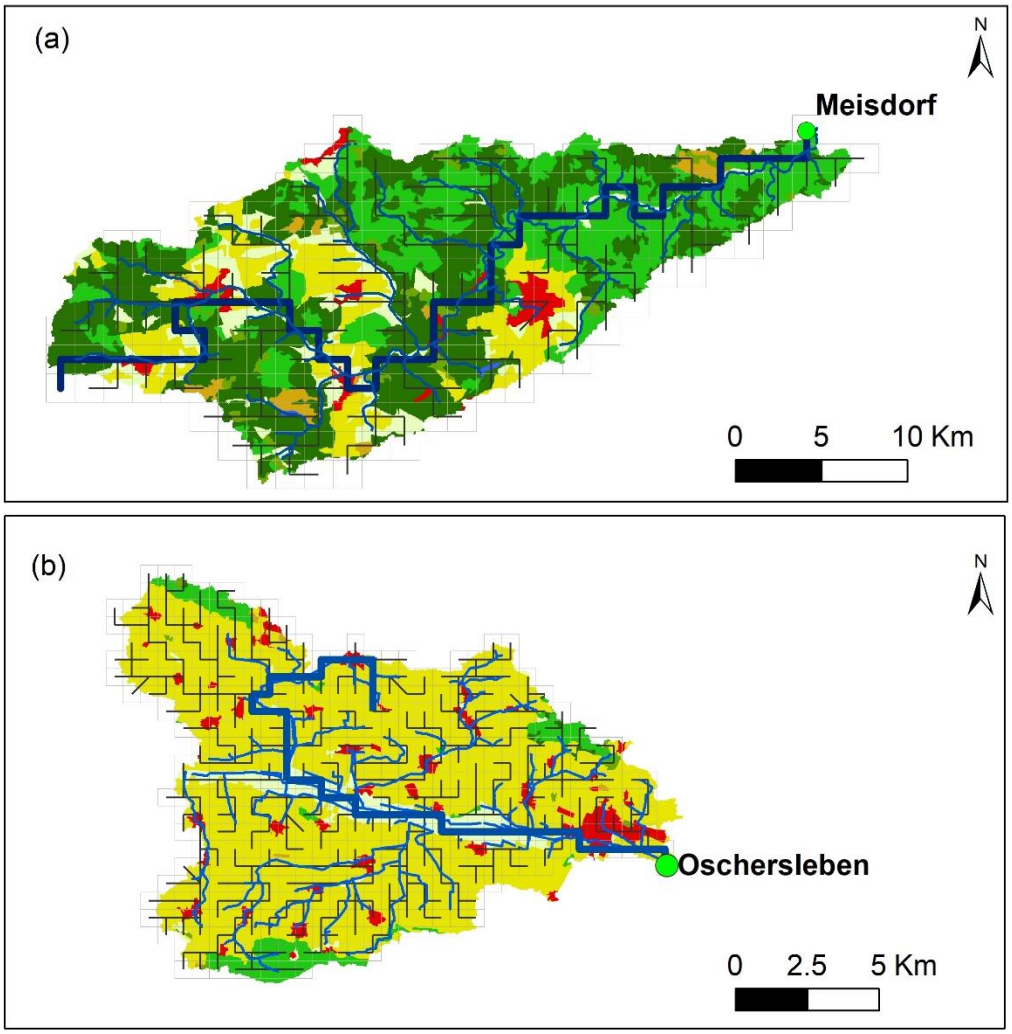

Figure S4.6. Main stems and model river network of (a) Upper Selke and (b) Großer Graben sub-catchments. The backgrounds are the land use type and the real river network from the LHW.

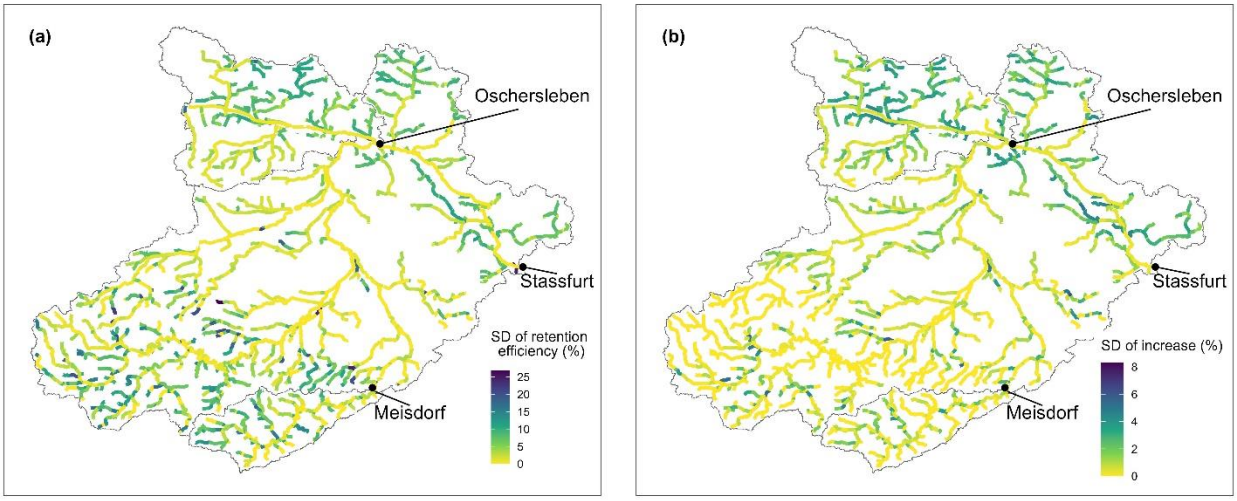

Figure S4.7. Spatial distribution of (a) the standard deviation (SD) of net nitrate retention efficiency in the baseline scenario and (b) the standard deviation (SD) of the percentage increase over baseline in the restoration scenario.

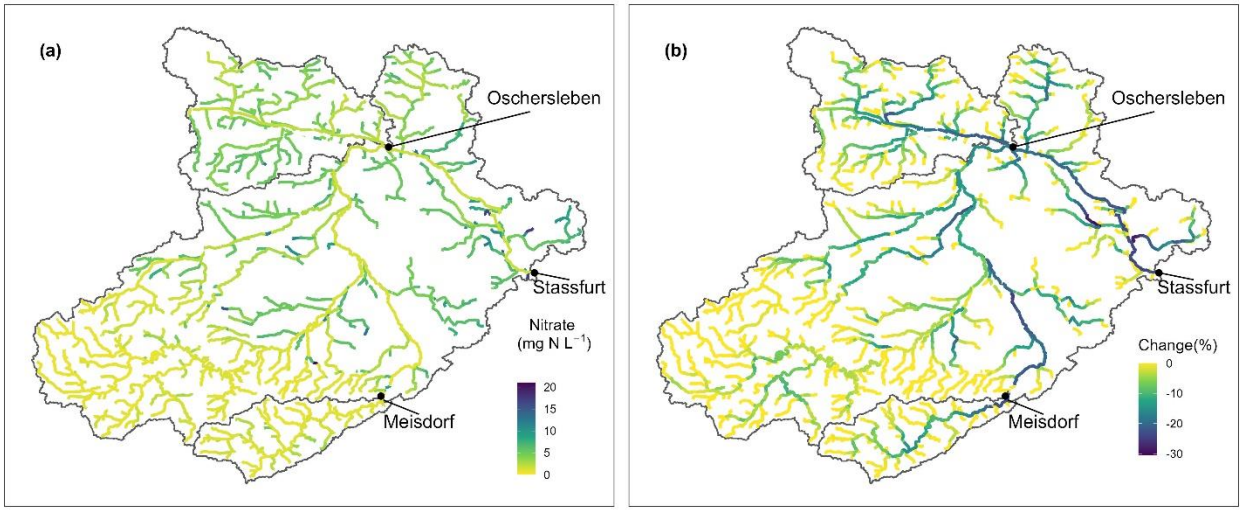

Figure S4.8. Spatial distribution of (a) summer mean nitrate concentration at baseline and (b) the relative change of summer mean nitrate concentration under scenario compared to baseline.

Table S4.1. The characteristics of the mHM-Nitrate model generated stream network of two representative sub-catchments (upper Selke and Großer Graben) at 1 km grid resolution. Values reflect the upper Selke, the values given in the parentheses stand for characteristics of the Großer Graben stream network.

Stream Order	Numbers (-)	Bifurcation ratio (-)	Total river length (km)	Drainage area (% of total area)
1st	47 (78)	2.9 (2.8)	75.5 (156.4)	46.6 (41.5)
2nd	16 (28)	5.3 (2.8)	44.0 (100.5)	23.3 (29.3)
3rd	3 (10)	3.0 (5.0)	15.4 (47.5)	11.8 (16.0)
4th	1 (2)	- (2.0)	26.4 (21.9)	18.3 (7.8)
5th	- (1)	- (-)	- (14.3)	- (5.4)

Note: Bifurcation ratio is defined as the ratio of the number of the streams of given order 'Nr' to the number of streams in the next higher order (Nr+1).

Table S4.2. River types and the potential natural sinuosity ranges of the Bode river network (Ministerium für Umwelt und Naturschutz Landwirtschaft und Verbraucherschutz des Landes Nordrhein-Westfalen, 2010).

River type	Description	Potential natural sinuosity
Type 5	Small coarse substrate-dominated siliceous highland rivers	1.25-2.0
Type 6	Small fine substrate-dominated calcareous highland rivers	1.25-2.0
Type 7	Small coarse substrate-dominated calcareous highland rivers	1.01-1.5
Type 9.1	Mid-sized fine to coarse substrate-dominated calcareous highland rivers	1.25-2.0
Type 9.2	Large highland rivers	1.06-1.5
Type 16	Small gravel-dominated lowland rivers	1.25-2.0
Type 17	Mid-sized and large gravel-dominated lowland rivers	1.25-2.0
Type 18	Small loess and loam-dominated lowland rivers	1.5-2.0
Type 19	Small streams in riverine floodplains	1.25-1.5

Chapter 5: Discussion

The objective of this study was to investigate the effects of drought and river restoration on nitrate concentration in a heterogeneous catchment (Bode) by utilizing a fully distributed catchment hydrological water quality model (mHM-Nitrate). The catchment experienced sequential drought from 2015-2018, and different nitrate concentration trends were observed in the forest- and arable-dominated parts of the catchment. The study began by examining the model's spatial transferability by comparing three calibration schemes. The results showed that multi-site calibration improved the mHM-Nitrate model's nitrate concentration performance at both calibration and validation stations and nitrate sampling locations compared to single-site calibration only at the catchment outlet. However, adding more calibration stations did not improve the model's nitrate concentration performance. The study concluded that it's vital to select gauging stations that represent all variations within the catchment area rather than just aiming for a higher number of stations for better model performance (Chapter 2). The well-calibrated and validated mHM-Nitrate model simulation results showed that the decline of nitrate concentration in the arable-dominated lowland area was due to the combined effect of less nitrate input to the river network and increased nitrate retention efficiency in the river network during the drought period (Chapter 3). Moreover, the study investigated the effects of stream restoration via stream re-meandering on nitrate retention in the Bode catchment, which is characterized by heavily modified stream network in the lowland arable area. The fully distributed process-based mHM-Nitrate model results indicated that small streams retained nitrate more efficiently than large streams as stream sinuosity at the stream network scale increased, and nitrate concentration decreased more in large streams than in small streams due to accumulative retention in the upper streams (Chapter 4).

5.1. Matching the model complexity with catchment heterogeneity

Catchment hydrological water quality models play an important role in supporting water quality management and investigating climate change and land use change scenarios. Catchments exhibit considerable spatiotemporal variation of climate conditions and spatial heterogenous characteristics, such as topography, land use, geology and soil type (Gao et al., 2018). The hydrological and biogeochemical processes, therefore, showed large heterogeneity at the catchment scale (Dupas et al., 2016; Rode et al., 2010). Due to the increased interest in land-use change and human activities, spatially distributed representations of water fluxes and state variables are required.

The model complexity in terms of hydrological and biogeochemical processes representation and associated parameterization increases from lumped to semi-distributed and fully distributed model. This is done to account for the heterogeneity of these processes at the catchment scale (Beven, 2001; McDonnell et al., 2007; Singh and Woolhiser, 2002). The hydrological modeling literature is still debating the advantages and disadvantages of two approaches: (a) increase model complexity under the presumption of facilitating a high degree of process heterogeneity, or (b) reduce model complexity and use simple models of complex systems (Beven, 2000; Orth et al., 2015; Schoups, van de Giesen and Savenije, 2008). Some researchers argued that as long as the analysis and interpretation appropriately account for

model structural and input data uncertainties, more complex hydrological water quality models have the advantage of increasing understanding of probable cause-effect relationships and system behavior at the cost of overparameterization (Birkel, Soulsby and Tetzlaff, 2014; Wade, Jackson and Butterfield, 2008). Another advantage of spatially distributed models is that they allow for a more accurate assessment of the effects of spatial changes in land use and specific-target mitigation (such as river restoration or pond implementation) (Tran, De Niel and Willems, 2018; Wagner and Waske, 2016). The critical processes must be adequately represented and parameterized within the model structure when models are parameterized at a smaller scale and then scaled up to a larger scale (Rode et al., 2010). For example, surface and subsurface runoff predominates nitrate transport and transformation at the small scale, while stream transport and transformation predominate at the catchment scale (Baffaut et al., 2015).

While others argue that increasing complexity in the model structure or in the spatial scale) does not guarantee improved simulations (Orth et al., 2015; Perrin, Michel and Andréassian, 2001). Another major problem is that some process representations in complex models have more conceptual than physical establishments, which can lead to inherent transferability issues that can only be effectively fixed through calibration (Lute and Luce, 2017). Additional parameters will be introduced when the model includes more processes. As a result, the main criticisms of fully distributed approaches are the equifinality problem and overparameterization (Beven, 1993; Beven, 2006). However, there are two opposing viewpoints on over-parameterization in the hydrological field. On the one hand, over-parameterization is seen as a flaw that raises questions about the model's reliability and robustness by introducing uncertainty in parameter determination (e.g.(Perrin, Michel and Andréassian, 2001; Seibert, Staudinger and van Meerveld, 2019)). On the other hand, the fact that a single natural process might have a number of alternative valid representations is thought to be a consequence of over-parameterization (Beven, 2006; Savenije, 2001).

Regionalization in catchment hydrological water quality models has been pursued to balance the model complexity and characterization of landscape heterogeneity in order to reduce overparameterization in models (Götzinger and Bárdossy, 2007; Hundecha and Bárdossy, 2004; Pokhrel, Gupta and Wagener, 2008). A multiscale parameter regionalization method (MPR) in the mHM model consists of two steps to estimate effective model parameters: first regionalizing the model parameters by transfer function based on catchment physical characteristics at finest resolution (the same as model input morphological data resolution), and then the regionalized model parameters are upscaled to model simulation resolution using appropriate upscale operators (Samaniego, Kumar and Attinger, 2010). This method preserves the sub-grid variability in the model parameters and reduces considerably the model complexity due to only the global parameters (coefficients of transfer functions) needing to be calibrated instead of model parameters in each grid. In addition to balancing the model complexity, such multi-resolution(level) implementation also reserves discharge and nitrate spatial information at specific locations. Moreover, the mHM-Nitrate model offers detailed spatial information that might serve as the basis for river restoration and land-based mitigation investigation. Due to the inadequate understanding of in-stream processes and the absence of observed data at river network scales, the regionalization technique for the nitrate submodule was only taken into account for the stream assimilatory uptake process in the mHM-Nitrate

model (Yang et al., 2019a). Further studies are needed to improve our understanding of stream retention processes (e.g., denitrification) at river network scale. The mHM-Nitrate model provides a promising framework to upscale stream denitrification rate with its controlling factors (e.g., nitrate concentration and temperature) at river network scale.

5.2. Implication of distributed hydrological water quality model calibration

Before relying too heavily on such scenario results, it is crucial to carefully validate internal variables and explicit process descriptions of the mHM-Nitrate model when interpreting the impact of stream restoration scenarios on nitrate concentration, especially as equifinality may cause scenario analyses to draw the incorrect conclusions about the behavior of the system. Calibration and validation of distributed hydrological water quality models are often performed using discharge measurements at the catchment outlet, which only provide integral information concerning the investigated catchment. In this study, the mHM-Nitrate model performance was temporally validated at eight gauging stations for both discharge and nitrate concentration for the period 2015-2019 and further spatially evaluated at an additional 94 nitrate sampling locations for the period 1994-2019 (Chapter 2). Results revealed that as the number of internal stations for calibrating the mHM-Nitrate model increased, the model performance of discharge at the catchment outlet in the validation period was similar as in calibration period among three calibration schemes. While the model performance for nitrate concentration decreased slightly at the catchment outlet from calibration to validation period among three calibration schemes. Overall, these results suggest that transferability of nitrate parameters is more likely affected by the multi-site calibration than hydrological parameters. This could be explained by different calibration stations that reflected different dominant meteorological and catchment characteristics, may activate distinct dominant hydrological processes at different sub-catchments (Cao et al., 2006; Dal Molin et al., 2020; Shrestha et al., 2016; Zhang, Srinivasan and Van Liew, 2008). In addition to affected by hydrological processes, nitrate processes are influenced by temporal variation of fertilizer application due to crop rotation and in-stream retention processes (Baffaut et al., 2015; Yang, Jomaa and Rode, 2019).

When changing from Scheme 1 (calibrated only at the catchment outlet) to Scheme 2 (calibration based on catchment outlet and two additional internal gauging stations) nitrate concentration modeling performance significantly improved at nitrate sampling locations. By including two additional internal calibration stations, the cumulative probability distribution of sensitive nitrate parameters (soil denitrification rate, in-stream denitrification rate and assimilatory uptake rate) were significantly different between Scheme 1 and 2. This is due to the various parameters are dominated by different catchment characteristics contained in the calibration stations. For example, in the Selke sub-catchment, soil denitrification rate was positively correlated to the area proportion of arable land in the upper Selke (outlet at Meisdorf), whereas there was no relationship for the entire Selke (outlet at Hausneindorf) (Yang, Jomaa and Rode, 2019). This demonstrates that the spatiotemporal transferability of model parameters is significantly impacted by the selection of calibration stations that represent different catchment characteristics. This finding suggests that distributed hydrological water quality models should be calibrated using multi-sites that contain more information of catchment characteristics in order to better constrain model parameters and assure accurate

representation of hydrological and water quality processes at internal locations (Chiang et al., 2014; Li, Weller and Jordan, 2010).

For the training and refinement of internal processes of the hydrological water quality model, choosing an appropriate calibration period with varying conditions is essential (Chuan-zhe, 2010; Singh and Bárdossy, 2012). For example, periods of heavy rain may result in soil saturation and enhanced soil denitrification, whereas droughts may result in soil cracking and the formation of preferential flow paths. Conventional calibration and validation periods are just a few events or years long, and they might not always involve rare or extreme events. In this study, the calibration period includes wet and dry years, thus drought-induced declines in nitrate concertation were well captured by mHM-Nitrate model (Chapter 3), demonstrating the transferability of model parameters under changing climate conditions.

Several studies also suggested that the calibration period should contain both high and low flow periods to increase the robustness of the model (Engel et al., 2007; Singh and Bárdossy, 2012). This could activate different internal processes (e.g., evapotranspiration, infiltration and runoff partition during high flow and low flow periods) and increase the confidence to apply the model in climate change scenarios. The assumption that model parameters are time-invariant may not be applicable when the meteorological and land use conditions have altered between the calibration and validation periods (Heuvelmans, Muys and Feyen, 2004; Merz, Parajka and Blöschl, 2011). Further studies are needed to investigate the temporal transferability of mHM-Nitrate model parameters under climate and land use change conditions.

5.3. The importance of high frequency and spatial monitoring for model calibration and validation

Benefitting from high-frequency (15 mins) water quality stations (Meisdorf, Hausneindorf, Stassfurt), the mHM-Nitrate model calibration under Scheme 2 compared to Scheme 1 improved model performance of nitrate concentration more in small streams (1^{st}-3^{rd}) than large streams (4^{th}-6^{th} stream order) in both forest and lowland arable area. This was probably caused by including the Meisdorf station in the calibration, which resulted in the parameter distributions considerably differing between Scheme 1 and Scheme 2. Furthermore, as stream order increased, the compensate for errors in the smaller upper streams may lead to good simulation performance at large streams. While the mHM-Nitrate model calibration using five additional stations (four of which had low frequency nitrate concentration observations) in Scheme 3 produced similar model performance of nitrate concentration compared to Scheme 2, this was due to the similar information content of discharge and nitrate concentration contained in calibration stations led to similar model parameters distribution between Scheme 3 and Scheme 2. This suggests that representative stations with high frequency monitoring might produce good model performance at interior sites in the watershed. It is recommended that choosing the representative stations which contain comprehensive information for calibration rather than the amount of stations, and that representative catchment characteristics should be taken into consideration while designing monitoring plans (Chen et al., 2012).

Several studies have shown that collection and interpretation of high-frequency nitrate data can be used to better understand and predict nitrate loads to receiving waters (Kirchner et al., 2004;

Neal et al., 2012; Outram et al., 2014; Rode et al., 2016a; Rode et al., 2016b; Rusjan, Brilly and Mikoš, 2008). For example, high-frequency measurements can capture high flow events that traditional grab sampling might miss, and they can increase the accuracy of model prediction by minimizing sample bias and data uncertainty (Hensley and Cohen, 2020; Hensley, Cohen and Korhnak, 2014; Rode, Osenbrück and Shrestha, 2013). The derived in-stream retention rates (e.g., assimilatory uptake rate, denitrification rate) from high-frequency measurements could be also used to validate the model simulated in-stream retention rates (Kunz et al., 2017c; Zhang et al., 2023).

The multi-site calibration of the mHM-Nitrate model in the Bode catchment showed the critical values of spatial observations of discharge and nitrate concentration (Chapter 2). Spatial observation of discharge and nitrate concentration at multi-site is essential to constrain model parameters since fewer parameter sets satisfy all the calibration criteria for all stations (Daggupati et al., 2015). As ground-based measurements are spatially limited or even completely lacking in developing and underdeveloped countries, remote sensing data that may provide continuous, high-resolution measurements of water balance components (e.g. evapotranspiration, soil moisture and groundwater storage) across time and space are an essential option for assessing the internal fluxes and states of the mHM-Nitrate model (Demirel et al., 2018; Immerzeel and Droogers, 2008; Karimi and Bastiaanssen, 2015; Xu, Li and Tolson, 2014). Further research could use both ground-based measurements and remote sensing data to comprehensively evaluate the spatial capabilities of the mHM-Nitrate model.

The mHM-Nitrate model underestimated the peak flow events in the mountain area (Chapter 3), which was due to the low density of precipitation observation stations. The number of climate stations increased before 1990s, afterwards, it declined due to optimization of observation stations. In addition, precipitation in mountainous areas is often underestimated due to topographic heterogeneity and wind-induced effects (Guidicelli et al., 2021; Kochendorfer et al., 2017). Since extreme events like floods that occur quickly cannot be recorded by a sparsely populated network of observation stations, spatial measurements are required to capture spatiotemporal changing weather conditions. Several studies showed that ground-based observation scarce mountainous areas may benefit from satellite-based precipitation observation (Lettenmaier et al., 2015; Michaelides et al., 2009). Therefore, further study might investigate at how remotely sensing precipitation affects the performance of the mHM-Nitrate model.

5.4. Limitations and future work

Although the mHM-Nitrate model showed good spatial and temporal performance for discharge and nitrate concentration in the study, there are some limitations: the groundwater representation in the mHM-Nitrate model was simplified, nitrate concentration of groundwater was initialed based on the land use type and geology type to differ the arable in the mountainous area and lowland area. A possible solution is based on the transit time distribution of water or storage selection functions to implicitly represent nitrate transport in groundwater (Nguyen et al., 2021). The mHM-Nitrate model might benefit from more regional and temporal measurements of groundwater nitrate concentration to better understand and refine the nitrate processes in groundwater.

Current stream restoration scenario considering sinuosity change according to the empirical equation between stream sinuosity and stream power, it is also worth to examine the effects of other stream morphological features (e.g., bedforms, pools) on stream nitrate retention at catchment scale coupling mHM-Nitrate model with physically based river network models (e.g., Networks with EXchange and Subsurface Storage, (Gomez-Velez and Harvey, 2014)) in future. Due to inadequate measurement at the river network, the river morphology represented in the mHM-Nitrate model is dependent on downstream hydraulic equations (stream width and depth related to discharge). More accurate river width and depth data in the river network may help to minimize the model uncertainty in stream retention as inexpensive unmanned aerial vehicles with photogrammetrically calibrated sensors become more widely available (Bandini et al., 2018; Kasvi et al., 2019).

- Nitrate processes representation at stream network could be improved in the mHM-Nitrate model. The existing mHM-Nitrate model's in-stream denitrification process did not distinguish between the water column and the hyporheic zone, but it might be developed in future to explicitly consider the various denitrification rates in the water column and hyporheic zone (e.g.,Cardenas, 2009; Gomez-Velez et al., 2015; Gomez-Velez et al., 2017; Gomez, Wilson and Cardenas, 2012; Kiel and Bayani Cardenas, 2014; Reisinger et al., 2016; Reisinger et al., 2015; Ye et al., 2012).
- The current stream denitrification process described in the mHM-Nitrate model was based on the relationship between denitrification rate and stream nitrate concentration and temperature. It may be possible to construct a new equation between the denitrification rate and other controlling factors (e.g., oxygen concentration, organic carbon concentration) as the high-frequency measurements increases (Jarvie et al., 2018; Jones et al., 2018).
- The impacts of climate and land use change on nitrate retention could be investigated based on the mHM-Nitrate model. As droughts are projected to become more frequent and server in the future (Hari et al., 2020; Spinoni et al., 2018), it is worthwhile to assess the effects of drought and land use change on hydrological processes and nitrate dynamics at the catchment scale. For example, Kong et al. (2022) reported that increasing nutrient flux due to deforestation can result the mesotrophic reservoir into a eutrophic state based on coupled catchment nutrient exports (HYPE) and reservoir ecosystem dynamics (GOTM-WET) models.
- Remote sensing observation data could be used to calibrate the mHM-Nitrate model and validate its internal fluxes and states. It would be possible to use the spatial data derived from remote sensing observations (e.g., evapotranspiration, soil moisture and total water storage) to calibrate the mHM-Nitrate model with more and easier access to remote sensing data. For example, Demirel et al. (2018) showed that including the spatial pattern of actual evapotranspiration derived based on MODIS into calibration objective function improved considerably the mHM model simulations.

Chapter 6: Summary

This study investigates the impact of multi-site and single-site calibration on the parameters' transferability of a new developed process-based catchment hydrological water quality model (mHM-Nitrate model) in the heterogeneous mesoscale catchment Bode (3200 km^2), Central Germany (Chapter 2). The mHM-Nitrate model was calibrated using three calibration schemes: (i) only calibrated at the catchment outlet (Scheme 1), (ii) calibrated at both the catchment outlet and two internal stations (Scheme 2), and (iii) calibrated at both the catchment outlet and seven internal stations (Scheme 3). The model performance for discharge was similar at the catchment outlet for the three calibration schemes. While for NO_3^- concentration, Scheme 2 performs better than Schemes 1 and 3 at the gauging stations. The spatial transferability of the model was further evaluated at 94 spatially distributed NO_3^- sampling locations, scheme 2 did better than scheme 1 and model performance across the sampling locations was similar for schemes 2 and 3. The findings indicate that in order to achieve optimal parameter calibration, it is essential to strategically choose gauging stations that include the entire range of catchment characteristics heterogeneity, rather than solely focusing on increasing the number of stations. In addition, this study provides practical recommendations for the selection of gauging stations during model calibration. It suggests that the presence of differences in cumulative parameter distributions can serve as an indication of which stations can offer additional and beneficial representation.

To explore the mechanism of sequential drought introduced nitrate heterogenous trends, model outputs and internal processes were compared between the drought period (2015–2018) and pre–drought period (2004–2014) (Chapter 3). Results showed that decline in stream nitrate concentration in the lowland area of the Bode watershed could be explained by less nitrogen export from the terrestrial and an increased in in-stream retention efficiency during the drought period. Nitrate concentration was relatively stable in the upper mountainous area of the catchment due to limited change in nitrate export and in-stream retention efficiency. The study found that, especially in the lowland region of the watershed, nitrate was mainly retained in the soil during the drought periods as opposed to being mobilized or transported. The Bode watershed is a typical mesoscale catchment in central Europe, having a mountainous headwater and an agricultural plain that experiences very little precipitation. We anticipate that catchments with geographical and climatic conditions comparable to those of the Bode catchment (i.e., wet mountain regions and dry lowland regions) would be particularly sensitive to changing weather conditions. In addition, the model is capable of accurately representing nitrate concentration in changing weather conditions, which might be used to study the effects of climate change.

Stream rehabilitation has received more attention recently in order to increase nitrate retention and reduce transport to downstream. Based on well calibrated mHM-Nitrate model, we examined the impacts of stream restoration via stream re-meandering on NO_3^- retention in the Bode catchment with a heavily modified stream network in lowland arable area (Chapter 4). Stream networks with various land uses and morphological characteristics exhibited significant spatiotemporal variation in stream NO_3^- retention rates, which were higher in agricultural streams than in forest streams. Small streams retained NO_3^- more effectively than large streams

as stream sinuosity increased at the stream network scale, while NO_3^- concentrations declined in large streams more than small streams due to accumulative retention in the upper streams. This study highlights the importance of stream re-meandering as a promising mitigation strategy to promote in-stream retention and decrease nitrate export at the stream network scale during the vegetative period, particularly at small streams in agricultural areas.

Reference

Baffaut, C., S. M. Dabney, M. D. Smolen, M. A. Youssef, J. V. Bonta, M. L. Chu, J. A. Guzman, V. S. Shedekar, M. K. Jha, and J. G. Arnold (2015), Hydrologic and water quality modeling: Spatial and temporal considerations, *Transactions of the ASABE*, *58*(6), 1661-1680.

Bandini, F., D. Olesen, J. Jakobsen, C. M. M. Kittel, S. Wang, M. Garcia, and P. Bauer-Gottwein (2018), Technical note: Bathymetry observations of inland water bodies using a tethered single-beam sonar controlled by an unmanned aerial vehicle, Hydrology and Earth System Sciences, 22(8), 4165-4181.

Beven, K. (1993), Prophecy, Reality and Uncertainty in Distributed Hydrological Modeling, Advances in Water Resources, 16(1), 41-51.

Beven, K. (2001), How far can we go in distributed hydrological modelling?, Hydrology and Earth System Sciences, 5(1), 1-12.

Beven, K. (2006), A manifesto for the equifinality thesis, Journal of Hydrology, 320(1-2), 18-36.

Beven, K. J. (2000), Uniqueness of place and process representations in hydrological modelling, Hydrol. Earth Syst. Sci., 4(2), 203-213.

Birkel, C., C. Soulsby, and D. Tetzlaff (2014), Integrating parsimonious models of hydrological connectivity and soil biogeochemistry to simulate stream DOC dynamics, Journal of Geophysical Research: Biogeosciences, 119(5), 1030-1047.

Cao, W., W. B. Bowden, T. Davie, and A. Fenemor (2006), Multi-variable and multi-site calibration and validation of SWAT in a large mountainous catchment with high spatial variability, Hydrological Processes, 20(5), 1057-1073.

Cardenas, M. B. (2009), A model for lateral hyporheic flow based on valley slope and channel sinuosity, Water Resources Research, 45(1).

Chen, Q., W. Wu, K. Blanckaert, J. Ma, and G. Huang (2012), Optimization of water quality monitoring network in a large river by combining measurements, a numerical model and matter-element analyses, J Environ Manage, 110, 116-124.

Chiang, L. C., Y. P. Yuan, M. Mehaffey, M. Jackson, and I. Chaubey (2014), Assessing SWAT's performance in the Kaskaskia River watershed as influenced by the number of calibration stations used, Hydrological Processes, 28(3), 676-687.

Chuan-zhe, L. (2010), Effect of calibration data series length on performance and optimal parameters of hydrological model.

Daggupati, P., N. Pai, S. Ale, K. R. Douglas-Mankin, R. W. Zeckoski, J. Jeong, P. B. Parajuli, D. Saraswat, and M. A. Youssef (2015), A Recommended Calibration and Validation Strategy for Hydrologic and Water Quality Models, Transactions of the Asabe, 58(6), 1705-1719.

Dal Molin, M., M. Schirmer, M. Zappa, and F. Fenicia (2020), Understanding dominant controls on streamflow spatial variability to set up a semi-distributed hydrological model: the case study of the Thur catchment, Hydrology and Earth System Sciences, 24(3), 1319-1345.

Demirel, M. C., J. Mai, G. Mendiguren, J. Koch, L. Samaniego, and S. Stisen (2018), Combining satellite data and appropriate objective functions for improved spatial pattern

performance of a distributed hydrologic model, Hydrology and Earth System Sciences, 22(2), 1299-1315.

Dupas, R., S. Jomaa, A. Musolff, D. Borchardt, and M. Rode (2016), Disentangling the influence of hydroclimatic patterns and agricultural management on river nitrate dynamics from sub-hourly to decadal time scales, Sci Total Environ, 571, 791-800.

Engel, B., D. Storm, M. White, J. Arnold, and M. Arabi (2007), A hydrologic/water quality model application protocol, Journal of the American Water Resources Association, 43(5), 1223-1236.

Gao, H., J. L. Sabo, X. Chen, Z. Liu, Z. Yang, Z. Ren, and M. Liu (2018), Landscape heterogeneity and hydrological processes: a review of landscape-based hydrological models, Landscape Ecology, 33(9), 1461-1480.

Gomez-Velez, J. D., and J. W. Harvey (2014), A hydrogeomorphic river network model predicts where and why hyporheic exchange is important in large basins, Geophysical Research Letters, 41(18), 6403-6412.

Gomez-Velez, J. D., J. W. Harvey, M. B. Cardenas, and B. Kiel (2015), Denitrification in the Mississippi River network controlled by flow through river bedforms, Nature Geoscience, 8(12), 941-945.

Gomez-Velez, J. D., J. L. Wilson, M. B. Cardenas, and J. W. Harvey (2017), Flow and Residence Times of Dynamic River Bank Storage and Sinuosity-Driven Hyporheic Exchange, Water Resources Research, 53(10), 8572-8595.

Gomez, J. D., J. L. Wilson, and M. B. Cardenas (2012), Residence time distributions in sinuosity-driven hyporheic zones and their biogeochemical effects, Water Resources Research, 48(9).

Götzinger, J., and A. Bárdossy (2007), Comparison of four regionalisation methods for a distributed hydrological model, Journal of Hydrology, 333(2-4), 374-384.

Guidicelli, M., R. Gugerli, M. Gabella, C. Marty, and N. Salzmann (2021), Continuous Spatio-Temporal High-Resolution Estimates of SWE Across the Swiss Alps – A Statistical Two-Step Approach for High-Mountain Topography, Frontiers in Earth Science, 9.

Hari, V., O. Rakovec, Y. Markonis, M. Hanel, and R. Kumar (2020), Increased future occurrences of the exceptional 2018-2019 Central European drought under global warming, Sci Rep, 10(1), 12207.

Hensley, R. T., and M. J. Cohen (2020), Nitrate depletion dynamics and primary production in riverine benthic chambers, Freshwater Science, 39(1), 169-182.

Hensley, R. T., M. J. Cohen, and L. V. Korhnak (2014), Inferring nitrogen removal in large rivers from high-resolution longitudinal profiling, Limnology and Oceanography, 59(4), 1152-1170.

Heuvelmans, G., B. Muys, and J. Feyen (2004), Evaluation of hydrological model parameter transferability for simulating the impact of land use on catchment hydrology, Physics and Chemistry of the Earth, Parts A/B/C, 29(11-12), 739-747.

Hundecha, Y., and A. Bárdossy (2004), Modeling of the effect of land use changes on the runoff generation of a river basin through parameter regionalization of a watershed model, Journal of Hydrology, 292(1-4), 281-295.

Immerzeel, W. W., and P. Droogers (2008), Calibration of a distributed hydrological model based on satellite evapotranspiration, Journal of Hydrology, 349(3-4), 411-424.

Jarvie, H. P., A. N. Sharpley, T. Kresse, P. D. Hays, R. J. Williams, S. M. King, and L. G. Berry (2018), Coupling High-Frequency Stream Metabolism and Nutrient Monitoring to Explore Biogeochemical Controls on Downstream Nitrate Delivery, Environ Sci Technol, 52(23), 13708-13717.

Jones, C. S., S.-w. Kim, T. F. Wilton, K. E. Schilling, and C. A. Davis (2018), Nitrate uptake in an agricultural stream estimated from high-frequency, in-situ sensors, Environmental Monitoring and Assessment, 190(4).

Karimi, P., and W. G. M. Bastiaanssen (2015), Spatial evapotranspiration, rainfall and land use data in water accounting – Part 1: Review of the accuracy of the remote sensing data, Hydrology and Earth System Sciences, 19(1), 507-532.

Kasvi, E., J. Salmela, E. Lotsari, T. Kumpula, and S. N. Lane (2019), Comparison of remote sensing based approaches for mapping bathymetry of shallow, clear water rivers, Geomorphology, 333, 180-197.

Kiel, B. A., and M. Bayani Cardenas (2014), Lateral hyporheic exchange throughout the Mississippi River network, Nature Geoscience, 7(6), 413-417.

Kirchner, J. W., X. Feng, C. Neal, and A. J. Robson (2004), The fine structure of water-quality dynamics: the(high-frequency) wave of the future, Hydrological Processes, 18(7), 1353-1359.

Kochendorfer, J., et al. (2017), The quantification and correction of wind-induced precipitation measurement errors, Hydrology and Earth System Sciences, 21(4), 1973-1989.

Kong, X., S. Ghaffar, M. Determann, K. Friese, S. Jomaa, C. Mi, T. Shatwell, K. Rinke, and M. Rode (2022), Reservoir water quality deterioration due to deforestation emphasizes the indirect effects of global change, Water Res, 221.

Kunz, J. V., R. Hensley, L. Brase, D. Borchardt, and M. Rode (2017), High frequency measurements of reach scale nitrogen uptake in a fourth order river with contrasting hydromorphology and variable water chemistry (Weiße Elster, Germany), Water Resources Research, 53(1), 328-343.

Lettenmaier, D. P., D. Alsdorf, J. Dozier, G. J. Huffman, M. Pan, and E. F. Wood (2015), Inroads of remote sensing into hydrologic science during the WRR era, Water Resources Research, 51(9), 7309-7342.

Li, X., D. E. Weller, and T. E. Jordan (2010), Watershed model calibration using multi-objective optimization and multi-site averaging, Journal of Hydrology, 380(3-4), 277-288.

Lute, A. C., and C. H. Luce (2017), Are Model Transferability And Complexity Antithetical? Insights From Validation of a Variable-Complexity Empirical Snow Model in Space and Time, Water Resources Research, 53(11), 8825-8850.

McDonnell, J. J., et al. (2007), Moving beyond heterogeneity and process complexity: A new vision for watershed hydrology, Water Resources Research, 43(7).

Merz, R., J. Parajka, and G. Blöschl (2011), Time stability of catchment model parameters: Implications for climate impact analyses, Water Resources Research, 47(2).

Michaelides, S., V. Levizzani, E. Anagnostou, P. Bauer, T. Kasparis, and J. E. Lane (2009), Precipitation: Measurement, remote sensing, climatology and modeling, Atmospheric Research, 94(4), 512-533.

Neal, C., et al. (2012), High-frequency water quality time series in precipitation and streamflow: from fragmentary signals to scientific challenge, Sci Total Environ, 434, 3-12.

Nguyen, T. V., R. Kumar, S. R. Lutz, A. Musolff, J. Yang, and J. H. Fleckenstein (2021), Modeling Nitrate Export From a Mesoscale Catchment Using StorAge Selection Functions, Water Resources Research, 57(2).

Orth, R., M. Staudinger, S. I. Seneviratne, J. Seibert, and M. Zappa (2015), Does model performance improve with complexity? A case study with three hydrological models, Journal of Hydrology, 523, 147-159.

Outram, F. N., et al. (2014), High-frequency monitoring of nitrogen and phosphorus response in three rural catchments to the end of the 2011–2012 drought in England, Hydrology and Earth System Sciences, 18(9), 3429-3448.

Perrin, C., C. Michel, and V. Andréassian (2001), Does a large number of parameters enhance model performance? Comparative assessment of common catchment model structures on 429 catchments, Journal of Hydrology, 242(3), 275-301.

Pokhrel, P., H. V. Gupta, and T. Wagener (2008), A spatial regularization approach to parameter estimation for a distributed watershed model, Water Resources Research, 44(12).

Reisinger, A. J., J. L. Tank, T. J. Hoellein, and R. O. Hall (2016), Sediment, water column, and open-channel denitrification in rivers measured using membrane-inlet mass spectrometry, J Geophys Res-Biogeo, 121(5), 1258-1274.

Reisinger, A. J., J. L. Tank, E. J. Rosi-Marshall, R. O. Hall, and M. A. Baker (2015), The varying role of water column nutrient uptake along river continua in contrasting landscapes, Biogeochemistry, 125(1), 115-131.

Rode, M., K. Osenbrück, and R. R. Shrestha (2013), Assessment of catchment response and calibration of a hydrological model using high-frequency discharge–nitrate concentration data, Hydrology Research, 44(6), 995-1012.

Rode, M., S. Halbedel Nee Angelstein, M. R. Anis, D. Borchardt, and M. Weitere (2016a), Continuous In-Stream Assimilatory Nitrate Uptake from High-Frequency Sensor Measurements, Environ Sci Technol, 50(11), 5685-5694.

Rode, M., G. Arhonditsis, D. Balin, T. Kebede, V. Krysanova, A. van Griensven, and S. E. A. T. M. van der Zee (2010), New challenges in integrated water quality modelling, Hydrological Processes, 24(24), 3447-3461.

Rode, M., et al. (2016b), Sensors in the Stream: The High-Frequency Wave of the Present, Environ Sci Technol, 50(19), 10297-10307.

Rusjan, S., M. Brilly, and M. Mikoš (2008), Flushing of nitrate from a forested watershed: An insight into hydrological nitrate mobilization mechanisms through seasonal high-frequency stream nitrate dynamics, Journal of Hydrology, 354(1-4), 187-202.

Samaniego, L., R. Kumar, and S. Attinger (2010), Multiscale parameter regionalization of a grid-based hydrologic model at the mesoscale, Water Resources Research, 46(5).

Savenije, H. H. G. (2001), Equifinality, a blessing in disguise?, Hydrological Processes, 15(14), 2835-2838.

Schoups, G., N. C. van de Giesen, and H. H. G. Savenije (2008), Model complexity control for hydrologic prediction, Water Resources Research, 44(12).

Seibert, J., M. Staudinger, and H. J. van Meerveld (2019), Validation and Over-Parameterization—Experiences from Hydrological Modeling, in Computer Simulation Validation: Fundamental Concepts, Methodological Frameworks, and Philosophical Perspectives, edited by C. Beisbart and N. J. Saam, pp. 811-834, Springer International Publishing, Cham.

Shrestha, M. K., F. Recknagel, J. Frizenschaf, and W. Meyer (2016), Assessing SWAT models based on single and multi-site calibration for the simulation of flow and nutrient loads in the semi-arid Onkaparinga catchment in South Australia, Agricultural Water Management, 175, 61-71.

Singh, S. K., and A. Bárdossy (2012), Calibration of hydrological models on hydrologically unusual events, Advances in Water Resources, 38, 81-91.

Singh, V. P., and D. A. Woolhiser (2002), Mathematical Modeling of Watershed Hydrology, Journal of Hydrologic Engineering, 7(4), 270-292.

Spinoni, J., J. V. Vogt, G. Naumann, P. Barbosa, and A. Dosio (2018), Will drought events become more frequent and severe in Europe?, International Journal of Climatology, 38(4), 1718-1736.

Tran, Q. Q., J. De Niel, and P. Willems (2018), Spatially Distributed Conceptual Hydrological Model Building: A Generic Top-Down Approach Starting From Lumped Models, Water Resources Research, 54(10), 8064-8085.

Wade, A. J., B. M. Jackson, and D. Butterfield (2008), Over-parameterised, uncertain 'mathematical marionettes' - how can we best use catchment water quality models? An example of an 80-year catchment-scale nutrient balance, Sci Total Environ, 400(1-3), 52-74.

Wagner, P. D., and B. Waske (2016), Importance of spatially distributed hydrologic variables for land use change modeling, Environ Modell Softw, 83, 245-254.

Xu, X., J. Li, and B. A. Tolson (2014), Progress in integrating remote sensing data and hydrologic modeling, Progress in Physical Geography: Earth and Environment, 38(4), 464-498.

Yang, X. Q., S. Jomaa, and M. Rode (2019), Sensitivity Analysis of Fully Distributed Parameterization Reveals Insights Into Heterogeneous Catchment Responses for Water Quality Modeling, Water Resources Research, 55(12), 10935-10953.

Ye, S., T. P. Covino, M. Sivapalan, N. B. Basu, H.-Y. Li, and S.-W. Wang (2012), Dissolved nutrient retention dynamics in river networks: A modeling investigation of transient flows and scale effects, Water Resources Research, 48(6).

Zhang, X., R. Srinivasan, and M. Van Liew (2008), Multi-Site Calibration of the SWAT Model for Hydrologic Modeling, Transactions of the ASABE, 51(6), 2039-2049.

Zhang, X., X. Yang, R. Hensley, A. Lorke, and M. Rode (2023), Disentangling In-Stream Nitrate Uptake Pathways Based on Two-Station High-Frequency Monitoring in High-Order Streams, Water Resources Research, 59(3), e2022WR032329.